CONTRACTOR REPORT

SAND82-8178
UC-62d
Unlimited Release

Molten Salt Receiver Subsystem Research Experiment Phase 1—Final Report Volume I—Technical

Babcock & Wilcox Company
Barberton, Ohio

Prepared by Sandia National Laboratories, Albuquerque, New Mexico 87185 and Livermore, California 94550 for the United States Department of Energy under Contract DE-AC04-76DP00789.

Printed October 1984

Printed in the United States of America
Available from
National Technical Information Service
5285 Port Royal Road
Springfield, VA 22161

NTIS price codes
Printed copy: A14
Microfiche copy: A01

SAND82-8178
Unlimited Release
Printed October 1984

MOLTEN SALT RECEIVER

SUBSYSTEM RESEARCH EXPERIMENT

FINAL REPORT: Phase I

Vol. 1 - Technical

Prepared by:

Babcock & Wilcox
A McDermott Company
Nuclear Equipment Division
Barberton, Ohio 44203

Submitted by:

Babcock & Wilcox
A McDermott Company
Contract Research Division
Barberton, Ohio 44203

November 29, 1982

Prepared for:

Sandia National Laboratories
Sandia Contract No. 84-2292B
B&W Contract No. 1081

Contractors Technical Report
Sandia Contract No. 84-2292B
Sandia Requestor: Dan Dawson 8453
Sandia Contracting Rep: Jack Hubner 8264

Abstract

This report presents the preliminary design of a molten salt receiver subsystem for application to solar thermal central receiver power plants. The design is applicable to a repowered utility electric plant or to a stand-alone plant. The receiver subsystem consists of an elevated quad-cavity receiver, a concrete tower to support the receiver, riser and downcomer piping within the tower to transport the salt to and from the thermal storage sub-system, heat absorption panels within the receiver cavities to absorb the incident radiant energy, and the pumps, tanks, piping systems, valves, controls and instrumentation necessary to provide safe and efficient operation of the receiver subsystem. Incident radiant energy is concentrated on the receiver cavity openings by a surround heliostat field. The design is based on a 320 MWt receiver sited at Barstow, California.

The report provides the design requirements necessary to detail the design of the receiver subsystem, a detailed description of the subsystem components, and the design methods employed to produce the design. A development plan highlights the areas of technical uncertainty along with the required development effort to resolve these uncertainties. Manufacturing processes were developed to establish the fabricability of the heat absorption panels. The cost and schedule from design through start up for the receiver subsystem are also provided. An executive summary of this report is available from TIC as SAND84-8178.

TABLE OF CONTENTS

TABLE OF CONTENTS (Continued)

TABLE OF CONTENTS (Continued)

TABLE OF CONTENTS (Continued)

TABLE OF CONTENTS (Continued)

LIST OF FIGURES

LIST OF FIGURES (Continued)

LIST OF FIGURES (Continued)

LIST OF FIGURES (Continued)

LIST OF FIGURES (Continued)

LIST OF FIGURES (Continued)

LIST OF TABLES

LIST OF TABLES (Continued)

EXECUTIVE SUMMARY

The Babcock & Wilcox Company, under contract to Sandia National Laboratories, has completed the preliminary design of a molten salt receiver subsystem for application to solar central receiver power plants. The design is applicable to a repowered utility electric plant or to a stand-alone plant. The receiver subsystem consists of an elevated quad-cavity receiver, a concrete tower to support the receiver, riser and downcomer piping within the tower to transport the salt to and from the thermal storage sub-system located at ground level, heat absorption panels within the receiver cavities to absorb the incident radiant energy, and the pumps, tanks, piping systems, valves, controls and instrumentation necessary to provide safe and efficient operation of the receiver subsystem. Incident radiant energy is concentrated on the receiver cavity openings by a surround heliostat field. Subcontractor support was provided by Martin Marietta Corporation, Black & Veatch Consulting Engineers, and Arizona Public Service Company.

The principal objectives of the program were:

- To evaluate receiver configuration improvements and select the configuration which maximized the performance/cost ratio of combined receiver and collector subsystems.
- To develop systems level requirements and specifications for the receiver subsystem.
- To prepare a cost effective preliminary design of a commercial receiver subsystem utilizing conventional design, shop fabrication, and field erection practices.
- To identify the requirements for a receiver subsystem research experiment and for a development plan to reduce any risks associated with the design and fabrication of a large scale receiver subsystem.
- To identify and resolve all uncertainties associated with the fabrication of the receiver heat absorption panels.

This summary presents the results of the program. First, the summary discusses the conceptual design evaluations that were made during the proposal phase to establish the quad cavity receiver as the base design. Next, the design requirements are presented establishing the functional requirements for the receiver subsystem, the design conditions, and the environmental requirements. A detailed description of the subsystem components is then given. Following the description of the components, the development requirements are outlined with a discussion of the need for a subsystem research experiment and appropriate laboratory tests. A 10 foot long tube panel was manufactured to prove acceptability of the fabrication procedures. The results of this effort are included. Finally, the cost and schedule are presented.

CONCEPT SELECTION

Prior to the contract work, the basic issues of the receiver type and the heliostat field configuration were evaluated. To understand the reasons for selecting the quad cavity receiver type with a surround heliostat field, it is necessary to make the comparison between the basic receiver concepts as follows:

- o external vs. cavity receiver
- o quad cavity with surround field vs. single cavity with North field

External vs. Cavity - The external receiver utilizes the heat absorption panels to form the external surface of the receiver. Because it eliminates the cavity and structural steel associated with the cavity shell, the external receiver has a simpler structure and, consequently, a lower capital cost. However, the exposure of the heat absorption panels leads to higher heat losses, relative to the cavity receiver, which in turn requires a larger heliostat field to compensate for the higher thermal losses. Evaluation of the design of an applicable external receiver indicated that the savings in the cost of the receiver structure did not make up for the increased cost of the heliostat field (Ref. 1).

Another major disadvantage of the external receiver is that it requires more care in the operation of the unit to ensure that the salt does not freeze within the receiver. The cavity receiver offers more protection against freezing. Each cavity in the quad design is insulated and doors are provided to seal off the cavity during shut down periods. Due to the insulated enclosure, the salt can be maintained in the liquid state during overnight, or for longer periods of time, without fear of freezing in the heat absorption panels. Doors may be supplied with the external receiver to minimize overnight heat losses. However, the curved surfaces require a more costly door arrangement, and would most likely have lower integrity door seals due to the overall complexity, thereby incurring higher heat losses than achievable with the cavity door seals.

The cavity receiver is designed mainly to minimize heat losses from the heat absorption panels by enclosing the panels within the cavity structure. Openings in the cavity face the heliostat field and are sized large enough to allow the concentrated radiant energy to impinge upon the heat absorption panels while sized small enough to minimize convective and radiative losses. In comparison with the external receiver, the cavity receiver heat losses are less, resulting in fewer heliostats for the same power levels. Based on previous studies (Refs. 1, 2, 3), it was concluded that the extra capital costs for the cavity receiver were more than offset by the reduction in heliostat field costs.

Quad Cavity vs. Single Cavity - Prior to the contract, studies (Refs. 1, 3) were performed to compare the quad cavity receiver using a 360° surround field with the single cavity facing a North only field. In these studies, it was concluded that the surround field arrangement was slightly more efficient, for a given power rating, than a North field arrangement, and consequently the surround field offered a slight reduction in total collector system cost. Also, in optimizing the tower and collector field layout, it was concluded that the surround field arrangement resulted in a considerably smaller tower and, therefore, lower tower costs. Sizing of the quad cavity concept indicated that it was a more compact arrangement, with shorter support spans for the structural steel resulting in less structural weight. Based on the preliminary sizing analysis, it was concluded that the quad cavity would incur less cost for structural steel, fabrication and erection than the single cavity*. Based on the evaluation performed in the early studies (Refs. 1, 3) on the costs of the collector field, tower and receiver, it was concluded at the beginning of the contract that the quad cavity receiver with a surround field was the preferred concept.

DESIGN REQUIREMENTS

The receiver subsystem is designed to meet the standards established by ASME, AISC Codes, etc., and the standards set by commercial practice as applied to products such as fossil fuel fired boilers. In general, these standards ensure that safety requirements are met, and that a high degree of reliability is ensured consistent with good economic practices. A "Requirement and Specification" document was produced which defines the necessary system requirements, applicable codes, requirements for design, fabrication, erection, quality assurance, and other special requirements. The general requirements are summarized below:

- The collector subsystem shall reflect solar radiation onto the receiver subsystem in a manner which satisfies incident heat flux requirements. Heat flux limits on the panels shall be established by consideration of thermal stress, temperature, fatigue damage, and corrosion limits.

- The receiver subsystem shall be designed to provide access for maintenance and inspection of the receiver, tower, panels, pumps, tanks, piping, controls, and other parts requiring maintenance.

---

*More recent results show that, while the quad cavity does in fact have less structural steel, the complexity of the arrangement and the much larger number of panels, supports etc. required, results in total costs that are very similar to those of the single cavity.

- The receiver subsystem shall be capable of functioning in the following normal modes of operation:

  ---cold startup
  ---diurnal startup
  ---sustained operation within the specified load range
  ---transient operation during cloud passage
  ---hot standby during prolonged cloud passage
  ---diurnal shutdown and overnight hold
  ---prolonged shutdown

- The receiver shall be capable of safe controlled shutdown resulting from upset and emergency conditions due to:

  ---molten salt pump trip
  ---heliostat field scram
  ---loss of power to the heliostat field
  ---loss of salt flow or pressure
  ---flow control valve malfunction
  ---adverse weather conditions

- The receiver subsystem shall be designed for a 30 year operating life.

- Considerations shall be given in the design to achieving high reliability by providing design and operating margins and utilizing sound engineering design practices.

The normal design conditions upon which the design is based are shown on Table 1 with the environmental requirements shown on Table 2. The receiver is designed to accommodate infrequent insolation peaks of 1100w/m^2 at salt flow rates 115% of normal. Nominal design salt temperatures are maintained at salt flow rates down to 25% of the nominal design condition.

TABLE 1 - NOMINAL DESIGN CONDITIONS

Reference Site	Barstow, California
Insolation (direct normal)	950 w/m^2
Design Point	Day 172 at Noon
Receiver Working Fluid	Molten Nitrate Salt 60% $NaNO_3$/40% KNO_3 Mixture by Weight
Design Absorbed Thermal Power	320 MW_t (1.09 X 10^9 Btu/Hr)
Minimum Absorbed Thermal Power	30 MW_t (0.1 X 10^9 Btu/Hr)
Salt Inlet Temperature	290C (550F)
Salt Outlet Temperature	565C (1050F)
Salt Flow Rate	367 Kg/sec (5.85 X 10^6 lbm/hr)

RECEIVER SUBSYSTEM DESIGN

The receiver subsystem is defined as shown in Figure 1 and includes the following components:

Receiver
Tower and Foundation
Receiver Structural Support
Salt Pumps
Riser/Downcomer in the tower
Miscellaneous Receiver Internal Piping
Controls
Valves
Insulation and trace heating
Auxiliary Equipment

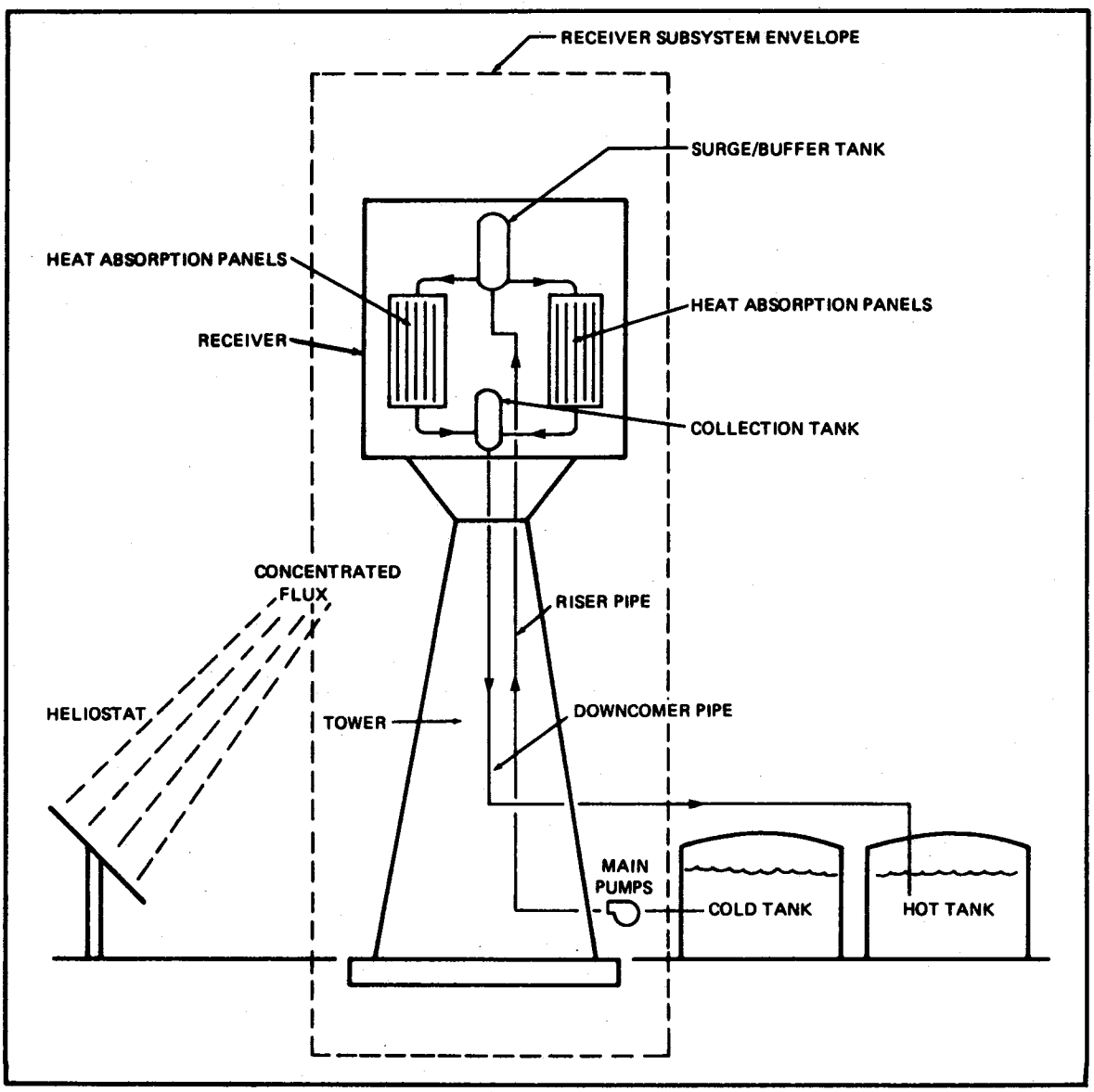

FIGURE 1 DEFINITION OF RECEIVER SUBSYSTEM

TABLE 2 - ENVIRONMENTAL REQUIREMENTS

Design	
Max. Change in Incident Flux	Caused by sharp edged, opaque cloud moving at 13 m/s (40 ft/s)
Maximum Wind Speed (for determination of receiver performance)	3.5 m/s (8 mph) at reference height of 10 m (33 ft.)
Temperature	Wet bulb 22C (74F) Dry Bulb 28C (82.6F)
Operating Temperature Range	-30C to 50C (-20F to 120F)
Earthquake	0.1g (ground response)
Survival	
Max. Wind Speed	40 m/s (90 mph)
Snow Load	240 Pa (5 psf)
Ice Layer	50 mm (2 inch) thick
Earthquake	0.25g (ground response)
Hail Diameter	25 mm (1 inch) Specific Gravity 0.9 Terminal Velocity 23 m/s (75 fps)

The receiver subsystem interfaces with other subsystems in the solar plant. The most important interface is with the heliostat field. While the heat flux in the receiver is defined by the receiver designer, some trial and error with the layout of the heliostat field is required to meet the receiver requirements. For the purposes of receiver design (after establishing actual heat fluxes) the interface is defined at the receiver aperture plane. The receiver subsystem interfaces with the thermal storage system at a point in the riser and downcomer pipes immediately outside the tower. The receiver controls interface with the plant master control subsystem. The receiver also requires electrical supply to the pumps, trace heating, lighting, etc.

A detailed description of the receiver subsystem is given in the following paragraphs covering the heliostat field, tower, cavity arrangement, flow circuits, heat absorption panels, materials, piping and tanks, steel structure, design verification, operation and control.

Heliostat Field - The receiver is situated near the south end of an almost circular field of heliostats (Figure 2) with the four cavities facing N, S, E, W as shown. A total of 10,500 Martin Marietta second generation heliostats was determined to provide the design power rating.

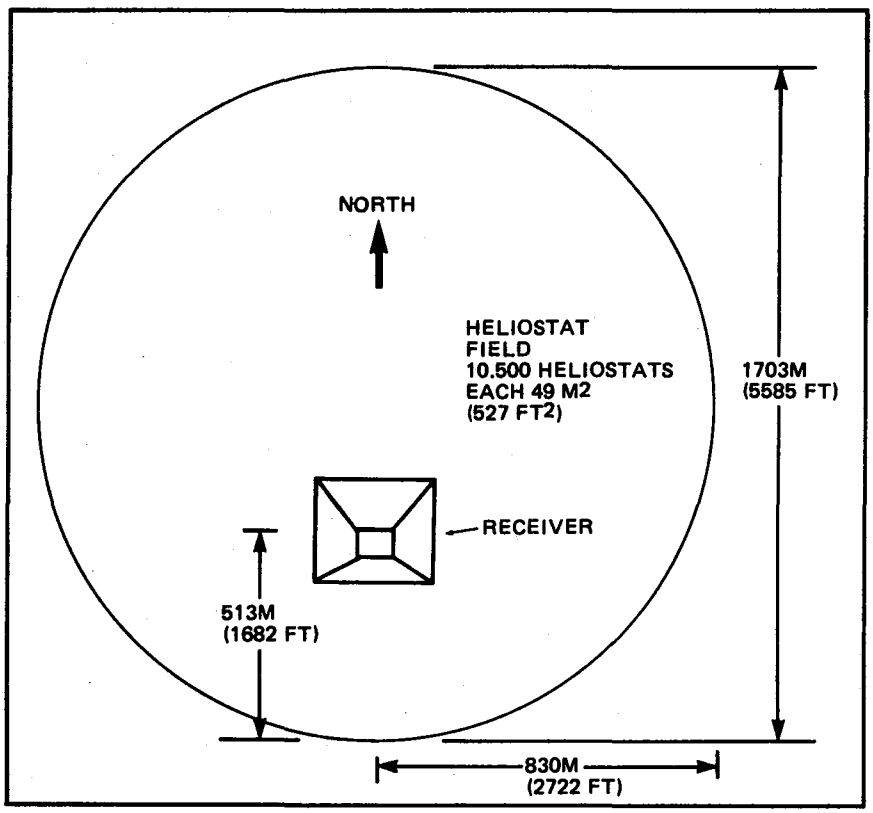

FIGURE 2 POSITION OF RECEIVER RELATIVE TO FIELD

Tower - To allow aiming of the heliostats onto the heat absorption panels within the cavity, the receiver is elevated by a tapered cylindrical, reinforced concrete tower. The tower is 508 ft. (155 m) high, with a top diameter of 60 ft. (18.3 m) and a base diameter of 80 ft. (24.4 m). The receiver is 106 ft. (32.3 m) x 105 ft. (32 m), 150 ft. (45.4 m) high, with a total weight resting on the tower of 2600 tons (2.36×10^6 Kg) (Figure 3).

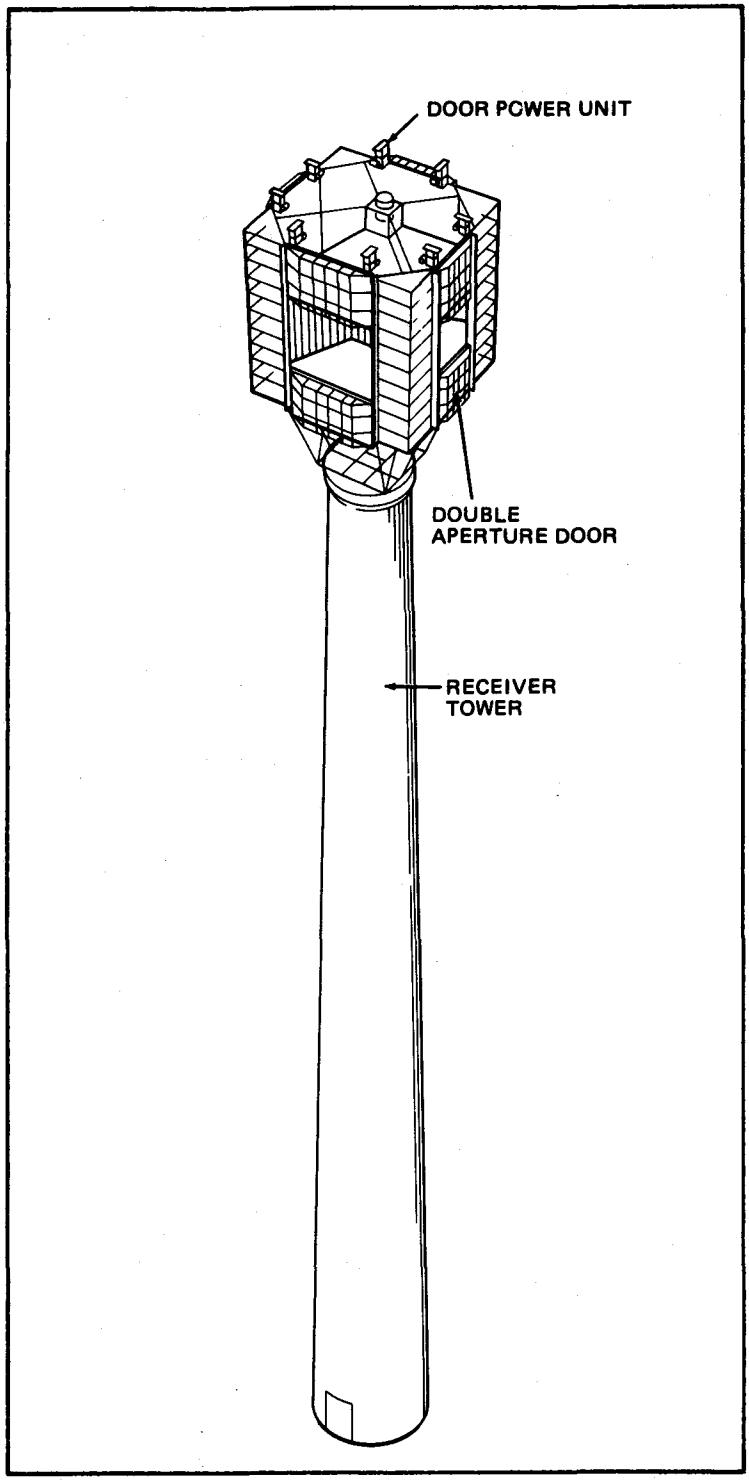

FIGURE 3 RECEIVER AND TOWER

Cavity Zones - The cavity zone arrangement is as shown in Figure 4. In the plan view shown, each of the four cavities is bounded by heat absorption panels, the aperture, and the casing which connects the panels to the aperture perimeter to form a sealed cavity. The heliostats beam the concentrated insolation through the square apertures to the heat absorption panels. Heat flux distribution on the panels is established by a distribution of aim points in the aperture plane. These aim points are located by groups of heliostats and thereby spread out the heat flux to optimize the use of the heat absorption panels.

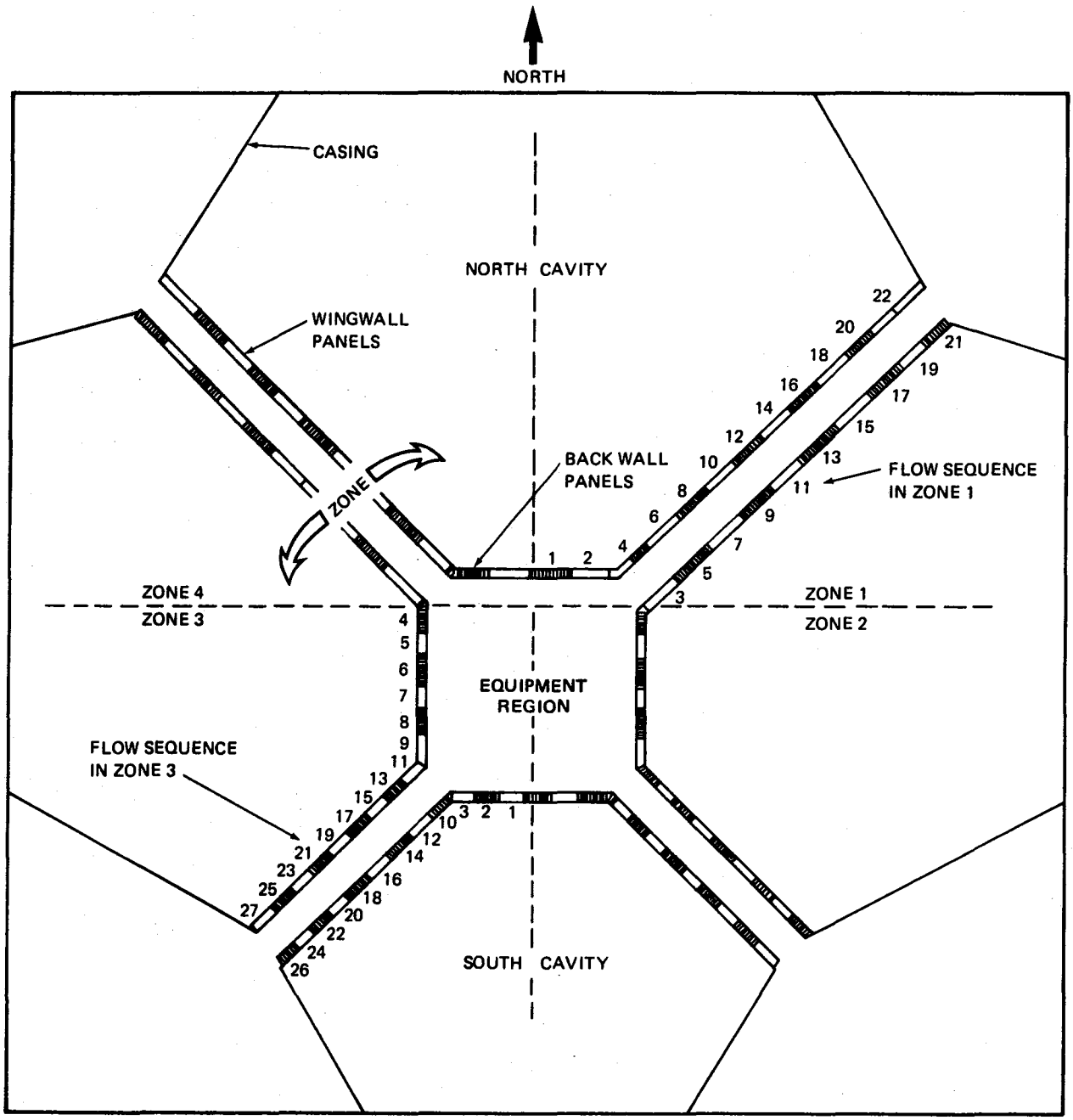

FIGURE 4 CAVITY ZONE ARRANGEMENT

The heat absorption panels are laid out in a 'X' shape to make maximum use of the heat transfer surface. A square area is left open near the center to accommodate structural supports, tanks, piping, and other equipment. The depth, height and width of the cavity were derived from earlier studies (Refs. 1, 2) and are based on considerations of optimal use of structural steel and thermal efficiency considerations.

There are four control zones in the receiver as defined by the dotted lines in Figure 4. Each zone operates as an independent flow circuit with cold salt entering each circuit at 550F (290C) and exiting at 1050F (565C). In each zone the flow passes from the back of the cavity to the outer corner. Typical flow paths are indicated where the individual heat absorption panels are numbered 1 through 22 in Zone 1 and 1 through 27 in Zone 3.

Basically, the cold salt is designed to enter at the center region where heat fluxes are high and flows to the outside where heat fluxes are lower. This flow arrangement prevents overheating in the regions where heat fluxes are high. The numbering of the panels also shows the path of the salt in crossing from one wing wall to the adjacent wing wall. This criss-crossing ensures the presence of cold salt in the high heat flux areas of both cavities and also helps to even out the effect of cloud transients which may effect one cavity more than the adjacent one.

Flow Circuit - The salt flow circuit is shown in Figure 5. Cold salt is pumped to the surge/buffer tank via the riser pipe by the main booster pumps located in the tower base. The surge buffer tank has a controlled salt level with an air cover gas to provide

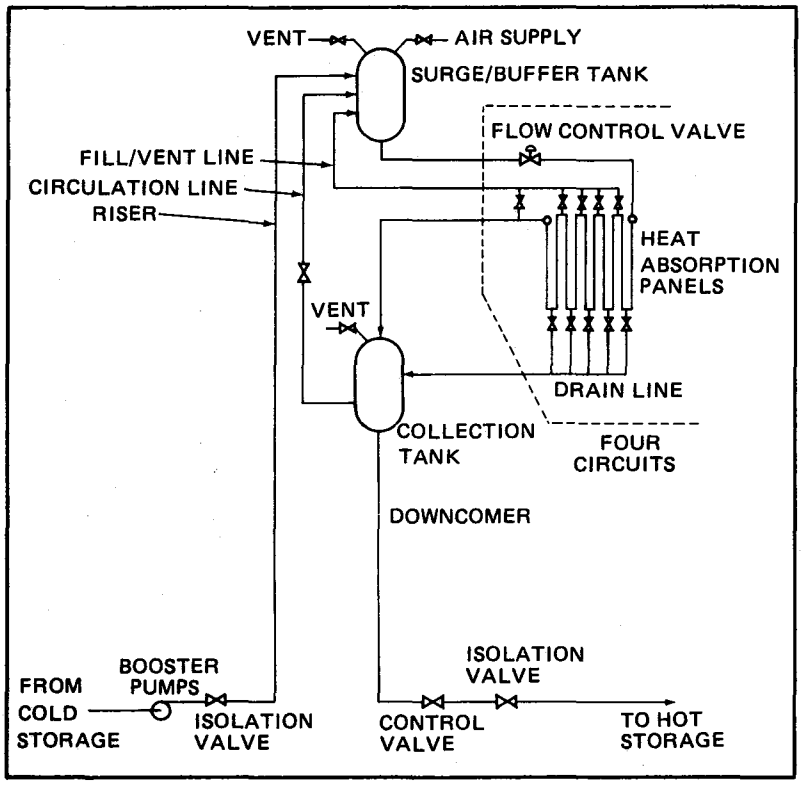

FIGURE 5 SALT PRESSURE BOUNDARY SCHEMATIC

isolation from pressure surges. From the surge/buffer tank the salt flows through the heat absorption panels to the collection tank. Within the heat absorption panels of each zone, the salt is heated from 550F (290C) to 1050F (565C). As indicated, the salt flows down in some panels and up in the adjacent panels. Each circuit or zone is controlled independently to maintain required flow rates and salt temperatures, and each flows into the collector tank where the salt streams are mixed. From the collection tank the salt flows down twin downcomer pipes to the hot storage tank located at ground level. The salt level in the collection tank is regulated by the control valves in the downcomer lines to ensure the required flow rate.

General Arrangement - The arrangement of components within the receiver is shown on the artists' sketch (Figure 6). The major features requiring amplification are the cavity layout, panel arrangement, wing wall features, central box region, tank locations, support structure, and doors. Table 3 gives general design data on the receiver subsystem.

TABLE 3 - GENERAL DESIGN DATA

Receiver Outer Dimensions	
Height	45.7 m (150 ft.)
Width E/W	32.3 m (106 ft.)
Depth N/S	32.0 m (105 ft.)
Total Receiver Wet Weight	2.36 X 10^6 Kg (2600 tons)
Tower Data	
Type	Reinforced Concrete
Height	155 m (508 ft.)
Base Dia.	24.4 m (80 ft.)
Top Dia.	18.3 m (60 ft.)
Number of Heat Absorption Panels	98
Active Panel Heat Absorption Area	2080 m^2 (22,400 $ft.^2$)
Receiver Thermal Efficiency	91%
Max. Incident Heat Flux on Panels	0.5 MW/m^2 (157,000 $Btu/Hr\text{-}Ft^2$)
Pressure Drop Through Receiver	2.8 MPa (400 psi)

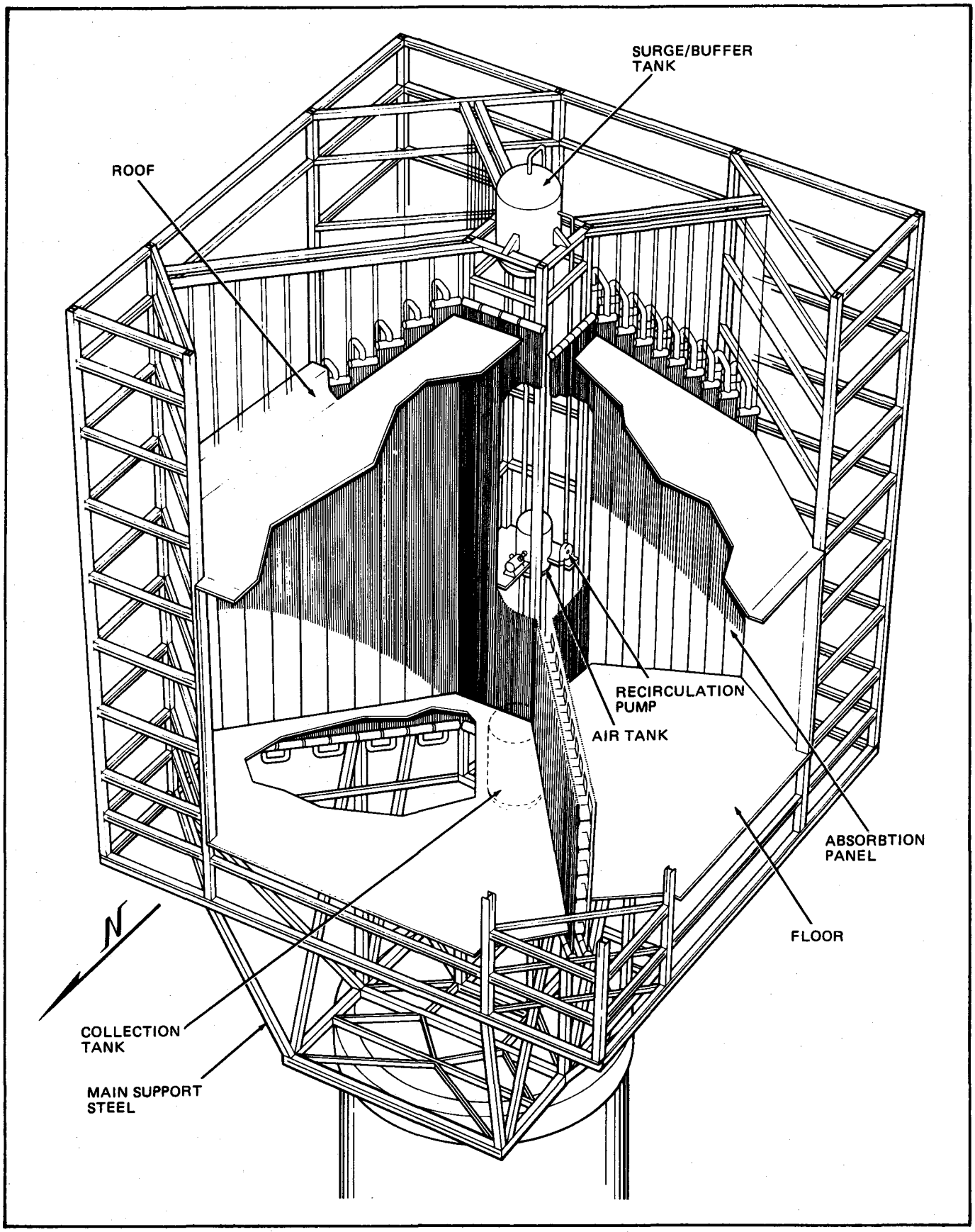

FIGURE 6 GENERAL ARRANGEMENT

As shown previously in Figure 4, each cavity is independently defined by several parts. Each cavity is bounded by panels, roof, floor, and casing which connects them to the aperture perimeter. Insulation is placed behind the panels, on top of the roof, under the floor, and behind the casing to insulate each cavity independently.

An insulated split door is located at each aperture and, when closed, is sealed at the junctures with the roof, floor, and casing to retain cavity heat. The split door enables one-half of the door to be used as a counter weight for the other half minimizing the power needed to operate the doors.

The panels are top supported by hangers from structural steel which runs directly above the line of each wing wall. The panels are supported by structural members and are allowed to expand in the horizontal and vertical downward directions. Those panels near the central box are the largest with decreasing panel lengths towards the outer corners of the receiver. Figure 7 shows the panels forming the double wing walls and highlights the panel insulation, steel supports, and interconnecting piping between walls.

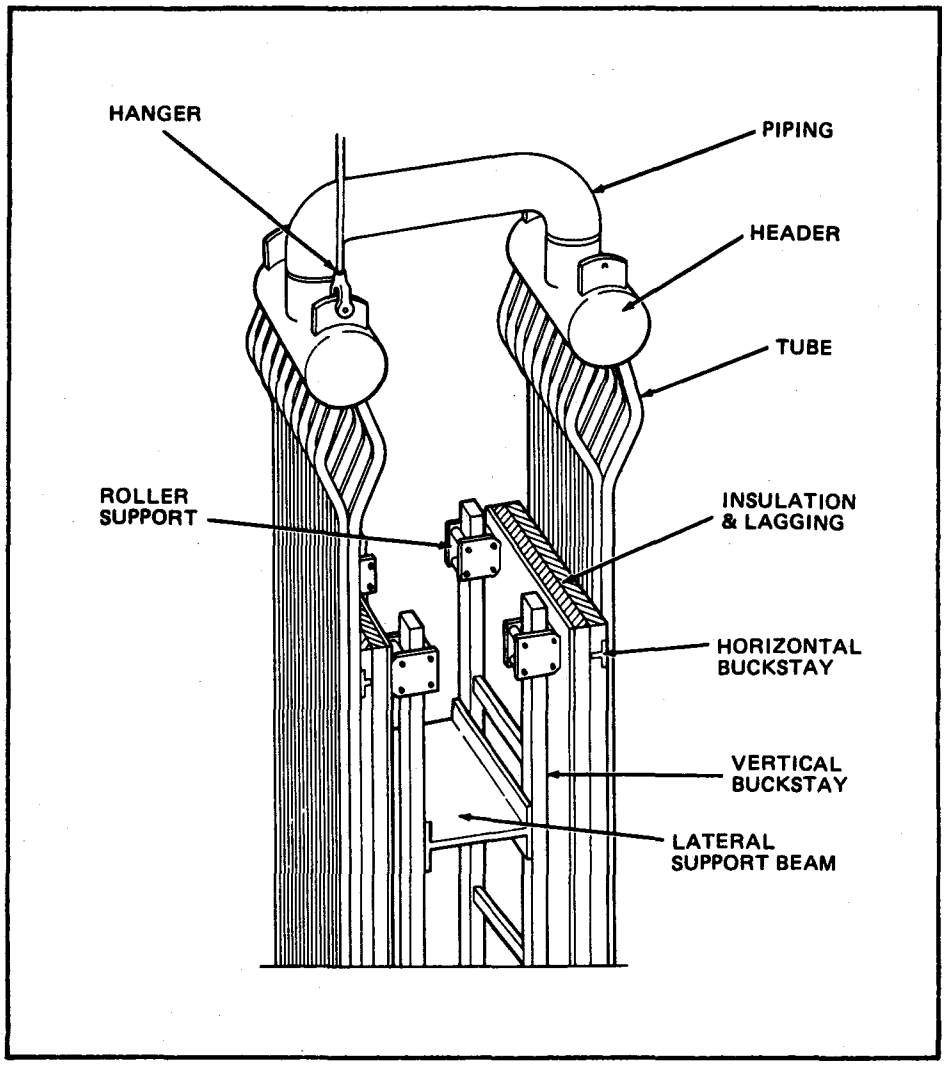

FIGURE 7 DOUBLE WING WALL

The central box region houses the surge/buffer tank at the top, the collection tank at the bottom, and, in between, the air tank to supply compressed air to the surge/buffer tank for emergency operation.

The receiver structure consists of standard wide-flange steel members arranged as a space truss that effectively surrounds each cavity and provides adequate support to the heat absorption panels, tanks, piping and other components. Loads on the receiver such as dead weight, seismic winds and others are transferred to a reinforced ring section at the top of the tower.

Heat Absorption Panels - The panels are comprised of a number of tubes welded together to form a membrane wall with a header at each end of the panel (Figure 8). Molten salt enters the header via a nozzle located at the center of the header, flows through the tubes and exits via a similar header at the opposite end. The tubes are 2" O.D. (50.8 mm) X 0.065 inch (1.65 mm) wall, made of Alloy 800H material. In the region of the panel where heat is absorbed, the tubes form a continuous membrane. A membrane wall was chosen to provide panel integrity, a light tight barrier and weathering protection for the insulation. Outside of the membrane wall region, the tubes are bent out of plane (safe ends) to provide flexibility to reduce stresses on the safe end to header weld connection. Panel materials are listed in Table 4.

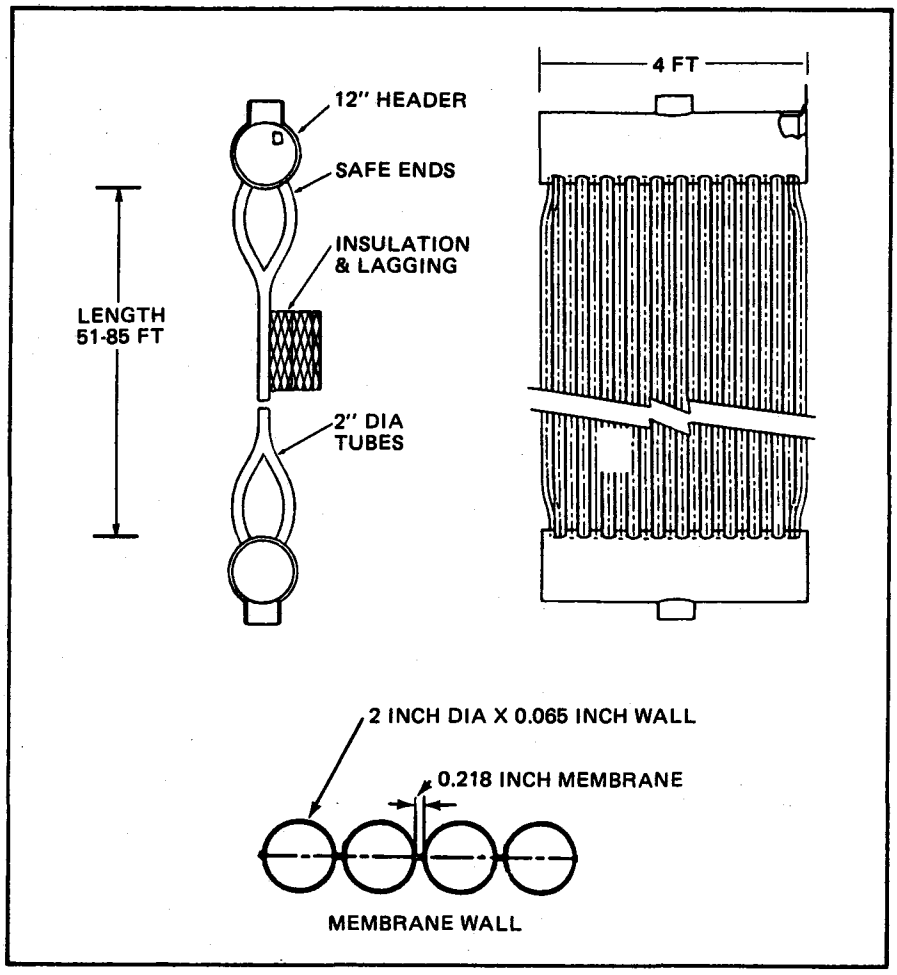

FIGURE 8 PANEL DESIGN

TABLE 4 - COMPONENT MATERIALS

Heat Absorption Panels	
Tubes	Alloy 800H
Safe Ends to Headers	304 SS
Headers	304 SS
Panel Buckstays (T)	304 SS
Vertical Buckstays	CS-SA 36
Piping	
Riser	CS-SA 106 GrC
Downcomer	304 SS
Panel Interconnecting Piping	304 SS
Tanks	
Surge/Buffer	CS-SA 515 Gr70
Collection	304 SS
Structural Steel	CS-SA 36
Panel Insulation	2" Med. Temp. Block 4" Int. Temp. Block 2" Kaowool K3000 (at gaps)

Panel sizes have been optimized for each zone. Because the south zones (2 and 3) have lower total energy input, the panel dimensions which best satisfy the energy requirements, heat flux inputs, and tube thermal stress requirements, are slightly different than those in the north zones (1 and 4). Table 5 shows the comparison of general dimensions of the panels.

TABLE 5 - ABSORPTION PANELS

	Zone 1 & 4	Zone 2 & 3
Number of Panels/Zone	22	27
Number of Tubes/Panel	22	15
Tube O.D. mm (in.)	50.8 (2.0)	50.8 (2.0)
Tube Wall Thickness mm (in.)	1.65 (0.065)	1.65 (0.065)
Length of Panel m (ft.)	26.0 (85.4) max.	26.0 (85.4) max.
(Header to Header)	19.4 (63.5) min.	15.7 (51.6) min.
Width mm (in.)	1220 (48)	813 (32)
Panel Dry Wt. (Avg) - Kg (lb)	1450 (3200)	977 (2150)

The panels are designed to be shop fabricated and shipped as an assembly complete with headers, insulation, and structural supports (Figure 9). The tubes forming the panel are restrained by horizontal Tee buckstays which are welded to pads on the tubes. These Tee buckstays are welded to the roller supports which allow the panel to expand vertically downward when heated. The assembly is also designed to allow expansion in the plane of the panel face. Insulation is attached to the panel by impaling the blocks on studs welded to pads on the tubes. Lagging is located at the back of the insulation and held in place by studs attached to the panel. The panel with insulation and lagging is attached to a structural support truss at the factory, and the motion of the rollers checked out before shipping. In the field, the gaps between the panels are covered by insulation and lagging such that the cavity has a continuous insulation/lagging boundary thereby minimizing conduction and convection heat losses. Design codes applicable to the panel assembly are listed in Table 6.

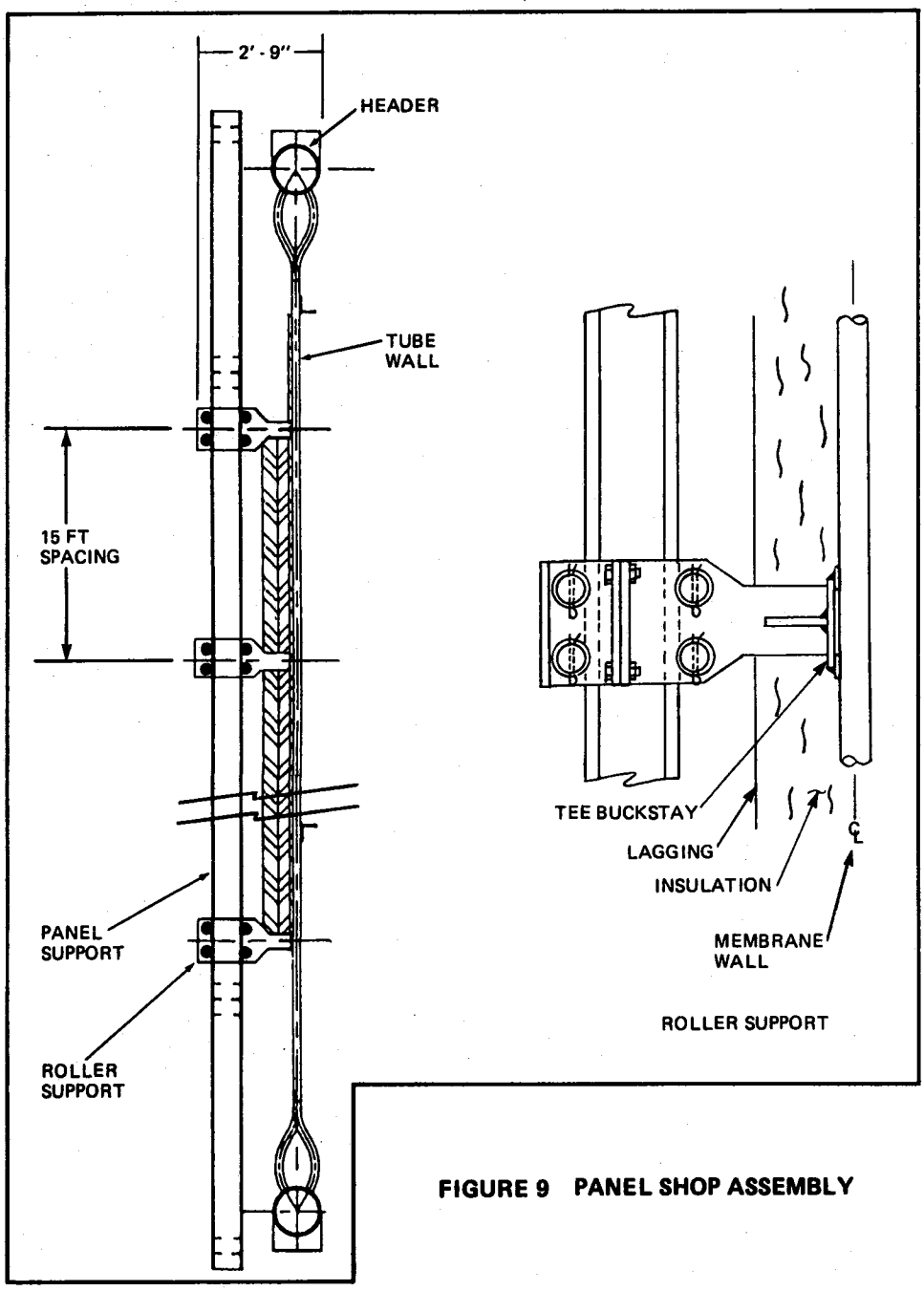

FIGURE 9 PANEL SHOP ASSEMBLY

TABLE 6 - CODES APPLICABLE TO PANELS

Tubes and Headers	Section I of the ASME Boiler and Pressure Vessel Code Power Piping Code, ANSI/ASME, B31.1
Remainder of Panel Assembly	Uniform Building Code American Institute of Steel Construction

Heat Fluxes - The panels have been designed to ensure successful operation for the life of the plant. Limits on heat fluxes were established based on thermal stress limits, creep-fatigue limits, and based on the maximum allowable metal temperature that will meet corrosion limits. Figure 10 shows the limits and the actual heat fluxes imposed on the panels in Zone 3. At the lower temperatures, the flux limit is established by maintaining thermal stresses in the elastic stress range. At the higher temperature the limit is established by maintaining the metal temperature at the inside of the tube under 1100F (593C). This temperature limit is based on the evaluation of corrosion data for alloy 800H in molten salt. The actual heat fluxes shown for the design point lie well below the limits in most regions thereby providing a healthy margin of safety. Detailed analysis of the panels has shown this margin to be necessary to accommodate uncertainties and the effects of skewed heating (fluxes not normal to the panel face). Based on detailed analysis and evaluation of the panel assembly, there is a high degree of confidence that the panels will perform successfully for the life of the plant.

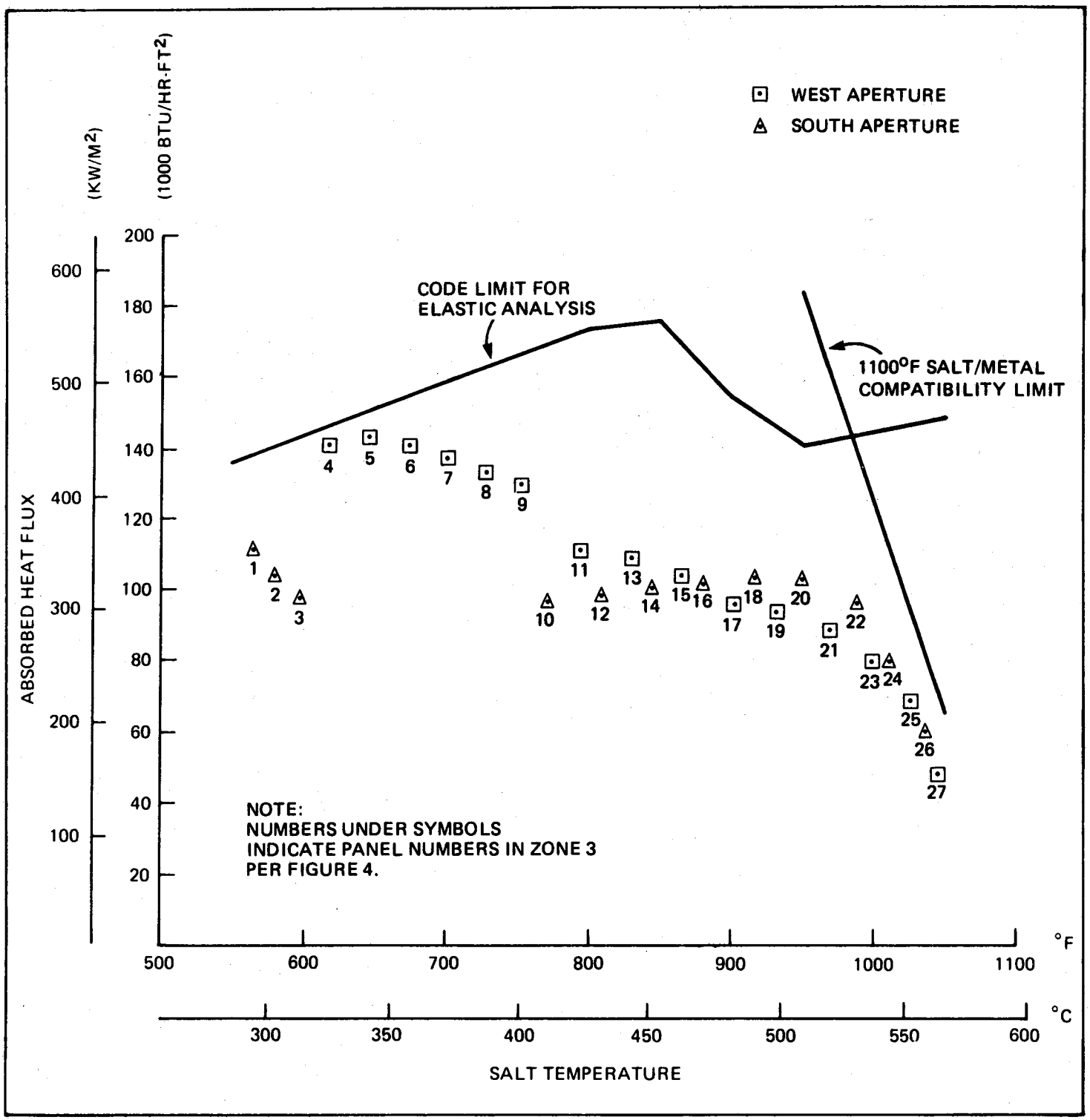

FIGURE 10 ZONE 3 PEAK FLUX AND LIMIT

Tanks - The major tanks in the system are the surge/buffer tank and the collection tank. The surge/buffer tank encloses an air space which dampens pump pressure surges. It also retains a salt inventory sufficient to buffer any difference that may exist under transient conditions between the salt needs for the panel and the flow supplied by the pumps.

The surge/buffer tank is sized to provide sufficient inventory to ensure continued flow in the panels during emergency conditions which may give rise to a loss of salt flow up the riser. A total flow, equivalent to two minutes of full flow, is available to cool the panels until the heliostat field can be de-focussed. To assure flow in the event of pump trips, the salt is forced through the panels by high pressure air from an air tank adjacent to the surge/buffer tank.

The collection tank is designed to collect flow from the four control zones. It also retains an inventory of hot salt to maintain temperature in the panels during overnight hold, in order to ensure quick start up in the morning. This is accomplished by pumping salt from the collection tank to the surge/buffer tank and back through the panels (Figure 5).

Piping - The major pipe sections are the riser and downcomer pipes and the panel interconnecting pipes. The 20 inch (508 mm) riser carries cold salt up the tower to the surge/buffer tank. Twin 14 inch (356 mm) downcomers carry the hot salt from the collection tank to the hot storage tank. Twin pipes are used for the downcomer to reduce the size of expansion bends within the concrete tower. The panels are connected by 10 inch (254 mm) diameter pipes. Materials for the cold pipes and tank are carbon steel; for the hot pipes and tank are 304 stainless steel. Table 4 gives a more detailed listing of the material selections.

Structural Steel - The structural steel provides support for the heat absorption panels, tanks, pipes, doors, maintenance platforms, elevator, and other miscellaneous items. It is designed to accommodate seismic loads, wind loads, platform loads, and dead loads, and transfer the loads to the concrete tower.

The main feature of the structure is a central support region which permits a large percentage of the receiver weight to be transferred directly to the concrete tower. Four triangular shaped corner regions support the remaining receiver weight and provide adequate stiffness to maintain lateral deflection within limits.

The five regions are interconnected by lateral supports which extend from the central box to the outer triangular regions. Loads on the wing wall panels are carried by these lateral supports, which run between the wing walls through to the five main support regions.

The structure was analyzed to ensure compliance with AISC, UBC, ANSI A58.1, and OSHA Codes. A finite element lumped mass dynamic analysis was performed on a model of the tower and receiver to assess the amplification of seismic effects at the receiver elevation. The results indicated that under the operational seismic load of 0.1g the load at the receiver would be 0.82g horizontal and 1.08g vertical.

A finite element analysis of the receiver structural steel was then performed with the seismic loads as inputs. In addition, the structure was analyzed for wind loads of 115 mph (55 psf) at the receiver elevation. Taking into account other dead loads and platform loads, the structural steel design was optimized for the loading conditions stated. Loading conditions and resultant steel weights are as indicated on Tables 7 and 8.

TABLE 7 - STRUCTURAL STEEL LOADS

Seismic	0.82 horizontal 1.08 vertical
Wind Load	1.44 KPa (30 psf) - ground 2.64 KPa (55 psf) - receiver
Platform Load	4.79 KPa (100 psf) with 407 M^2 (4370 ft^2) area.
Dead load	
Receiver Internals (wet)	
Panels & Buckstays	0.67×10^6 Kg (1.47×10^6 lbs)
Tanks	0.29×10^6 Kg (0.64×10^6 lbs)
Piping, Roof, Floor, Misc.	0.31×10^6 Kg (0.68×10^6 lbs)
Total Receiver Internals (wet)	1.26×10^6 Kg (2.79×10^6 lbs)
Doors/Frame/Mechanism	0.114×10^6 Kg (0.25×10^6 lbs)
Total Dead Load	1.38×10^6 Kg (3.04×10^6 lbs)

TABLE 8 - RECEIVER WEIGHT

Receiver Internals (wet)	1.26×10^6 Kg (2.79×10^6 lbs)
Doors	0.11×10^6 Kg (0.25×10^6 lbs)
Platforms	0.09×10^6 Kg (0.19×10^6 lbs)
Main Steel	0.91×10^6 Kg (1.99×10^6 lbs)
Total Dead Weight (wet)	2.37×10^6 Kg (5.22×10^6 lbs)

Doors - Each cavity has a two piece door over the aperture which can be closed during long hold periods to seal off the cavity and minimize heat losses to the environment. The door is divided horizontally with each half moving vertically up or down. Vertical motion of the door is preferred over horizontal motion because it exerts equal forces on the door tracks ensuring a more reliable operation. To save weight, the doors employ a space frame design fabricated from aluminum tubing. The inside surface of the doors is covered by 6 inches (15 mm) of insulation which in turn is covered by sheet steel to isolate the door structure from the cavity hot air.

Pumps - The main salt booster pumps, located at the base of the tower are two half capacity pumps each with a 2600 KW (3500 HP) variable speed motor.

Design Verification - Following the establishment of design requirements and design principles, the major features of the receiver were defined. To establish a design which meets requirements, thermal-hydraulic analysis was performed to optimize the heat transfer surfaces, cavity geometry etc., and Code type stress analysis was done. After the general features of the design were established, detailed analysis of the design was performed to verify performance, and to ensure that the entire receiver met the imposed thermal, deadweight, wind and seismic loads. A brief outline of the analysis performed is as follows:

- Thermal-hydraulic analysis was performed to verify performance, verify thermal efficiency, and provide boundary conditions for detailed stress analysis.
- ASME Code calculations for pressure boundary parts were completed.
- Thermal stresses in panels and panel/header junctions were analyzed to ensure the components met thermal stress limitations for steady state and transient conditions.
- Elevated temperature and fatigue analysis of critical areas in tubes was performed to ensure the panels met the lifetime operational requirements.
- Finite element analysis of steel structure and doors for wind and seismic effects was performed to minimize structural steel weight.
- Analysis of tower and receiver for seismic effects was performed to assess amplification at the receiver and achieve optimum design of tower and receiver.

Operation and Control - The operating procedures for the receiver subsystem are designed for safe, efficient collection of thermal energy. The plant control system supports these goals by providing automatic plant control, while also providing warnings and alarms for system failures. Operating procedures encompass two major divisions: normal operation and abnormal operation.

The control system sets the salt outlet temperatures within the system by modulating flow using control valves at the inlet to the heat absorption circuits. Control is accomplished with a quasi-feedforward algorithm using salt temperature measurements at the outlet of each panel to protect the system from cloud transient effects. Performance of the control system has been verified by computer simulation of the effect on the receiver subsystem of typical cloud transients.

Normal operations center around the diurnal cycle for the plant and are designed for maximum utilization of daylight hours for power collection. Important features of normal operation are:

- Automatic control to maintain salt outlet temperature within specified limits during varying load conditions and cloud transients.
- Automatic protection of the receiver panels from overheating which could occur following the passage of clouds across the collector field.
- Minimum of 25% full load flow rate at design salt outlet temperatures to ensure flow stability in all panels.
- Forced recirculation of salt within the tower with doors shut for hot standby and overnight hold.
- Gravity draining of salt for prolonged system shutdown.

Abnormal operations are the responses to a system failure of some type. Procedures for abnormal operation are designed to ensure safe operation with minimum impact on the system resulting from various failure modes. Important features of abnormal operation are:

- Emergency flow for a minimum of two minutes available from the surge/buffer tank supported by air pressure in the event of salt booster pump stoppage. This allows 2 minutes for the operation of emergency power systems to defocus the heliostats.
- Redundant instrumentation and voting circuits to assure reliable shutdown of the equipment during emergency events.
- Redundant flow control valves used in parallel, on panel circuits, to ensure flow in the panels in the event of valve blockage or inadvertent closure.

SRE DESIGN AND DEVELOPMENT PLAN

To support the development of a large scale commercial receiver subsystem, a Subsystem Research Experiment (SRE) was defined along with a complementary Development Plan identifying analytical studies and laboratory tests. Together the SRE and Development Plan will resolve uncertainties in the design and fabrication of the full size units, reduce design margins, simplify design features, and lead to lower cost units.

A two step SRE program is proposed. First, a 5 MW_t receiver is proposed for testing at the Central Receiver Test Facility in Albuquerque. Successful testing of the 5 MW_t unit will prove out some of the basic design features of the unit and develop acceptance of the design by the utilities. Second, a 30 MW_t receiver test is proposed at, as yet, an unidentified facility. The major advantage of the larger test unit is that it will test the full size panels. Since the panel and its support structure are generally considered to be the critical parts of the receiver component, testing under a wide variety of steady state and transient conditions would provide valuable data on performance, mechanical integrity, and the ability to accommodate thermal expansion. Test of a 30 MW_t size unit would greatly facilitate design extrapolation to larger sizes. The major benefits of a 30 MW_t test unit are listed as follows:

- Allows more accurate prediction of large commercial unit performance.
- Would prove out the control system applicable to the large units.
- Would demonstrate the integrity and reliability of door seals.
- Allows more accurate prediction of fabrication costs for the panels and the fabrication and erection costs of the structure.

The proposed Development Plan identifies analytical studies, and laboratory testing to support development of the commercial receivers. The development work is more in the nature of proof tests designed to lower the maintenance and capital costs of the components. No issues are identified which need resolution before building a large scale receiver. The major development areas are:

- Re-assessment of mechanical design limits on the heat absorption panels to determine if flux limitations can be increased with resulting reductions in receiver costs.
- Examination of innovative approaches to panel restraint to minimize complexity and reduce costs.
- Molten salt corrosion testing of alternate panel materials to ascertain the viability of lower cost materials.
- High flux insulating materials tests to examine the effects of accident conditions on the insulating materials.
- Salt properties verification tests.
- Reinforced concrete tower design studies to further examine the tower/receiver interface to minimize the number of parts and reduce costs.
- Dynamic response studies to optimize tower/receiver structure configuration.

PROCESS DEVELOPMENT

Conventional fabrication techniques were used wherever possible to fabricate the receiver subsystem. One area that required development was the tube to tube weld along the tube length to form the membrane wall. The concept of a membrane wall has been used for many years to fabricate boiler wall panels. For boilers, however, the membrane weld process is relatively straight forward. Since the panels are constructed with thick walled (0.140 inch - 3.6 mm), carbon steel tubes, a sub-arc weld process adequately produces the desired quality weld. Essentially this process is relatively straightforward since it does not demand close fit ups or a high degree of cleanliness to meet quality standards.

By contrast, the membrane weld process for the receiver panels is somewhat more difficult since it uses thin wall, Alloy 800H tubes (0.65 inch - 1.65 mm thick). The relatively thin walls require much more care than boiler tubes during the weld process to prevent burn through. Also, the weld process for Alloy 800 needs to be conducted with a higher degree of cleanliness than is necessary for carbon steel.

Two methods of producing the membrane wall panel were pursued. One, to use weld deposits along the entire tube length to form the membrane; the other to develop a drawn tube with an integral fin. The results of the two approaches are shown in Figures 11a and 11b.

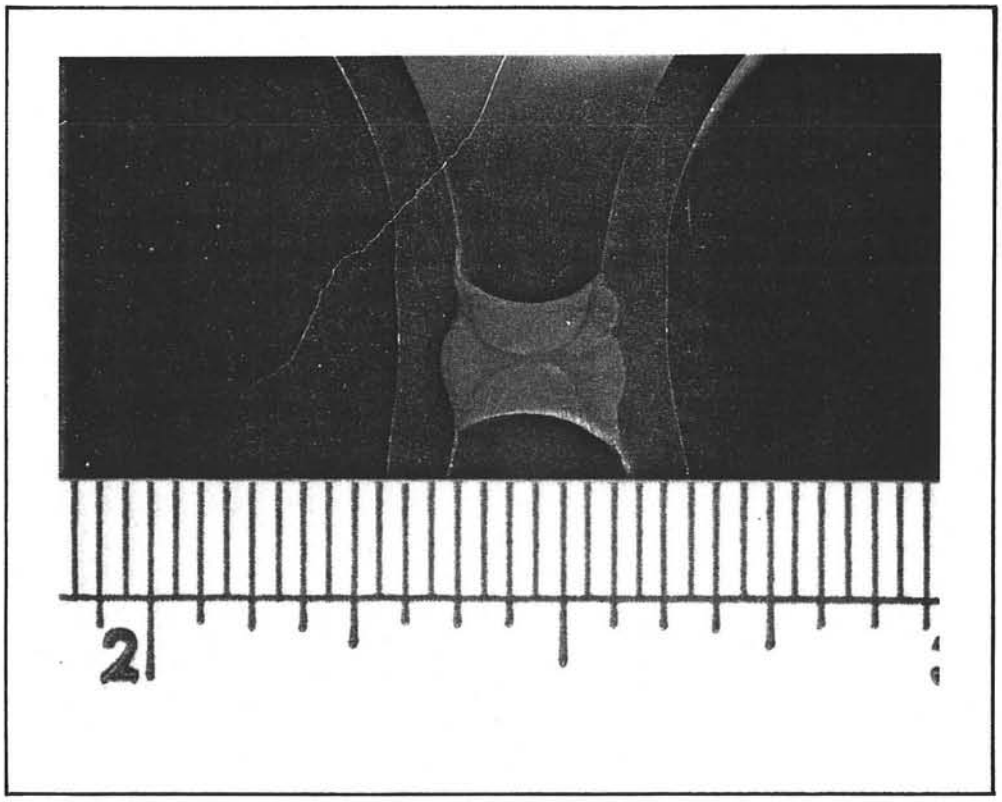

FIGURE 11a
TUBE TO TUBE MEMBRANE WELD

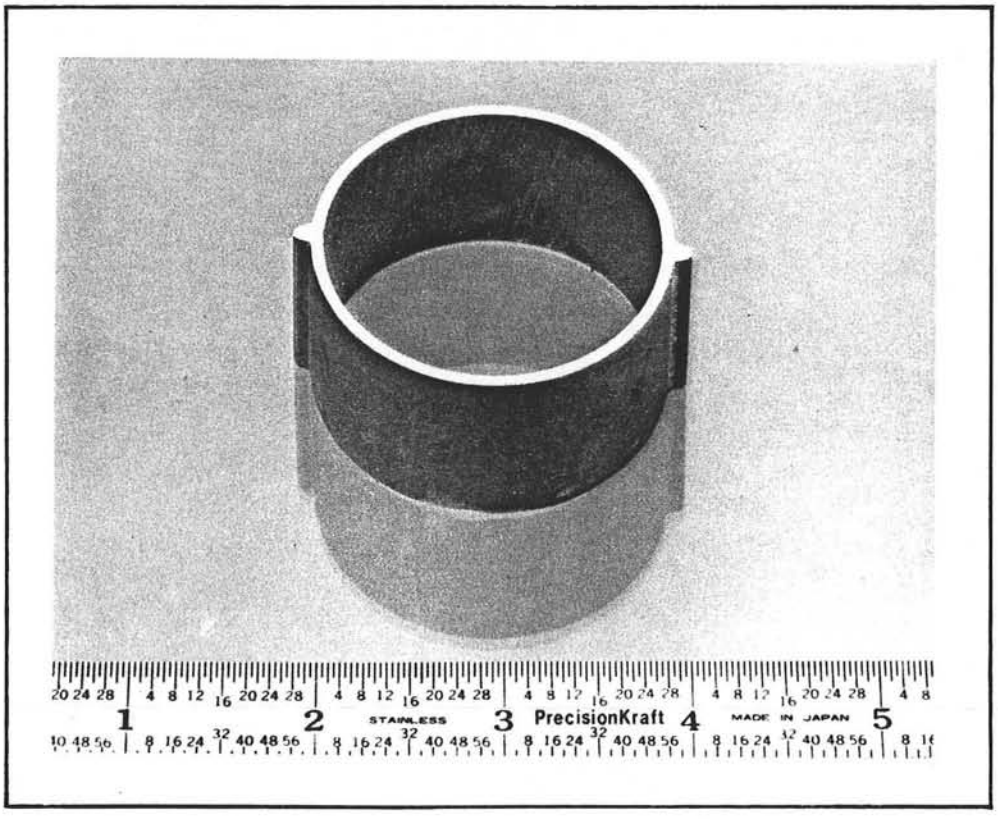

FIGURE 11b
DRAWN TUBE WITH INTEGRAL FIN

In the weld deposit method, two weld passes (one on top of the other) are laid on the tube outside at one location and another two weld passes are laid down on the outside diametrically opposite the first two. A MIG process was used with water cooling inside the tube to control the penetration depth of the weld and to control the weld contour. Tubes with these external fins can then be laid fin-to-fin and the fins welded together using a TIG process to form the membrane panel.

An alternate approach was to develop a cold drawn tube with an integral fin. Again, the fins were fused together using a TIG process to form the membrane panel. Both approaches resulted in welds with contours which blend in well with the tube profile offering very low stress concentration factors. Metallographic examination and tensile tests of mock ups verified the integrity of the attachments. Both approaches to the fabrication process are acceptable, however, based on the limited data at present, the weld deposit method appears to be the more economic approach.

To demonstrate the fabrication process used to assemble the membrane panel, the safe ends and connection to the header, a 10 foot (3.05 M) long mock up was fabricated. The mock up used 8 Alloy 800H tubes, with 304 stainless steel safe ends, and a 304 stainless steel header at one end (Figure 12). The attachment on the tubes was also demonstrated. The welds were inspected by visual and dye penetrant methods. The entire assembly was successfully hydrotested.

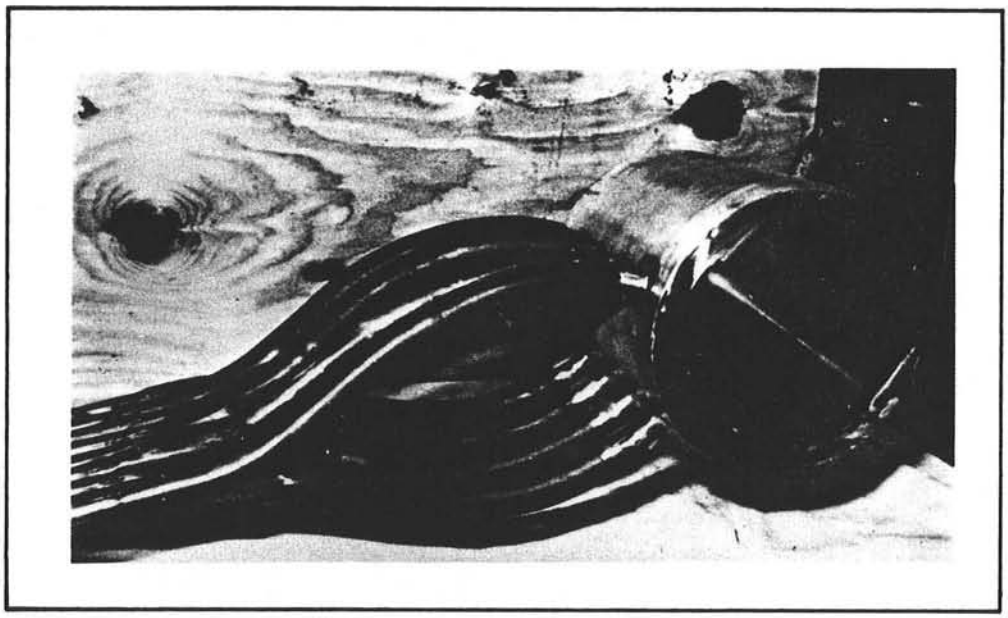

FIGURE 12

The completion of the 8 tube panel showed that the development of the basic fabrication processes, which are applicable to large size panels, have been successfully demonstrated. Remaining development efforts only need to concentrate on methods to utilize the same fabrication processes to produce large numbers of full size panels at low cost.

COST AND SCHEDULE ESTIMATE

Plans, schedules, and cost estimates were developed for shop fabrication and field erection of the full scale receiver subsystem. The proposed construction methods are based on conventional techniques and those developed as part of this contract. An integrated design, shop fabrication, and field erection schedule for the subsystem is shown in Figure 13. A cost estimate for this work is presented in Table 9. This estimate is based on standards data, actual cost data from previous contracts, vendor quotations, and catalog prices. Costs are expressed in current dollars (November 1982).

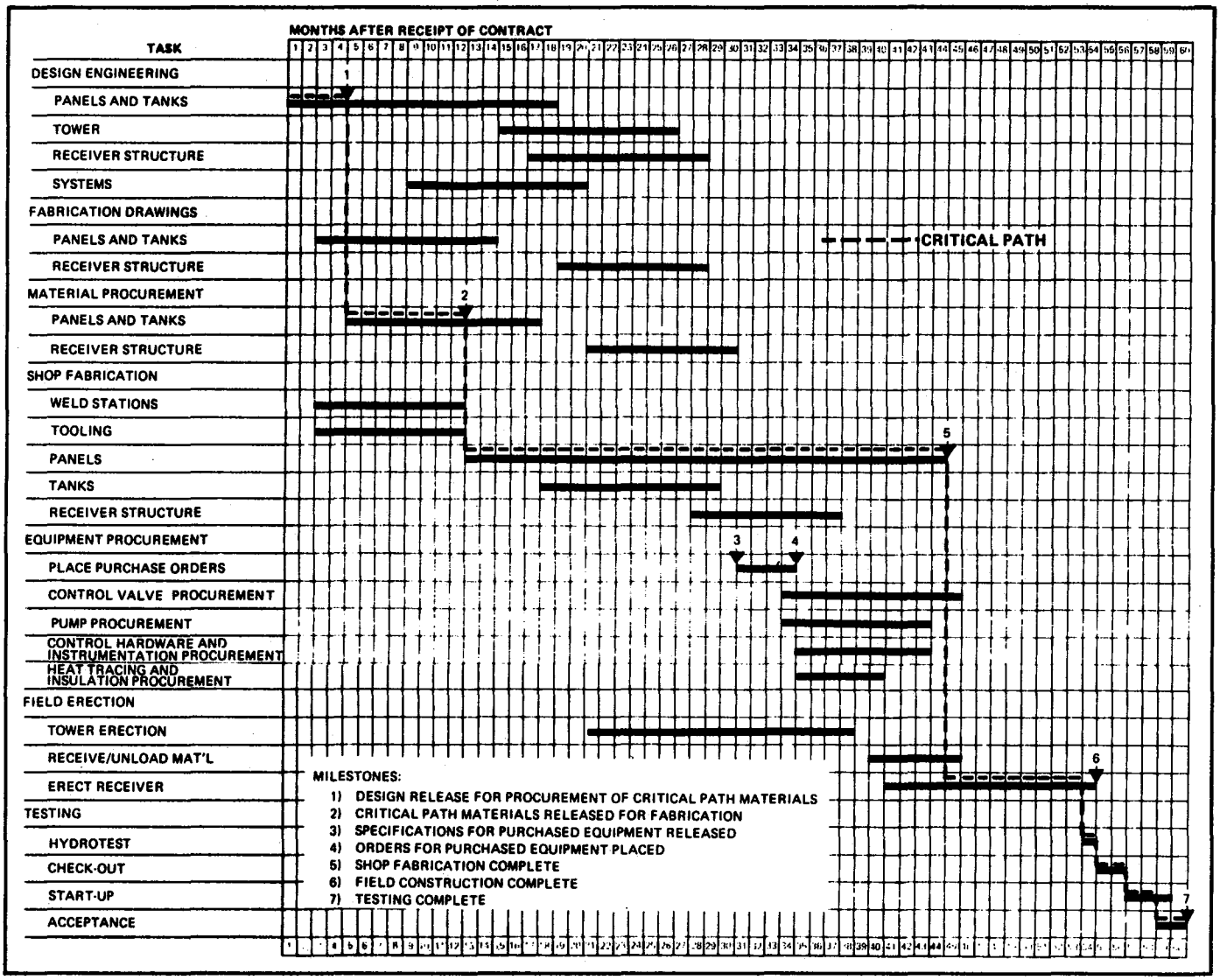

FIGURE 13 DESIGN, FABRICATION AND FIELD ERECTION SCHEDULE

TABLE 9 - COST ESTIMATE FOR RECEIVER SUBSYSTEM
(In Thousands of Dollars)

Receiver		
o Engineering	1,943	
o Fabrication		
Panels and Insulation	17,054	
Surge/buffer Tank	455	
Collection Tank	578	
Structural	5,415	
Procured Equipment[1]	4,824	
o Erection	23,752	
Subtotal		54,021
Tower		
o Foundation and Erection	3,932	
o Electrical Equipment[2]	2,247	
o Accessories[3]	985	
o Procured Equipment	3,898	
Subtotal		11,062
Systems		
o Engineering	625	
o Testing	709	
Subtotal		1,334
Indirect Costs[4] (15% on all Items Except Receiver and Systems Engineering)		9,577
TOTAL		72,994

NOTES:

1. Includes pumps, valves, piping, compressor, air tank, trace heating, door motor and mechanism, instrumentation, and controls.
2. Includes all electrical equipment except lighting, communications, and lighting protection.
3. Includes stairs, elevator, lighting, communications, lighting protection, ventilation equipment, and painting.
4. Indirect costs cover field costs, field engineering, procurement, and construction management.

REFERENCES

1. Conceptual Design of Advanced Central Receiver Power system, EG-77-C-03-1724, Martin Marietta Aerospace, Denver, CO, September, 1978.

2. "Saguaro Power Plant Solar Repowering Project," Final Report, Executive Summary and Vols. I, II, & III, DOE/SF10739-1, 2, 3, & 4, Arizona Public Service Company, Phoenix, AZ, July 1980.

3. "Advanced Conceptual Design for Solar Repowering of the Saguaro Power Plant," DOE/SF 11570 - 1, 2, & 3, Arizona Public Service Company, Phoenix, AZ, April, 1982.

CONCLUSION

The preliminary design effort has established that current technology will successfully support the design, fabrication, and operation of large scale solar thermal receivers. It is projected that a large receiver subsystem (320 MWt) can be operable 5 years after award of contract at a total cost of approximately $76M. It is recommended that research and development efforts be continued with emphasis on sub-scale component tests with the objective of a) proof testing critical components and demonstrating technical feasibility to potential users, and b) refining designs to lower capital and maintenance costs.

1.0 INTRODUCTION

1.1 Objectives of Study

This report describes the results of a study headed by the Babcock & Wilcox Company, under contract to Sandia National Laboratories (SNLL), to develop receiver subsystem and component designs for large solar thermal central receiver stand-alone or repowering applications using molten nitrate salt as the heat transfer medium. The principal objectives of the program were:

a) To develop systems level requirements and specifications.

b) To evaluate receiver configurations and select the configuration which optimizes the cost/performance of the combined receiver and collector subsystems.

c) To prepare development plans intended to resolve all uncertainties associated with the design, fabrication, erection and operation of the full scale commercial receiver subsystem.

d) To prepare a cost effective design of a commercial receiver utilizing conventional design, shop fabrication, and field erection practices.

e) To prepare shop fabrication and field erection plans, schedules, and cost estimates.

1.2 Technical Approach

During the course of the study, receiver subsystem and component specifications were developed; performance, structural, and control system analyses were completed; development needs were identified; and fabrication and erection plans, schedules, and cost estimates were prepared.

The work effort was organized into the following ten tasks:

Task 1 - Review of the Molten Salt Receiver Subsystem (RS) Specification

The RS specification from the SNLL Statement of Work was reviewed and recommendations were made.

Task 2 - Definition of RS Requirements

The existing literature on molten salt central receivers was reviewed and the requirements for the design, fabrication, operation, and maintenance were identified. The Receiver Subsystem Requirements Specifications document was prepared.

Task 3 - RS Concept Selection

A parametric evaluation of candidate receiver configurations was completed. The evaluation criteria included:

a) subsystem and component performance

b) structural integrity

c) capital and operating costs

d) maintainability

e) development needs

Based on this evaluation, a quad-cavity receiver was selected as the optimum configuration. A membrane wall panel construction with one-sided heating was selected for use as the heat absorption surface.

Task 4 - RS Design and Analysis

A Design Analysis Plan was prepared and detailed design of the subsystem and components selected during Task 3 was completed. The design effort addressed:

a) estimation of receiver efficiency

b) sizing and arrangement of the heat absorption surface area

c) physical arrangement of major components and associated piping

d) thermal/mechanical code analyses of structural and pressure boundary parts

e) selection of materials

f) control system design

Task 5 - RS Cost and Fabrication Plan

A "Shop Fabrication and Field Construction Plan" was prepared. This document included fabrication and erection plans, schedules, and cost estimates.

Task 6 - Receiver Fabrication Process Development

Welding methods were developed for the fabrication of the membrane panel. Particularly important development issues included:

a) tube-to-tube joining via membranes

b) tube-to-header joining using stainless steel safe-end

c) panel-to-lateral support connection

d) field repair of individual tubes

Following the development of the welding methods, a 10 foot long, 8 tube wide, panel was fabricated with a header attached to demonstrate the use of the various welding approaches.

Task 7 - RS Subsystem Research Experiment and Development Plan

Problem areas and uncertainties associated with the full sized receiver subsystem were identified and a program through which these uncertainties could be resolved was developed. The plan consisted of two parts.

a) SRE Design - a program of subscale modeling to demonstrate design adequacy and operational capability.

b) Development Plan - a program of analytical studies, and field and laboratory testing to resolve specific areas of uncertainty.

Task 8 - Phase II Plan and Proposal*

A proposal for Phase II was to be written based on the plan developed in Task 7 and the proposal outline provided in the RFP.

Task 9 - Reports and Data

Reports were prepared in accordance with SNLL requirements and to document significant accomplishments. In addition to monthly reports, the following documents were prepared.

a) Mid-term Report

b) Shop Fabrication and Field Construction Plan

c) Fabrication Process Development Plan

d) Receiver Subsystem Requirements and Specifications

e) Design Analysis Plan

f) Final Report

Task 10 - Program Management

The program was managed and controlled to assure satisfactory completion of all tasks in accordance with the program plan.

---

*This task was deleted from the contract.

1.3 Project Organization

The Babcock & Wilcox Company was supported in the completion of this study by Martin Marietta Aerospace, Black & Veatch Consulting Engineers, and the Arizona Public Service Company. The specific responsibilities of each team member are summarized in the following paragraphs.

Babcock & Wilcox

Babcock & Wilcox provided project management and coordination of subcontractors' activities. Other responsibilities included receiver concept selection and design, preparation of construction plans, schedules, and cost estimates, and the definition of development needs.

Martin Marietta

Martin Marietta designed the collector field and provided flux distribution input used for receiver surface sizing and arrangement. They also provided the control system design and instrumentation requirements, and prepared the Receiver Subsystem Requirements and Specifications Document.

Black & Veatch

Black & Veatch designed and prepared field erection plans and cost estimates for the tower and foundation; the piping, valves, and pumps; and, the insulation and trace heating.

Arizona Public Service

Arizona Public Service provided information on the operation and maintenance requirements of the receiver subsystem from a utility's viewpoint.

All of the subcontractors participated in the review and assessment of the receiver concept, design, and operation.

1.4 Design Evolution

Detailed design of the receiver subsystem components followed the approach outlined in the proposal and design analysis plan. As presented in both of these documents, the preferred receiver configuration is a quad cavity with four control zones.

The initial design used the single wing wall concept with heating on the wing walls from both sides and exposed lateral buckstays providing seismic and wind restraint for the panels. The exposed supports were cooled with screen tubes. The network of exposed buckstays, both horizontal and vertical, added greatly to the complexity of the design and introduced potential problems related to the thermal/mechanical behavior of the buckstay-to-panel connection.

At one stage of the design development, an analysis of the single wing wall design indicated that stress limits due to wind and seismic loads could be met with no lateral supports other than at the upper and lower headers. At this stage a concept was pursued where no external supports were added to the wing wall. However, the natural frequency of the panels was considered too low to ensure absence of wind induced vibration, and resulted in lateral supports again being considered for the wing walls. After re-evaluating the problems with exposed buckstays, namely, the general complexity, the potential problems with the buckstay to panel attachment, the complex temperature distribution of the buckstay arrangement, and the difficulty of replacing panels, it was decided to pursue a design using one sided heating on the panels with supports protected from the heat flux.

Since the concept of exposed buckstays had already been explored with negative results, it was decided that a "double wing wall" configuration would be used. This design placed the lateral supports between the wing walls of adjacent cavities and resulted in all of the absorption panels being heated from one side only.

Switching to the double wing wall design required that the wing wall absorption tubes be re-analyzed for one-sided heating. This new analysis generally confirmed conclusions drawn from the previous analyses of the single wing wall and back wall - that the peak flux levels were too high in some areas of the receiver. Lowering the peak heat fluxes then required additional panel surface. Rather than incurring additional costs in developing new flux maps by re-aiming the heliostats, it was decided to approximate the new fluxes by inspection and extrapolation of the initial flux maps.

The design changes and re-sizing resulted in the double wing wall configuration that is presented in the main body of this report. Detailed descriptions of the major component designs and analyses are included. Pertinent information on the analyses of the original single wing wall design is presented in the appendices. Section 8.0 includes a more detailed discussion of the design changes that were made and the conceptual trade studies that were performed to produce the final receiver configuration.

2.0 RECEIVER SUBSYSTEM DESIGN

The components and interface of the Receiver Subsystem (RS) are depicted in Figure 2.1. The major components of the subsystem are the quad-cavity receiver, tower, tower piping, main booster pumps, and controls. Major interfaces are with the collector subsystem, thermal storage subsystem piping, master control system, and electrical power systems.

2.1 General Description

An artist's sketch of the receiver and tower is shown in Figure 2.2. The quad-cavity receiver sits on top of a 155m (508.5 ft.) concrete tower. The cavity overall dimensions are 32m (105 ft.) x 32.9m (108 ft.) and 45.7m (149 ft.) high. Total wet weight of the receiver is 2.36×10^6 kg (2600 tons). The tower houses the main riser and downcomer piping, main booster pumps, and auxiliary equipment.

The major parts of the salt pressure boundary are shown in Figure 2.3. Incoming cold salt at 290C (554F) is pumped to the top of the tower by two high pressure booster pumps through a riser pipe. The incoming salt is collected in a surge tank and distributed to four heat absorption circuits where it is heated to 565C (1049F). The hot salt is collected in a collection tank and flows through two downcomer pipes to the bottom of the tower and into the hot storage tank. A control valve at the bottom of the downcomer is used to control the flow rate in the downcomer and as an energy dissipation device.

Insolation comes from a full 360° heliostat field that is biased to the north side of the receiver. The heliostat field is designed to supply sufficient power, with 950 W/M^2 insolation at solar noon on the summer solstice (designated as the design point), through the four apertures of the quad-cavity receiver to achieve 320 megawatts of absorbed thermal power. The key interface item is the heat flux distribution on the heat absorption panels. A complete set of heat flux distributions or maps, needed for design, have been supplied by the Martin Marietta Aerospace Corporation.

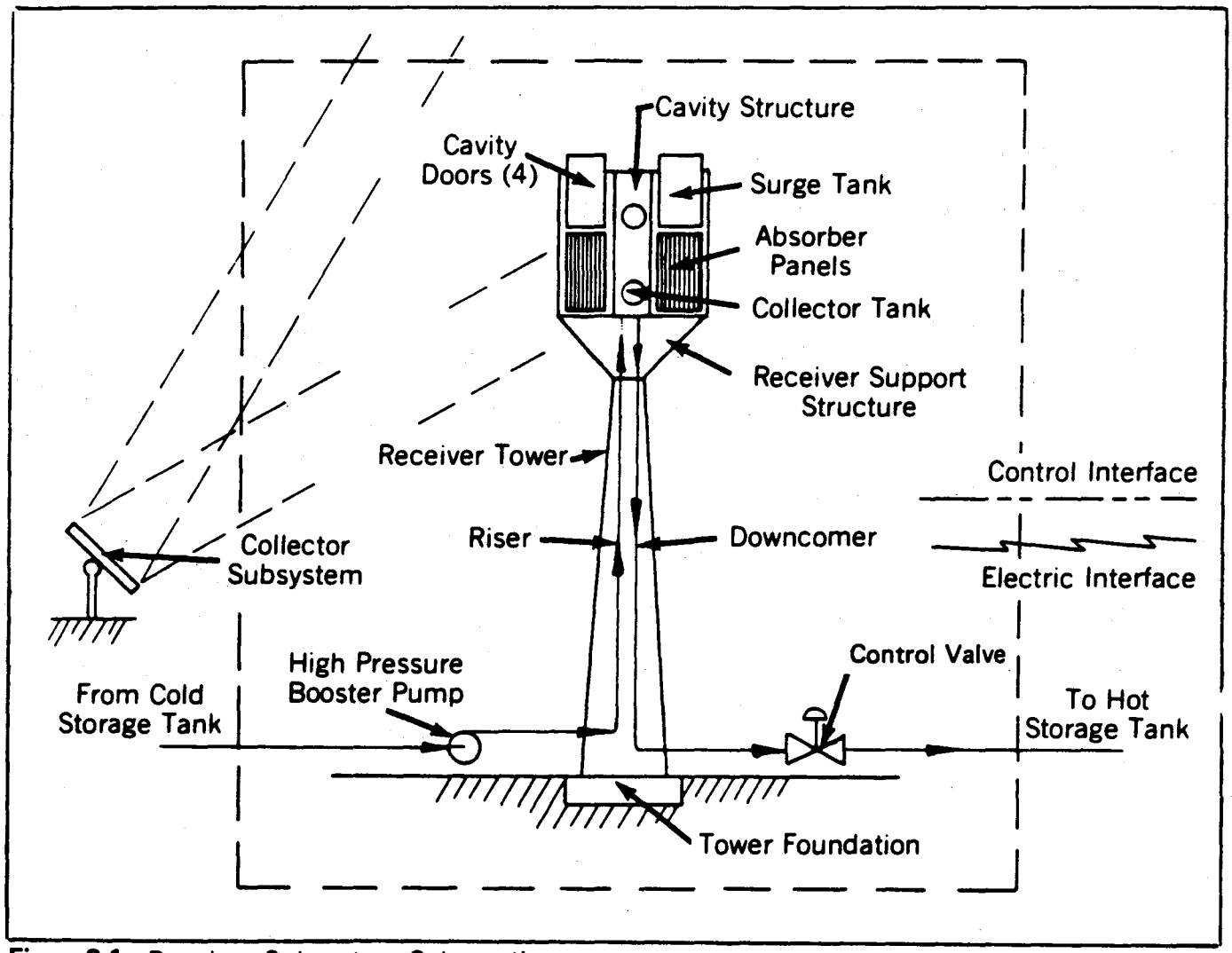

Figure 2.1 Receiver Subsystem Schematic

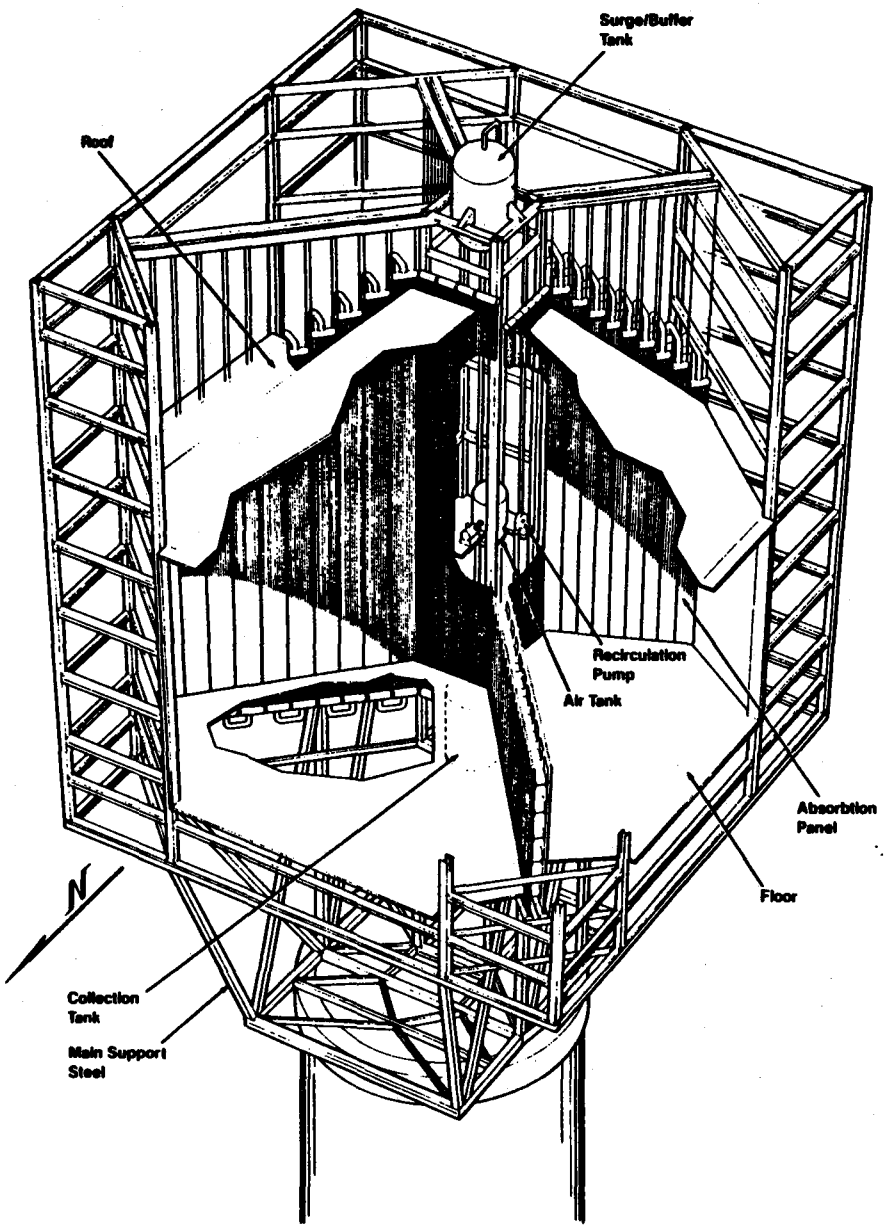

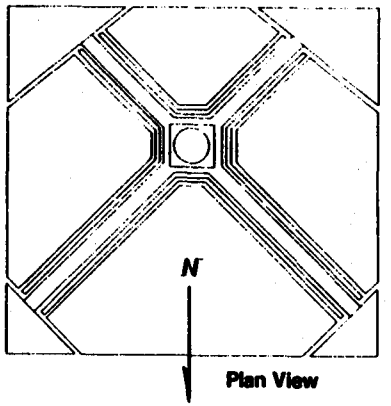

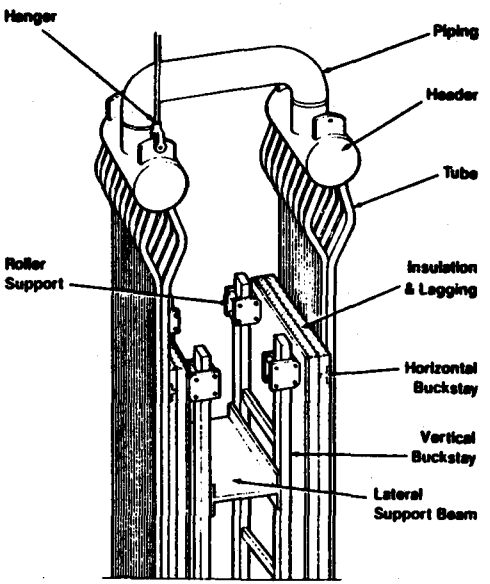

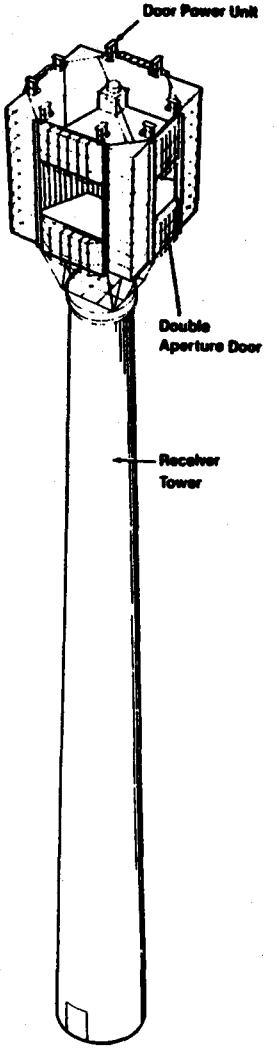

FIGURE 2.2

Quad-Cavity Molten Salt Receiver Subsystem

Babcock & Wilcox

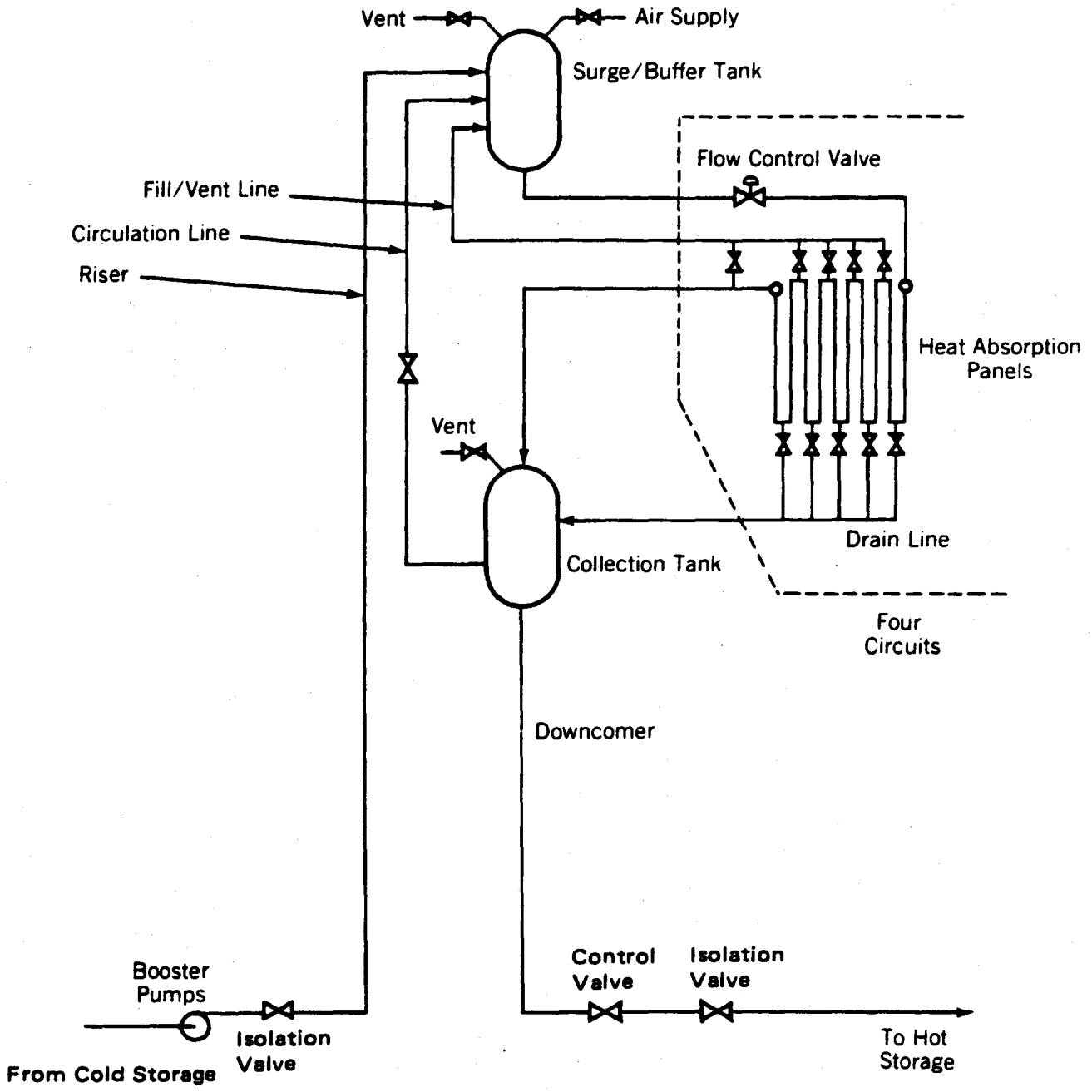

FIGURE 2.3 - SALT PRESSURE BOUNDARY SCHEMATIC

The heat flux distributions can be controlled by heliostat (or collector field) aim strategies. The interface requires B&W to evaluate the effect of a given distribution on the salt temperature profile through the heat absorption circuit and the tube metal temperatures in terms of stress and corrosion limits. Iteration is required to ensure that the actual fluxes are consistent with allowable stresses in the heat absorption panels.

The receiver cavity houses the heat absorption panels, salt tanks, roof, floor, control valves, and miscellaneous supports and hardware. The absorption panels are arranged to form a box at the center of the cavity with two parallel "wing" walls extending to each outside corner of the cavity. The absorption panels are formed from tubes welded together to form a membrane wall.

2.1.1 Panel Design

The layout of the heat absorption panels can be seen in the artist's sketch. The panels forming the center box are termed "back wall" panels; those extending to the outer corners of the cavity are termed "wing wall" panels. A major feature of the panel is the membrane wall construction. Figure 9.1 shows the general dimensions, number of tubes, and other details of the panels.

The panels are flat in the heat absorption areas with the tubes bent into inlet and outlet headers to provide flexibility for thermal expansion. Supports are welded to the back of panel to support insulation, retain rigidity, and resist wind and seismic loads.

2.1.2 Panel/Header Assembly Design

The panel/header assembly is shown in Figure 9.4. The assembly comprises tubes, headers, lateral supports, panel insulation, support

frame, and roller assembly (to allow expansion during operation). The complete assembly is shop fabricated and shipped to the site as shown. The pressure boundary design criteria is Section I of the ASME Boiler and Pressure Vessel Code.

The tube material is Alloy 800H, chosen for its excellent elevated temperature properties. The headers are 304 stainless steel. The bent tube between the panel Alloy 800H tube and the header is 304SS ensuring that the critical tube/header junction is made with similar materials. Structural support parts that operate at high temperatures (such as the panel lateral support) are 304SS. Other structural parts, such as the vertical buckstays are A36 carbon steel.

The arrangement of panels as installed in the cavity is shown in Figure 9.2. It shows the arrangement, the piping connecting the panels, and panel supports. Note that the wing wall panels decrease in length towards the outside of the cavity. The change in length is made to accommodate the heat flux pattern and save panel material.

As shown, the panels are hung from the top and allowed to expand downwards when heated. The supports are welded to the back of the panels to provide lateral restraint and to move downwards with the panels.

2.1.3 Tanks

The receiver subsystem contains three major tanks - surge/buffer tank, collection tank, and an air receiver tank. Figures' 9.5 and 9.6 show the the configuration of the surge/buffer tank and the collection tank. The air receiver tank is shown on Figure 2.4.

The surge tank's primary purpose is to receive salt from the thermal energy storage system and to distribute the molten salt to the various receiver zones. An air supply is furnished to the tank to permit

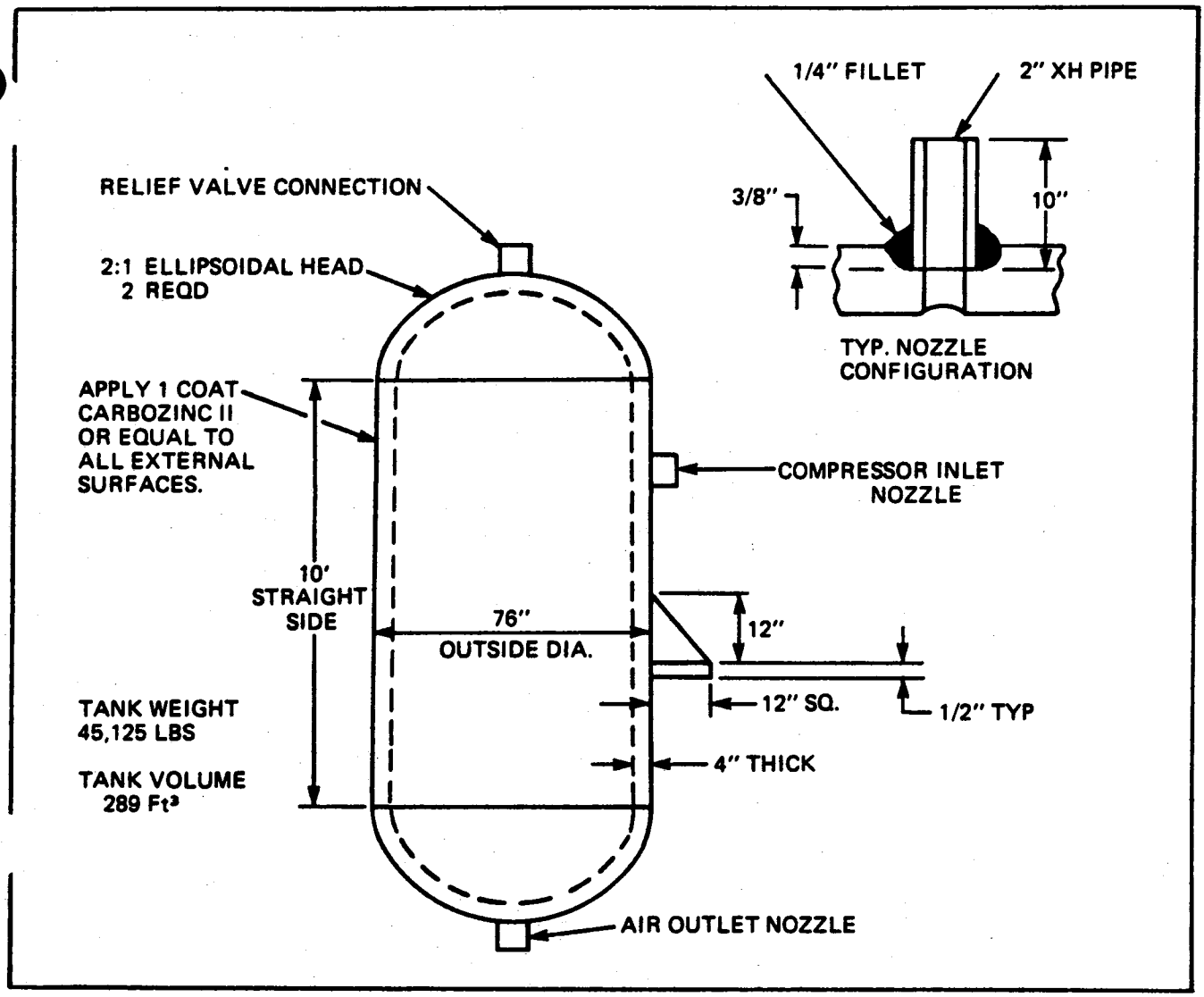

NOTES:
1. Tank to be designed, fabricated, and code stamped per ASME section VIII, Division 1, latest edition.
2. All main seams shall be RT inspected.
3. Design conditions - 1800 psi at 200°F.
4. Material - SA-515 Gr70 or equal - shell, head, & supports.
   - SA-106 GrB - Nozzles
5. Four support pads as shown on tank are required. The pads are to be attached to tank wall by use of 3/8" fillet welds all around.

FIGURE 2.4 - AIR RECEIVER TANK

continuation of the molten salt flow through the receiver during a pump or electrical failure. The collection tank receives the molten salt from the receiver and sends it to the hot storage tank. The collection tank serves as a fill tank and drain tank as well. An air tank and compressor provide compressed air to the surge tank during emergency shut-down conditions. The compressed air forces the salt out of the surge tank thereby maintaining flow in the panels. The design parameters are the pressure, temperature, volume, and mechanical loads. The design criteria is provided in Section VIII Division 1 of the ASME Boiler and Pressure Vessel Code. Material selection is based on availability, costs, manufacturability, and mechanical properties compatible with the design requirements. The tanks (excluding the air tank) are insulated with 8 inches of intermediate temperature block insulation and protected by aluminum lagging. Trace heating is installed on the surge and collection tanks in order to heat the tanks prior to filling with molten salt.

2.1.4 Cavity Design

The unit is designed to 320 MWth with 290C (554F) salt inlet temperature and 565C (1049F) salt outlet temperature. The heat absorption panels are designed as a once-through unit with four zones (circuits). Zones 1 and 4 are identical and zones 2 and 3 are identical as shown in Figure 2.5. Zone 1 receives insolation from the north and east fields and zone 2 from the south and east fields. Zone 1 has 22 heat absorption panels which are 1.23 meters (48.8") wide, Zone 2 has 27 panels which vary in width from 1.23 meters (48.8") to .8 meters (32"). The molten salt passes through the panels in a serpentine manner. The cavity is formed by the absorption panels, a roof, a floor and a casing type closure between the panels and the aperture door (see Figures 9.8,

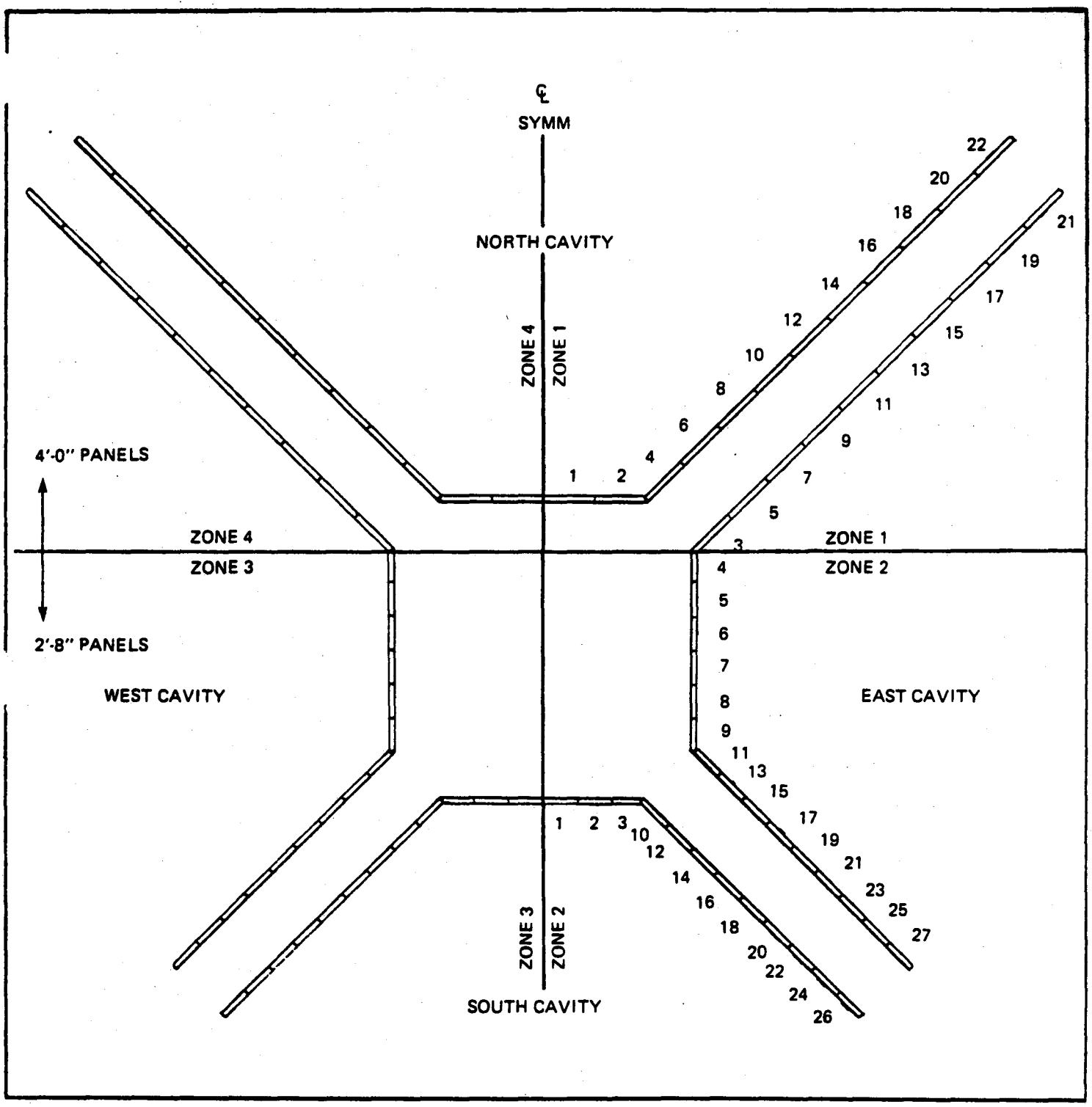

FIGURE 2.5 - PANEL LAYOUT

9.10, amd 9.14). The roof, floor, and casing consist of packed insulation panels supported and restrained by external steel members. Field insulation is applied at the panel joints to minimize heat loss (see Figures 9.12, 9.13, and 9.14).

The main support structure supports the internal components and accommodates deadweight, wind and seismic loadings. The configuration selected consists of a box like tower structure at the center of the receiver with 4 triangular corner towers. The 5 sections are tied together by beam members located between the receiver wing panels. This total structure is bottom-supported by a network of trusses which is in turn anchored to the concrete tower. The design criteria is in accordance with the American Institute of Steel Construction (AISC).

2.1.5 Doors

Each cavity of the receiver has a two piece door which can be closed during adverse weather and at night for the purpose of retaining heat. The structure consists of trusses made from aluminum to minimize weight. The face of the door (nearest the cavity) is covered with a series of packed insulation panels similar to that which comprises the cavity roof and floor. The door mechanism for raising and lowering the door consists of a motor, gear reducer, and a roller chain drive. The door moves on a vertical track which is attached to main steel. A flexible seal is provided on the door to limit heat loss when the door is closed.

2.1.6 Tower

The solar receiver is supported by a reinforced concrete tower which is 155 meters (508.5 ft) tall, with a top diameter of 18.3 meters (60 ft) and a base diameter of 24.4 meters (80 ft), (see Figure 2.6).

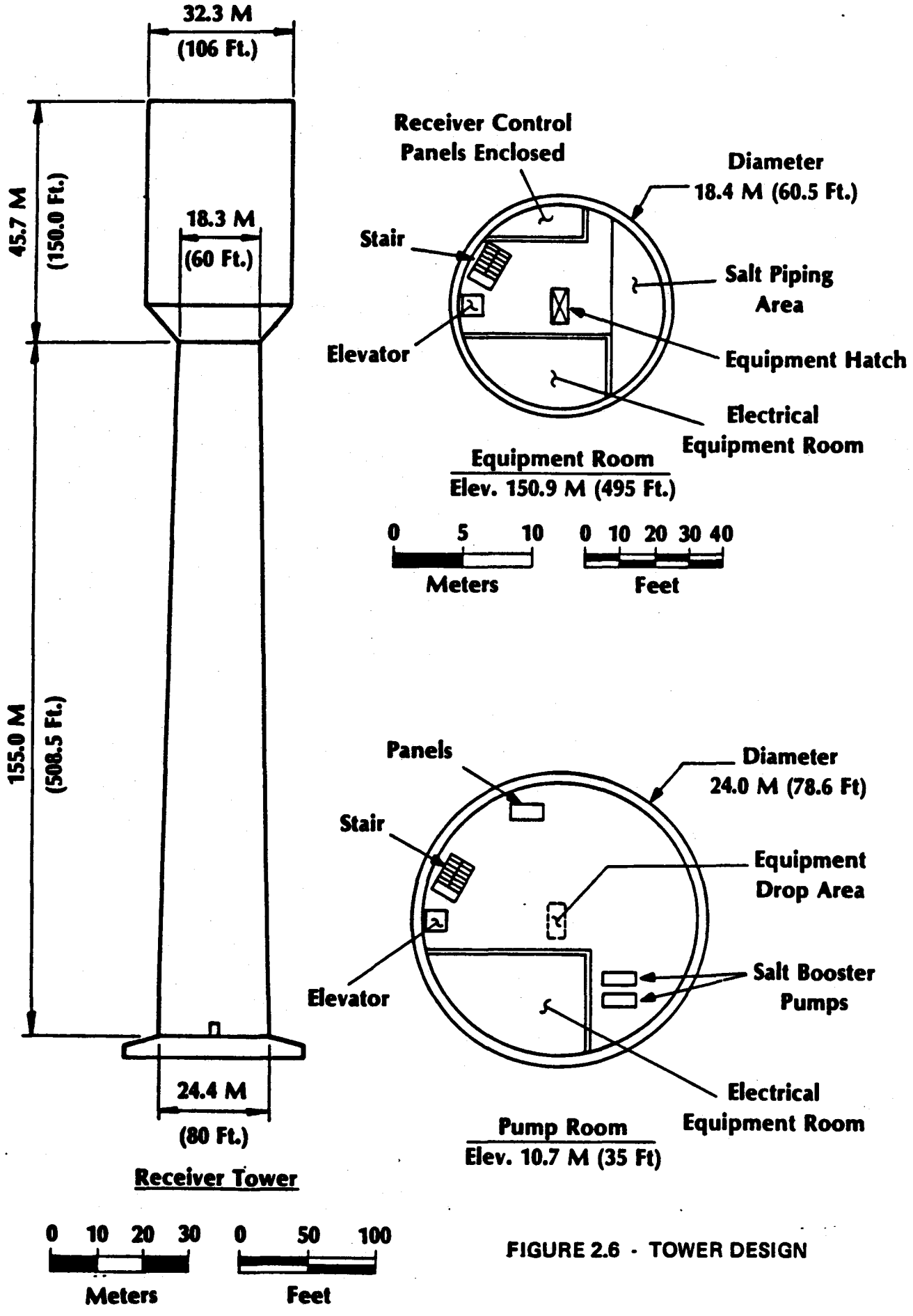

FIGURE 2.6 - TOWER DESIGN

The shell thickness is a constant 0.381 (1.25 ft.), except at the top, the shell is locally thickened to accommodate the receiver support steel. The design was established on the basis of ACI 307-79. The analysis is presented in Subsection 2.6, Tower Design.

The tower foundation is a circular reinforced concrete mat; the bearing capacity of the soil is assumed to be adequate, so piles are not needed. The dimensions of the foundation are 40.2 meters (132 ft) diameter and 4.4 meters (14.5 ft) thick under the shell; it tapers to 2.2 meters (7.25 ft) thick at the outside diameter. The design is in accordance with ACI 318-77. The design was established on the basis that there is no uplift on any portion of the foundation under lateral loading. The maximum settlement over the life of the solar plant will be less than 2.54 cm (1 inch) or 1.9 cm (.75 inch) differential between points across the diameter of the foundation.

The tower also houses receiver subsystem equipment. The receiver booster pumps are located in the pump room at elevation 10.7 meters (35 ft) and an equipment room, which houses receiver control panels, is located at elevation 151.1 meters (495 ft). Tower accessories include an elevator which travels from grade to the top of the tower, a caged ladder from the pump room to the equipment room, a stairway from grade to the pump room, a stairway from the equipment room to the top of the tower, piping support embedments, lighting protection, aircraft obstruction lighting, access platforms, interior lighting, communications equipment, raceway, and ventilation system.

2.1.7 Controls

The control system is designed mainly to control the salt flow rate in order to maintain the desired outlet salt temperatures when

possible yet to limit temperatures in the receiver during rapid flux transients when outlet temperature fluctuations are unavoidable thereby protecting the receiver salt pressure boundary. Limits are set on salt temperature which are derived from maximum allowable metal temperatures in the heat absorption panels.

The system uses a quasi-feed forward control. Header temperatures are monitored by thermocouples and the information fed forward via an algorithm to anticipate maximum salt temperatures.

The control system has been designed, evaluated, and hardware defined. Computer simulations were used to predict the response of the control system to cloud transients. Based on these evaluations, the system is shown to be controllable within the temperature constraints even in severe environments. Details of the control system design are given in Section 4.2 and Appendix C; the piping schematic is shown in Figure 9.3.

2.1.8 Auxiliary Equipment

The cold salt booster pumps are half capacity pumps which lift the cold salt from near the bottom of the tower to the receiver surge/buffer tank. Each pump is designed to deliver 12.2 m^3/min. (3200 gpm) to the surge/buffer tank at design conditions. Since the flow rate of salt through the receiver will vary significantly throughout the day, the pumps are provided with variable speed drive motors. This arrangement will save energy costs associated with throttling the salt flow by a modulating control valve.

The subsystem contains a 500 mm (20") Schedule 100 carbon steel riser that connects the discharge header of the two booster pumps to the surge/buffer tank. Two 350 mm (14") extra strong stainless steel

downcomer pipes are routed between the collection tank and the bottom of the tower. A control valve in the downcomer pipe at the bottom of the tower modulates the flow of hot salt from the receiver and ensures that the downcomer line remains full of fluid. At the maximum flow rate, a portion of the fluid pressure (due to fluid elevation head in the tower piping) is dissipated as friction pressure drop in the downcomer; the remaining available pressure provides sufficient head for salt flow to the hot storage tank. At lower flow rates, the pressure drop in the downcomer decreases and the control valve dissipates that part of the remaining head which exceeds the pressure drop needed for flow to the hot salt tank.

The temperature of the receiver control equipment room is controlled by heating and cooling elements. A 2200 Btu/min (11 ton) condensing unit and 113.28 m^3/min. (4000 cfm) air handling unit provides cooling for the equipment room. Heating is provided by electric resistance heating coils in the air ducts. Redundant condensing and air handling units are provided because of the critical nature of this service.

2.2 Material

Materials were selected to provide adequate strength and corrosion resistance in the operating environments with the additional objective to minimize base material costs.

2.2.1 Material Selection

Carbon steel was selected for the low temperature service of the riser piping and surge/buffer tank. Carbon steel provides favorable strength and acceptable corrosion resistance at temperatures below the maximum operating temperature of 400°C (750°F).

The panel interconnecting piping, collection tank, and downcomer operate in a higher temperature environment (normally as high as 565°C (1050°F)); consequently, the increased mechanical strength and corrosion resistance of 304 stainless steel was considered necessary.

The panel heat absorption tubes operate in temperature environments up to 620°C (1148°). Consequently, Incoloy 800 was selected to provide satisfactory strength and corrosion resistance in the high temperature environments.

The mechanical strength of the component alloys are compared in Figure 2.7. The corrosion rate data upon which corrosion allowances were based are described in Section 3.2.2. The available data pertaining to the corrosion resistance of the selected alloys in molten nitrate salt is very limited and often exhibits wide scatter. Thus, it will be prudent to reassess the material choices based on the results of on-going and future test programs.

2.2.2 Corrosion Allowances

Table 2.1 summarizes the corrosion allowances used in sizing the heat transfer surface for the receiver components.

Limited data are available for salt-side corrosion rates; however, data presented in Reference 1 was used to establish salt-side corrosion rates for the carbon steel components, and test data per Reference 2 and 3 was used to establish salt-side corrosion rates for the Incoloy 800H and 304 stainless steel components.

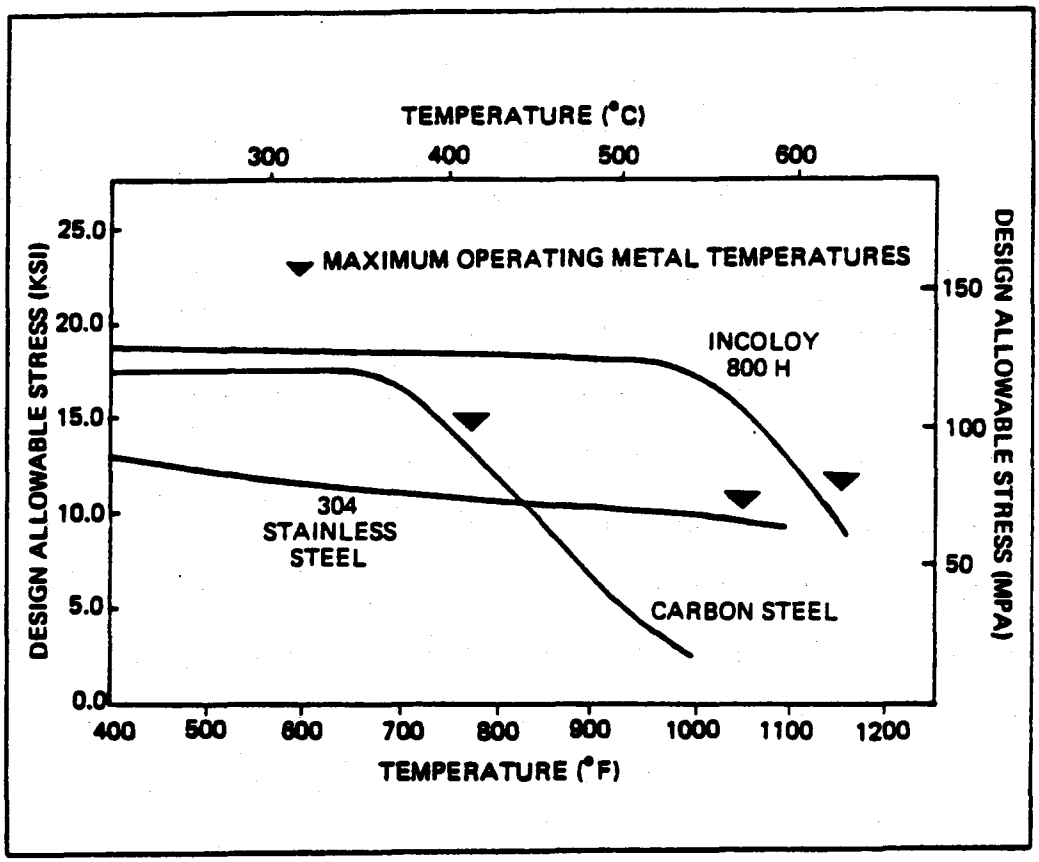

FIGURE 2.7 - DESIGN ALLOWABLES VERSUS TEMPERATURE

TABLE 2.1

Material Corrosion Allowances

Component	Material	Maximum Salt Side Operating Temps. °C (°F)	Salt Side Corrosion MM (mills)
Riser Piping	Crbn Stl	315 (600)	.10 (4.0)
Surge/Buffer Tank	Crbn Stl	400 (750)	1.27 (50.0)
Heat Absorption Tubes	Incoloy 800H	600 (1100)	.30 (12.0)
Panel Interconnecting Piping and Downcomer	304 Stnless Steel	566 (1050)	.15 (6.0)
Collection Tank	304 Stnless Steel	566 (1050)	.15 (6.0)

2.3 Thermal/Hydraulic Design

The objective of the thermal/hydraulic design of the receiver panels is to provide a heat absorption surface capable of providing high reliability over a 30-year period at the flux levels anticipated in the design. The major mechanisms which may lead to degradation of the panel are creep/fatigue damage resulting from thermal stresses generated within the panels and corrosion of the panel material in the molten salt environment. These mechanisms may be quantified and limits established for panel operation which assure long life and high reliability.

The selected panel design uses 2-inch (outside) diameter tubes with a .065 inch wall thickness and a flow rate at design point of approximately 79,000 lbs. per hour per tube. In the two control zones on the north side of the receiver, this translates into a pass width of approximately 4 feet (22 tubes per panel) and in the south zones a pass width of 2 feet, 8 inches (15 tubes per panel). This panel design provides a good balance between heat absorption capability and system pressure drop in addition to keeping fabrication costs low through the use of the relatively large 2 inch tube.

2.3.1 Allowable Heat Fluxes

In order to assure a receiver panel design capable of high reliability and long life, two major limits must be established. First, a maximum allowable stress level must be set based on long panel life. The establishment of such a limit can be a very difficult task because of the complex, inelastic conditions imposed on the material by the thermal loading. Simplified elastic design rules, however, may be employed to establish such a stress limit and heat absorption limits may then be set to remain below this limit.

In order for a simplified elastic analysis to form the basis of a reasonable model, the stresses calculated by elastic methods must be low enough to allow shakedown of the material under cyclic loading to pure elastic action. Based on the philosophy of the ASME code, this limit is assumed to be twice the yield strength (2Sy), or where it is larger, the cyclic yield stress is employed by using the term $3Sm_t$. Meeting this limit, it is believed based on preliminary evaluation, provides reasonable assurance that the panel will survive a 30-year life. While the elastic limits were used to establish allowable stresses, a more detailed creep/fatigue analysis was performed as discussed in Section 2.4.

The second of the two major design limits is based on the corrosion properties on Incoloy 800H in molten salt. Investigations into the corrosion properties of Incoloy 800H (Ref. 2, 3) have indicated a sharp increase in corrosion rates above 600°C (1112°F). Based on this, a metal temperature limit of 593°C (1100°F) was used to establish the limit for each absorption.

Figure 2.8 presents the heat flux limit, as a function of salt temperature, below which these two design limits are met for straight-on heating of individual tubes. This plot is based on a simplified stress analysis which follows.

Simplified Panel Thermal Analysis

The elastically calculated thermal stress in a tube may only be accurately calculated by two-dimensional methods which calculate detailed 2-D temperature profiles. The detailed geometry of the tube and web and the proper detailed incident flux must be included. Also, since the tube is held at discrete points, a true plane strain condition does not exist

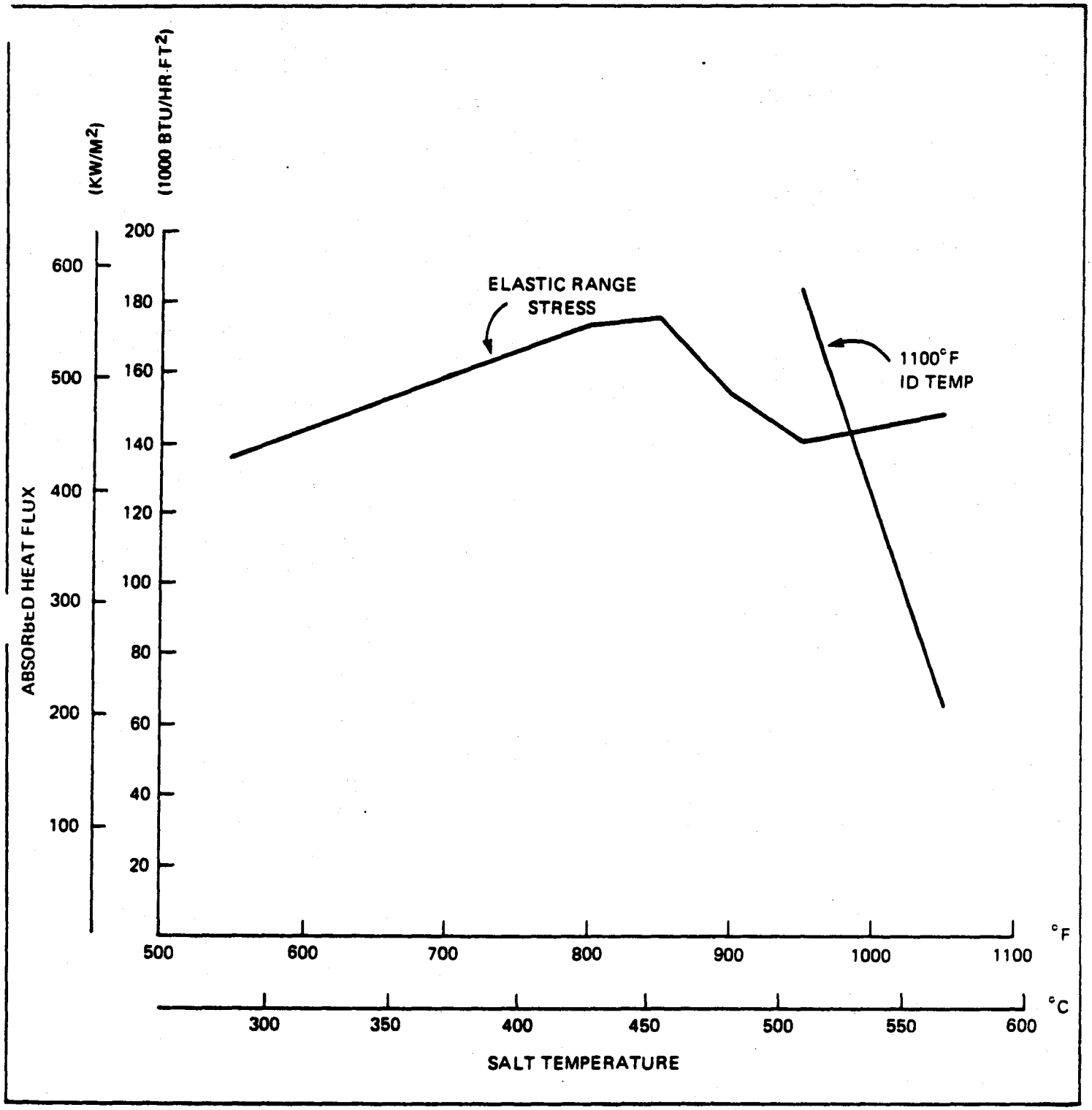

FIGURE 2.8 - ALLOWABLE ABSORBED HEAT FLUX

and so 3-D effects of attachment may be present also. The calculation of the stresses requires the use of the Babcock & Wilcox finite difference membrane wall code or a finite element code. Because these methods are cumbersome for an iterative solution, a simpler alternate method presented in this section has been used to generate basic panel heat transfer limits.

Basic Heat Flux Limits

The stresses generated in the crown of a tube exposed to radiant heat flux are due to non-uniform heating circumferentially and through thickness gradients caused by cooling on the inside surface. As a first approach, then, simple equations for thermal stresses may be superimposed to result in an approximate relation for stress. Consider the tube cross section shown below (Figure 2.9).

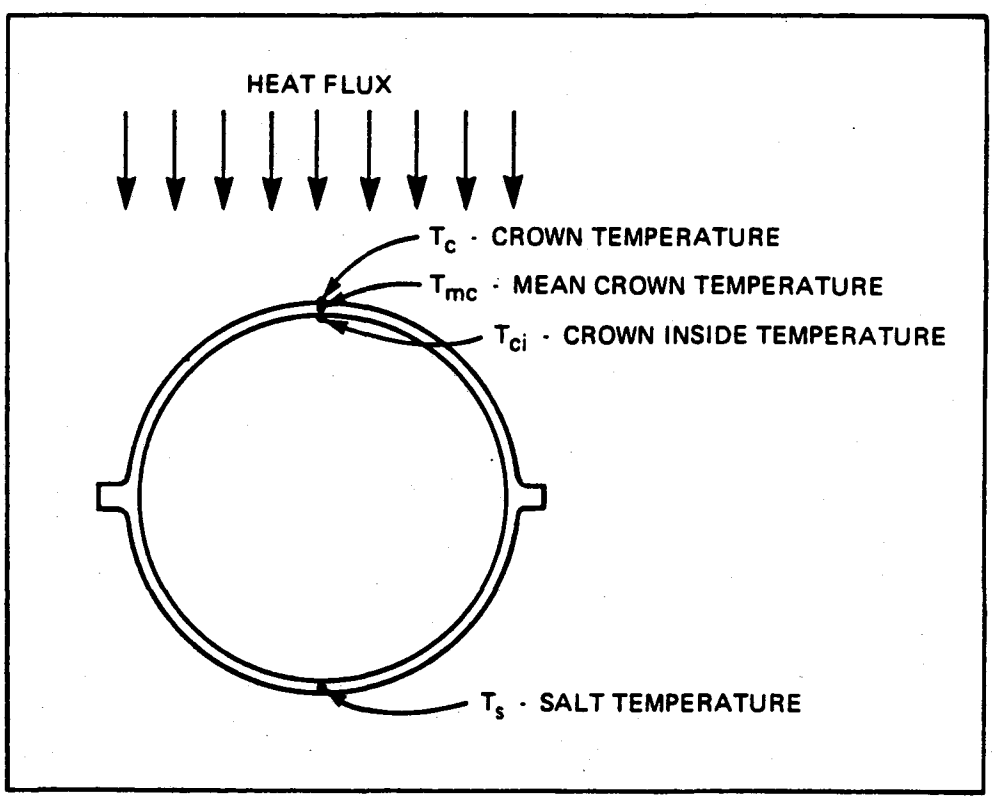

FIGURE 2.9 - TUBE WALL TEMPERATURES

T_c is the crown outside wall peak temperature, T_{ci} is the crown inside wall temperature, T_{mc} is the mean temperature at the crown, and T_s is the salt temperature. A total average metal temperature, T_m, for the cross section may also be defined. The stress in tube, presumed to be a beam with a temperature distribution through its depth is given by:

$$\sigma = E\alpha\ (T_{mc} - T_m) \qquad (1)$$

and for the tube wall at the crown, presumed to be a plate with a through-thickness gradient the stress is:

$$\sigma = E\alpha\ (T_c - T_{ci})/2(1 - \nu) \qquad (2)$$

Superimposing these, the crown outside wall stress is approximated by

$$\sigma = E\alpha\ [(T_{mc} - T_m) + (T_c - T_{ci})/2(1 - \nu)] \qquad (3)$$

Now the mean crown temperature, T_m, may be replaced by

$$T_{mc} = (T_c + T_{ci})/2 \qquad (4)$$

and T_m may be calculated in an approximate may as follows.

The flux distribution on the front side of the tube is approximately a cosine, thus the mean wall temperature profile is roughly a cosine on the front side of the tube, and salt temperature on

the back side. Integrating this around the tube, and neglecting, for now, the metal in the membrane,

$$T_m = \left[\int_{-\frac{\pi}{2}}^{\frac{\pi}{2}} (T_{mc} - T_s) \cos\theta d\theta \right]/2\pi + T_s$$

$$\text{or } T_m = T_s + .318\ (T_{mc} - T_s) \qquad (5)$$

Substituting the expression for T_m and T_{mc} into equation (3) we have:

$$\sigma = E\alpha\ [(T_c + T_{ci})/2 - (T_s + .318\ ((T_c + T_{ci})/2 - T_s)) + (T_c - T_{ci})/2(1 - \nu)]$$

$$\text{or} \quad \sigma = E\alpha\ [.954\ (T_c - T_s) + .523\ (T_c - T_{ci})]/1.4 \qquad (6)$$

Equation (6) can be used as the basis for establishing the allowable stresses and heat fluxes in the tubes. Results obtained by using equation (6) have been compared to the more accurate results from two dimensional computer analysis for tubes without a membrane and tubes with a membrane. The comparison is as follows.

a) No membrane - equation (6) within 3% of FE program.

b) Membrane - equation (6) overpredicts the stress by roughly 10%.

In the case of the latter, i.e., tubes with a membrane, equation (6) was still used to establish allowables because the error will allow some margin for the effects of skewed heating and other unknowns. Preliminary evaluation suggests that the additional stress due to skewed heating range from 0 to 50% and, therefore, the use of equation (6) is considered prudent, as a basic limit, with the effect of skewing and the membrane considered on a panel by panel basis.

For the present stage of analysis, equation (6) has been used to set basic allowable heat fluxes. While further evaluation will probably lead to modification of the allowable curves in some parts of the flow circuit, the present analysis is sufficiently accurate on which to base the design.

One-dimensional conduction may be employed to find the temperatures required by Equation (6). These relationships are:

$$T_{ci} = T_s + q\ (d_o/d_i)/h \qquad (7)$$

$$T_c = T_{ci} + q\ (d_o/2K_m)\ (\ln\ (d_o/d_i)) \qquad (8)$$

where

h = convection heat transfer coefficient

q = absorbed flux at crown

d_o = outside diameter

d_i = inside diameter

k_m = metal conductivity

the heat transfer coefficient used is given by:

$$Nu = .023\ Re^{.8}\ Pr^{.33} \qquad (9)$$

$$Nu = hd/k$$

Salt properties provided by SNLL have been used and values for Inconel properties have been taken from the ASME code.

The equations for calculating the tube stress as a function of flow, salt temperature, and flux have been employed in an iterative procedure to find the heat flux, for any salt temperature, which produces the allowable stress in the tube, or, if it is lower, the flux which results in an 1100°F inside tube temperature for design point conditions in the panels. The limits on flux have been calculated based on the marginally lower (Zone II) flow per tube (see Table 2.2 and Figure 2.8).

TABLE 2.2

FLUX LIMITS VS. SALT TEMPERATURE

Salt Temp.	Flux Limit (stress)	(1100F I.D.)
550°F	136,000	
600°F	143,500	
650°F	151,200	
700°F	159,000	
750°F	165,200	
800°F	173,200	
850°F	176,700	
900°F	154,100	
950°F	140,500	183,000
1000°F	144,700	126,300
1050°F	148,200	65,400

2.3.2 Heliostat Aiming

2.3.2.1 Background

Previous studies have indicated that the use of a single heliostat aim point per cavity often results in unacceptable flux distributions, especially with regard to peak-to-average flux ratios. It has also been demonstrated that such flux distributions can be smoothed-out by the use of multiple aim points. A specification of the coordinates of multiple aim points and the associated heliostat groups constitutes an aiming strategy. The aiming strategies adopted from the ACR Phase II Program have been found inadequate, and a re-aiming of the heliostat field was initiated with the purpose of reducing peak fluxes, providing balanced fluxes on two-sided heating panels, and providing flux distributions along the flow paths that are consistent with ID temperature limit requirements.

The development of suitable aiming strategies for a cavity receiver is made difficult by the fact that the incident fluxes at a point on the receiver are effected by a large number of heliostats spread over a significant portion of the collector field, while each element of reflective surface in the heliostat field illuminates a relatively large area on the receiver surfaces. In other words, there can be no point-to-point mapping between the collector field and the receiver.

In the past, the development of aiming strategies has been based to a large extent on trial and error techniques. A novel technique has been developed during the present program that

permits a more systematic approach to aiming, and is the subject of the discussion to follow.

The technique to be described hinges on the construction of two types of maps, to be referred to as image maps and domain maps, respectively. The first of these is used to establish the magnitude of permissible shifting of aim point coordinates (relative to the center of the aperture) as a function of heliostat location. The second is used to identify the heliostat groups that effect the flux distribution at a given receiver location, and to determine the sense and direction of aim point coordinate shifting required to achieve a desired flux distribution. A third element of the technique is the TRASYS computer code, which is used extensively to evaluate and verify the aiming strategies.

2.3.2.2 Assumptions and Guidelines

The principal assumptions and guidelines adopted for this study are listed below:

1. The focal length = slant range for all heliostats.
2. Perfect focusing, implying that the central rays of the reflected beams from all minor elements of a given heliostat intersect at a common focal point.
3. Inaccuracies due to mirror and aiming imperfections are eliminated by the use of an "effective" solar intercept angle of 50 minutes of arc intercepted by the actual sun.
4. All aim points are in the aperture plane.

5. The aiming strategies should not result in perceptible increases in spillage losses when compared to single-point aiming.

Assumptions 1 through 3 are idealizations that have been shown to have negligible effects on the accuracy of the results of the present study. Item 4 was adopted following initial studies which indicated that there are not significant benefits derived (in this case) from aiming strategies involving aim points outside of the plane of the aperture. Item 5 requires no elaboration.

2.3.2.3 Development and Use of Image Maps

The pertinent elements of the applicable radiation geometry are depicted on Figure 2.10. Consider an arbitrary point M in the heliostat field, surrounded by an elemental mirror area dM "aimed" at the focal point F at the center of the aperture plane. (Aiming in the present context means that the axis of the reflected beam goes through F). The reflected beam will be conical in shape, with the angle 2δ determined by the effective intercept angle of the solar disk. The reflected beam will form an elliptical image on the aperture plane, whose semi-major axis will be denoted by a. The size of this image is a function of the intercept angle and the distance from the mirror (point M) to the focal point F (this distance depends on the tower height and the location of the mirror).

If L represents the dimension of the aperture (Figure 2.10), the difference $(L/2 - a)$ approximates the maximum permissible shift in aim point coordinates of the heliostat at the location M.

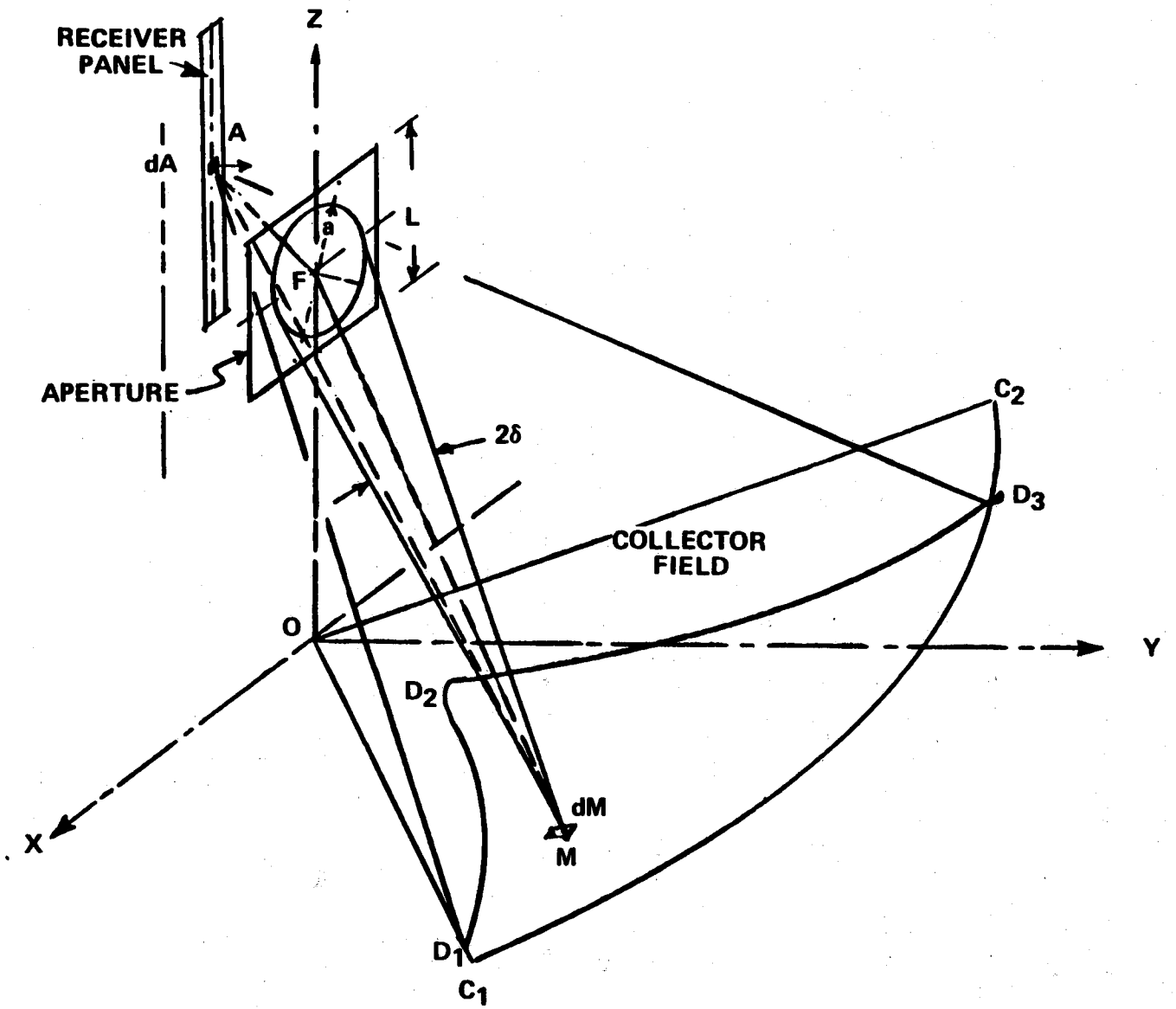

FIGURE 2.10 - RADIATION GEOMETRY

Next we must determine which heliostats have the same size image (dimension a). It has been shown during the ACR Phase II program that the iso-lines connecting heliostats associated with constant image sizes may be approximated by circles described by the following equations:

$$y_o = \underline{a} \,/\, 2 \sin \delta$$
$$r = \sqrt{y_o^2 - H^2}$$

where y_o represents the distance between the tower and the center of the iso-line circle, H is the tower height, r is the radius of the circle, and $\underline{a}$ is the semi-major axis of the (constant) image represented by the iso-line. These equations apply to vertical aperture planes only; and by virtue of symmetry, the locus of the centers of the circles is the collector field axis that is perpendicular to the aperture plane. A set of iso-lines such as just described constitutes an image map. An example is shown on Figure 2.11 for the East field. For the East aperture L/2 = 21.3 Ft. Hence the aim point of a heliostat located on the circle labeled 14' (for example) may be shifted from the center of the aperture, in any direction within the plane of the aperture, by an amount equal to 21.3 - 14 = 7.3 Ft., without effecting spillage losses. Similar maps have been constructed for the North and South apertures.

2.3.2.4 Development and Use of Domain Maps

With reference to Figure 2.10, consider the elemental surface dA loated at point A on a receiver panel. That portion

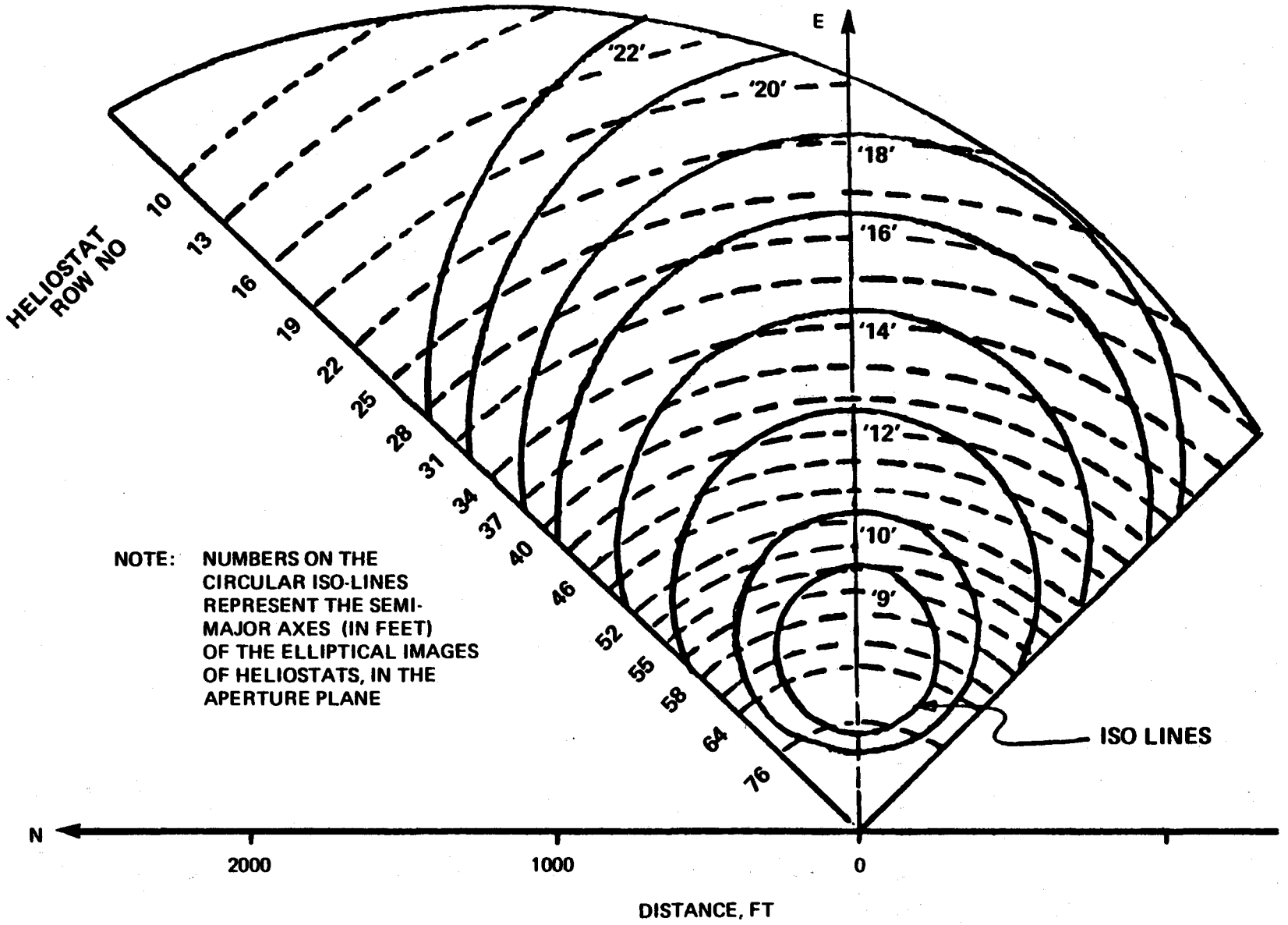

FIGURE 2.11 - IMAGE MAP - SOUTH FIELD

of the heliostat field that contributes to the flux level at A will be referred to as the domain of dependence of A, and it is indicated on Figure 2.10 by the area $C_1D_1D_2D_3C_1$. The boundary of the domain consists of two parts: The line $D_1C_1D_3$, which coincides with a portion of the boundary of the collector field; and the line $D_1D_2D_3$ established by the "optics" of the receiver/collector radiation interface (as explained later). In particular, the shape and position of this line depends on the coordinates of the aim points of the heliostats inside the domain.

The relationship between the area and shape of the domain of dependence and the incident fluxes on the elemental area dA is non-linear, and its evaluation is outside the scope of this study. for the purpose of developing aiming strategies, it is usually sufficient to use the domain maps for qualitative specifications of aiming requirements, including the identification of the heliostats involved in the re-aiming, and the sense and direction of the required shift in their aim points.

The "optical" portion of the domain boundaries - such as line $D_1D_2D_3$ on Figure 2.10 - represent lines of intersections between the plane of the heliostat field and tori, whose dimensions are determined by the effective intercept angle δ, and the coordinates of the receiver and aim points involved. This is demonstrated below.

Points A, F, and M of Figure 2.10 have been reproduced on Figure 2.12 with two additional points M' and M'' on the heliostat

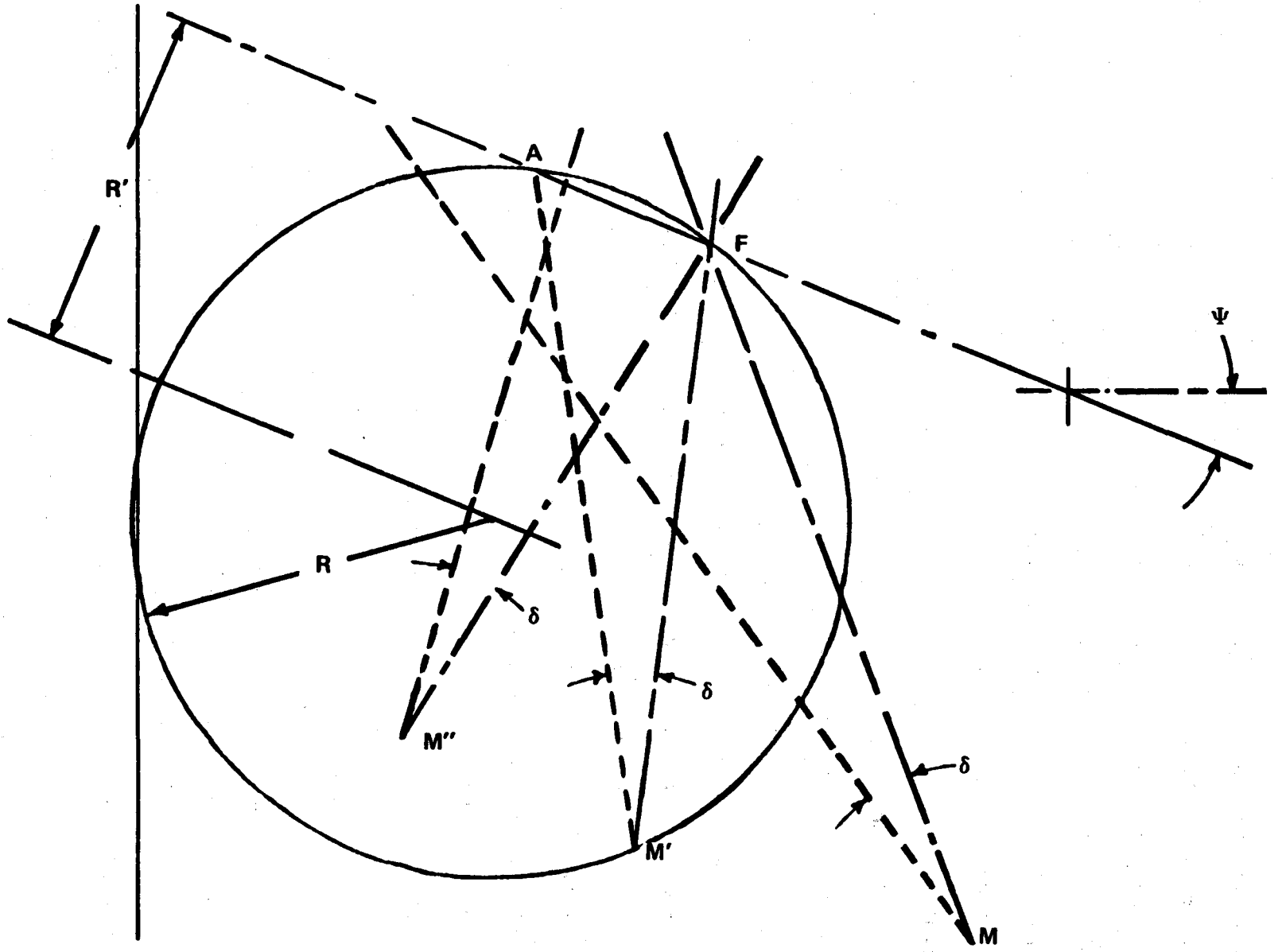

FIGURE 2.12 - GEOMETRICAL BASIS FOR THE CONSTRUCTION OF DOMAIN MAPS

field. The axes of the reflected beams from these three mirror elements all go through their common aim point F, and subtend the same conical angle δ. It is seen that point A (on the receiver panel) is fully enveloped by the beam produced by M, it is barely touched by the beam from M', and it is completely missed by the beam from M''. It may be readily shown that the locus of points such as M' that form the included angle δ with the two fixed points A and F is a circle going through A and F and having a radius:

$$R = AF / 2 \sin \delta$$

where AF represents the distance between points A and F. It is further evident, that heliostats located inside this circle cannot contribute to the fluxes at A, whereas those located outside or on the circle, will effect the incident fluxes at point A, provided that F represents their common aim point.

The circular locus of the points of type M' may be expanded into a special locus by the rotation of the circle around an axis going through points A and F. This generates a torus as shown on Figure 2.13, with

$$R' = R \cos \delta \cong R$$

since $\cos \delta \cong 1$

For the pair of points A and F, the torus divides the universe into two regions: Heliostats inside the torus cannot effect the incident fluxes at A, whereas all heliostats outside and on the surface of the torus will contribute to the fluxes at

A, provided, of course, that all heliostats under consideration are aimed at F. Consequently, the intersection of the torus with the plane of the heliostat field determines the domain of dependence of point A defined earlier. Pertinent elements of this geometry are depicted on Figure 2.13.

Referring to the small sketch on the upper left hand corner of this figure, it is seen that as the elevation of point A is lowered, the angle Ψ between the line AF and the horizontal is decreased until a point is reached where the plane of the heliostat field and the torus have a common point of tangency. This represents a transition from a doubly-connected to a singly-connected domain, as illustrated on Figure 2.14. The shaded areas on this figure represent the domains of dependence of three points on panel 9 on the North-East wall of the East cavity, corresponding to elevations 21, 20.6 and 15 Ft. above the elevation of the aim point.

Note that a very small change in elevation near the "transition height" results in a substantial change in the shape and area of the domain of dependence, with corresponding changes in incident fluxes along the panel. It follows that transition heights are associated with steep longitudinal flux gradients - a fact that has been verified by TRASYS runs. These gradients can be considerably reduced, however, by the use of multiple aimpoints.

The transition height is represented by the following equations:

$$\Psi t_r = \cos^{-1} (1 - H/R)$$

$$z_{t_r} = AF \sin \Psi_{tr}$$

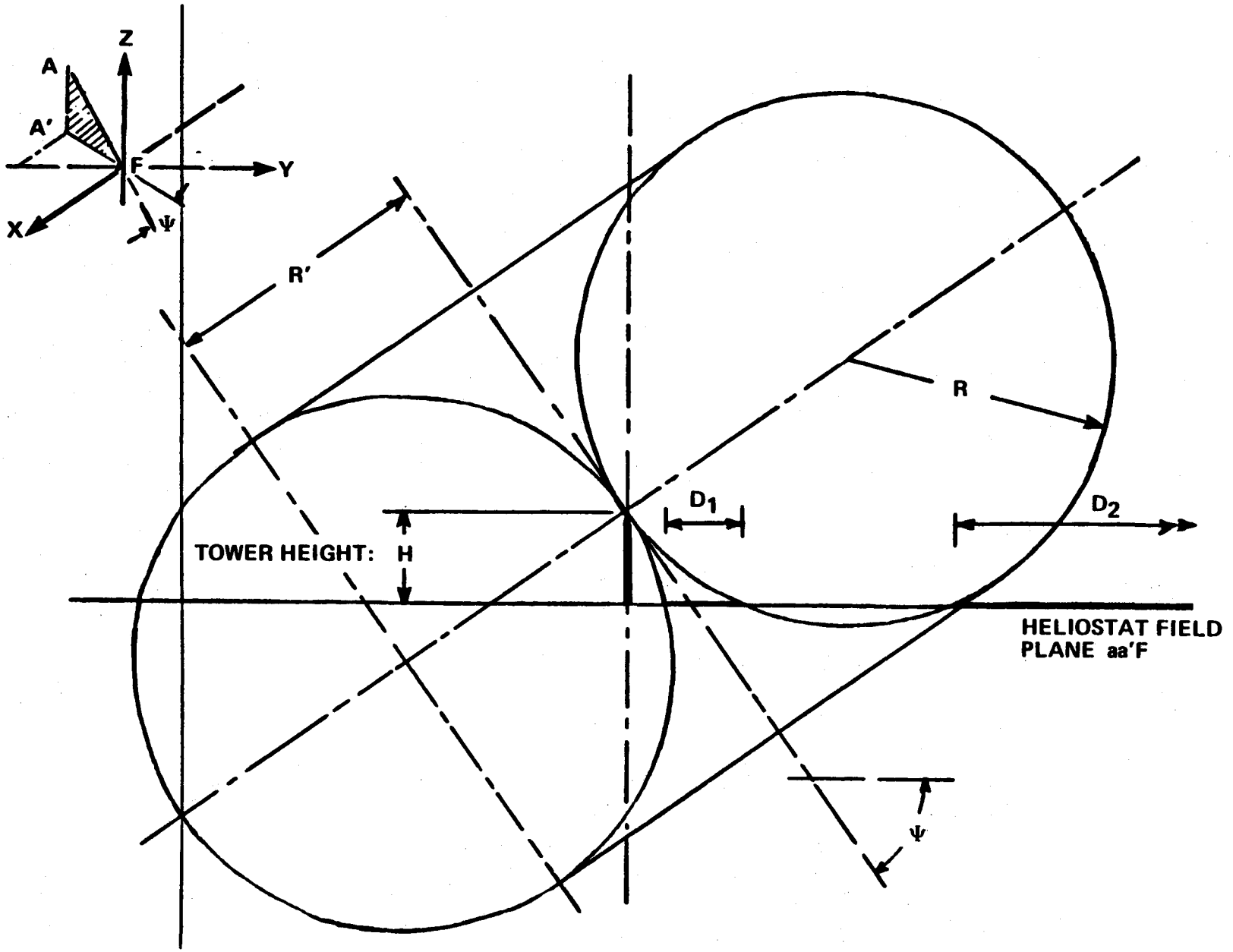

FIGURE 2.13 - PRINCIPLE OF CONSTRUCTION OF DOMAIN MAPS

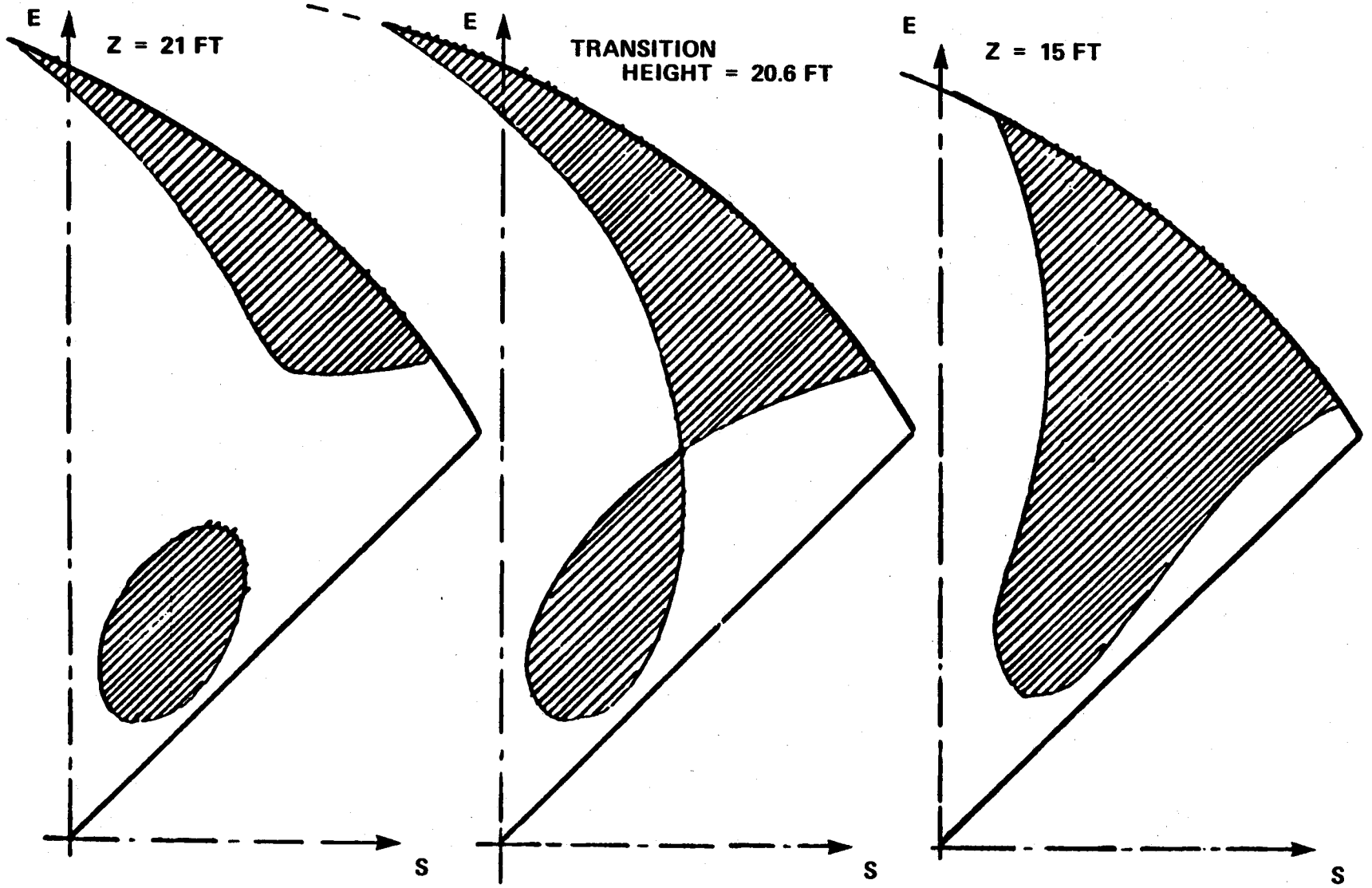

FIGURE 2.14 - TYPICAL DOMAIN MAPS NEAR TRANSITION POINT (EAST CAVITY - NORTH WALL)

where Ψ_{tr} represents the value of the angle associated with the transition, H is the tower height, z_{tr} is the transition height.

Further examples of domain maps are shown on Figures 2.15 and 2.16. Figure 2.15 shows the the domain boundaries as a function of elevation for Panel 1 in the South cavity, with single point aiming. It is evident from inspection that peak fluxes on this panel will occur at at elevation of 10 Ft. because it encompasses a larger portion of the heliostat field than the other domain boundary lines (a fact verified by TRASYS runs).

It may also be inferred from the map that one way of smoothing this flux profile is by raising the aim points of the heliostats in the region abcd, and lowering the aim points within the region cdef. This will result in a lowering of the fluxes at the 10 Ft. level, and an increase in fluxes at the -2 and -5 Ft. levels. If all the aim points in the South field would be raised by 10 Ft, the z=0 Ft line would become the z=10 Ft line, with corresponding decrease in fluxes. On the other hand, raising only the heliostats in regions abdc would shift lines ab and cd and decrease the heat flux between the 0 and 10 Ft. elevations.

Figure 2.16 shows another example of domain mapping, where a decrease in flux levels was achieved by a combination of low and high aiming.

2.3.2.5 Typical Results

Figure 2.17 depicts the final aiming strategy for the East cavity. A variety of combinations of horizontal and vertical shifting in aim points has been applied, as indicated by the

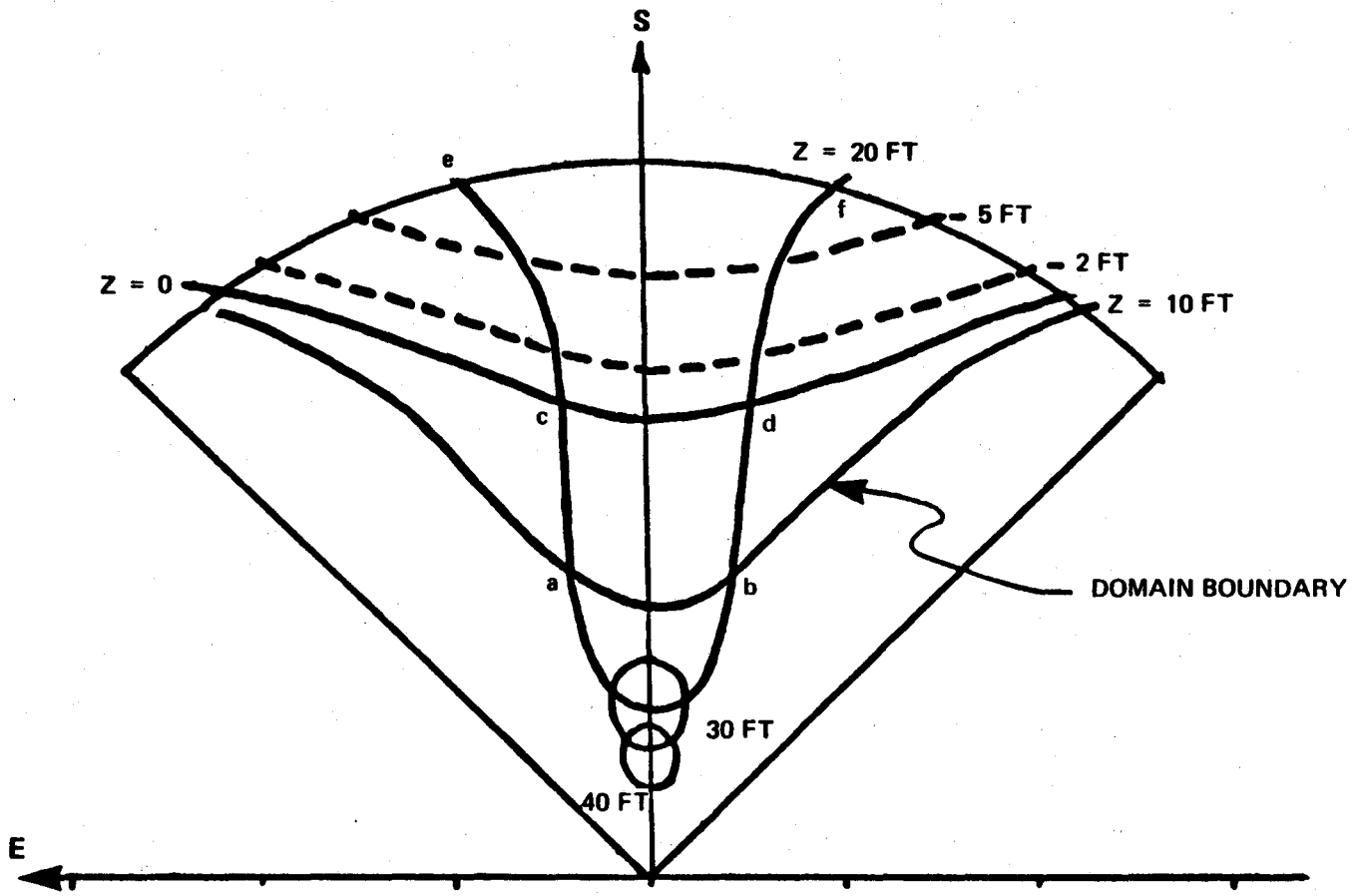

FIGURE 2.15 - TYPICAL DOMAIN MAP (SOUTH CAVITY - PANEL 1)

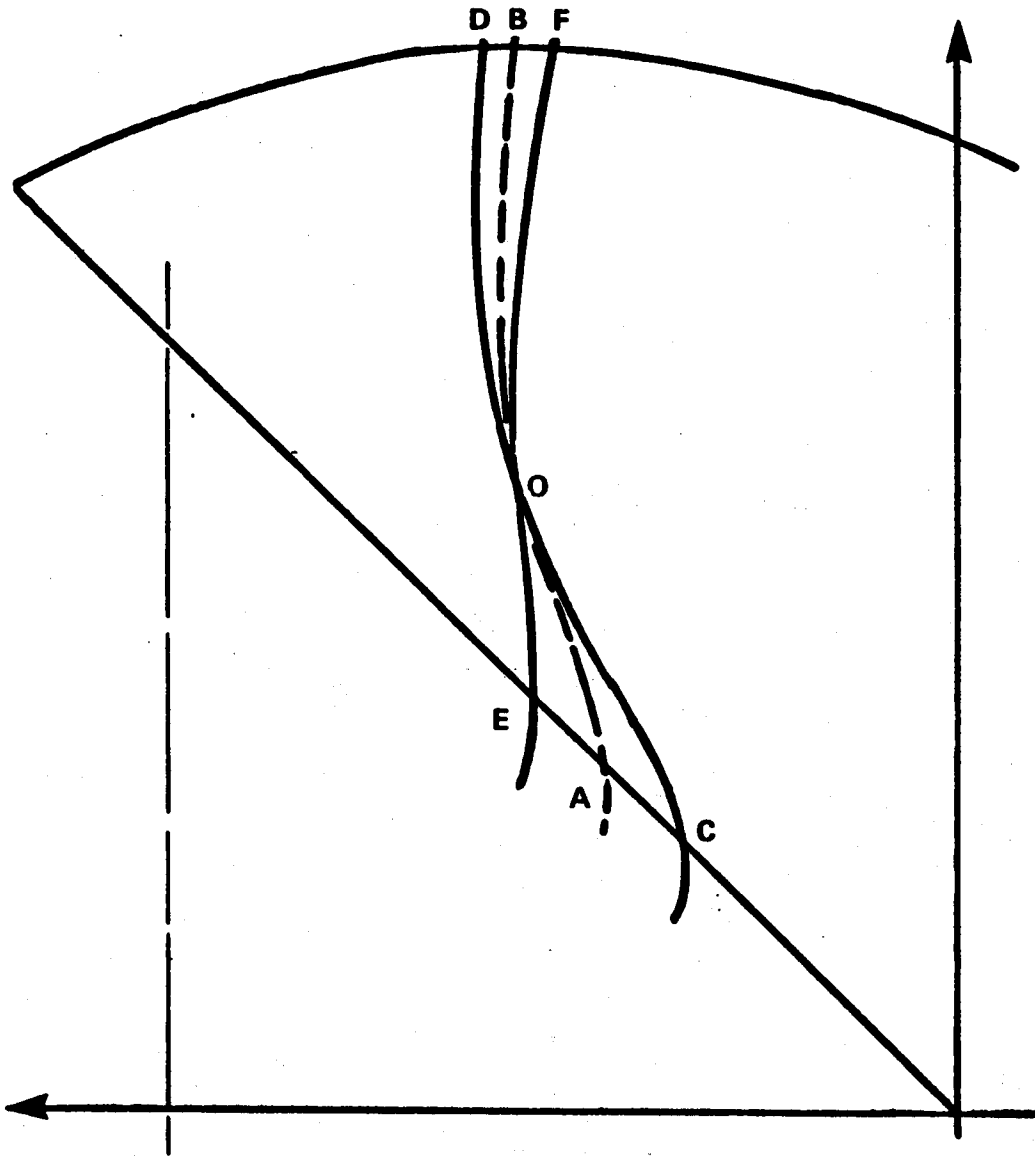

AB : ZERO AIM

EF : ΔZ POSITIVE

CD : ΔZ NEGATIVE

TO DECREASE FLUXES: AIM LOW IN REGION BOD; AND AIM HIGH IN REGION EAO

FIGURE 2.16 - APPLICATION OF DOMAIN MAPS TO RE-AIMING (EAST CAVITY, PANEL 10 SE)

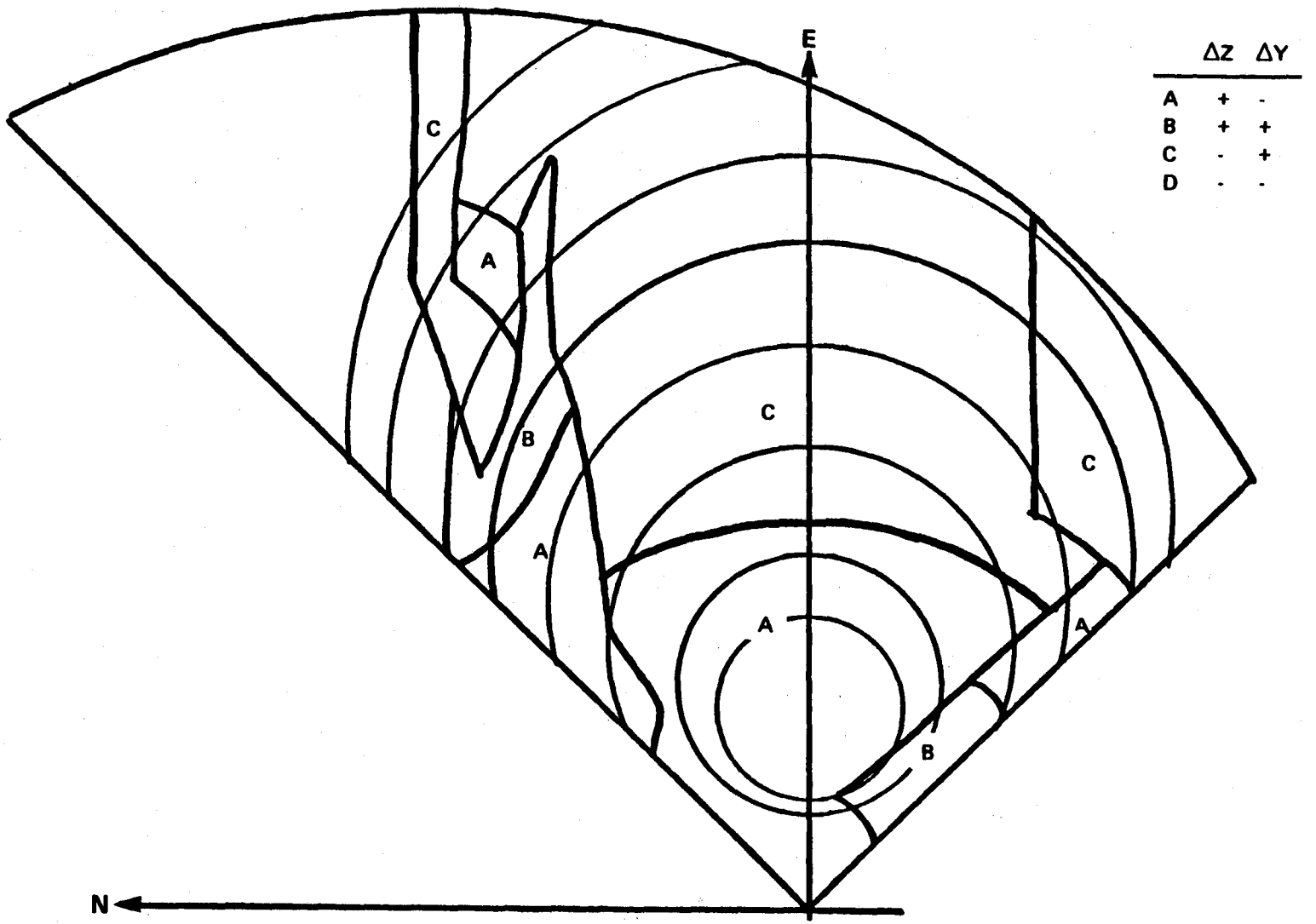

FIGURE 2.17 - FINAL AIMING STRATEGY (EAST CAVITY, DESIGN POINT)

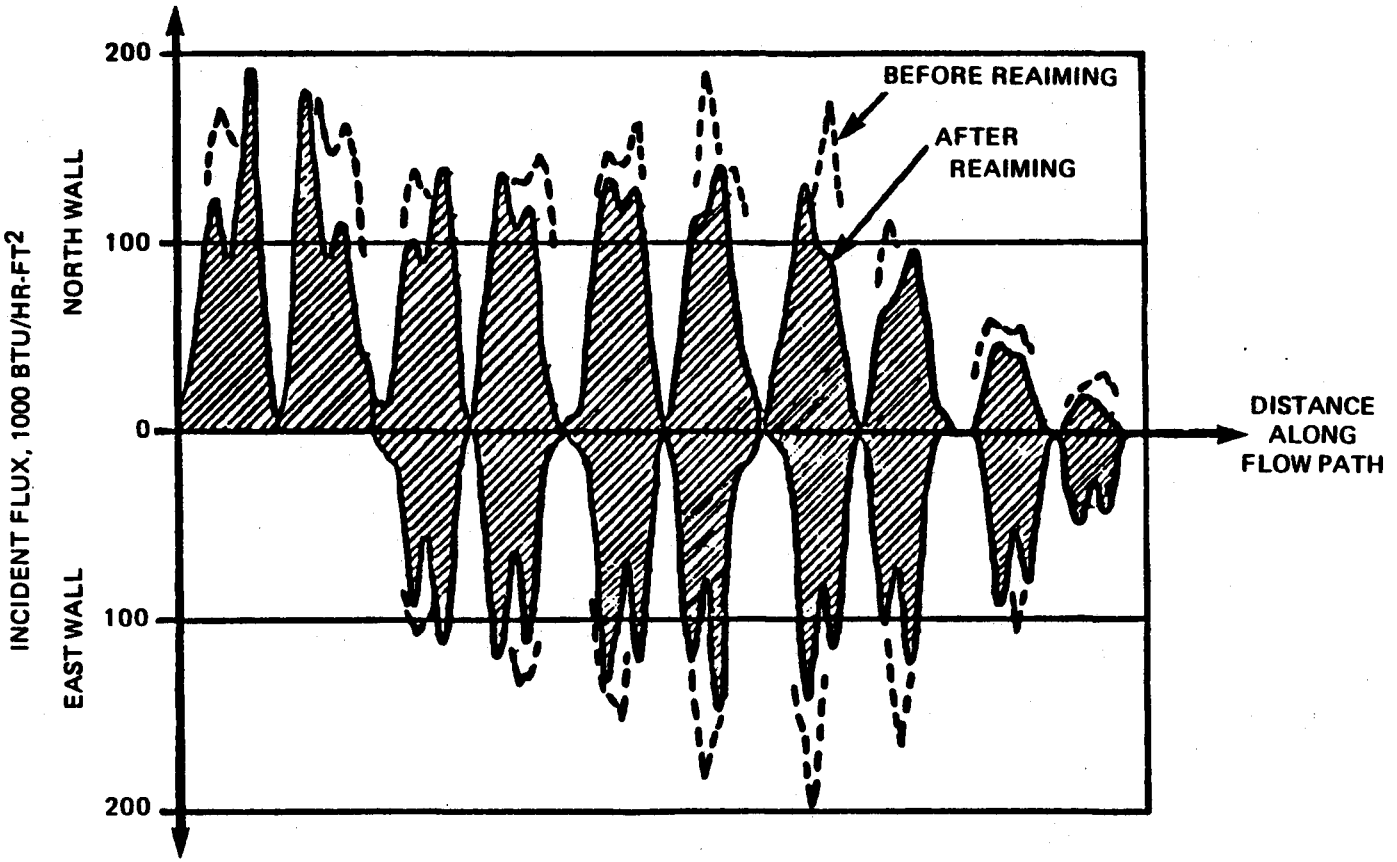

FIGURE 2.18 - EFFECT OF RE-AIMING ON FLUX PROFILES, ZONE 1, DESIGN POINT

letters, A, B, C, and D. The superimposed image map, represented by the circular iso-lines, establishes the magnitude of aim point coordinate changes for each category.

Figure 2.18 shows a computer plot of incident fluxes along the flow path for Zone 1. The shaded areas represent the flux profiles achieved with the aiming strategies developed by the use of the new technique. The dashed curves indicate the peaks in the previous flux profiles. The improvement associated with the new technique is quite evident, especially with regard to reduction of the peaks in the high temperature area.

2.3.2.6 RS Aiming Strategy

The aim point coordinates and associated heliostat locations are listed in Addendum A, Table A1, A2, and A3, of the Receiver Subsystem Requirements and Specification (Appendix A).

2.3.3 Actual Heat Fluxes

The heat flux occuring on the heat absorption surface within the receiver cavities is a function of:

- cavity geometry
- heliostat field geometry
- heliostat aim strategy
- sun location and insolation level

The goal of receiver design is to arrive at a combination of these which result in the required power level (at design point solar conditions) with a distribution of heat flux on the absorption surface which does not exceed the heat absorption capability of the receiver panels.

The heat absorption capabilities of the receiver panels have been described in Section 2.3.1 and presented as a maximum allowable flux vs. salt temperature. These limits are a function of the panel sizing described in Section 2.3.4. The important aspects of the panel heat flux which determine if these limits are met are the individual panel peak heat flux, and the individual panel absorbed power which establishes the salt temperatures within the system. The peak panel fluxes and absorbed power for the current design are shown in Figures 2.19 through 2.22. Based on these, peak fluxes as a function of salt temperature are shown in Figures 2.23 and 2.24, compared to the absorption capabilities of the panels. As can be seen, a significant amount of margin exists over much of the design. On the back wall of the north cavity, however, the limit is slightly exceeded. The margin in the design is believed to be sufficient to cover:

- Additional aiming refinement to reduce north cavity back wall fluxes.

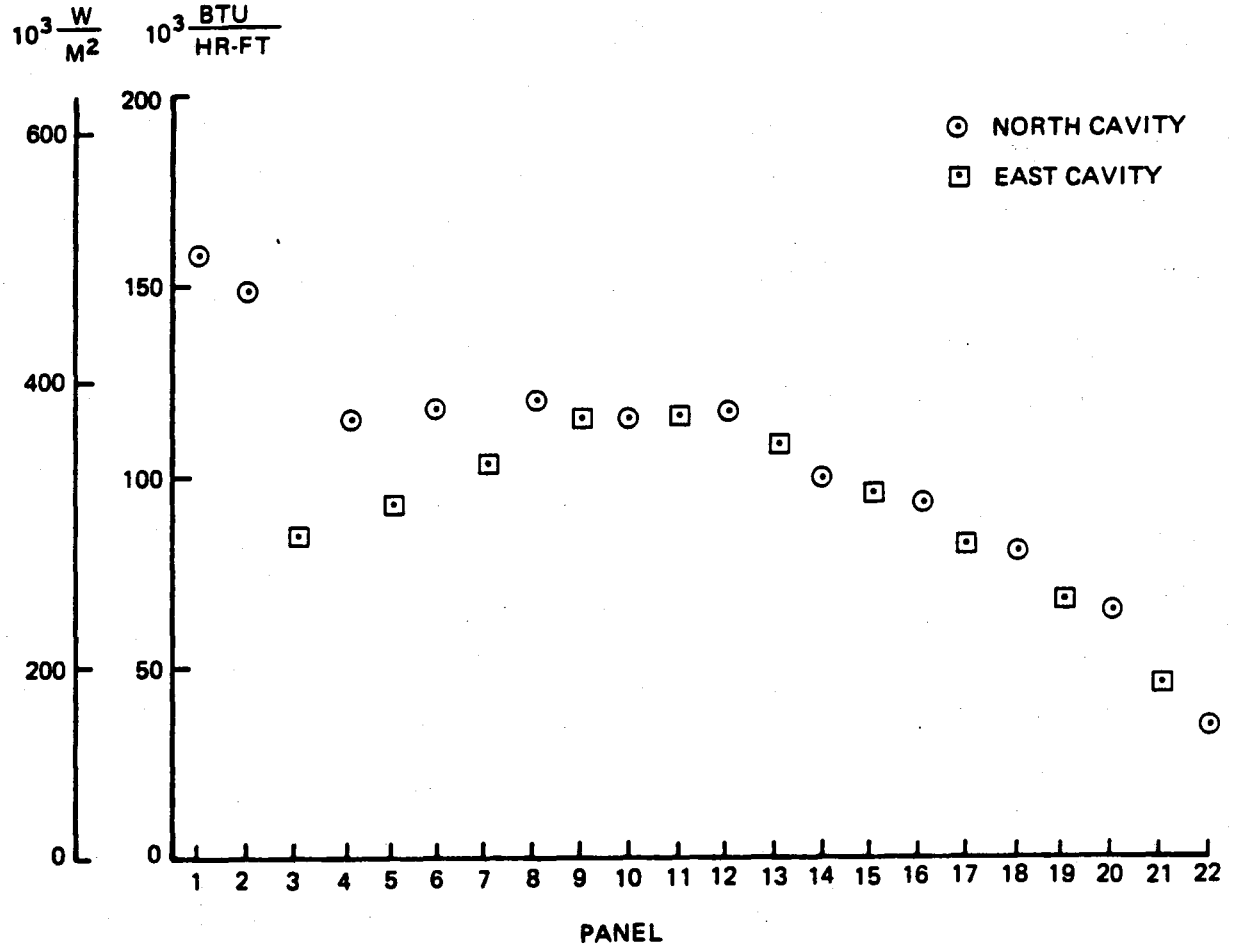

FIGURE 2.19 - ZONE 1 PEAK FLUXES

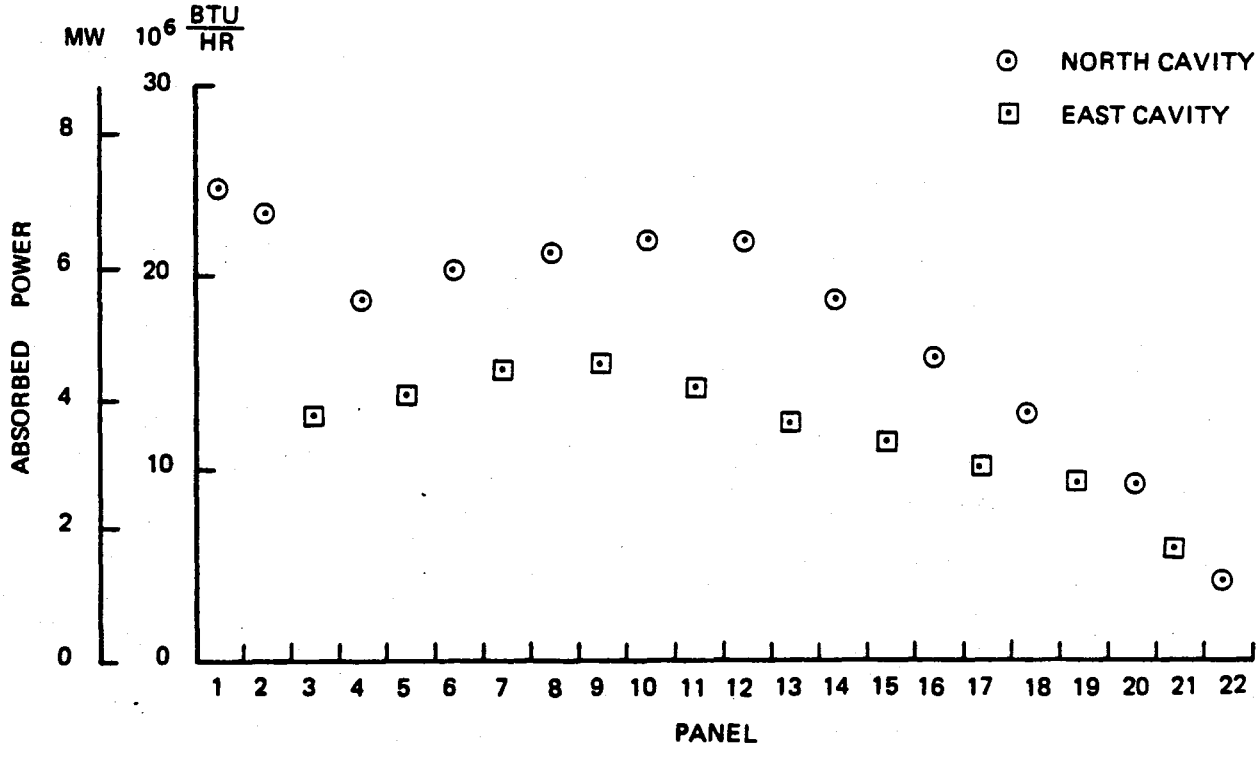

FIGURE 2.20 - ZONE 1 ABSORBED POWER

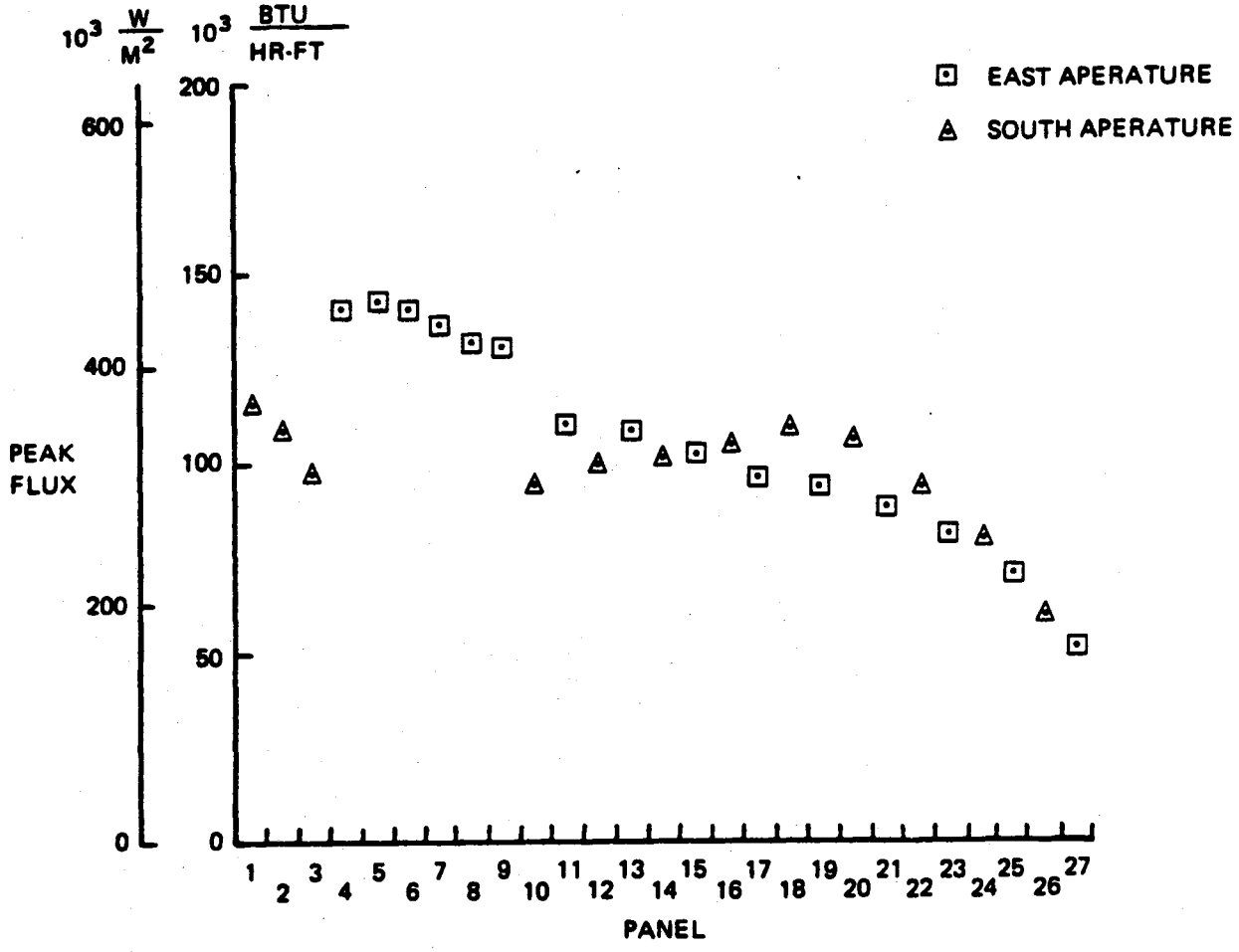

FIGURE 2.21 - ZONE 2 PEAK FLUXES

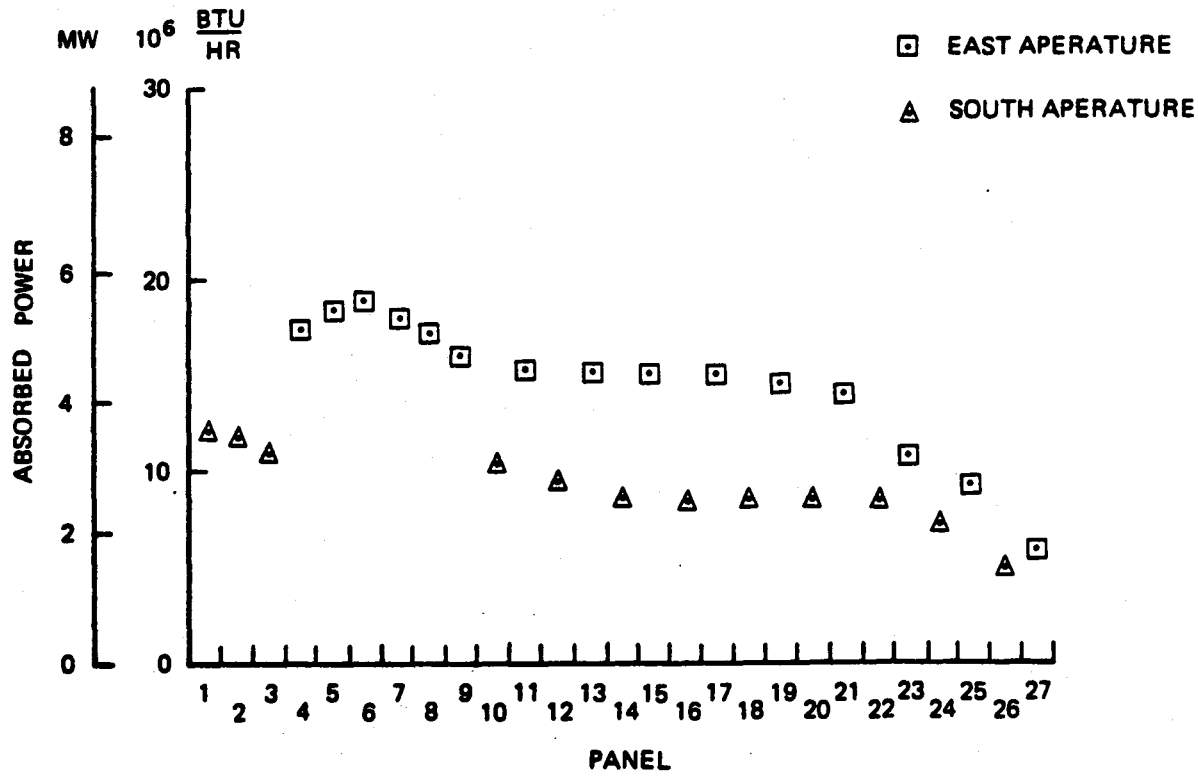

FIGURE 2.22 - ZONE 2 ABSORBED POWER

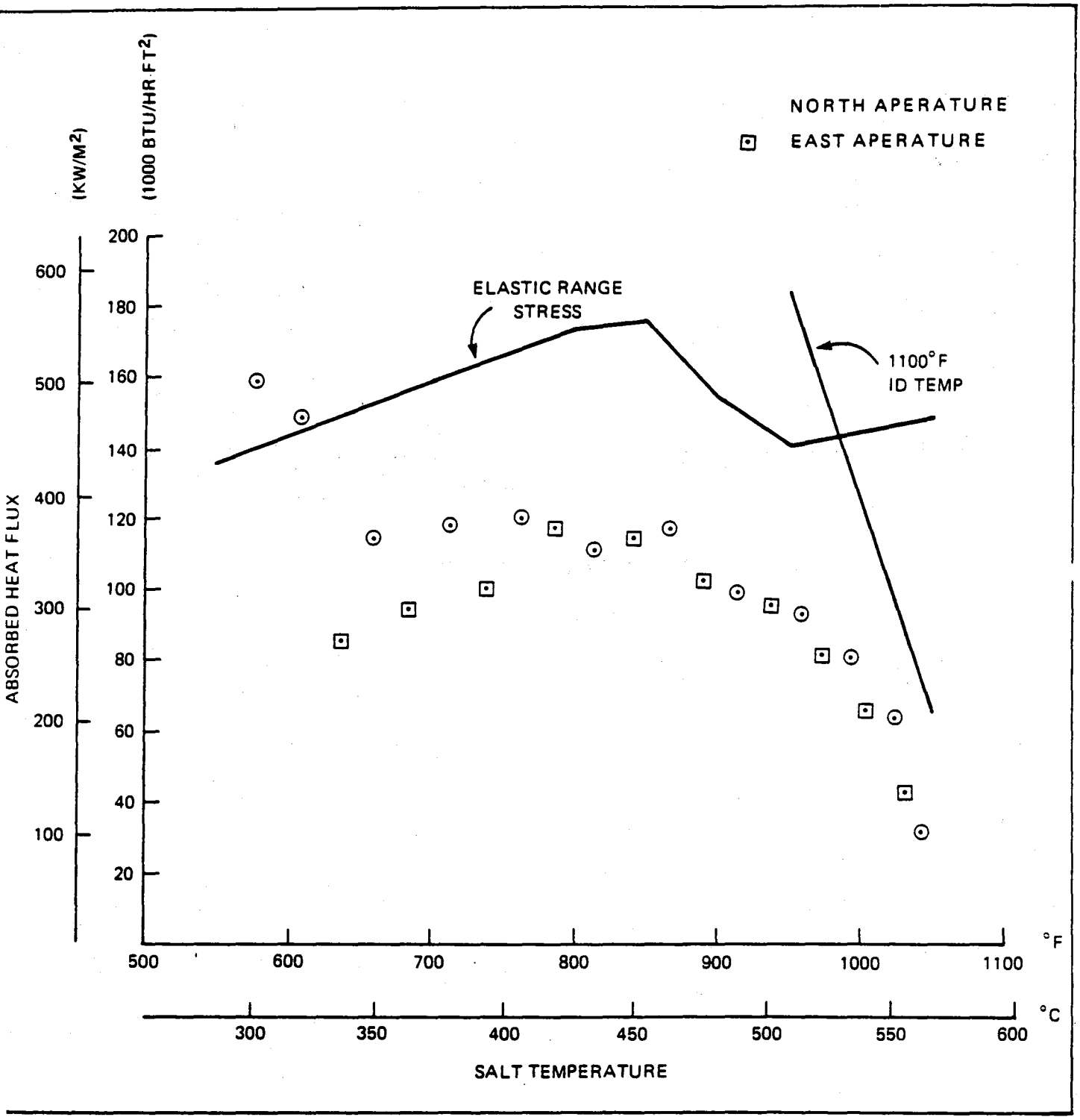

FIGURE 2.23 - ZONE 1 PEAK FLUX AND LIMIT

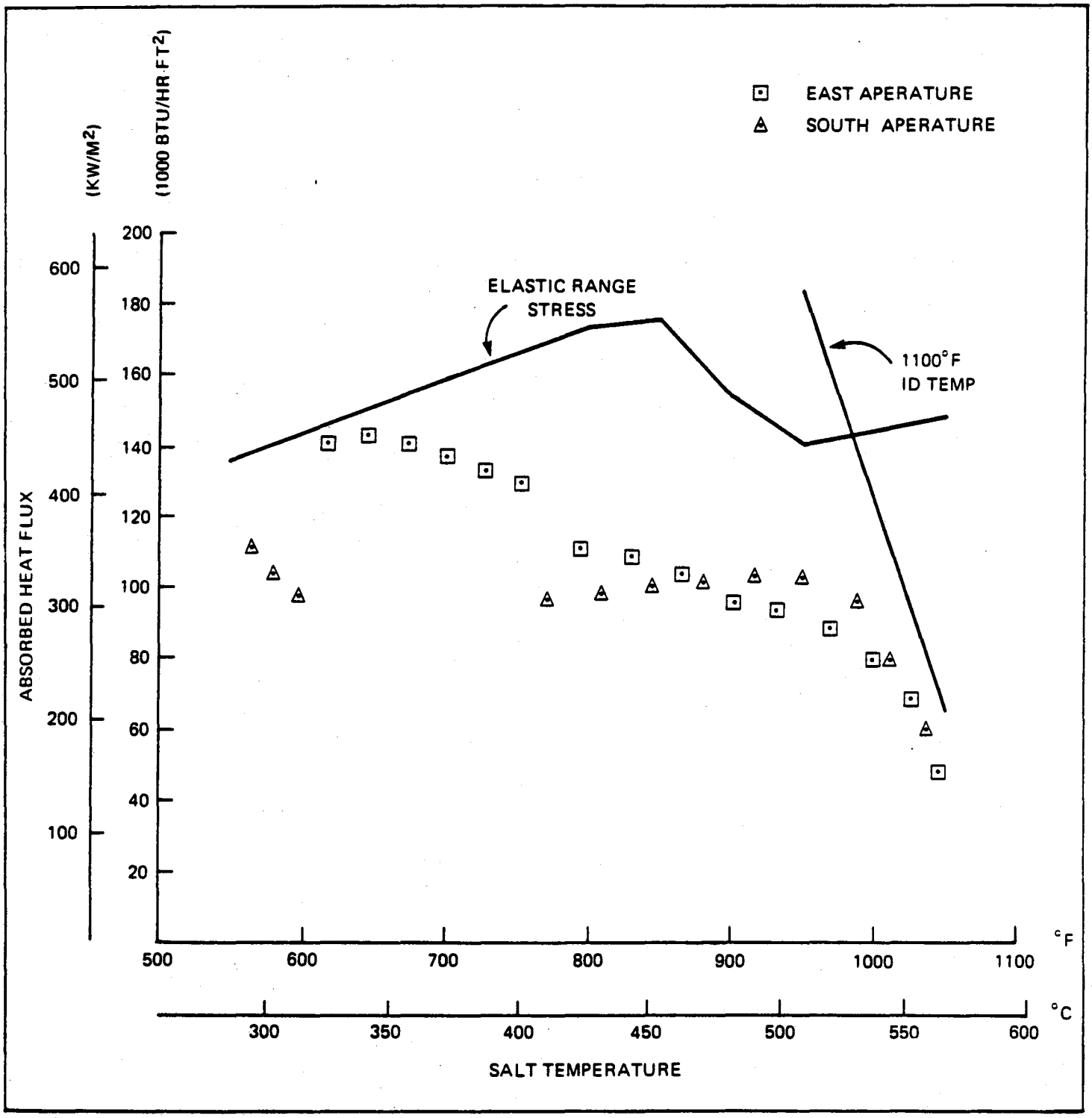

FIGURE 2.24 - ZONE 2 PEAK FLUX AND LIMIT

- Skewed heating effects which can reduce the allowable heat flux limit in some panels by as much as one-third.
- Peak insolation conditions.
- Daily and yearly flux distribution variations.
- Cloud transient conditions.
- Flux prediction errors.
- Design uncertainties such as salt properties, metal properties, tube thickness variations, etc.

Overall the heat flux levels predicted are felt to support prediction of receiver panel life of 30 years.

The prediction of heat fluxes for the current design is based upon the aiming philosophy described in the proceeding section. These studies were based on the heliostat field and receiver geometry of the Alternate Central Receiver Power system, Phase II [Ref. 1] Commercial Receiver Design Update. As studies progressed, it became apparent that flux levels possible with this receiver configuration would not allow sufficient margin below the allowable flux limits to permit conservative design. Because of this, the surface within the receiver cavities was increased by scaling up the geometry and increasing the area of each wing wall. Fluxes from the previous design were then scaled down based on the assumption that increases in surface by geometric scaleup of the receiver geometry leave the distribution of flux relatively unaffected, while reducing its magnitude in inverse proportion to the surface increase. This scaling process, while approximate, is sufficiently accurate for the purposes of sizing.

2.3.4 Panel Sizing

The receiver heat absorption surface is made up of vertical panels, each conducting the molten salt flow for one pass of heat pickup. The goal of sizing these panels is to achieve the most economical coverage of the surface without exceeding the limitations of the panel material. In order to achieve this goal, the following design objectives are set.

- Maximum heat transfer coefficient is desirable to maximize the allowable heat flux without overheating or overstressing the tube material.
- Minimum flow circuit pressure drop is desirable to minimize the energy requirements of the booster pumps.
- Maximum tube diameter is desirable to minimize panel fabrication costs by reducing the total number of tubes and welds.
- Panel widths must be held below a reasonable limit to avoid large lateral heat flux and salt temperature differences.

To meet these objectives, the designer has the flexibility to select the tube diameter and the salt flow per tube or number of tubes in a pass (since total salt flow is prescribed). These two parameters also set the pass width. A parametric study comparing many configurations of varying pass width and tube diameter was conducted. Based on the criteria described above, a two inch diameter tube with 79,000 lbm/hr salt flow per tube was selected. A discussion of the relationship between panel sizing and the criteria for economic design follows.

Thermal Stress

The factor limiting the allowable heat flux for most of the surface within the receiver is the allowable thermal stress. As shown in Section 2.3.1, for a given geometry, this thermal stress is a function of the tube wall resistance, heat transfer coefficient, and the absorbed heat flux. For a .065 inch tube wall thickness and a specified maximum thermal stress limit, the allowable heat flux will be a function of the heat transfer coefficient as shown in Figure 2.25. This allowable heat flux limit is not sensitive to tube diameter or salt temperature, although the heat transfer coefficient and allowable stress limits are. As can be seen, with higher heat transfer coefficients, higher heat fluxes are allowable. This allows economic design by minimizing the total surface required to absorb the design power.

Pressure Drop

To achieve a desired heat transfer coefficient, the designer has the freedom to select a tube size, then set the flow per tube to the value required by the heat transfer coefficient correlation. Figure 2.26 illustrates the relationship between tube diameter and pass width for various heat transfer coefficients. For the same coefficients, Figure 2.27 presents pressure drops, as a function of tube diameter, for flow dircuits covering a given area. As can be seen in Figure 2.26, small diameter tubes require wide pass widths for the same total flow and heat transfer coefficient. Wide passes with small tubes, however, are shown in Figure 2.27 to offer lower pressure drops for the same heat transfer coefficients.

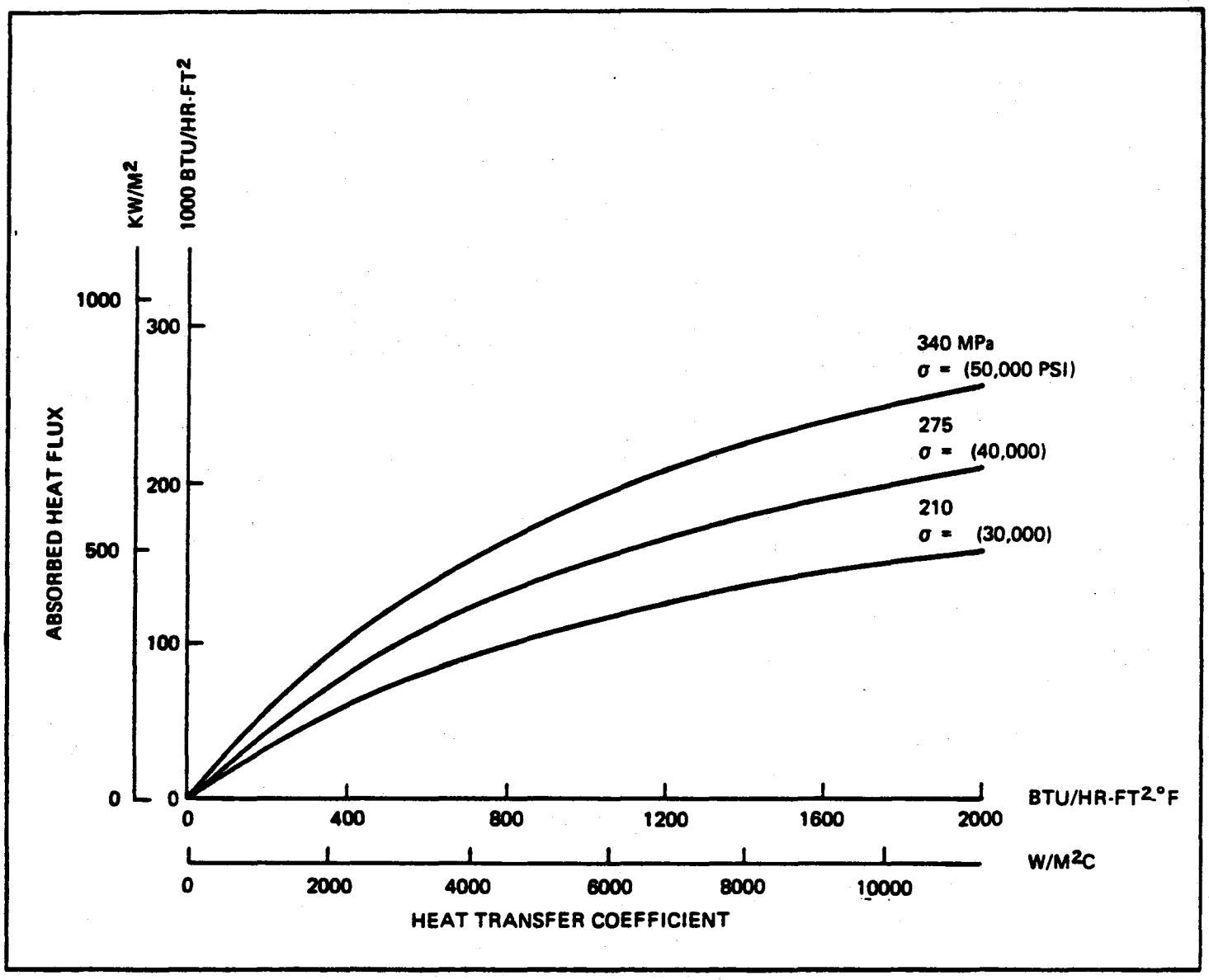

FIGURE 2.25 - PREDICTED TUBE THERMAL STRESS

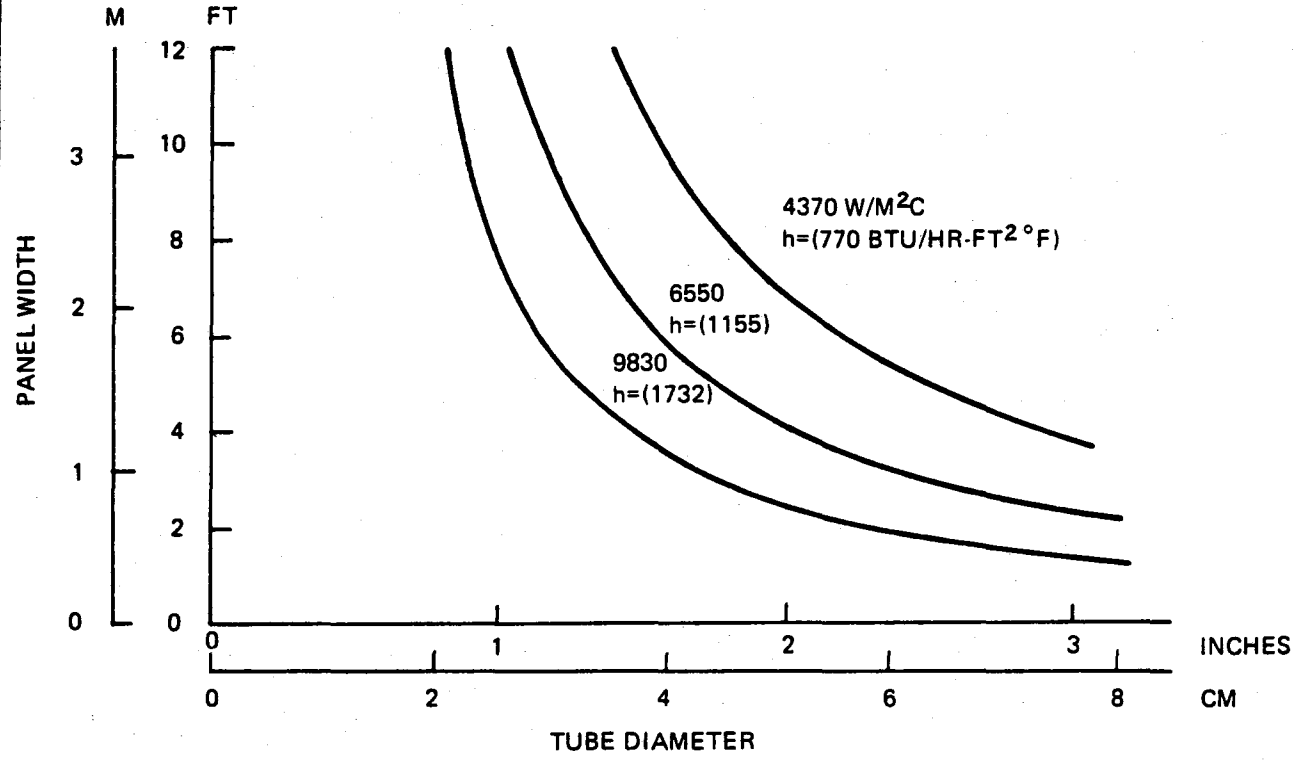

FIGURE 2.26 - PANEL SIZING FOR EQUIVALENT HEAT TRANSFER COEFFICIENT

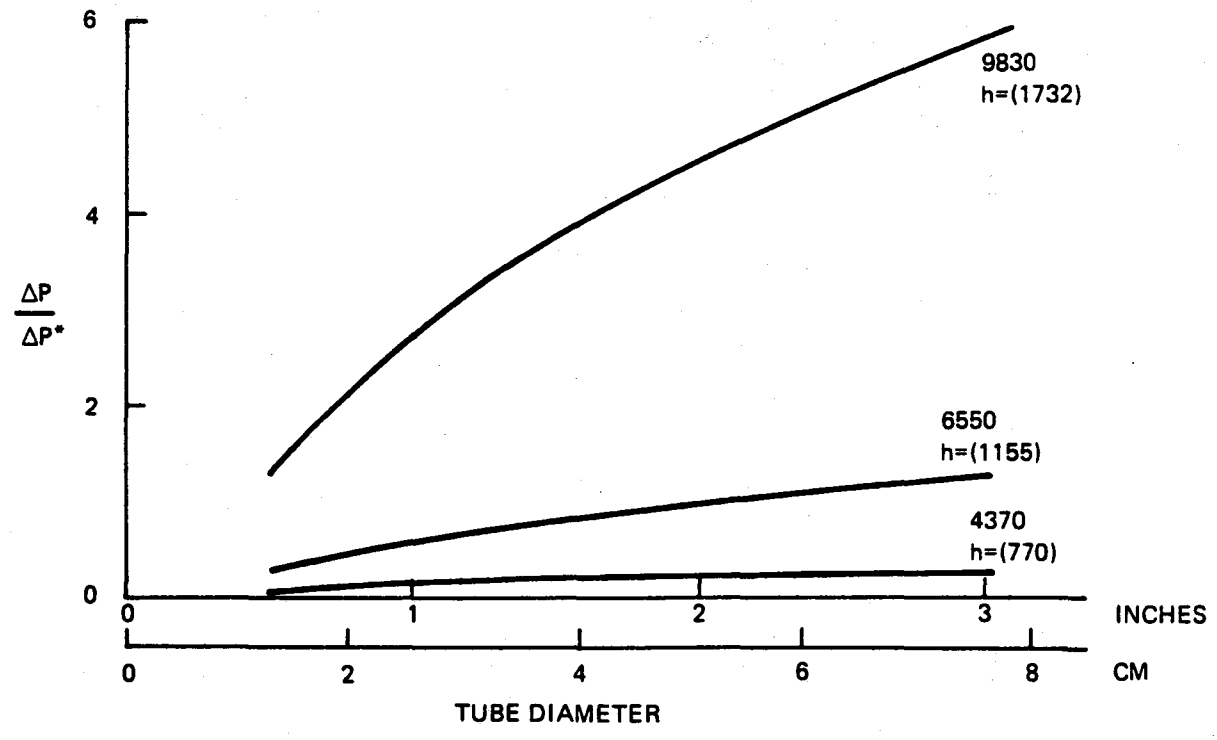

FIGURE 2.27 - RELATIVE PRESSURE DROP WITH EQUIVALENT HEAT TRANSFER COEFFICIENT

Tube Diameter

Aside from the impact on heat transfer coefficient and pressure drop, there is an important direct effect of tube diameter on panel cost. For larger tubes, fewer total tubes will be required to cover a given total surface. This reduces the number of welds in the panel and thus total fabrication costs. This effect is important as the panels are a major cost item in the receiver subsystem.

Panel Width

Lateral heat flux gradients across a panel result in non-uniform heating of the salt within the tubes and lateral differences in metal temperatures. This will tend to cause deflections and stresses within the panels which are difficult to quantify and accommodate by prudent design. These effects are minimized however if relatively narrow pass widths are used.

Summary of Panel Sizing

Combining considerations of the four criteria; namely, thermal stress, pressure drop, tube diameter, and panel width, the two inch diameter tube with approximately 79,000 lb/hr per tube was selected as the best compromise. This selection offers a design with:

- Relatively few tubes and welds
- Adequate heat transfer coefficient (in the 800 - 1200 btu/hr-ft^2 range)
- Relatively narrow pass widths and thus minimum concern over lateral gradients
- Total panel friction pressure drop at design point of approximately 310 psi and a circuit pressure drop of

approximately 390 psi (including piping and header losses). This value is relatively high but within panel pressure limits and within currently available booster pump technology.

2.3.5 Membrane Sizing

The web geometry is established by observing the temperature/stress change that results for a given incremental change in width and thickness. Table 2.3 summarizes the results for various web sizes. 1/16" increments (width, length) were evaluated using the Membrane Wall Program (Program 158). Optimization of the web dimensions was based on limiting web temperature, balancing elastic axial stress between the tube crown and the web, fabriction costs, and welding limitations. A 0.218" width and a 0.125" thickness were selected because this combination resulted in lower web temperatures and stresses than those at the tube crown. Also, fabrication costs for this configuration were lower than for other geometries investigated. The following significant results were obtained:

1. Decreasing web width decreases web axial stress considerably while tube axial stress increases slightly.
2. Decreasing web thickness increases web axial stress considerably while tube axial stress remains constant.
3. Maximum tube crown temperature remains constant for any web size.
4. Maximum web temperature decreases with decrease in web width but increases for decrease in web thickness.

The conclusion reached is that a web dimension of 0.218" x 0.125" is optimum for solar receiver application yielding a lower maximum temperature and stress than those present in the tube.

TABLE 2.3

MEMBRANE DIMENSIONING

$Q = 100{,}000$ Btu/Hr-Ft^2 (One-Sided Heating)

Web Size Width x Thickness	Axial Stress, KSI $\sigma_{webmax}/\sigma_{tubemax}$	Temperature, °F $T_{webmax}/T_{tubemax}$
3/8" x 1/8"	-57 -28	329 192
5/16" x 1/8"	-45 -30	265 192
1/4" x 1/8"	-33 -32	205 192
3/16" x 1/8"	-23 -33	153 192
1/4" x 1/4"	-26 -32	178 192
1/4" x 3/16"	-28 -32	184 192
1/4" x 1/8"	-32 -32	204 192
1/4" x 1/16"	-51 -32	280 192

2.3.6 System Hydraulics

The heat absorption panels are arranged in multi-pass, serpentine flow paths. Based upon previous studies [Ref. 1], a four control zone configuration was selected. Cold salt flow is introduced to the receiver zones in high flux regions, and proceeds toward the lower flux regions with hot salt flow exiting each zone at the end of the wing wall. This flow path provides the maximum utilization of the panel heat absorption capability.

The resulting configuration has 22 heat transfer passes in each of the two zones on the north side of the receiver, and 27 passes in each of the two southerly zones (Figure 2-5).

Pressure Drop Summary

Figure 2.3 illustrates the main parts of the subsystem. The molten salt flow path for the receiver subsystem begins at the main salt booster pump at the base of the riser. From here, flow is pumped up the riser to the surge/buffer tank located at the level of the panel upper headers. Flow then splits into the four control zones, passes through the main flow control valves, and the heat transfer surface. Hot salt exiting the control zones is recombined in the collection tank located at the level of the panel lower headers and then exits the tower via a downcomer. Flow passes through the energy dissipation control valve at the base of the downcomer where the unusable static pressure remaining in the salt is broken down.

Maximum pressures occuring within the unit will occur at design point conditions but with an absorbed thermal power 15% higher than design point corresponding to an assumed solar direct isolation level

of 1100 w/m^2 incident on the collector field, as opposed to the design value of 950 w/m^2. This condition results in 15% higher flow rates and 32% higher pressure drops within the system.

Pressures within the system are based on the collection tank pressure where the static head salt pressure for a column of salt rising to the surge buffer tank salt level is maintained (65 psi). This assures positive pressure throughout the system, thus avoiding the formation of voids within downflowing salt. Table 2.4 summarizes the design point pressure drops within the heat absorption panels. The absorption panels are designed for a maximum operating inlet pressure of 513 psi to allow for operation at maximum (115%) power.

TABLE 2.4

Design Point Pressure Drops

	North	South
	Zones I & IV	Zones II & III
Salt Flow (lb/hr)	1.754×10^6	1.171×10^6
Passes	22	27
Tube/Pass	22	15
Pressure Drops (psi)		
Tube Friction	283	314
Header Losses	70	65
Piping Connections	15	8
TOTALS	368	387

The main booster pumps at the base of the 20 inch diameter riser consist of two half capacity vertical multistage pumps, each with 3500 H.P. variable speed motors, and are designed to support 115% of design flow in the system. The downcomer consists of two 14 inch lines with a control valve at its base to dissipate pressure and control flow out of the collection tank so its level may be maintained.

Circulation Line

Between the collection tank and the surge/buffer tank, a circulation line exists with a circulation pump which allows a 10% forced recirculation flow during hot standby. This flow allows the use of the surge/buffer tank and collection tank inventory as heat storage to maintain panel temperatures for overnight hold.

Downflow Stability

With the heat absorption panel arrangement incorporated in the design, half of the panels contain salt flowing downward, while it is being heated. This configuration of "heated downflow" in parallel tubes has led to problems in various types of heat exchange equipment in the past. This condition is due to the upward buoyancy force on the fluid which will tend to increase with decreasing flow velocity. This will tend to further decrease velocity in some tubes, and can lead to flow imbalances which could be detrimental to the operation of a receiver.

The nature of this problem depends upon the relative balance between pressure differentials due to gravity (buoyancy) forces, and those caused by frictional effects. For the solar receiver design presented, however, frictional effects outweigh the buoyancy effects such that even at low flow rates associated with minimum (25%) power

operation, no problems are expected and only minimal caution is required during startup to avoid the problem.

The pressure differential between the upper and lower headers of a heat absorption panel is the combination of the gravity and frictional effects, with gravity negative as it acts in the flow direction:

$$\Delta P = \Delta P_{frictional} - \Delta P_{gravity}$$

Because of its nature, the frictional pressure drop decreases with decreasing flow. With heat input being constant, flow reductions result in higher salt temperatures within a tube and thus lower salt densities which result in a smaller gravity term as well. Because the system pump sets up the pressure differential between panel headers required to force the total flow through the panel, a reduction in frictional pressure drop due to a flow perturbation in a single tube results in a pressure imbalance which tends to accelerate the flow in that tube, returning flow to its original value which is stable. A reduction in the gravity pressure drop, however, because it appears as a negative term, results in a pressure imbalance which tends to decelerate the flow further. The stability of a panel flow/heat absorption condition, therefore, depends upon the balance of the stabilizing friction drop effect vs. the destabilizing buoyancy effect. If the formulation for both terms are written, and appropriate derivatives are taken, the stability is found to depend upon the non-dimensional parameter:

$$[32f/\pi^2 d^5 \rho^2 g\beta]\ \dot{m}^2/\Delta T \text{ or } [2f/dg\beta]\ v^2/\Delta T$$

where,

f - is the tube friction factor

d - is the tube inside diameter

ρ - is the salt average density

β - is the salt volume coefficient of expansion

ΔT - is the header temperature difference

$\dot{m}'$ - is the per tube mass flow rate

v - is the salt velocity

If this parameter is greater than unity, stability is indicated.

For the current unit, this parameter is found to be:

$$6.417 \times 10^{-7} \ (lbm^2/hr^2-{}^oF) \times \dot{m}^{\ 2}/\Delta T$$

Figure 2.28 illustrates the stable and unstable operating regions based on this parameter, along with the operating region of the unit. For the minimum operating power level of 25%, flow per tube in the unit will be approximately 19500 lb/hr/tube and the maximum temperature rise in a pass is less than 40^oF. The stability parameter for this case is 6.1.

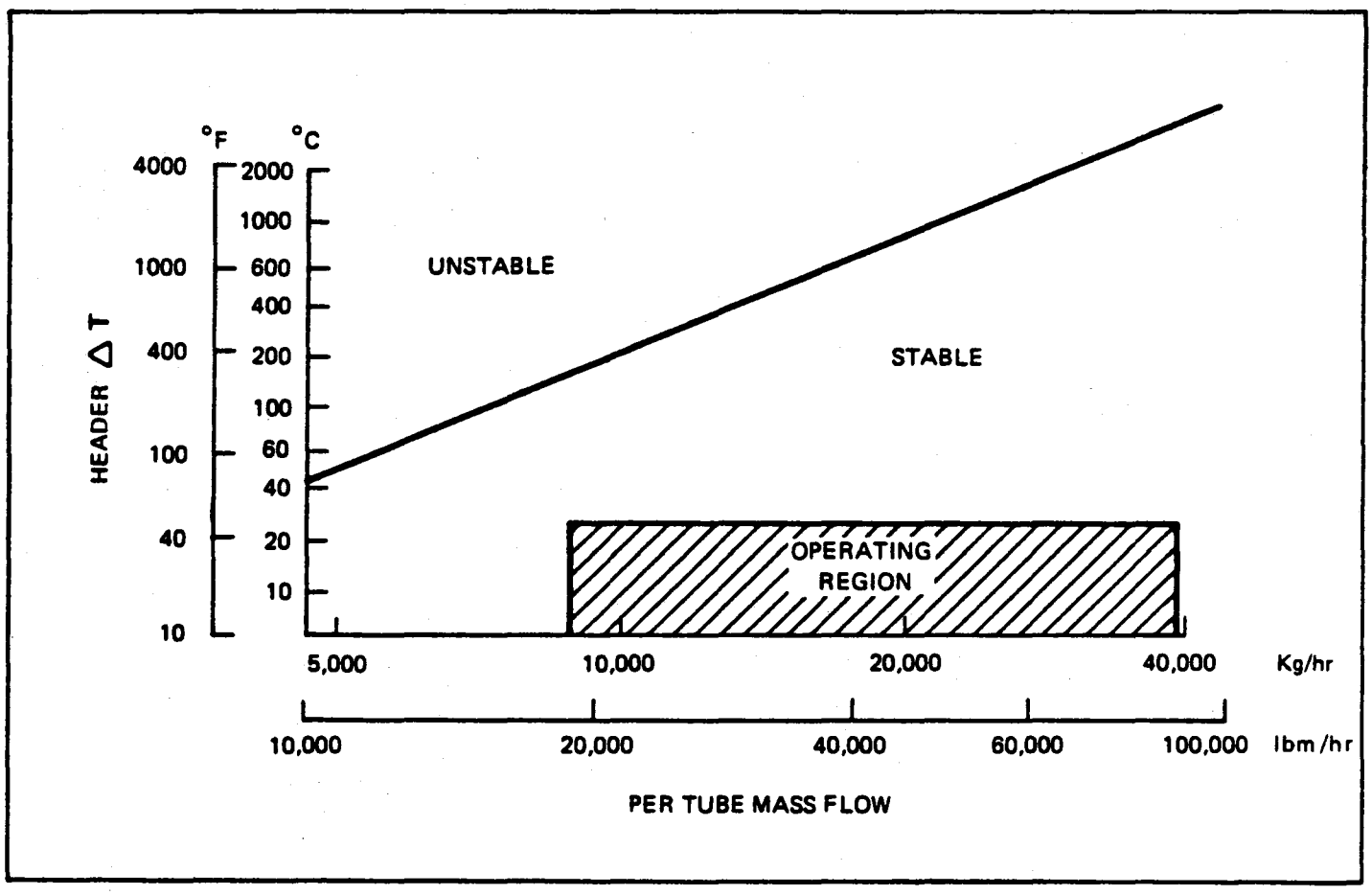

FIGURE 2.28 · DOWNFLOW STABILITY MAP

At design point flow, this factor is approximately 100.

As a point of caution, however, at flows below 25%, the stability factor drops quickly. Thus startup should be performed by establishing 25% flow before significant power is focused on the receiver. This avoids initiation of recirculation in the panels which would continue as power was ramped up.

2.3.7 Receiver Efficiency

Accurate prediction of solar receiver efficiency* is of great importance in establishing the overall first cost of a complete solar central receiver thermal power generating system. Over-prediction of the efficiency of a central receiver would result in the specification of a disproportionately smaller number of heliostats than otherwise would have been required (additional heliostats of necessity are far-field heliostats and thus of lower efficiency than average in terms of input to the receiver aperture). For example, if total heliostat requirements for a 100 MWe plant were underestimated by 5%, the plant would underperform. The total cost to supply the additional heliostats required to meet performance would cost as much as $8M (if in fact they could be added). Contrarywise, overestimation could lead to an oversize plant, the cost of which may be judged uneconomic.

An evaluation of receiver efficiency requires the development of analytical techniques. In developing these techniques, thermal losses from the cavity were separated into the following mechanisms:

---

*The thermal efficiency of a cavity receiver is defined as the ratio of the total energy retained by the working fluid (molten salt) to the total energy entering the aperture.

- Radiation losses
  - --Infrared reradiation
  - --Reflection (visable)
- Convection
- Conduction

Methods were determined which estimate natural convection, reradiation, reflection, and conduction losses. This section describes these methods briefly and presents the estimate of the efficiency of each cavity of the receiver. A more detailed description of the calculations is found in Appendix F. The resulting calculated losses are found in Tables 2.5 and 2.6 and Figures 2.29 and 2.30.

Radiant Losses

Radiation losses were calculated using a two banded spectral model for emissivities. Aperture view factors were calculated for each cavity surface and checked to insure that the total view factor for the aperture was equal to one. Average temperatures were estimated by integrating the emissive powers over each cavity surface. It was assumed that the radiant temperature of the sky and ground was $400^{\circ}K$. This corresponds to a radiant background flux of 44 $Btu/Hr\text{-}Ft^2$. This flux may seem low considering that the ground temperature may be as high as $580^{\circ}K$ (194 $Btu/Hr\text{-}Ft^2$), however, it must be remembered that the aperture sees the sky by oblique reflection from the mirrors.

Reflection

Since the surfaces with incident solar flux are not absolutely black, the effect of reflection was computed and added to the radiant losses. It was assumed that five percent of the incident light was

TABLE 2.5

RECEIVER LOSSES

Total Receiver Insolation - 1.201×10^9 Btu/Hr

	N	S	E/W
Total Insolation Absorbed	$.4197 \times 10^9$	$.1446 \times 10^9$	$.528 \times 10^9$
Incident	$.4571 \times 10^9$	$.1594 \times 10^9$	$.5836 \times 10^9$
Losses			
Radiant			
Re-radiation	.0135	.00496	.0215
Reflection	.00457 (1%)	.00136 (.85%)	.0055 (.94%)
Convection			
Natural	.018	.0080	.0264
Conduction			
Roof	.000385	.000200	.000600
Floor	.000255	.000132	.000400
Wall (panels)	.000688	.000188	.00118
TOTAL	.0374	.0148	.0556
Percent Loss Per Cavity (cavity loss/cavity power)	8.18%	9.31%	9.53%

TABLE 2.6

RECEIVER LOSSES IN PERCENT OF TOTAL

	N	S	E/W	Total
RADIANT				
IR Reradiation	1.12	.41	1.79	3.32
Visable Reflection	.38	.11	.46	.95
CONVECTION				
Natural	1.5	.67	2.20	4.37
CONDUCTION				
Roof	.032	.017	.050	.099
Floor	.021	.011	.030	.062
Walls	.057	.016	.098	.171
				8.97

Receiver Efficiency = 91%

N = North Cavity

S = South Cavity

E/W = Total East and West Cavities

diffusely reflected to either the aperture or another cavity internal surface. The proportion of reflected light that remained in the cavity was estimated using a catalog of view factors (Reference 4).

Convective Losses

Cavity receiver convective losses have been the subject of much research and controversy. After investigating available methods, it was decided to use the method of Clausing (References 5, 6, 7). This method solves three equations simultaneously to yield values for aperture velocity, cavity temperature, and heat transport.

In order to be assured of reasonable accuracy, the convection coefficients were calculated on a panel by panel basis with separate coefficients for the ceiling, floor, and other inactive surfaces. For these coefficients to be calculated, it was necessary to estimate the surface temperatures. For inactive surfaces, an estimate was made of total incident and radiant flux, and therefore, the equilibrium radiant temperature. For active surfaces, typical temperature profiles around the tubes and along the length of the tubes were averaged by integration (in the case of radiation, the flux was averaged). This yielded an equation for average temperature as a function of average salt temperature and tube temperature. Convective losses were calculated using the temperature difference between the average panel temperature and the temperature of the air inside the cavity.

Conduction Losses

Conduction losses were estimated with a simple conduction model using conductivities and insulation thicknesses for each surface.

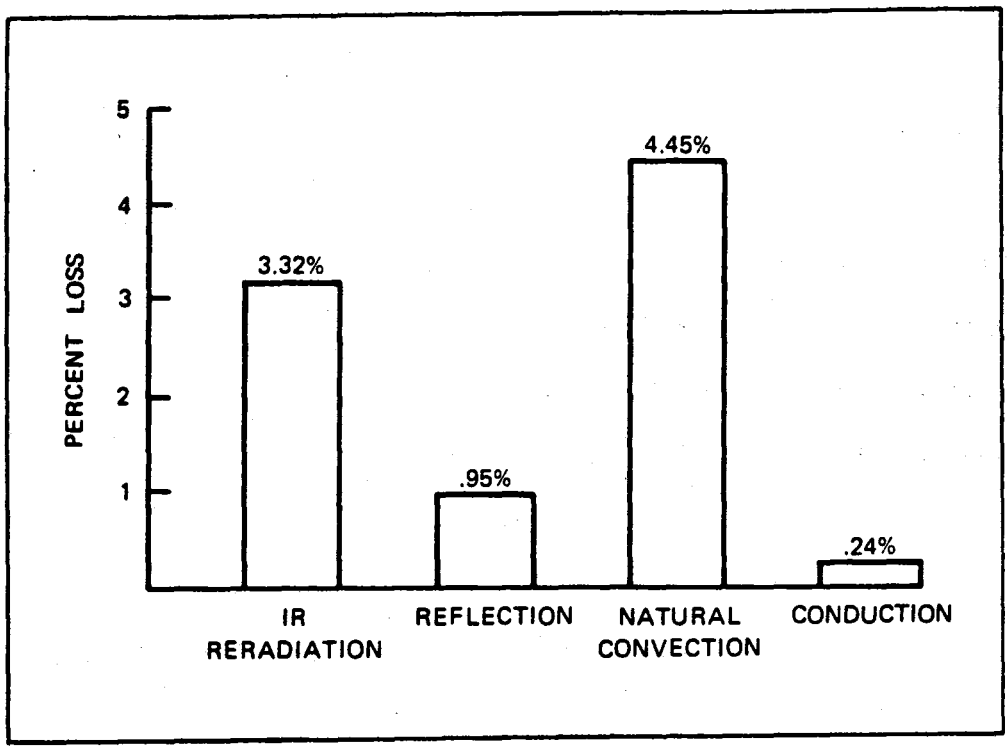

FIGURE 2.29 - RECEIVER LOSSES BY TYPE

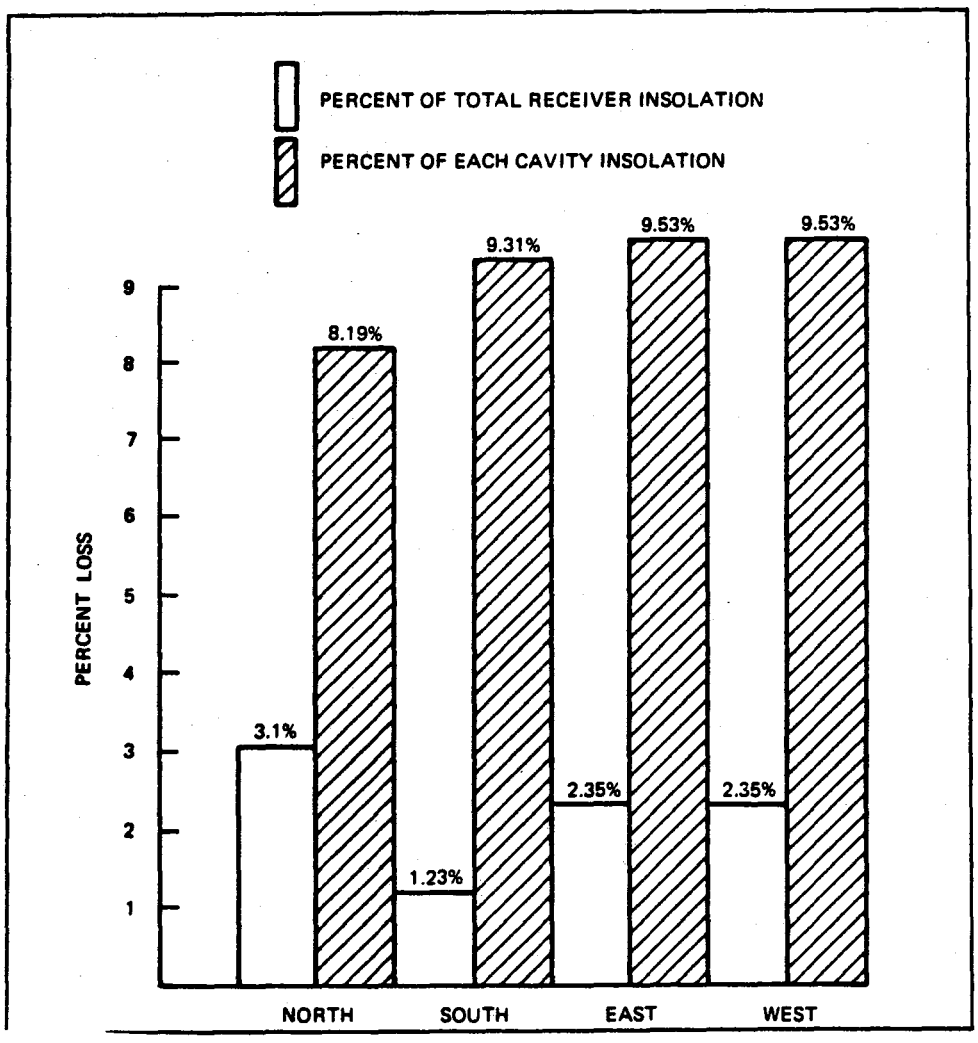

FIGURE 2.30 – RECEIVER LOSSES BY CAVITY

Uncertainties in Convection Calculations

Because of the nature of the calculations, it is probably prudent to put a tolerance of about 30% on convention losses. Until data can be taken from a receiver with dimensions and temperature differences on the same order of magnitude as the receiver design, it will be difficult to extrapolate the correlations. Therefore, it is necessary to estimate the possible errors associated with convective losses.

1) Boundary layer effects - vertical tubes can be viewed as a flat surface with a roughness when the tube diameter is small in comparison to the laminar sub-layer. With this design, the sub-layer is less than 3/16 inch. The value of this thickness is large at the bottom of the tubes and small at the top where the flow is more fully developed. It is expected that this effort will result in a slight reduction (less than 10%) in the predicted natural convection losses.
2) The heat transfer correlation used in this analysis was derived from the dry cryrogenic nitrogen data. Under operating conditions, the actual fluid will be a mixture of air and a small percentage of water vapor. Property variation could therefore yield a significant error (+20%).
3) Since carbon dioxide and water vapor will be present in the air, it will be reasonable to expect that infrared radiation from the tubes will be absorbed by the air within the cavity and convected out. This effect becomes more pronounced as the cavity size increases and is estimated to reduce overall receiver efficiency by as much as one percent.

4) The heat transfer model assumes a flow distribution through the receiver which allows the use of external receiver heat transfer correlations. Variations in this distribution could inhibit or enhance heat transfer in the cavity and alter the average cavity temperature.

Summary of Results

The overall receiver efficiency, at design point conditions, was estimated to be 91%. The major losses were found to be natural convection with 4.45 percent of the total insolation and radiation with 4.27% of the total insolation.

These convective calculations are based upon a correlation of small scale cryrogenic experiments using dry nitrogen as a working fluid and have no basis in full scale tests. Therefore, it is expected that these results may be accurate to + 30% of the calculated losses. The prediction of radiation losses are directly dependent upon the accuracy of shading factors whose error may be + 20%. This suggests that the range of receiver efficiency will be between 89% and 93%. However, some losses such as forced convection and infrared absorption by the air within the cavity have not been included in the calculations due to the complexity and uncertainty of the solutions. These effects may be significant in a receiver of this size.

It was found that these values could be as much as 30% off of the nominal predicted values and that further testing is required on receiver cavities of larger scale.

2.4 Mechanical Design of Pressure Boundary

This section covers the mechanical design of the panels, headers, and tanks. The interconnecting piping is discussed along with the main riser and downcomer piping in Section 3.1.

2.4.1 Design of Panel Assembly

General Description

The panel assembly consists of a number of tubes formed into a membrane wall, headers, insulation, and bracing steel. Two widths of panels are required for this receiver, namely 4'-0 and 2'-8" widths. Figure 9.4 shows the construction of a typical panel assembly. Various lengths of panel are required depending on the location within a given cavity. Panels in a wing wall, for instance, vary in length according to a 2:1 slope of heated panel surface. The panel assembly is shop fabricated which facilitates erection by minimizing field installation work. The lateral support system with the panels, (in position) serves to restrain the membrane panel removing loads such as wind and seismic.

Codes

The basic mechanical design criteria applied to the receiver tubes and headers is Section I, "Power Boilers" of the ASME Boiler and Pressure Vessel Code and in accordance with the Power Piping Code, ANSI/ASME B31.1. The remainder of the panel assembly meets the requirements of the Uniform Building Code (UBC) and the Standards of the American Institute of Steel Construction (AISC).

Panel Supports

The major components of the panel support arrangement are shown on Figure 2.31. The heat absorption panels are designed with horizontal buckstays attached to the tubes via small lugs welded to the tubes. Roller connections attached to the horizontal buckstays permit thermal growth in the vertical direction and transfer lateral loads to vertically oriented wide flange members (vertical buckstays) that are bolted directly to main structural steel. Single angle bracing welded to a pair of vertical buckstays forms a plane truss enabling the panel assembly to transfer lateral loading in a side to side direction. Six inches of shop installed insulation is placed on the backside of each panel and is in direct contact with the tubes. Aluminum lagging and tie-backs hold the insulation in place but the buckstays attached to the panel support the insulation weight. Expansion joints in the lagging allow for differential thermal expansion.

Vertical plug seals held in place by lagging connect adjoining panels and insulation, effectively sealing the cavity enclosure. Two joint closures are shown in Figures 2.32 and 2.33.

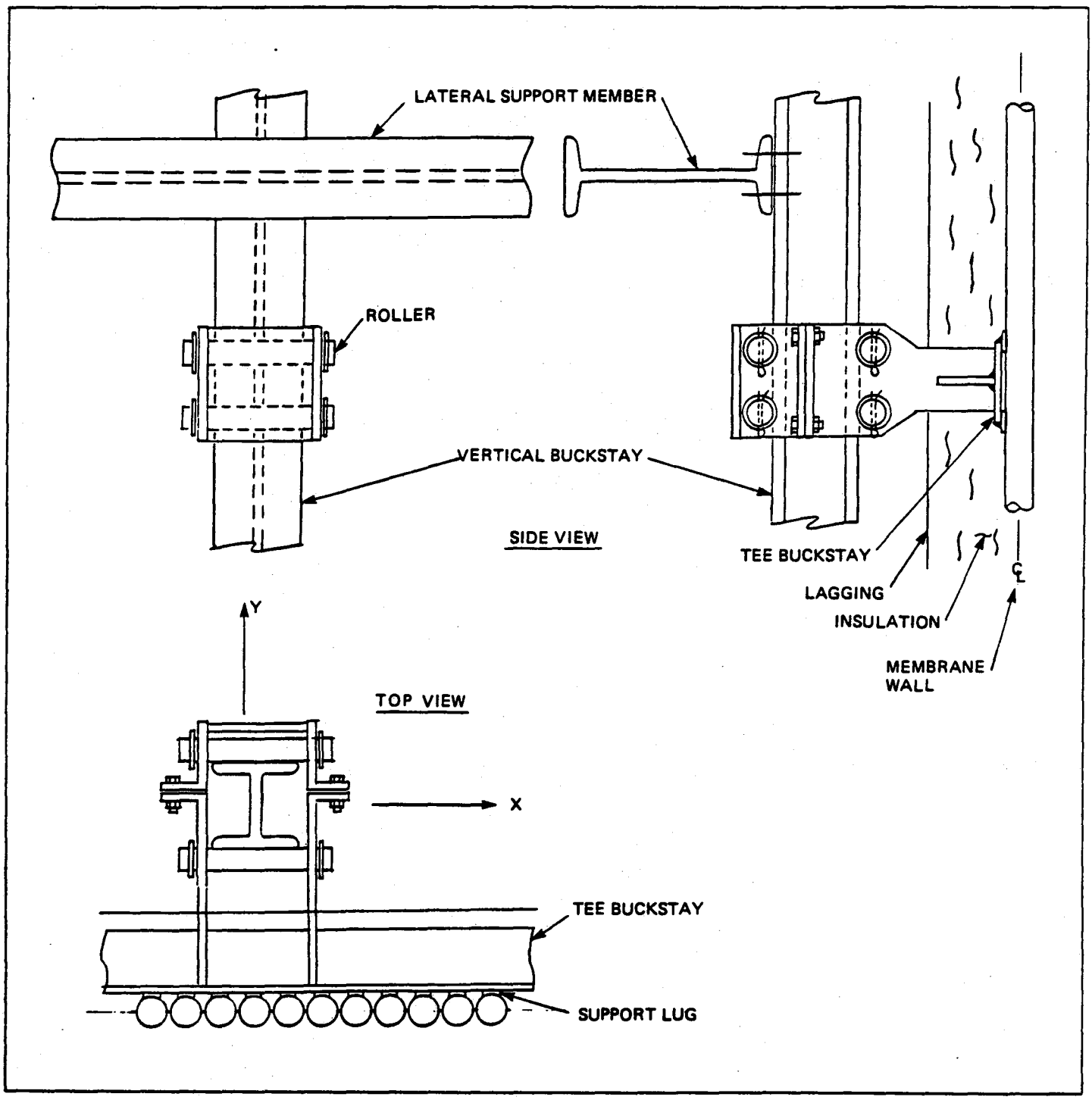

FIGURE 2.31 · PANEL SUPPORTS

THE BABCOCK & WILCOX COMPANY

POWER GENERATION DIVISION

REVISIONS			MICRO-FILM
DASH NO.	DATE	DESCRIPTION	ORIG.

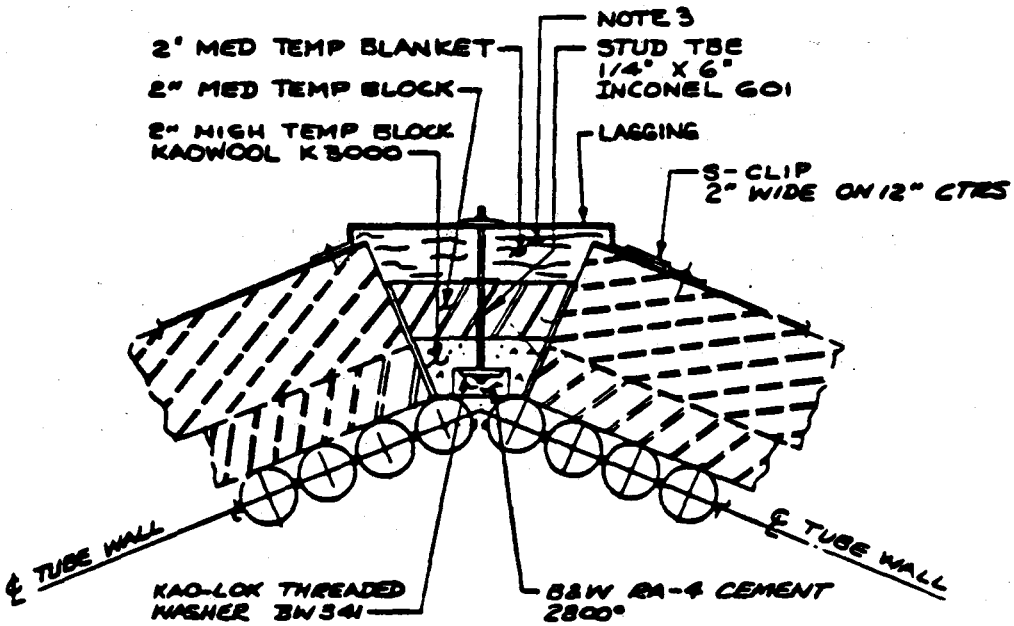

SECTION R-R

ANGLE JOINT CLOSURE ASSY

FIGURE 2.32

DWG. BY LAMB	CHK'D RGK	ANGLE JOINT CLOSURE ASSY	SCALE NV	DATE 10-20-82
PASSED BY RGK	APP'D		DRWG. NO.	A-

BRUNING 16635

FORM BBW 1067 A-8

THE BABCOCK & WILCOX COMPANY

POWER GENERATION DIVISION

REVISIONS			MICRO-FILM
DASH NO.	DATE	DESCRIPTION	ORIG.

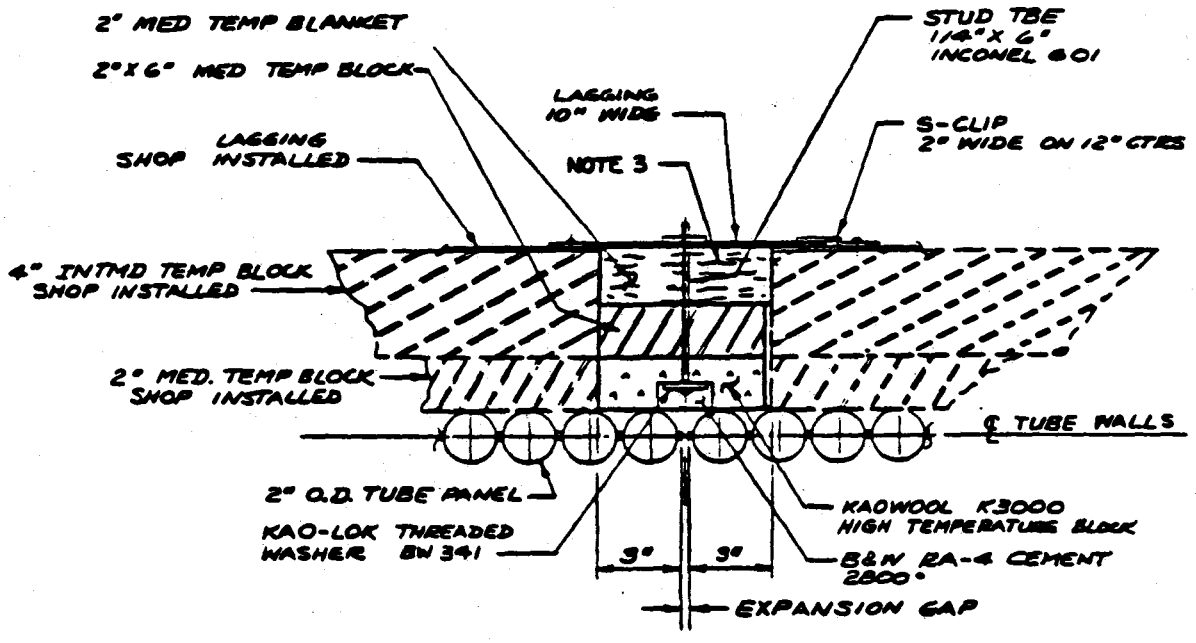

SECTION S-S

PANEL JOINT CLOSURE ASSY

FIGURE 2.33

DWN. BY LAMB	CHK'D RGK	PANEL JOINT CLOSURE ASSY	SCALE NV	DATE 10-20-82
PASSED BY RGK	APP'D		DRWG. NO.	A-

BRUNING 16635

FORM BGW 1987 A-2

Structural Connection

In position, the absorption panels are hung from top support steel to accommodate thermal growth similar to a conventional boiler. Maximum elongation for the longest panel is approximately 9 inches. The vertical buckstays are hung by separate hangers. The weight of the horizontal buckstays, roller connections, and insulation is supported by the receiver panels. Four bolt connections tie the vertical buckstays to main steel and are shown in Figure 2.31. The spacing of members framing into the vertical buckstays is set to avoid interference with the roller connections. The members include struts and diagonals of the panel assembly and main steel beams.

The depth of the wing wall is based upon the physical distance between panels of different cavities required to place the lateral support system. Since a minimum distance yields a smaller overall receiver size, the depth of the panel assembly and the main steel members was kept to a minimum (set at 5'-0" from centerline of panel walls).

Materials

Due to prevailing high temperature (1050^{o}F maximum), Type 304 stainless steel was selected as the material for the lugs, tee-buckstays, and roller connection. The vertical buckstays and diagonal bracing shall be A36 carbon steel.

Material selection for the pressure components of the panel assembly are SB-163 800H Incoloy for the absorption tubes, TP 304 SA 312 stainless steel for the headers, and TP 304 SA 213 for the tube safe ends.

Stress and Deflection Requirements

The panel design is established on the basis of internal pressure, deadweight, frequency of vibration, wind, seismic, and thermal loads. The spacing between lateral buckstays has been set at 15'-0 for the membrane wall design. This is based on a horizontal earthquake loading using a seismic factor of 0.82 which controls over a wind load of 30 psf. To check the spacing, the absorption panels are assumed to act as beams having fixed supports at the lateral buckstays. The resulting bending moment is therefore,

$$M_x = \frac{w\ell^2}{12}$$

where ℓ = spacing and w = horizontal load = 10.38 lbs/in

$$M_{xa} = F_{bx} S_x (1.33) = 54620 \text{ in-lb}$$

where $F_{bx} = 0.66 F_{yield} = 0.66 (15.28 \text{ ksi}) = 10.08 \text{ ksi}$

$(T = 1100^{\circ}F)$

$S_x = 4.07 \text{ in}^3$ (one 4'-0 panel)

1.33 = increase for non-gravity load.

M_{xa} = allowable bending moment

F_{bx} = allowable bending stress

S_x = panel section modulus

Maximum spacing between buckstays is

$$\ell \leq \sqrt{\frac{12 \text{ Mxa}}{w}}$$

$$= \sqrt{\frac{12 (54620)}{10.38}}$$

$$= 20'-9"$$

Due to the presence of insulation and to prevent cracking of paint on the receiver surface, maximum panel deflection between restraints is limited to,

$$\Delta_{max} \leq \frac{\ell}{360} = 0.500 \text{ in.}$$

$$\Delta_{max} \text{ (earthquake)} = \frac{w^4}{384\ EI} = 0.302 < 0.500 \text{ in.}$$

where E = modulus of elasticity (Inconel 800H @ T = 1100°F)

I = moment of inertia of a panel

The absorption panels are designed to exceed a natural frequency of 5 hertz which is above that of the tower. Figure 2.34 shows the effect on frequency when the unsupported length is increased. Three types of boundary conditions are considered - pin-pin, pin-pin w/tension, and clamped-clamped. The frequency of the membrane wall was also determined to be a controlling factor for establishing the proper spacing of buckstays. For fully restrained supports and neglecting the effects of tension,

$$f = \frac{[(2i + 1)\ \frac{\pi}{2}\ ]^2}{2\pi\ell^2} \left(\frac{EI}{m}\right)^{1/2}$$

where i = 1 for first mode shape

ℓ = spacing (inches)

E = Young's modulus for Inconel 800H at T = 1100°F

I = moment of inertia of a 2" O.D. x 0.65" tube

m = mass = $\frac{WT.}{g}$, WT. = weight of tube and fluid per inch of length

g = 386.0 in./s^2

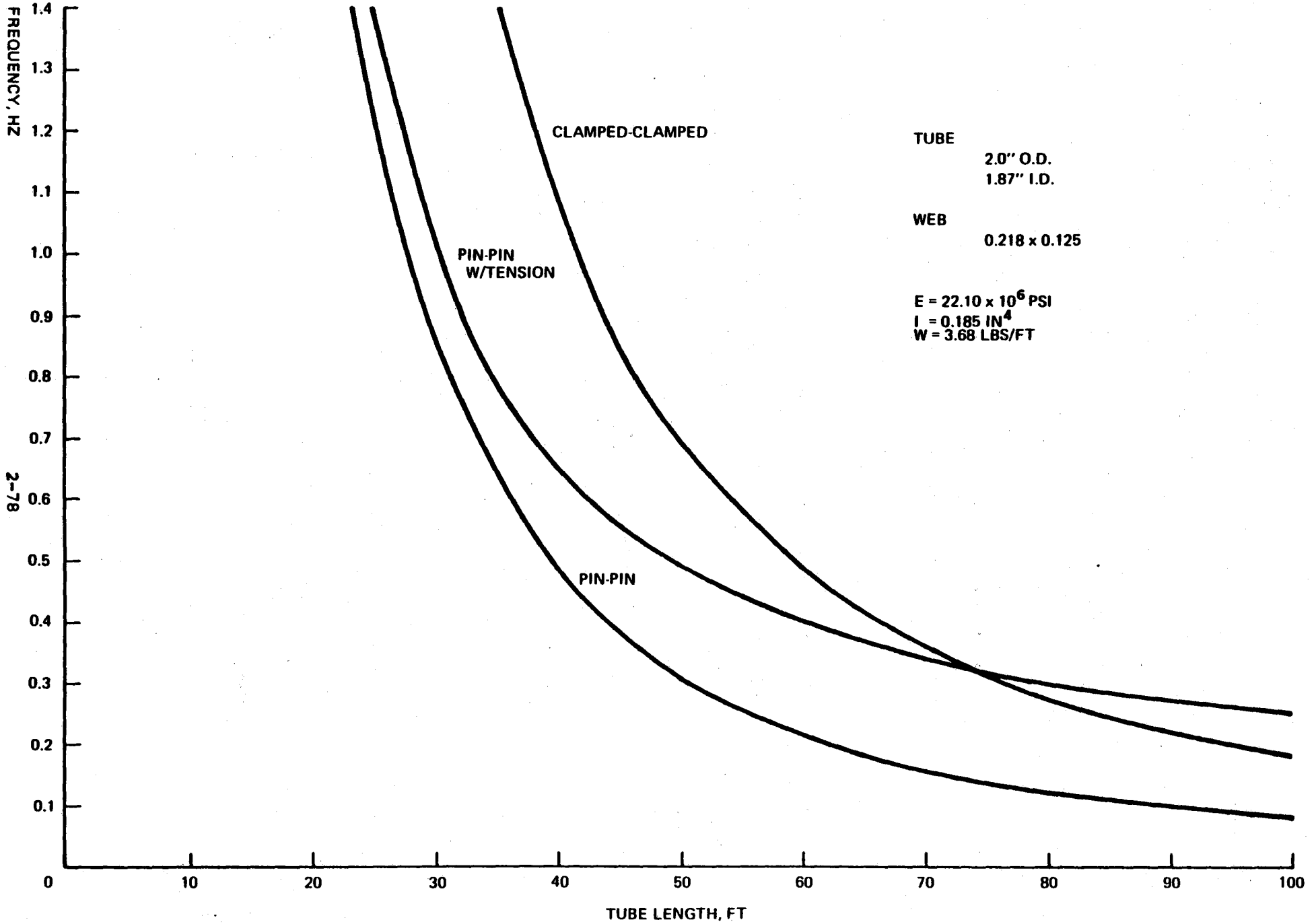

FIGURE 2.34 - FREC 'CY VS. TUBE LENGTH

Solving for l when f = 5 hertz,

$$l = 194" = 16.2' > 15'\text{-}0$$ which is adequate.

Considering the effects of tension on frequency will yield an even greater spacing.

The maximum tensile stress due to deadweight is 430 psi. Longitudinal and hoop stress due to an internal pressure of 600 psi design is,

$$\sigma_{hoop} = \frac{Pr}{t} = \frac{600(0.935)}{0.065} = 8631 \text{ psi}$$

$$\sigma_{long} = \frac{Pr}{2t} = 4316 \text{ psi}$$

where P = pressure, psi

r = inside radius of tube, in.

t = minimum wall thickness, in.

Various locations were examined in the north cavity and checked for combined stress. Table 2.7 highlights the results.

TABLE 2.7

Stresses Due Seismic, Dead Load & Pressure

	Stress in psi				Allowable Stress	
Panel 1	Seismic	Axial	Pressure	Total	S_m	1.33 S_m
Top	6885	430	4316	11631	11900	15863
Bottom	6885	0	4316	11201	11900	15863
Panel 22						
Top	6885	345	700	7930	9800	13063
Bottom	6885	0	900	7785	9800	13063

S_m = allowable stress of Inconel 800H (ASME Section 1)

The greatest stress ratio exists in Panel 1 of the north cavity near the top and is

$$\sigma_{ratio} = 0.73 < 1.00 \text{ for combined stress.}$$

The allowable stress S_m is used for dead load and pressure stress limit. A one-third increase is permitted for evaluating the seismic plus steady state stress limit.

The deflection that results from thermal bowing is insignificant and does not control the spacing of lateral restraints. Using a linear through-wall thickness gradient, an expression for the thermal moment can be obtained. Assuming that no rotation occurs at the supports, a single span can be analyzed for thermal bowing.

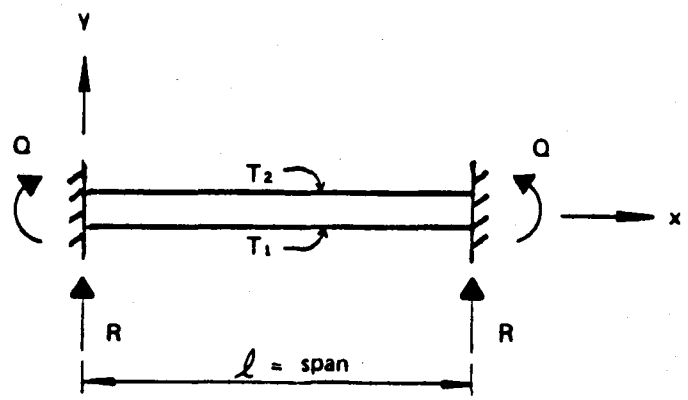

$T_2 > T_1$

$\Delta T = T_2 - T_1$

$$Q = \frac{\alpha \Delta T E I}{d} =$$

$$= \frac{8.99 \times 10^{-6} (280)\ 25.7 \times 10^{6} (0.185)}{2}$$

$$= 5984 \text{ in-lbs}$$

$$\sigma_2 = \frac{M}{S} = \frac{5984}{0.185} = 32.346 \text{ per (for a linear gradient)}$$

$R = 0$

$S_Y = 0$ at $\ell/2$

Where

T	=	Temperature, °F
α	=	Coefficient of thermal expansion, in/in
E	=	Modulus of elasticity, psi
I	=	Moment of inertia of tube, $in.^4$
d	=	Tube outside diameter, in.
Q	=	Fixed-end moment, in-lbs.
S	=	Section modulus of tube, $in.^3$
σ	=	Bending stress, psi
R	=	Support reaction
S_Y	=	Deflection

For the analysis of the fixed end beam with an applied ΔT as shown, the thermal moment is not a function of span but is linearly proportional to $\frac{\Delta T}{d}$. The thermal axial stress that results from the thermal moment represents the stress for generalized plane strain. Releasing the fixed end supports would increase deflection due to an imbalance of heating of two adjacent spans. The maximum thermal stress due to the imposed restraint is 32.4 KSI and corresponds to an average metal temperature of 700°F for which S_m = 15.7 KSI and

$$32.4 < 3\ S_m = 47.1 \text{ KSI}$$

where $3\ S_m$ = the acceptable elastic stress (approximately 2 x yield stress). The receiver panel therefore meets the stress and deflection requirements for design.

Tube Sizing

The tube wall thickness selected for this design is 0.065 in. Several locations were checked throughout the receiver based on the following assumptions. Fluid temperatures and pressures are linearized throughout a circuit where T_{inlet} = 554°F and T_{outlet} = 1050°F, and P_{inlet} = 513 psi and P_{outlet} = 30 psi. A static head of 65 psi was considered for each location. A maximum metal temperature of T_{fluid} + 200°F was used and corrosion of 12 mils applies for metal temperatures greater than 1000°F. Panel 1 (north cavity) is the controlling design. The results are shown in Table 2.8.

TABLE 2-8

Summary of Tube Design Cases

T_f,°F	T_m,°F	P_{oper} PSI	P_{des} PSI	S,PSI	t_{reqd}, ins	Corrosion Allowance Mils
561	761	578	600	15900	0.0470	0
607	807	525	547	15700	0.0442	0
777	977	336	358	15700	0.0336	0
828	1028	272	294	14700	0.0298	12
950	1100	95	117	13700	0.0185	12

Operating steady state conditions — P = 578 psi max., T = 1050°F max.

Design conditions — P = 600 psi Max., T = 1050°F max.

$T_m = T_f + 200^{\circ}F < 1100^{\circ}F$

$t = \frac{PD}{2S+P} + 0.005\,D + e$ per ASME Boiler Code, Section 1

$t \geq 0.047 < 0.065$ in.

Corrosion = 0 for $T_m < 600^{\circ}F$
= 2 mils for $600^{\circ} < T_m < 1000^{\circ}F$
= 12 mils for $1000^{\circ} < T_m < 1100^{\circ}F$

$\frac{t_{reqd}}{t_{used}} = \frac{0.047}{0.065} = 0.72 < 1.00$

P = pressure
T_f = fluid temperature
T_m = maximum metal temperature
S = allowable stress
D = tube O.D.
e = corrosion allowance

The tube ends (bents) are designed to provide an efficient, reliable attachment of the membrane wall panel to the headers. A wall thickness of 0.188 in. was selected primarily based on the tube to header weld. Figure 9.1 shows the design of the tube bend. Principle loads are internal pressure, panel deadweight, and thermal loading. Thermal loading consists of two components. First, differential thermal expansion between two tubes of a panel which is a function of the flux distribution across the panel width. This stress has been determined to be negligible due to the flexibility of the bends. Second, thermal shock caused by rapidly changing fluid tempeatures at the tube to header junction. During a heliostat trip these stresses can be significant surpassing yield strength. Assuming a linear temperature ramp over a 150 sec. time period, the header experiences a maximum $\Delta T = 120^{\circ}F$ for a fluid $\Delta T = 450^{\circ}F$ which is calculated using empirical formulas. Neglecting heat transfer through the junction and assuming the tube temperature to equal changing fluid temperaure, then the thermal stress becomes

$$\sigma = E \alpha \Delta T = 22.1 \times 10^{6} \ (10.3 \times 10^{-6}) \ 120^{\circ}$$

$$= 27{,}300 \text{ psi} < 3 S_m = 42{,}600 \text{ psi}$$

E = modulus of elasticity, psi

α = coefficient of thermal expansion, in/in

σ = thermal stress in tube, psi

and exists in the outlet header of Pass 27, Zones 1 and 4.

Headers

Headers form the connection between the receiver panel and the crossover pipe. Two lengths of headers are used throughout the receiver (4'-0 and 2'-8) which agree with the panel width. Standard flat heads, 2" thick, are used to conserve space. Panel tubes enter the header at a transition angle of 30° with no reinforcement. The crossover pipe attaches to the opposite side with a 1/2" x 2 1/4" reinforced nozzle. Details of the header are shown in Figure 9.1.

The upper header is supported by two 1" rod hangers and carries the entire weight of the panel assembly minus the vertical buckstays. The upper header therefore experiences deadweight bending and shear stress with superimposed internal pressure load whereas the lower header sees an additional static pressure load and negligible deadweight stress. Pressure and temperature vary along the circuit (or zone) therefore the design is based on header location. The controlling header analysis is at the inlet header of the circuit where a design pressure of 600 psi and temperature of $550^{\circ}F$ is used.

The design of the tube-to-header junction was established to minimize stress concentrations. The bent tube ends are welded directly to the header using backing strips. Since the presence of the backing strips represent a sizable head loss in the receiver, their removal is justifiable. A longitudinally split header is then required in order to remove the backing strips during fabrication.

Loads include internal pressure, deadweight, and thermal stress. Maximum design pressure for the inlet header of Pass 1, Zone 1, is 600 psi when $T_{fluid} = 550^{\circ}F$. For the same panel, maximum deadweight bending stress occurs and is

$$\sigma_b = \frac{M}{S} = \frac{16000(40)^2}{48(360)} = 1482 \text{ psi}$$

and shear stress is

$$\sigma_v = \frac{VQ}{It} = \frac{8000(6.13)^2}{360(2)(0.50)}(0.50)2 = 5118 \text{ psi}$$

M = bending moment
S = section modulus
V = shear force
Q = statical moment of inertia
I = moment of inertia
t = tube thickness
σ_v = shear stress
σ_b = bending stress

The headers are also subjected to thermal loads that develope when fluid temperature suddenly changes. The maximum thermal load is expected to occur at the header ligaments. Two transients responsible for thermal shock are heliostat trip and cloud transients. The greatest resultant stress is 29.5 KSI which is in the inelastic range and was determined from a linear temperature ramp defined by a $\Delta T = 450^{\circ}F$ and a 150 sec. time period. Cyclic loading conditions were evaluated for a design life of 10,000 cycles (approx. one transient per day for 365 days per year for 30 years). Fatigue analyses for the header ligaments indicate a safe fatigue life of 100,000 cycles. The usage factor is then 0.10.

A Bijlaard analysis was performed for the tube-to-header juncture using loads calculated from the yield stress of the material. The results of the analysis can be proportioned to the actual stresses. For an axial tensile stress of 883 psi (maximum) and bending stress equal to 287 psi, the following stresses were calculated.

σ_m = 478 psi

$\sigma_m + \sigma_b$ = 2488 psi

where σ_m = membrane stress

σ_b = bending stress

Header sizing is based on internal pressure and follows standard Code procedure.

$$t_{hoop} = \frac{PR}{SE - 0.6P} = 0.465 \text{ in.}$$

$$t_{Long} = \frac{PR}{2SE + 0.4P} = 0.220 \text{ in.}$$

P = 600 psi (design pressure)

R = 5.89 in. (inside radius)

S = 13500 psi (max. allowable stress at T = 600°F)

E = 0.65 (longitudinal weld joint efficiency)

0.59 (ligament efficiency)

Corrosion allowance = 0.006 in.

t_{reqd} = 0.465 + 0.006 = 0.471 < 0.500 in.

The required thickness does not include tolerance and therefore the headers must be ordered by minimum wall thickness.

The tubes are offset by 30° from the vertical to provide clearance for welding the attachments. A 15° offset, however, could theoretically be possible with the longitudinal ligament efficiency still controlling (E = 0.59) over the diagonal efficiency.

Summary of Panel Assembly Design

The panel assembly is designed to be completely fabricated in the shop. The assembly is supported from top steel and is bolted to main lateral support members. Roller connections allow for thermal expansion of the absorption panels. The connections transfer lateral load from horizontal buckstays spaced at 15'-0 intervals. Determination of restraint spacing is based on longitudinal tube stress and deflection due to pressure, seismic, thermal, and dead loading.

Tube thickness requirement is 0.047 in. per ASME Power Boiler Code, Section 1. Actual tube thickness is 0.065 in. The tube to header junction has been evaluated for static and thermal shock loads and found to be adequate at a tube wall thickness of 0.188 in. and a header wall thickness of 0.50 in. The header nozzle was found to require reinforcement of 1/2 in x 2 1/4 in.

Material selection for the pressure components of the panel assembly are SB-163 800H incoloy for the absorption tubes, TP304 SA 312 stainless steel for the headers, TP 304 SA 213 for the tube ends. Material for the lugs, tee-buckstay, and roller connection is TP 304 stainless steel. The vertical buckstay and bracing uses A36 carbon steel.

2.4.2 Surge/Buffer and Collection Tank

The surge/buffer tank and collection tank are part of the receiver subsystem. The surge tank has the following functions, (a) receives molten salt from the thermal energy storage system and distributes it to the various zones in the receiver, (b) is part of the circulation system in which salt is circulated thru the receiver during cloud cover and night-time operation. Air pressure is supplied to the surge tank to assist in maintaining receiver circulation in case of pump or electrical failure, (c) receiver venting is provided thru the surge tank.

The collection tank receives molten salt from the receiver and distributes the salt to the thermal energy storage system. It serves as a fill tank for the receiver and also part of the circulation system for night-time storage.

The basic input required for design of the tanks are:

--geometry - volume, number of nozzles, location, etc.

--design pressure

--design temperature

--thermal transients

--mechanical loads - wind, seismic, snow, etc.

--pipe loads on nozzles

--heat loss limits

--support requirements

The design criteria for the tanks are those identified in the ASME Boiler and Pressure Vessel Code for Unfired Vessels - Section VIII Division 1 and implemented by B&W Company Standards. Each tank design is discussed in the following paragraphs.

Surge Tank

Functional requirements established the tank volume at 1885 cubic feet (14000 gal.), the design pressure at 600 psi, and the design temperature at 800°F. The geometry of the tank is shown on Figure 9.5 and is based on such factors as ability to ship, manufacturability, availability of heads, plate, optimization of weld seams, etc. Ellipsoidal heads were selected to minimize stresses at the head to shell juncture and the recognition that ellipsoidal heads which have the same thickness as the shell will be of comparable strength.

The material selected considers the corrosive nature of the fluid, material properties at the design temperatures, availability, cost and fabricability. SA-515Gr70 is the plate material and SA-181Gr70 is the nozzle forging material. SA-106GrC will be used for those nozzles which can be made from piping material.

The minimum wall thickness for the ellipsoidal heads and shell is determined from ASME Section VIII Division 1 Code formula (UG-27) for the shell.

$$t = \frac{PR}{SE-0.6P}$$

$$= 3.71"$$

where, P = design pressure = 600 psi

R = inside radius = 72 inches

S = allowable stress for SA-515Gr70 = 12000 psi @ 800°F

E = Joint Efficiency = 1.0 (Full radiography of weld joints)

t = min. wall thickness (inches)

UG-27a(1) for Ellipsoidal Head

$$t = \frac{PD}{2SE-0.2P}$$

$$= 3.62"$$

D = Inside Diameter (inches)
= 144"

Ordered thickness was set at 4 inches to allow for reinforcement at openings, provide for machining of the head to shell juncture due to out of roundness, and to provide for a corrosion allowance.

Nozzle configuration is selected from the catalogue of nozzles acceptable to the Unfired Pressure Vessel Code. All nozzles are welded types (i.e., no bolted closures) to minimize leakage and maintenance.

The tank is supported from main steel by four support lugs. Slotted holes are provided in the lugs to account for thermal expansion. The tank is fully insulated to minimize heat loss. Trace heating is provided to warm the tank prior to filling.

Collection Tank

The approach used for the design of the collection tank is similar to that used for the surge tank. The volume requirement is 1885 cubic feet. The design pressure is 90 psig and the design temperature is 1050°F. The configuration of the collection tank is shown on Figure 9.6. The minimum wall thickness of shell and head is 0.70 inch. Because of the corrosive nature of the salt at 1050°F, the material selected is an austenitic material SA-240 Grade 304. Nozzle forgings will be of SA-182 Gr 304 material.

2.4.3 Thermal Analysis of the Absorption Tubes

Design of the receiver panel geometry involved using thermal hydraulic technology to establish panel width, height, tube diameter, tube thickness, design pressure, design temperature, and flux pattern. Based on this information a stress analysis of the absorption tube was performed to verify that the design selected was structurally adequate for the intended service. Section 2.4.1 covers the stress analysis of the tube for mechanical loads and compliance with the ASME Boiler Code requirements. The section also included the analysis of the header to tube junction for a thermal shock resulting from loss of site power. These analyses conclude that the geometry selected meets acceptable stress and deflection limits.

This particular section provides the method and results of the thermal analysis of the absorption tube which evaluates creep damage, fatigue damage, and total strain due to thermal stresses caused by heat flux.

Thermal Analysis

Three thermal stress models were investigated in which the tube geometry remained fixed while being subjected to different heat flux patterns, namely - normal, skewed, and a varying flux over the full length. Figures 2.35 thru 2.37 shows the three heat flux loading patterns being applied. Figure 2.38 shows the finite element model variations used to optimize the Finite Element Model. A detailed account of the various analyses is covered in the appendix. The results are summarized in Table 2-9. These results essentially indicate that compared to normal type heating, typical stresses will increase for

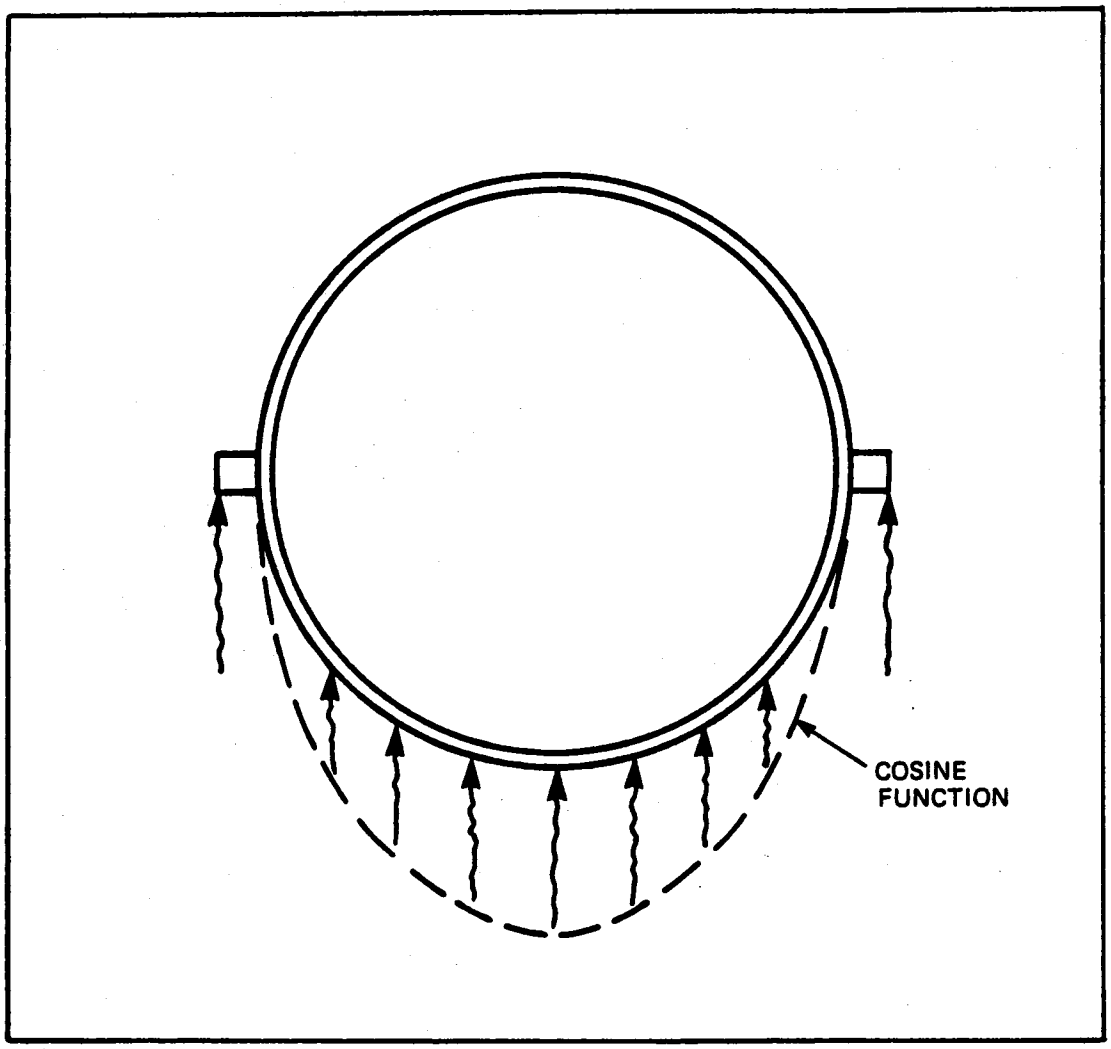

FIGURE 2.35 - THERMAL LOAD DIRECT HEATING

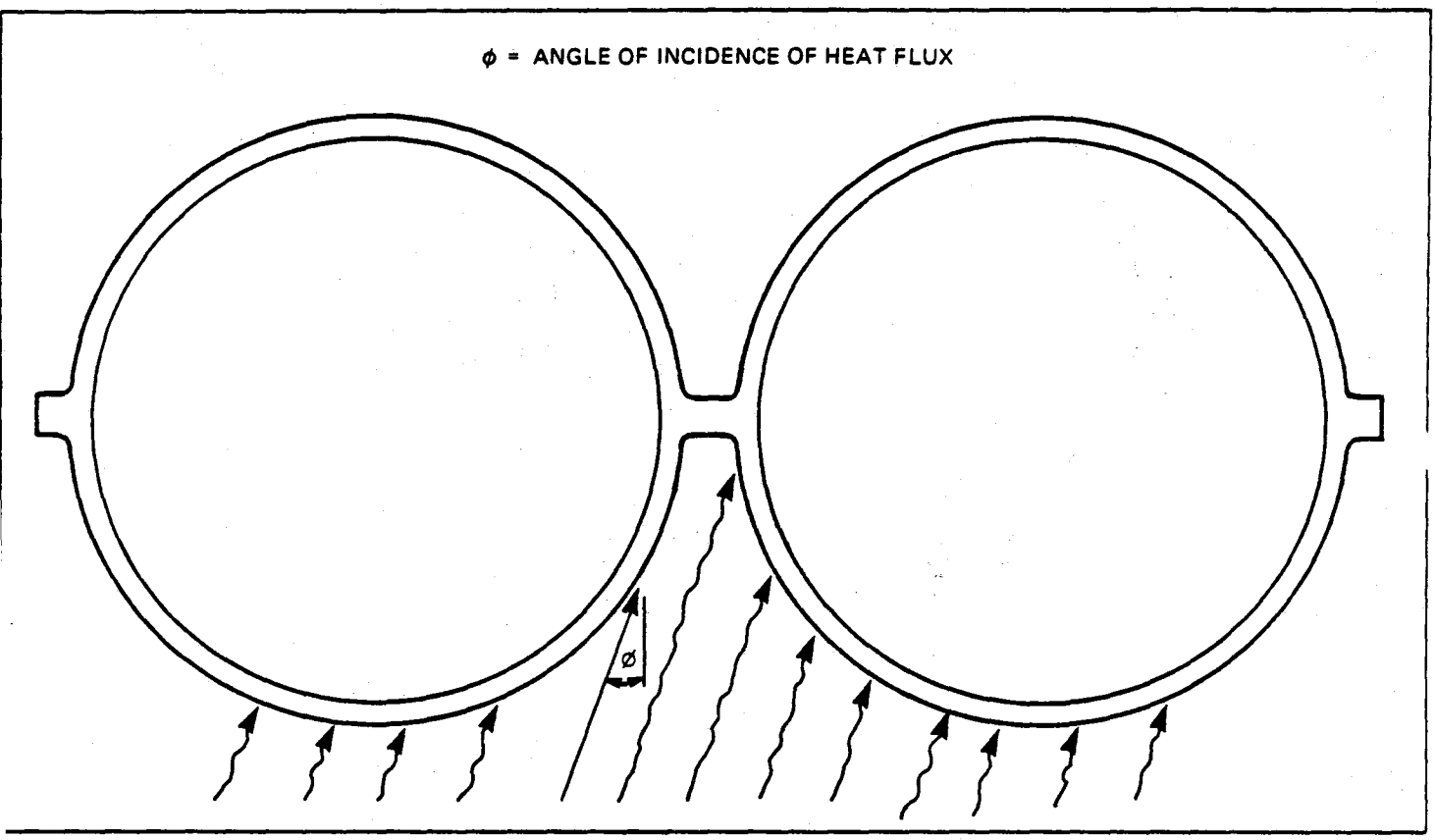

FIGURE 2.36 - THERMAL LOAD SKEWED HEATING

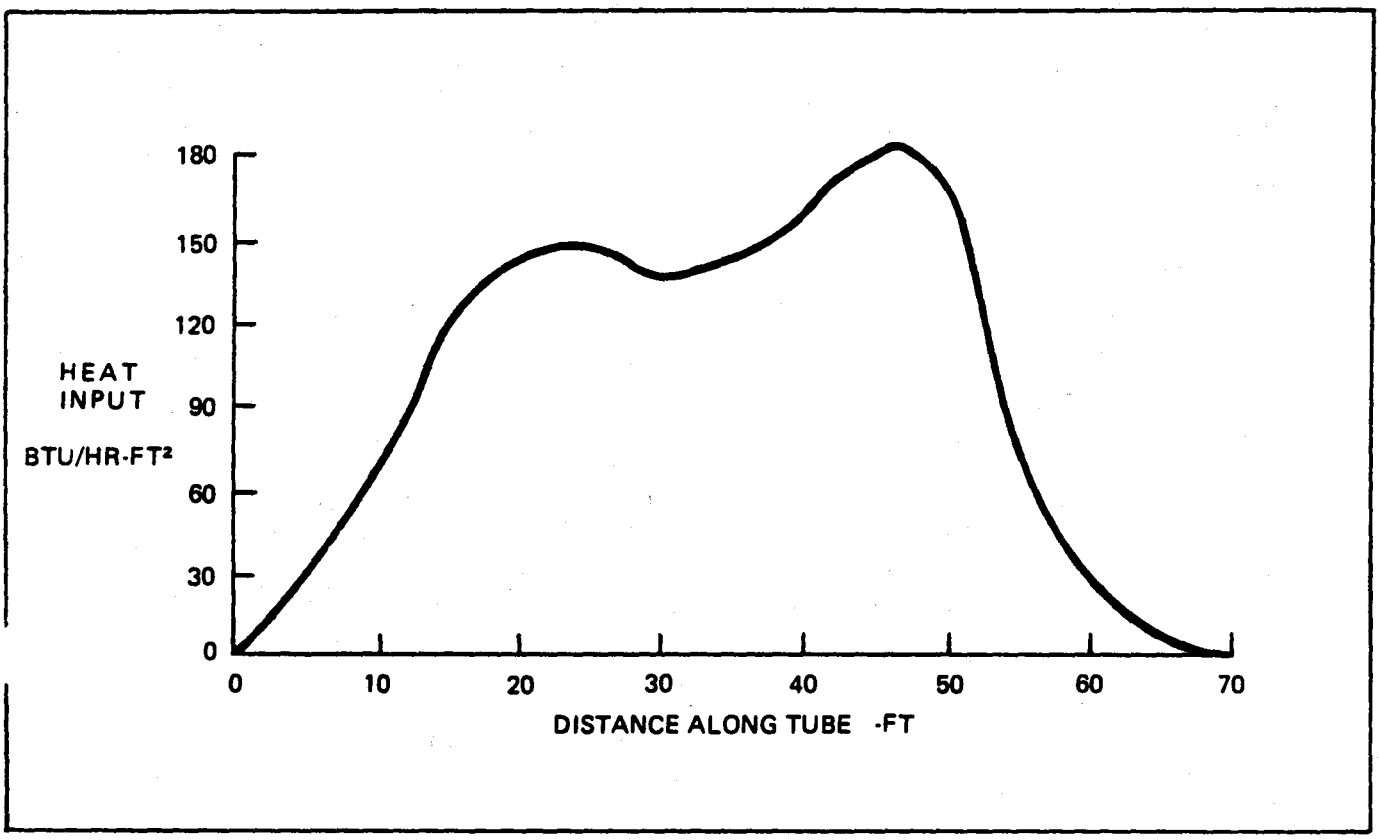

FIGURE 2.37 - FULL TUBE ANALYSIS

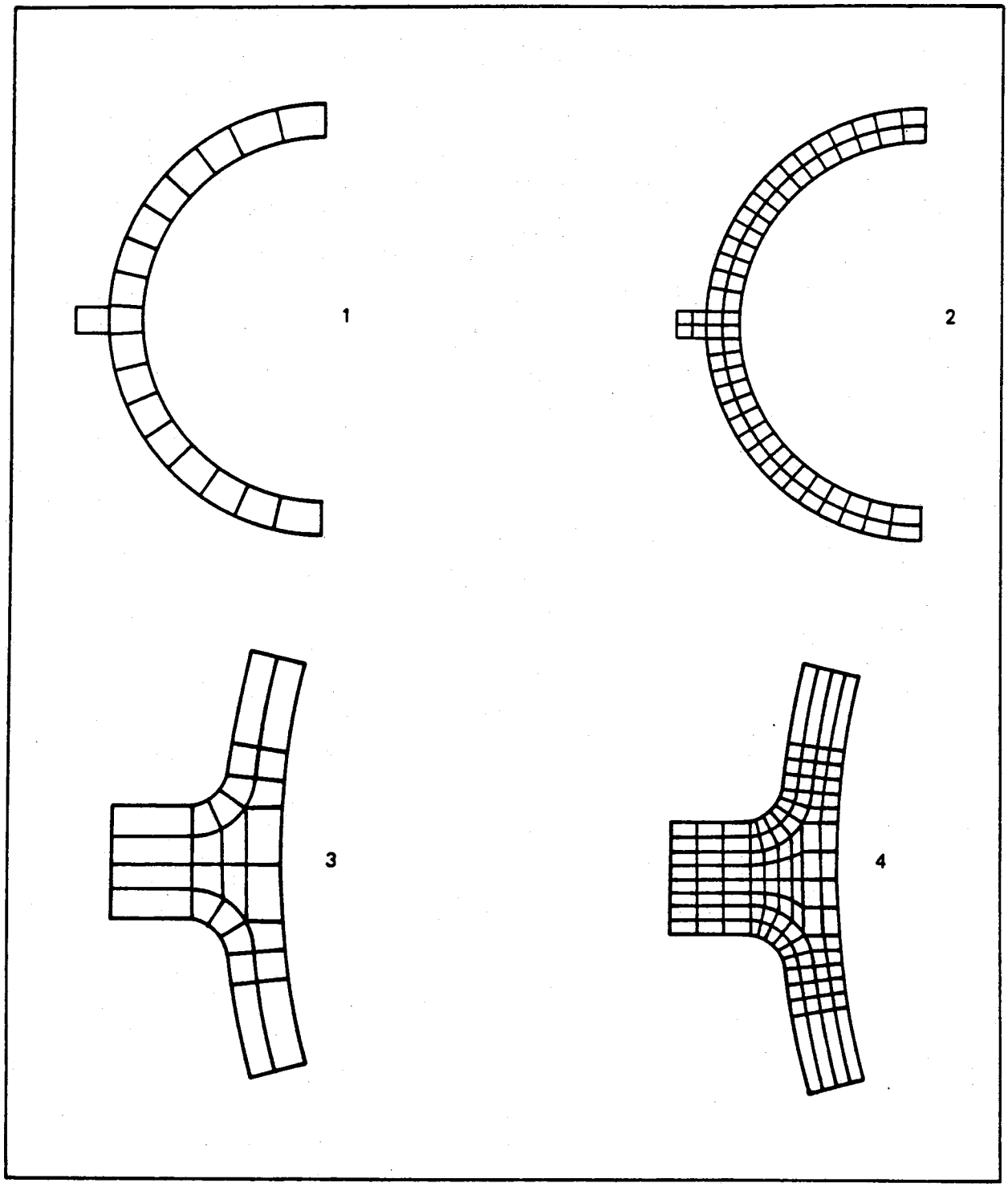

FIGURE 2.38 - MATH MODELS

TABLE 2.9

	STRESS	
MODEL	TUBE	WEB
BASE (Normal Heat Flux)	33 KSI	40 KSI
SKEWED	+ 35%	- 50%
FULL TUBE	- 30%	+ 10%

Influence of heat Flux Profile

on Tube Stresses

skewed heating (the maximum metal temperature stays the same while the average tube metal temperature decreases) and tube stresses will reduce when considering the overall heat flux along the length of the tube (full heat flux is not continuous along the full tube length).

At this time it should be noted that the analytical effort is based on two sided heating since early design configuration considered heating of this type. The final design uses one sided heating and therefore the numerical results associated with this thermal portion are qualitative.

The full length tube thermal analysis is based on a tube free to bow. The final design configuration has the tube restrained and so; the analysis must be considered qualitative. The results contained in the Appendix E indicate the stress profile still decreasing for a restrained tube length of approximately 15 feet which is the restraint span presently being used.

Combining effects of skewed heating and full length heat results in approximately a standoff. Sufficient analytical effort has been performed to make the prediction that the final panel design calculations will meet the design criteria.

Creep/Fatigue Analysis

The final portion of the thermal stress evaluation involves the analytical effort necessary to verify that the absorption panel tube as currently designed will not fail in fatigue or result in excessive distortion or rupture as the result of creep. This complex analysis was performed conservatively using simplified techniques developed from previous work. The basis for the approach taken is found in the B&W Internal Report "Elastic and Inelastic Creep/Fatigue Evaluations of Solar Receiver Panel Tube Based on Code Case N-47" by Dr. K. Hsu. The results of this method as applied to this receiver is attached as Appendix B. A summary of the results follow -

- Stresses were obtained at various locations throughout the receiver from which the critical stress points were defined. The most critical point was found to be one which sees a heat flux of 155000 BTU/hr-ft^2 and a salt temperature of 600°F. The maximum thermal stress at this point is 47000 psi. Figure 2.39 and Table 2.10 provide the stress profile for the condition noted.
- For the fatigue analysis, a conservative operation cycle was defined (Figure 2.40). Since the maximum stress is well above yield stress, the fatigue analyses has to be based on an inelastic approach using effective strain range versus cycles to failure methods. The inelastic strain range was calculated as 1.833×10^{-3} inch/inch.
- The failure criteria was based on the conservative approach taken in Code Case N-47 of the "ASME Boiler and Pressure Vessel Code, Section III, Nuclear Power Plant Components." The result of the fatigue analysis is a usage of 0.82 with an allowable of 1.0.

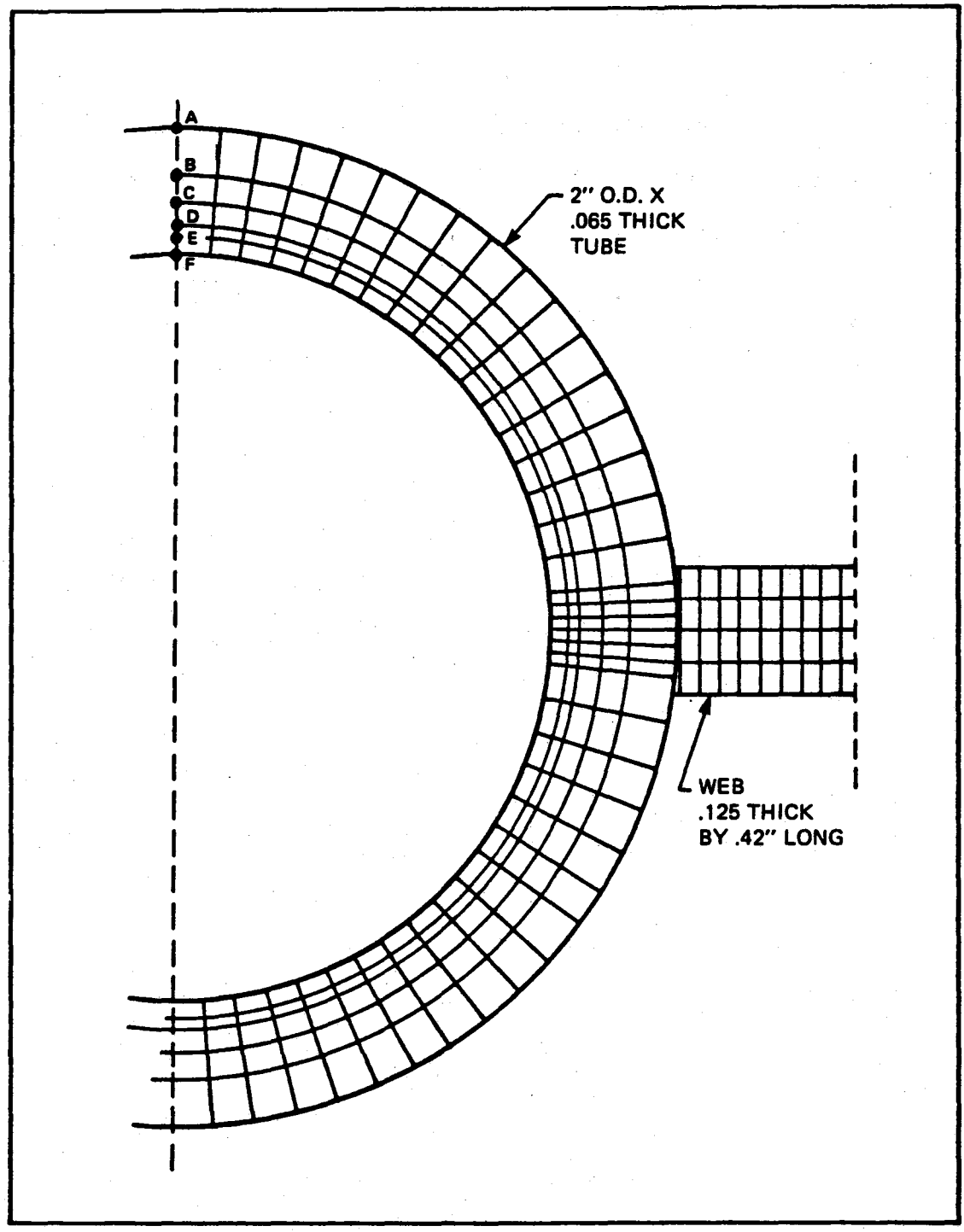

FIGURE 2.39 - TUBE/WEB MODEL

TABLE 2.10 STRESS PROFILE

TUBE* RADIUS	STRESS COMPONENT	(PSI) PRESSURE	(PSI) THERMAL	(PSI) PRESSURE + THERMAL
1.000" (A)	r	-268	0	-268
	θ	7223	-9263	-2040
	z	58	-47064	-47006
0.975" (B)	r	-268	148	-120
	θ	7223	-2272	4951
	z	58	-36949	-36891
0.960" (C)	r	-268	152	-116
	θ	7223	1968	9209
	z	58	-30941	-30883
0.950" (D)	r	-268	115	-153
	θ	7223	5087	12310
	z	58	-26631	-26573
0.942" (E)	r	-268	61	-207
	θ	7223	7541	14764
	z	58	-23259	-23201
0.935" (F)	r	-268	0	-268
	θ	7223	9578	16801
	z	58	-20485	-20427

* See Figure 2.39

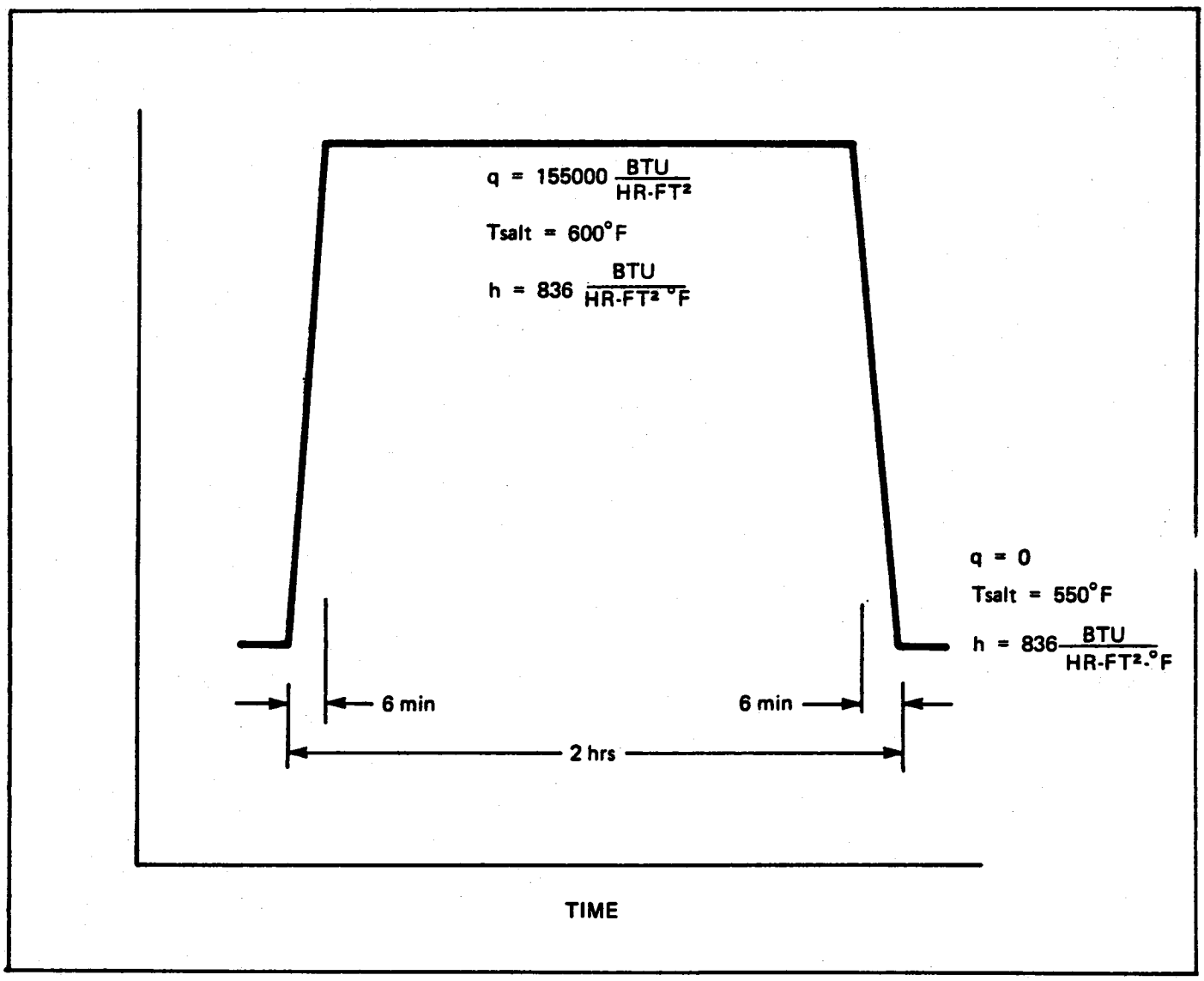

FIGURE 2.40 - ASSUMED THERMAL TRANSIENT EVENT

- The damage due to creep was found to be negligible for the two points evaluated. Figure 2.41 shows the location of the worse case stress/strain point in the receiver with respect to the damage envelope for the tube material. This point being within the envelope and therefore acceptable.
- In addition to performing a creep-fatigue analysis using the techniques of ASME Nuclear Code Case N-47, analysis was performed using the proposed "Supplemental Elevated Temperature Rules for Section VIII Division 1" (Appendix D). Essentially the results are identical since creep is negligible (low heat flux, high salt temperature).

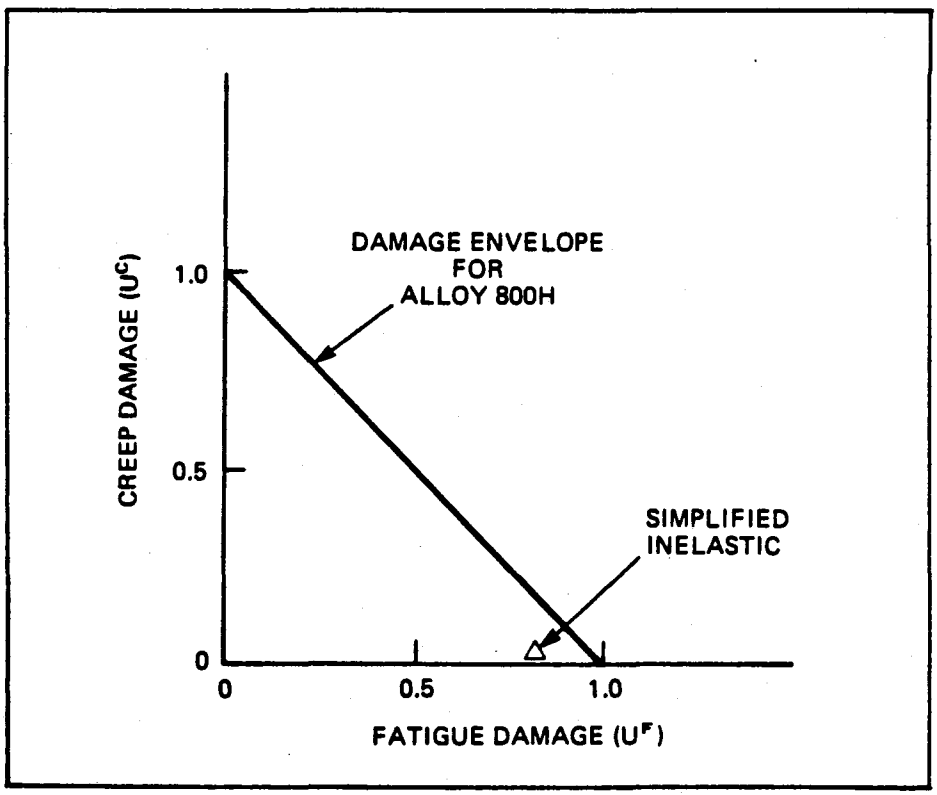

FIGURE 2.41 - CREEP–FATIGUE DAMAGE ENVELOPE

2.5 Design of Receiver Structure

The receiver structure consists of the structural steel which supports the heat absorption panels and other components, and the cavity doors.

2.5.1 Structural Steel

The structural steel is the structure above the top of the reinforced concrete tower which supports the panels, tanks, roof, floor, etc., and transfers receiver loads to the reinforced concrete tower. Because of the similarity between the requirements for design of the structural steel for a fossil fired boiler and the steel for this receiver, the proposed structural steel design is derived from boiler steel design principles with some modifications.

Major Support Areas

The quad-cavity support structure is unique because of the cavity configuration that outlines the regions available for structural steel (Figure 2.42).

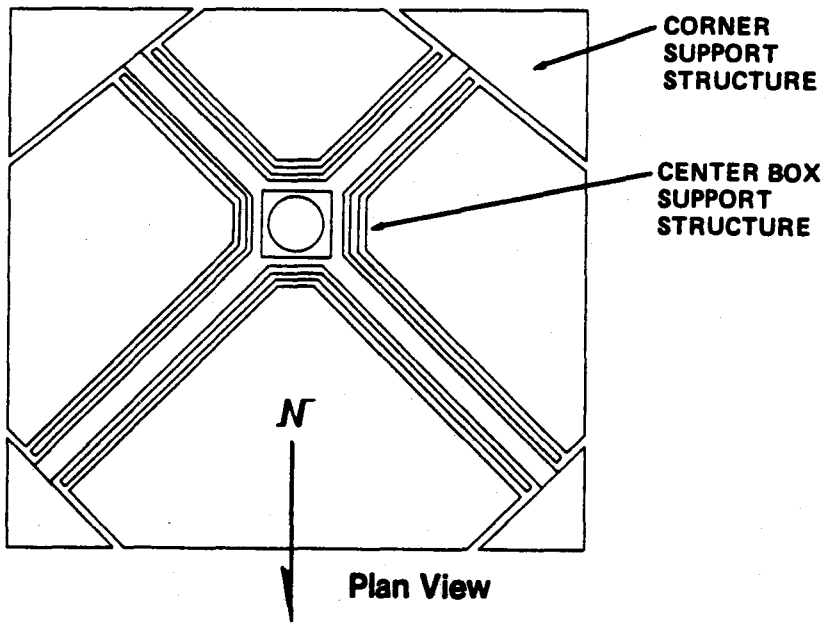

FIGURE 2.42 - STRUCTURAL SUPPORT BY FIVE MAJOR REGIONS

The structural steel has to provide support for a number of components and withstand wind and seismic loadings to maintain stresses and deflections within allowable limits. This is easily accomplished in the quad-cavity design by using five main structural support regions; the four corners and the center box. Tying these five regions together provides a balanced, efficient structure, with less material required than for other designs such as a single cavity receiver. Details of the structural arrangement are shown in Figures 9.16, 9.17, and 9.18.

Lateral support members which tie the corners to the center box run between the double wing walls. This steel furnishes the lateral restraint to the receiver walls. Spacing between the double walls is designed to provide space for the required lateral support system and yet is minimized to keep the overall size of the receiver to a minimum. The interconnecting steel members between the central box and the four corners are designed to transfer the lateral loads acting on the components within the center box to the stiffer outside corners. The resulting distribution of horizontal load permits a greater number of reaction points to exist (diagonal bracing) offering efficient use of the structure. The bracing of the corners therefore provides the structure's stability and lateral rigidity. Loading from the five regions is collected by a network of trusses referred to as the tower attachment and is then transferred to the concrete tower.

The central box structure, comprised of four columns, horizontal beams, and diagonal bracing, supports approximately 75% of the total receiver weight. Because of the high loading from the receiver panels, tanks, and piping, each column is well braced to carry the axial loads.

Each of the four corners consists of three columns and bracing which produces the structure's stiffness. This corner steel also defines the aperture openings and supports the aperture door frames.

The cavity enclosure requires support externally. Lightweight, open-web steel joists support the cavity roof and posts support the floor. Enclosure walls are supported by horizontal members which frame into main steel.

Lateral Support System

The wing wall support system is shown in Figure 2.43. This sketch establishes the minimum wall to wall distance of 5'-0". The resulting receiver size is 108'-0" for the north and south faces and 104'-9 for the east and west faces. The vertical members, or "buckstays," of the panel assemblies are bolted to lateral support members. The weight of the vertical buckstay is supported from top steel. Their purpose is to provide support for the main steel lateral supports. With this support, the axial load carrying capacity of the member is more than doubled for a given single WF shape. The diagonally oriented members (shown in sections 'F-F' and 'E-E' of Figure 9.16 are lateral header supports. These members also collect vertical buckstay weight and transfer the load to top steel hangers. Two hangers are shown per diagonal.

Pressure Boundary Support

Membrane wall panels and headers are hung from the top of the structure to accommodate the downward thermal growth of the walls. The panels are then tied to main steel at various elevations to absorb lateral loads from wind and earthquake. Tanks are supported by the four central columns using support feet connections. Constant load hangers and horizontal ties remove piping loads and permit flexibility for thermal expansion.

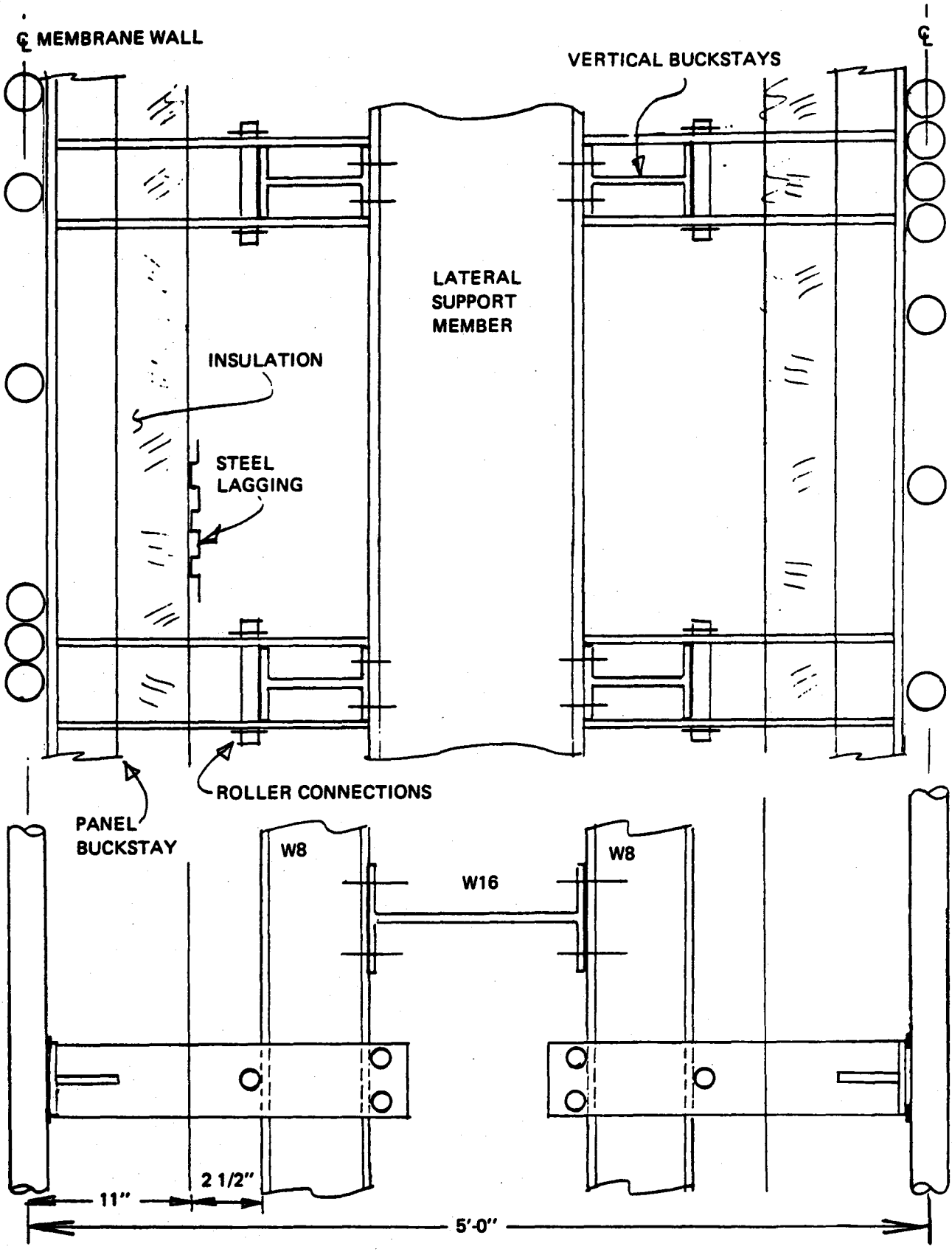

FIGURE 2.43 - LATERAL SUPPORT SYSTEM

Tower Attachment

The tower attachment steel is composed of an arrangement of vertical and horizontal trusses (Figure 9.15). Four main trusses overhang the tower to support the cavities (sections 'A-A' and 'C-C'). Diagonal braces (sections B-B and D-D) give additional support to the corners.

The arrangement of the attachment steel is complex because of the transition from the large square section of the cavity base to the much smaller, circular tower. While the design is viable, at this stage, further design efforts, with a larger tower diameter, may significantly reduce the complexity and cost of the attachment steel.

Access

Platforms are placed at three elevations to provide access to upper header piping, lower header piping, and the recirculation pump/compressor area. Access to other equipment such as the door mechanism or the cavity man-way is via the upper and lower platforms. Stairs are located in the southeast corner of the receiver and a 12-man elevator is in the southwest corner.

Codes

Applicable codes used for design include the American Institute of Steel Construction (AISC), the Uniform Building Code (UBC), and local codes.

Loads

The receiver structure was analyzed using an earthquake base response of 0.15g computed for Seismic Zone 3 (per UBC 1973) with a Use Factor of 2.0 and a 30 psf basic wind pressure.

earthquake (operational) - 0.82g (horizontal)

1.08g (vertical)

wind load - 30 psf (basic ground pressure)

55 psf (receiver level)

The cavity enclosure is designed to minimize heating of the structural steel. Lagging and insulation are designed to minimize the escape of hot air from the cavities. Structural members are cooled by natural convection of outside air vented through the structure.

Effect of Tower Diameter

The design concept began with a receiver/tower combination utilizing a 42'-3" tower attachment at the interface. The receiver structure above the tower is designed to meet the allowable lateral deflection (per AISC) of:

$$\Delta = \frac{h}{200} = \frac{150(12)}{200} = 9"$$

where h = the height of the receiver in feet.

With the 42'-3" diameter tower, this deflection criterion could not be met. The excessive rotation of the tower attachment steel created high displacements and it was concluded that the tower diameter was inadequate. The deflections were reduced within the allowable limits when a 60' diameter (top) was used. Maximum lateral displacement therefore controls the design of the attachment steel whereas the steel above elevation 548'-0" is designed according to allowable stress.

In order to minimize the total cost of the tower/receiver subsystem, Black & Veatch was asked to determine the cost and seismic acceleration levels of several top diameters for the reinforced concrete tower. It would then be the responsibility of Babcock & Wilcox to pick the final top diameter for overall economy. The three top diameters chosen by Black & Veatch for consideration were 12.9 meters (42'-3"), 18.3 meters (60'-0"), and 24.4 meters (80'-0"). In order to have a reasonable taper, the diameters at the base of the tower were respectively chosen to be 19.8 meters (65'-0") 24.4 meters (80'-0"), and 30.5 meters (100'-0").

Results of response spectrum analyses of the three towers indicate that seismic accelerations tend to increase with increasing top diameter. For the operational earthquake, horizontal accelerations at the top of the receiver were respectively 0.61 g, 0.65 g, and 0.77 g for the three top diameters considered. Corresponding vertical accelerations were 0.86 g, 0.88 g, and 0.97 g. In all cases, survival earthquake accelerations were almost exactly double operational earthquake accelerations. The cost (1982 dollars) of each tower was estimated to be $3.0 million, $3.5 million, and $4.9 million, respectively for the three top diameters considered. These cost estimates include only the cost of the reinforced concrete tower and its foundation; the cost of accessories is not included.

From results of this study, Babcock & Wilcox chose the 18.3 meter (60'-0") tower for overall economy when considering combined tower and receiver costs. Results elsewhere in this report reflect the 18.3 meter (60'0") tower.

Structural Analysis

The structural analysis was performed primarily to determine structural adequacy of the structure, the tonnage of steel required to support the Quad-Cavity Receiver, and to check the steel arrangement for design improvement. Because of the complex geometry of the structure, the finite element program, FESAP, was employed for the analysis.

The geometry of the 3-dimensional model is shown in Figure 2.44. The model consists of 331 nodes and 1025 beam elements. Preliminary member sizes were estimated by hand and their corresponding properties provided input data for the model. An iterative process followed by adjusting the sizes according to output data which consists of element stresses and displacements. This process was continued until acceptable stresses and deflections were obtained.

Horizontal loading applied in the east-west direction was assumed to control member sizes. In actual design analysis, other directions would be investigated. Those directions are north-south and a direction parallel with one wing wall. Steel weight is based on member sizes and includes connection weight which is equal to 10% of member weight.

The seismic accelerations are based on dynamic response modelling using calculated steel/tower stiffness and mass. Any significant changes in these values will have impact on the seismic accelerations. Past experience on other solar receiver studies indicates that the seismic "g" values used for this evaluation are representative and we have no reason to change these values at this time.

The total steel tonnage is 2188 tons and the total wet receiver weight is 5216 tons. All structural members are rolled sections of A36 material readily available with standard type bolted connections.

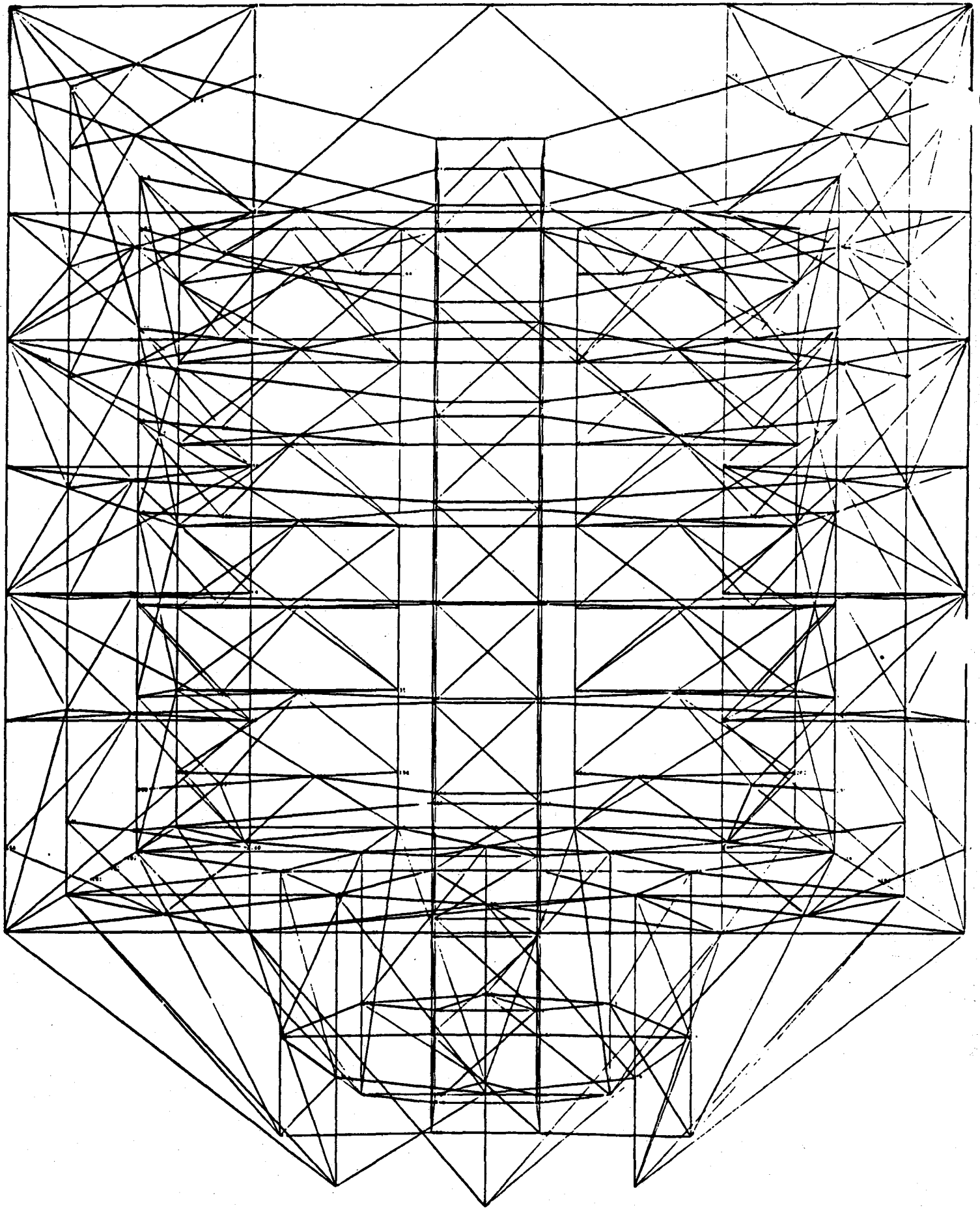

FIGURE 2.44 - FINITE ELEMENT MODEL - STRUCTURE

Excessive lateral deflections determined the tower diameter of 42'-3" to be inadequate and as a result, a tower diameter of 60'-0 was selected. Figure 9.15 identifies the 42'-3" tower attachment steel arrangement for which the steel tonnage was determined. A revised steel arrangement for the attachment is shown in figures' 2.45 and 2.46 for the 60'-0" diameter.

Conclusion

The structural design arrangement meets the design criteria for the identified loads. Standard methods of steel construction were used for the design and finite element used for the analysis. No major problems exist with the design although areas for improvement would include redesign of tower attachment steel, bracing optimization, and improved dynamic response modeling. Any future modifications or studies concerning the design, however, would not significantly reduce the estimated steel tonnage.

Tables 2.11 and 2.12 summarize receiver weights and conclude the structural analysis.

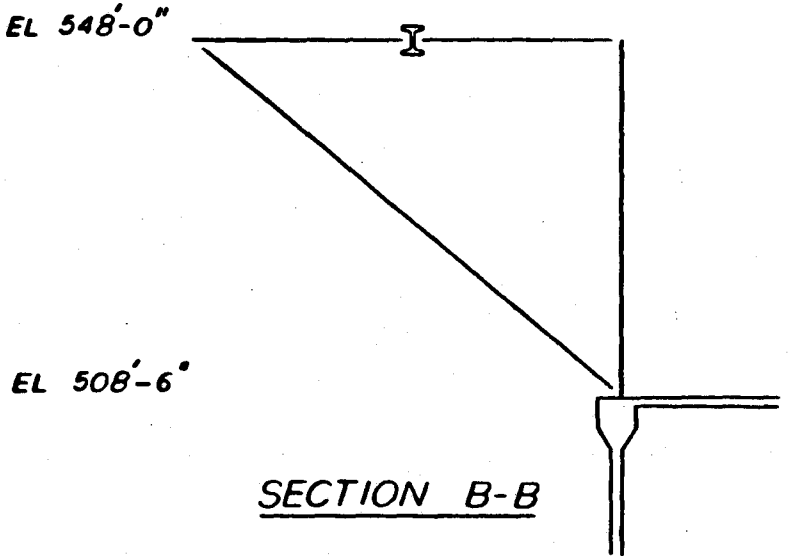
EL 548'-0"
EL 508'-6"
SECTION B-B

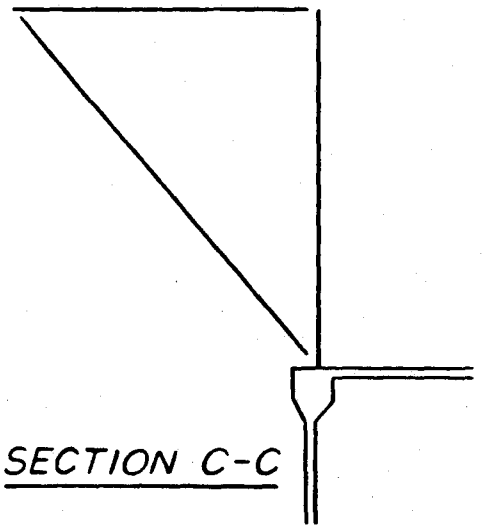
SECTION C-C

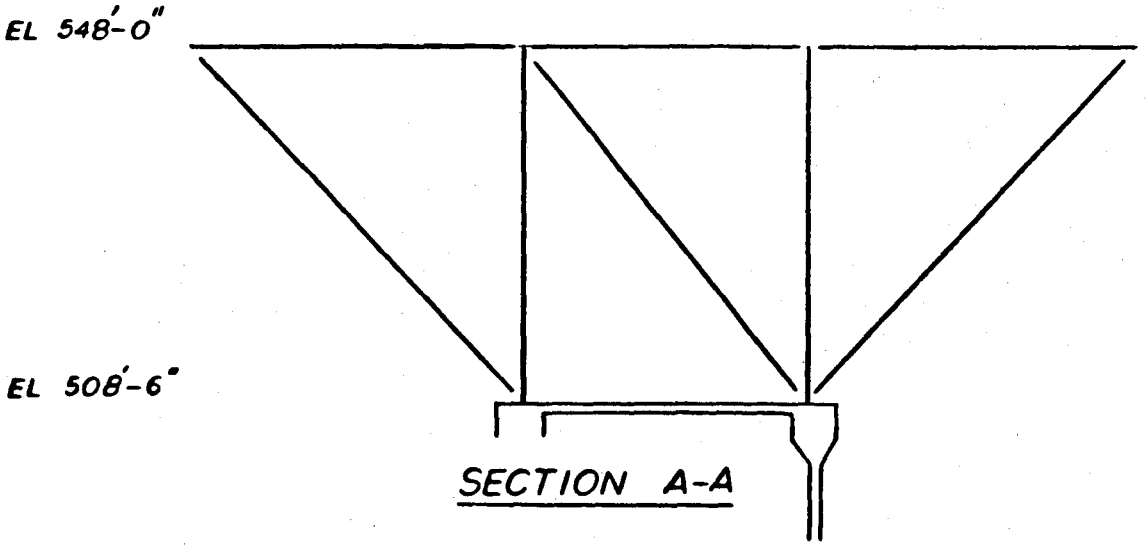
EL 548'-0"
EL 508'-6"
SECTION A-A

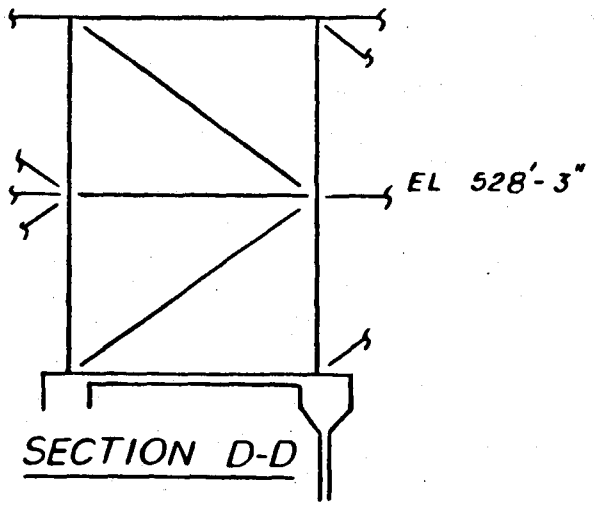
EL 528'-3"
SECTION D-D

FIGURE 2.45

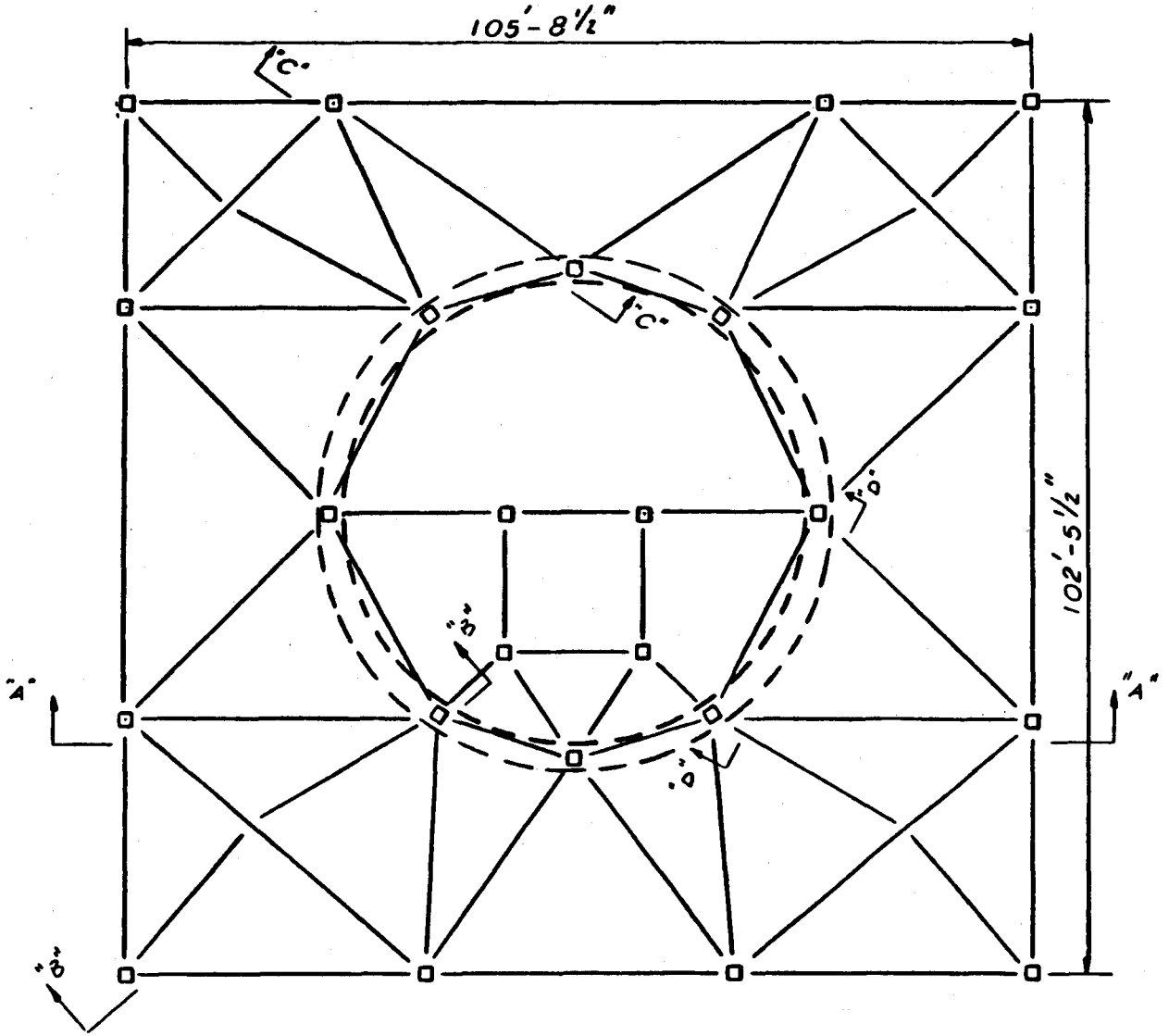

ELEVATION 548'-0"

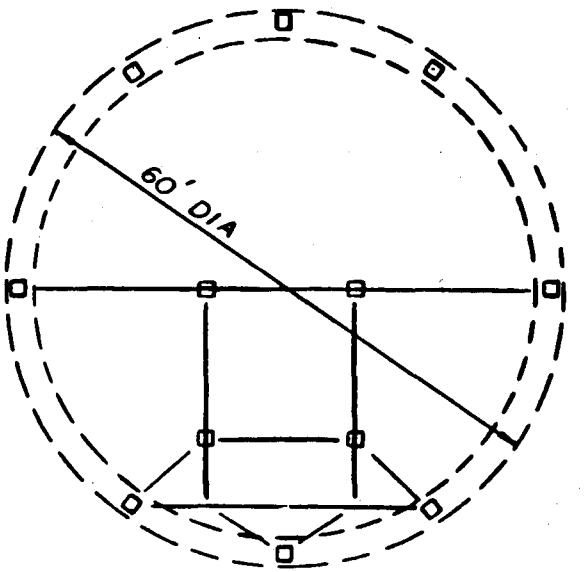

ELEVATION 508'-6"

FIGURE 2.46

TABLE 2.11 Main Steel Weight

Platform and Cavity Enclosure Loads

Platform Area	4,373 sq. ft.	
" Dead Load		86.3 kips
" Live Load		437.3 kips
Cavity Roof Area	7,619 sq. ft.	
" Dead Load		162.0 kips
" Live Load		172.8 kips
Cavity Floor Area	77,651 sq. ft.	
" Dead Load		115.0 kips
" Live Load (Eq.)		123.1 kips
Cavity Wall Area	11,890 sq. ft.	
" Dead Load		178.0 kips
" Live Load		192.0 kips

Platform and Cavity Steel

Platform Steel (includes support steel or cavity roof and floor)	95 kips
Cavity Wall Steel	99 kips
Subtotal	194 kips

Main Steel Weights

Main Steel (connections included)	
Columns	804 kips
Vert. Bracing	381 kips
Horiz. Beams	706 kips
Base Plates	103 kips
Subtotal	1994 kips

Table 2.12 Total Receiver Weight

Component Weights

	Total Wts.	Salt Wt.
Surge Tank	331 kips	187 kips
Collection Tank	262 kips	187 kips
Air Supply Tank	46 kips	
Miscellaneous Equipment	10 kips	
Panels, Interconnecting Piping	1206 kips	600 kips
Vertical Buckstays	264 kips	
Platform Area Dead Load	86.3 kips	
Cavity Enclosure Dead Load		
Roof	161 kips	
Floor	115 kips	
Walls	178 kips	
Riser	40 kips	33 kips
Downcomers	12 kips	8 kips
Miscellaneous Piping	70 kips	60 kips
Doors (incl. Frame, Insul. and Lagging)	167 kips	
Door Track	70 kips	
Elevator	10 kips	
Platform and Cavity Steel	194 kips	
Main Steel	1994 kips	
Total Wet Rcvr Wt.	5216 kips	1075 kips
Total Dry Rcvr Wt.		4141 kips

2.5.2 Doors

Each cavity of the receiver has a two-piece door which can be closed during adverse weather conditions or at night to minimize heat loss in the receiver. Figure 9.18 depicts the structure for the north cavity door which is representative of the other three doors. The north door is the largest in size and weight while the east, west, and south doors are smaller, respectively. Table 2.13 below identifies the estimated size and weight of the door structures.

TABLE 2.13 DOOR DATA

Door Location		Weight (Approx.)
North	54'-10" x 54'-10"	31460 lbs
East	45'-0" x 45'-0"	22230 lbs
South	31'-10" x 31'-10"	12625 lbs
West	45'-0" x 45'-10"	22230 lbs

The structure chosen for the door is a space frame. The space frame along with a variable cross section and the use of aluminum structural tubing were employed to minimize the weight of the doors. Figure 2.47 reflects the complexity of the door structure. The aluminum structural tubing is composed of round and square tubing of 6061-T6 material.

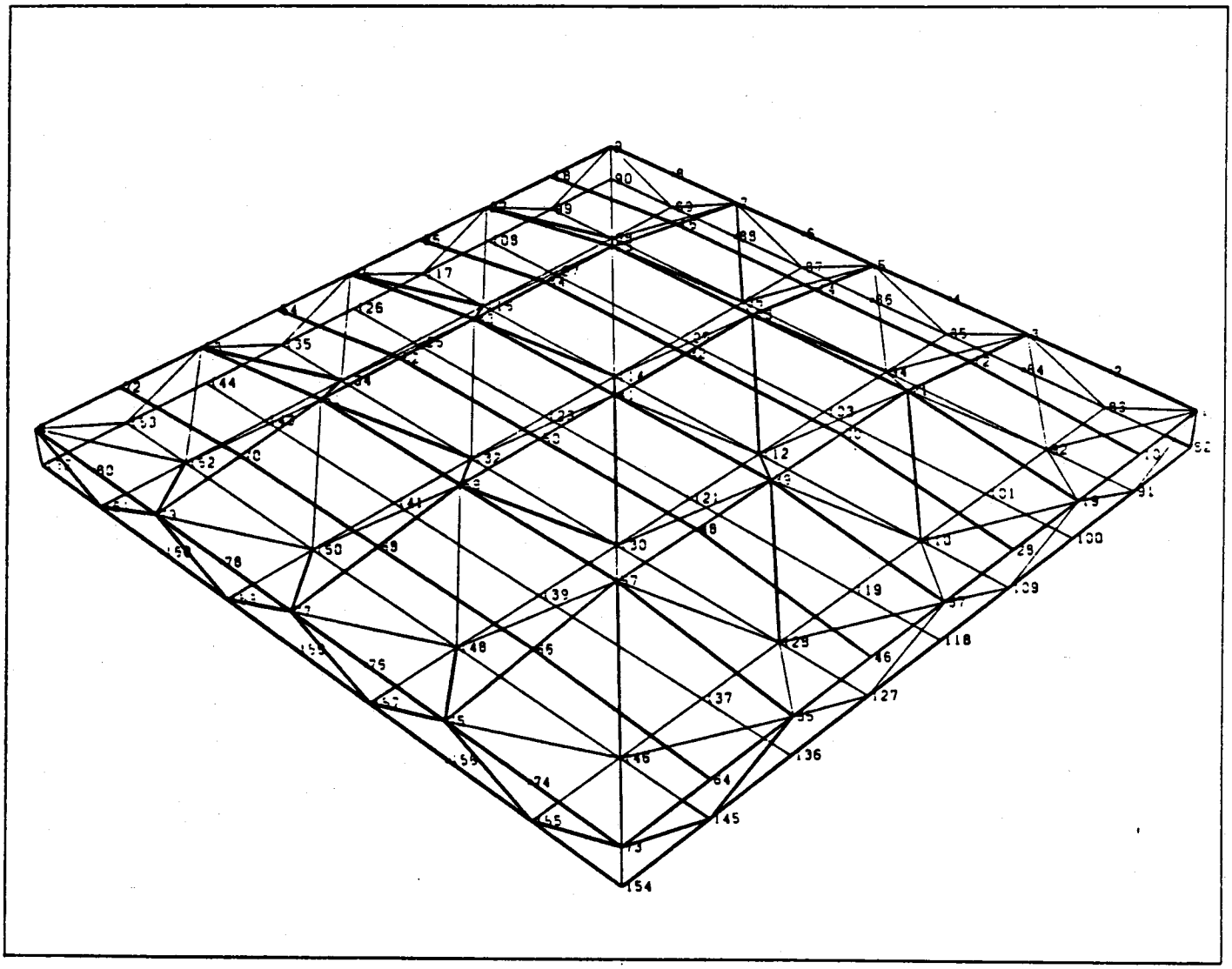

FIGURE 2.47 - TYPICAL DOOR MODEL

The side of the door facing the cavity is covered with a 1/8 inch thick layer of aluminum. Over the aluminum sheet is 2" of medium temperature insulation and 4 inch of intermediate temperature insulation. The final surface is then covered with a 12 gauge croloy sheet. This insulation assembly is attached to the door surface as packed panels. The side of the door facing outside the cavity is covered with a heat shield for a distance of approximately one-half the height of the door. The heat shield is 1/8 inch thick stainless steel and is designed to protect the door structural members from flux spillage when the doors are open and the receiver is in operation. A heat shield is also provided along the edge of the doors at the contact point between the two doors. The heat shield is painted with a solar reflective white paint (Pyromark Series 2500). The cavity doors are sized to withstand wind, seismic, and dead loads.

The doors have been designed to be raised and lowered by a motor and gear box arrangement. The motors have been sized to permit the doors to be raised and lowered while overcoming the dead weight of the doors, the vertical component of the wind load experienced on the door face, and the friction forces associated with the interface between the doors and the door rails. The mechanical connection between the upper and lower doors is provided by chain sprockets and a roller chain located on each side of the door. The motor and gear box arrangement was sized to raise or lower the doors in thirty seconds. Faster response times for closing

the doors were considered for emergencies. A fast closing door satisfies emergency operation assuming that the door can be protected against the high aperture heat flux by some material, possibly an ablative type. However, investigations into ablative materials indicated that there were no materials which would provide protection against the flux levels experienced. By leaving the doors open and providing a two minute reserve capacity in the Surge Tank, sufficient time would be available to initiate a back-up electrical system to de-focus the heliostats.

During nighttime operation, the closed doors must effectively seal the cavity to minimize convective losses. This is accomplished using a 3" diameter Tadpole seal which is attached to the door. The seal is shown in the door drawing of Figure 9.18.

2.6 Tower Design

The arrangement of the receiver support tower is shown in Figure 2.48, with a pump room near grade and an equipment room near the top of the reinforced concrete tower. The spatial arrangement of equipment floors is based on consideration of access, maintenance, and safety requirements. Tower accessories include an elevator which travels from grade to the roof at the top of the shell, a stairway from grade to the pump room, a stairway from the equipment room to the top of the shell, a caged ladder from the pump room to the equipment room, piping support embedments, lightning protection, aircraft obstruction lighting, access platforms, interior lighting, communication equipment, raceway, and a ventilation system.

2.6.1 Design of Tower and Foundation

The analysis and design of the receiver support tower meets the requirements of paragraph 3.2 and 3.4.3 of the "System Components Specification and Requirements." The reinforced concrete tower is 155 meters (508.5 ft.) tall, with a top diameter of 18.3 meters (60.0 ft.) and a base diameter of 24.4 meters (80.0 ft.), as illustrated in Figure 2.48. The top diameter of the tower shell is established from the framing requirements for the structural steel supporting the receiver. The tower/receiver interface is illustrated in Figure 2.49. The base diameter was determined from stress analyses which evaluated reasonable tapers, concrete shell thicknesses and reinforcement requirements. The design meets provisions of ACI 307-79, "Specification for the Design and Construction of Reinforced Concrete Chimneys." Seismic forces were computed for Seismic Zone 3 (per UBC 1973) with a Use Factor of 2.0. Wind forces were computed for a 1.44 kPa (30 psf) basic wind pressure.

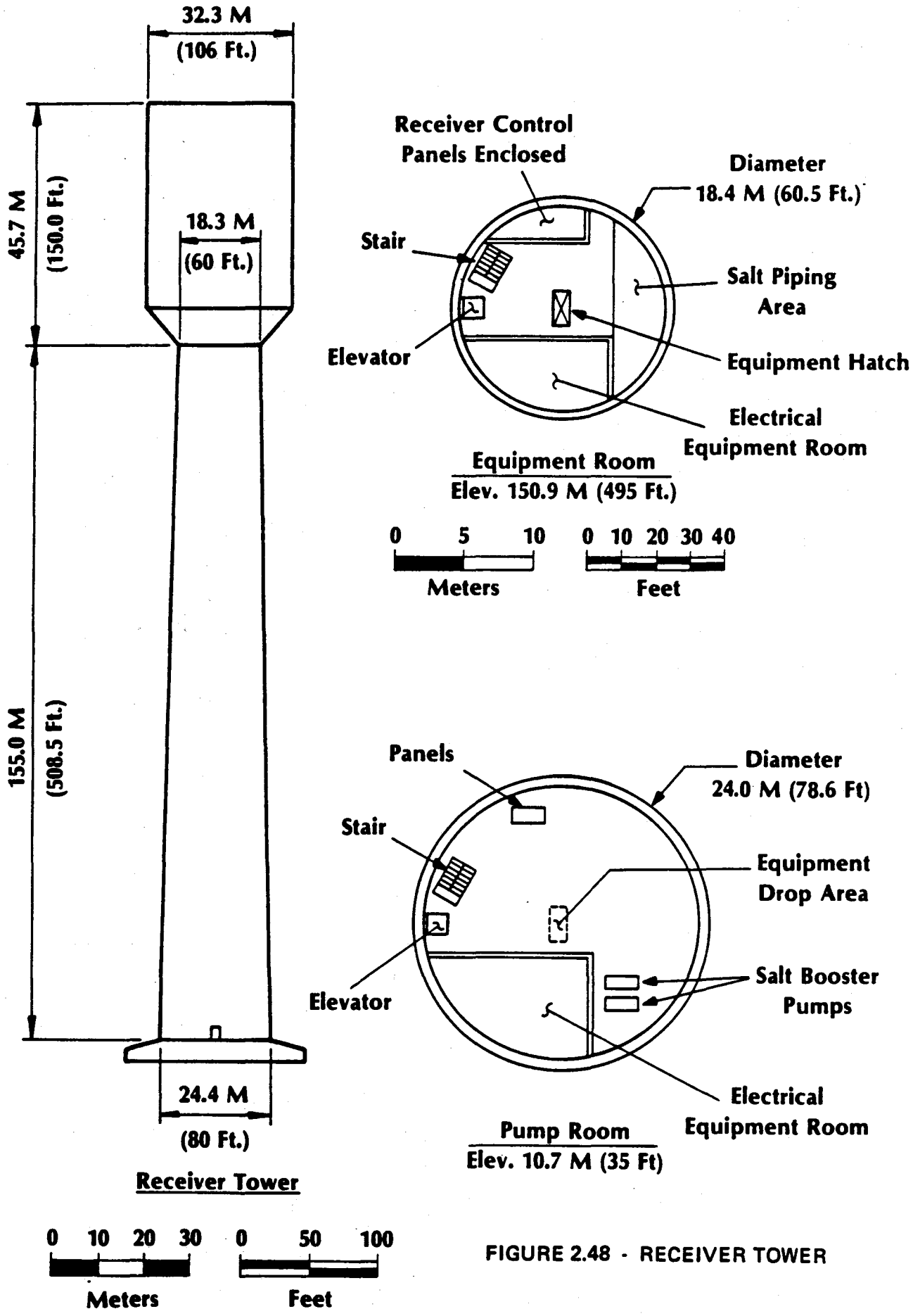

FIGURE 2.48 - RECEIVER TOWER

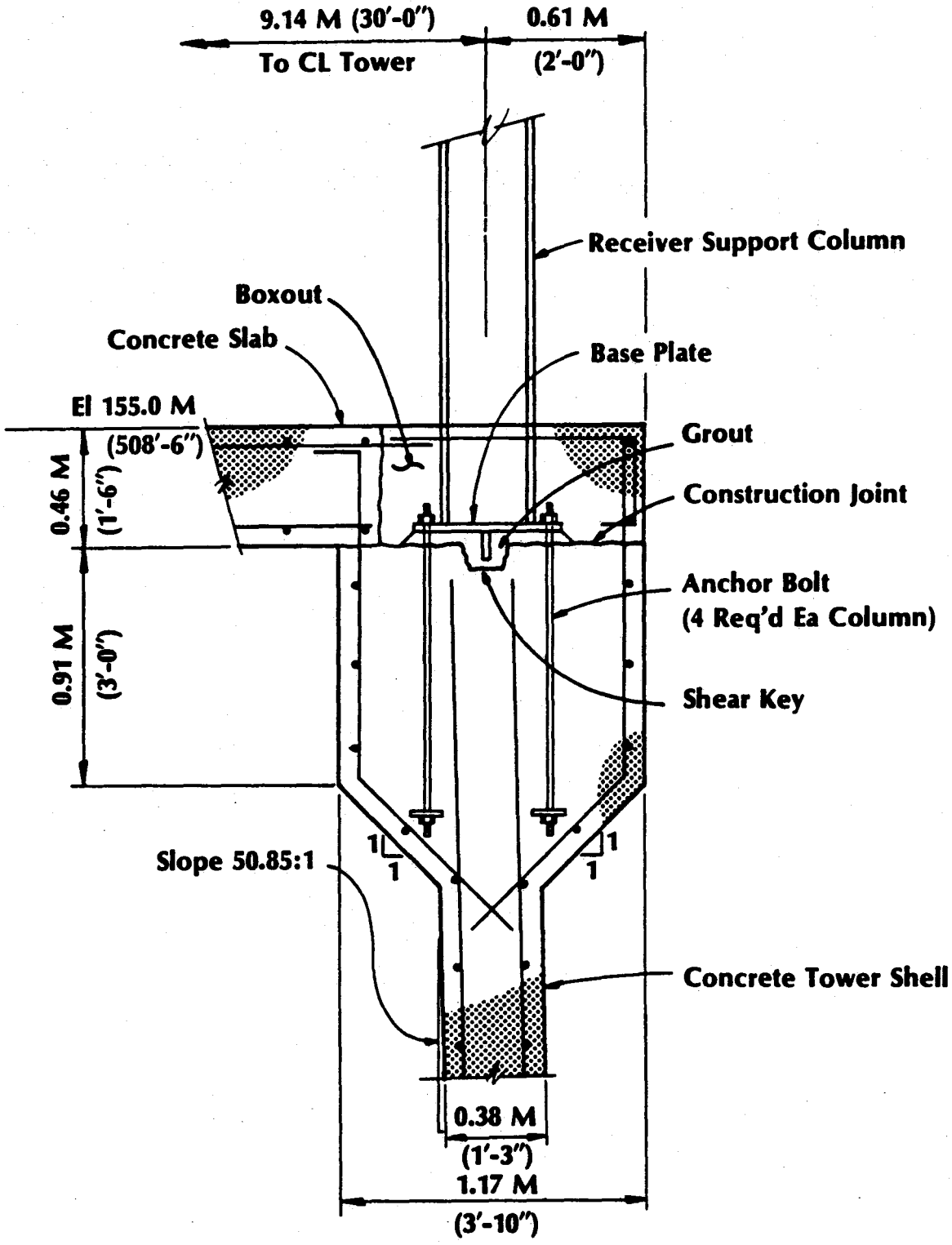

FIGURE 2.49 - TOWER/RECEIVER INTERFACE

Black & Veatch used its priority computer program, "Reinforced Concrete Chimney Design and Analysis," for the tower design. The user inputs the lateral forces, trial thicknesses and diameters; the program computes the vertical and circumferential reinforcement requirements, resulting stresses in the concrete and reinforcement for various load combinations, and the quantities of concrete and reinforcement. Wind and seismic forces due to the receiver were included by adding a concentrated shear and moment at the top of the concrete tower.

The tower foundation is a circular reinforced concrete mat, designed in accordance with ACI 318-77. No uplift is permitted on any portion of the foundation under lateral loading. The maximum settlement over the life of the solar plant will not exceed 0.025 m (1 inch) or 0.019 m (0.75 inches) differential between points across the diameter of the foundation. The maximum bearing stress on the soil is assumed to be less than the allowable bearing stress; otherwise piles would be used. In order to prevent uplift, the foundation mat is 40.2 meters (132.0 ft.) in diameter, 4.4 meters (14.5 ft.) thick under the shell and tapering to approximately 2.2 meters (7.25 ft.) at the outside diameter. The resulting bearing stress on the soil under dead load and earthquake is 400 kPa (8300 psf).

2.6.2 Seismic Analysis

Although the ACI 307-79 Specification provides suitable guidance for the design of the reinforced concrete receiver support tower, this approach offers no data for the seismic design of the receiver. Therefore, a seismic response spectrum analysis of the final tower design was performed in order to provide accelerations for design of the

receiver components and other associated equipment and piping. This analysis was performed using a version of computer program "SAP IV" (originally developed at the University of California at Berkeley and enhanced by Black & Veatch).

A lumped mass, or "stick," model of the tower and receiver was first developed. This model had twenty-two mass points, with the twelfth mass point at the top of the concrete shell. The receiver was modeled with mass and stiffness data provided by Babcock and Wilcox. The first five natural frequencies and modal participation factors for both horizontal and vertical motion are summarized in Table 2.14.

The Nuclear Regulatory Commission (NRC) Regulatory Guide 1.60 horizontal and vertical ground level design response spectra were normalized to 0.10 g and 0.25 g for the operational and survival earthquakes, respectively.

TABLE 2.14

NATURAL FREQUENCIES AND MODAL PARTICIPATION FACTORS (MPF)

Frequency Number	Horizontal Motion		Vertical Motion	
	Frequency (Hz)	MPF	Frequency (Hz)	MPF
1	0.37	21.0	4.06	24.0
2	1.47	11.1	8.78	9.70
3	3.03	9.67	15.5	6.87
4	5.82	6.67	20.7	3.32
5	8.53	4.90	26.1	4.03

$$MPF = \frac{\Sigma\, m_j\, a_j}{\Sigma\, m_j\, a_j^2}$$

These spectra are shown in Figure 2.50 and 2.51. Damping for the tower was taken to be 0.01 and 0.02 of critical damping for the operational and survival earthquakes, respectively. These low values of damping better reflect the actual damping in a simple, chimney-like structure than do those of NRC Regulatory Guide 1.61 which are more appropriate for complex structures with a multiplicity of components.

For any particular mass point, the modal acceleration is equal to the modal displacement (normalized with respect to the mass matrix by SAP IV) times the modal participation factor times the spectral acceleration for the frequency associated with that mode. The maximum probable acceleration for any mass point is then taken as the square root of the sum of the squares of the modal accelerations.

For horizontal motion, four modes are required in order to be within 3.6 percent of the result using ten modes; this indicates that there is considerable "whipping" action at the receiver level (for this particular, generally conservative, ground motion). For vertical motion, the result for one mode is within 5.7 percent of the result using 5 modes.

The maximum absolute horizontal and vertical accelerations of the tower are plotted in Figure 2.52, and the key values are summarized in Table 2.15. The horizontal "whipping" effect is shown in the figure. The ground motion is amplified considerably, especially for vertical motion, as a result of the first natural frequency falling near the peak acceleration values of the response spectrum. It should be noted that the accelerations are fairly insensitive to changes in the shell design because natural frequencies are, simplistically, proportional to the

square root of stiffness divided by mass. Changing the shell thickness to increase stiffness also changes the mass, so the natural frequencies are only changed in a minor way.

TABLE 2.15

SEISMIC ACCELERATIONS AT RECEIVER

	Operational		Survival	
	Horizontal	Vertical	Horizontal	Vertical
Damping	1%	1%	2%	2%
Ground Acceleration	0.10 g	0.10 g	0.25 g	0.25 g
Top of Tower Acceleration	0.33 g	0.54 g	0.66 g	1.08 g
Top of Receiver Acceleration	0.65 g	0.88 g	1.29 g	1.73 g

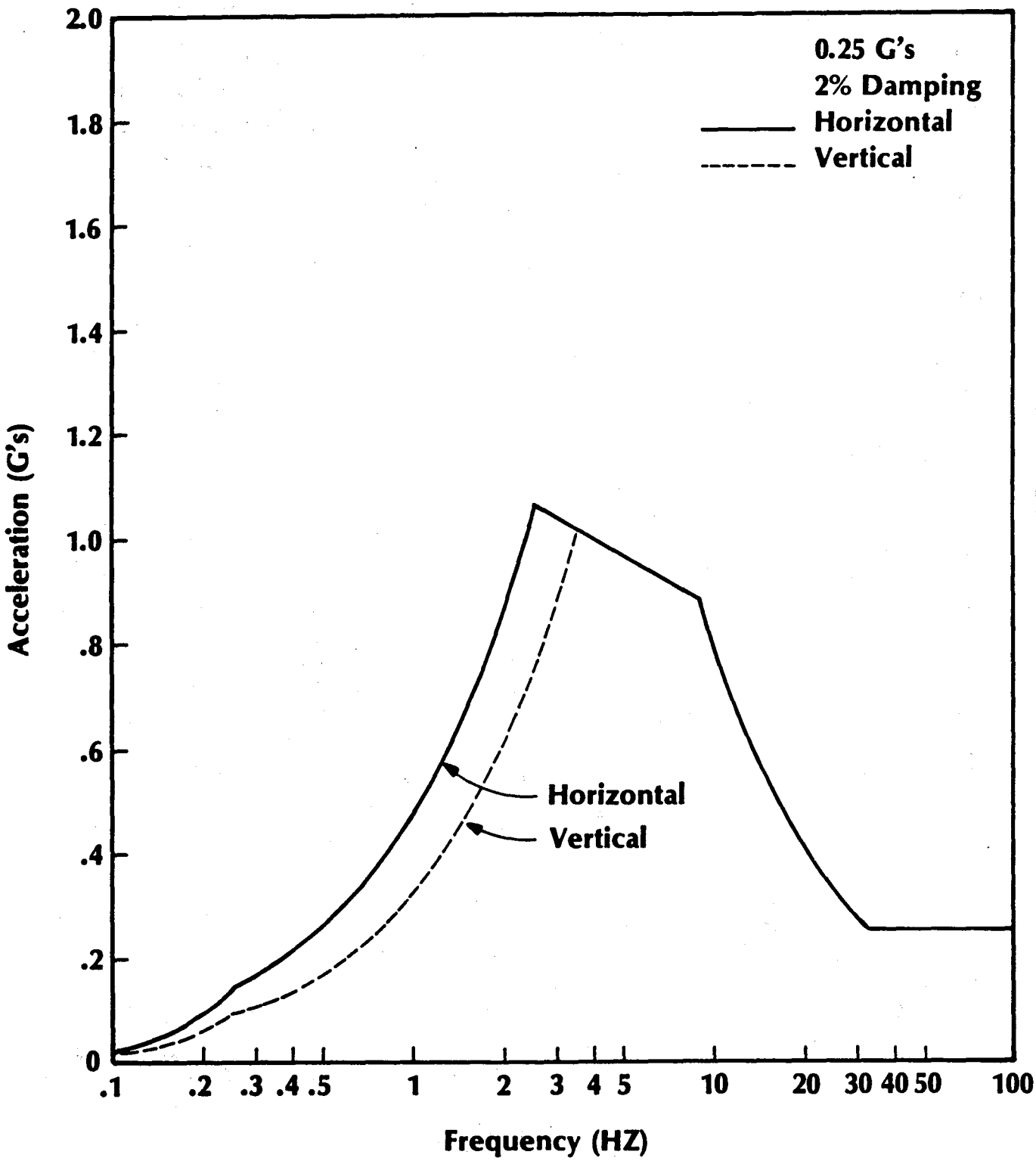

FIGURE 2.50 - SURVIVAL EARTHQUAKE GROUND RESPONSE SPECTRA

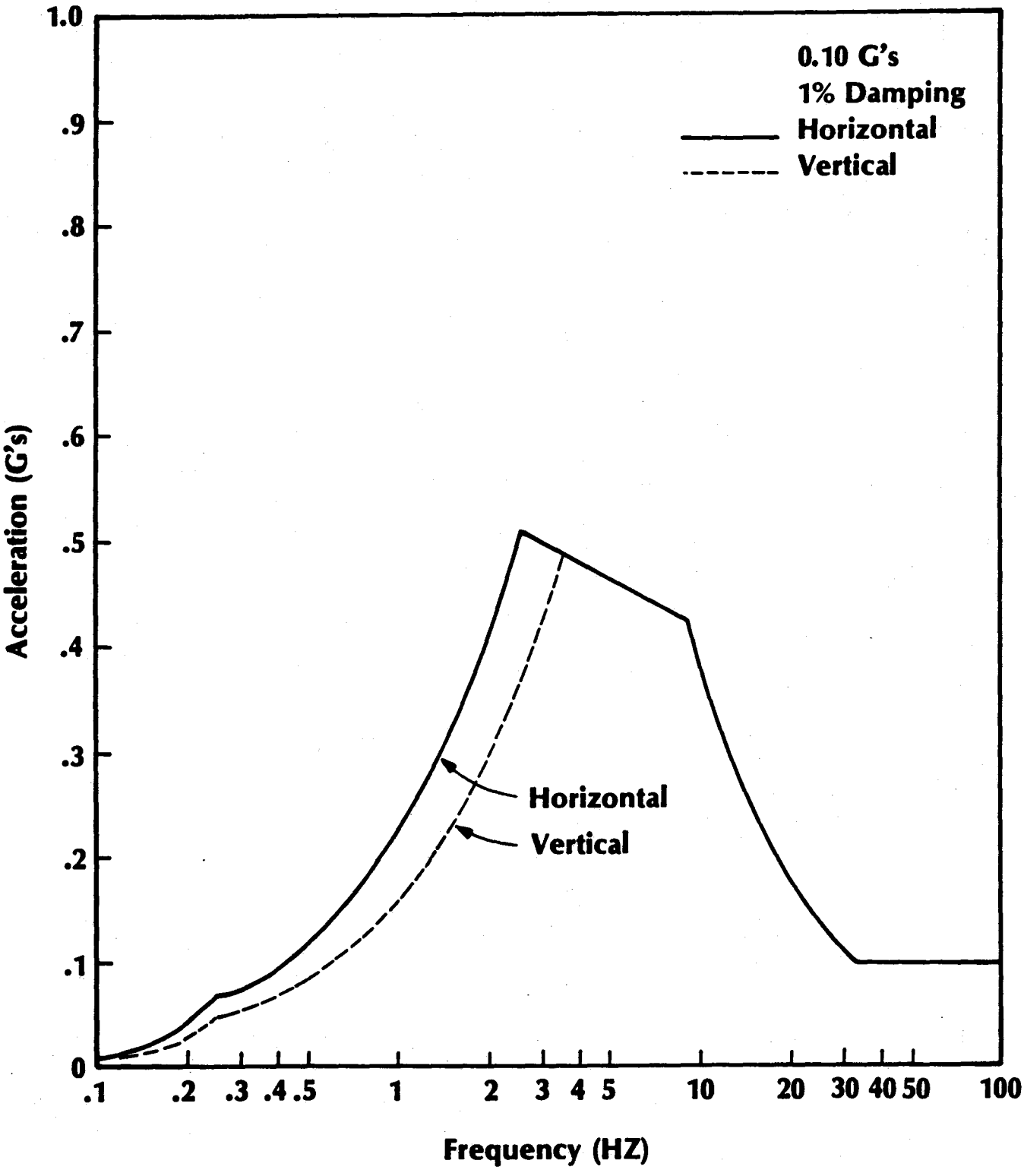

FIGURE 2.51 - OPERATIONAL EARTHQUAKE GROUND RESPONSE SPECTRA

Response Spectrum Analysis (NRC 1.60)
Operational EQ — 0.10g — 1% Damping
Survival EQ — 0.25g — 2% Damping

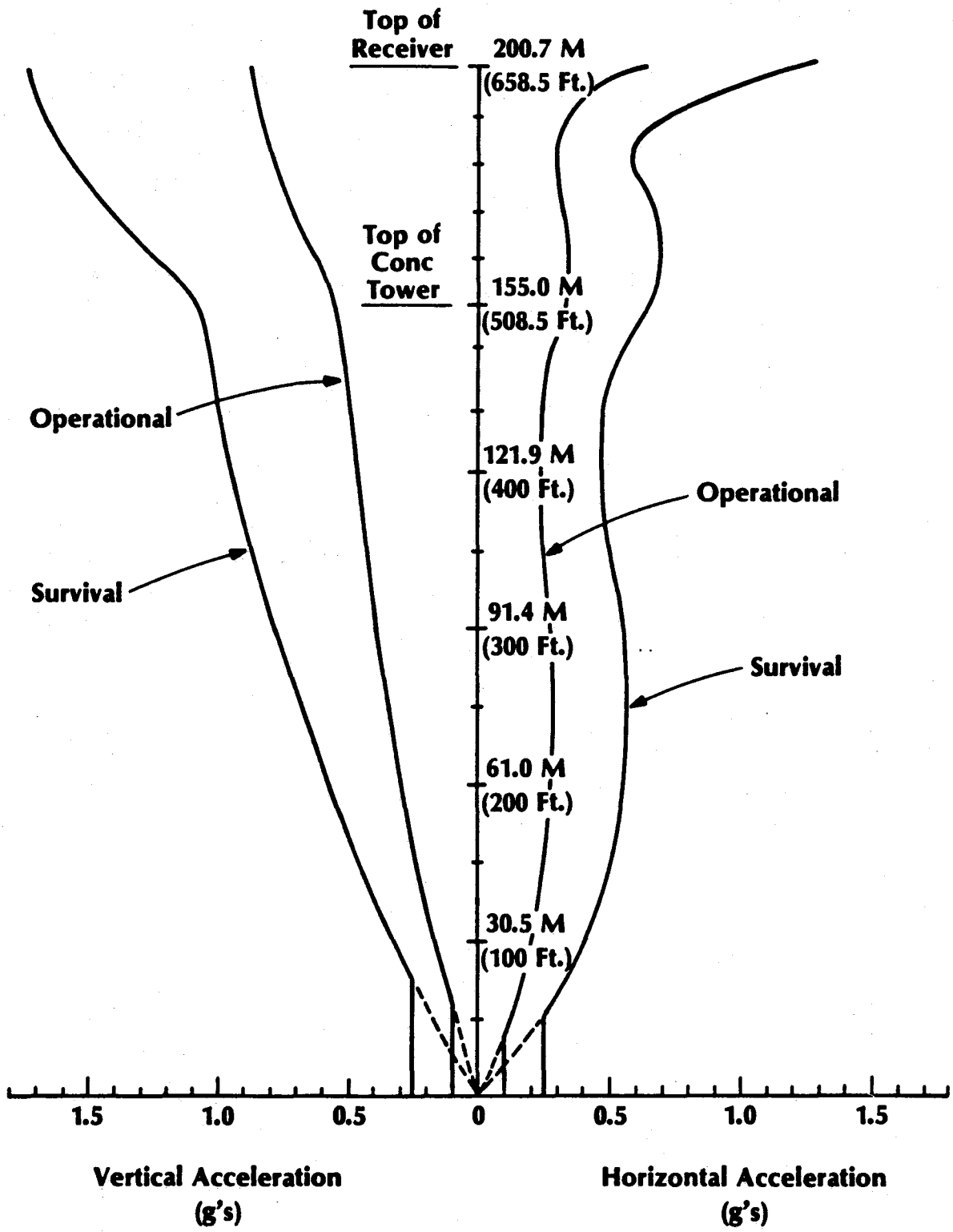

FIGURE 2.52 - SEISMIC ACCELERATIONS

3.0 BALANCE OF SUBSYSTEM

The balance of the receiver subsystem consists of the piping system, electrical distribution system, motors and drive mechanisms, recirculation pump, and booster pumps.

3.1 Piping System

The receiver piping system provides the salt flow link between the energy storage subsystem and the solar receiver and conducts the salt from the surge/buffer tank through the panels to the collector tank. For the purpose of this study, the hot and cold piping interfaces with the energy storage subsystem exist .03 meters (1 ft.) outside the receiver tower.

3.1.1 Piping Arrangement

The piping arrangement was selected to minimize piping costs, accommodate the anticipated thermal stresses of the piping system, and allow convenient draining of the lines. A schematic arrangement of the piping is shown in Figure 3.1. First, the piping arrangement of the main riser and downcomer is presented, followed by arrangement of the piping internal to the cavity.

Main Riser and Downcomer

The physical arrangement of the receiver cold salt supply and hot salt discharge piping is shown in Figures 3.2, 3.3, and 3.4.

The expansion loop arrangement utilized in the routing provides the required thermal flexibility of the piping system such that acceptable loads are imposed on the nozzles of the receiver tanks and booster pumps. The dimensions of each loop were selected such that they

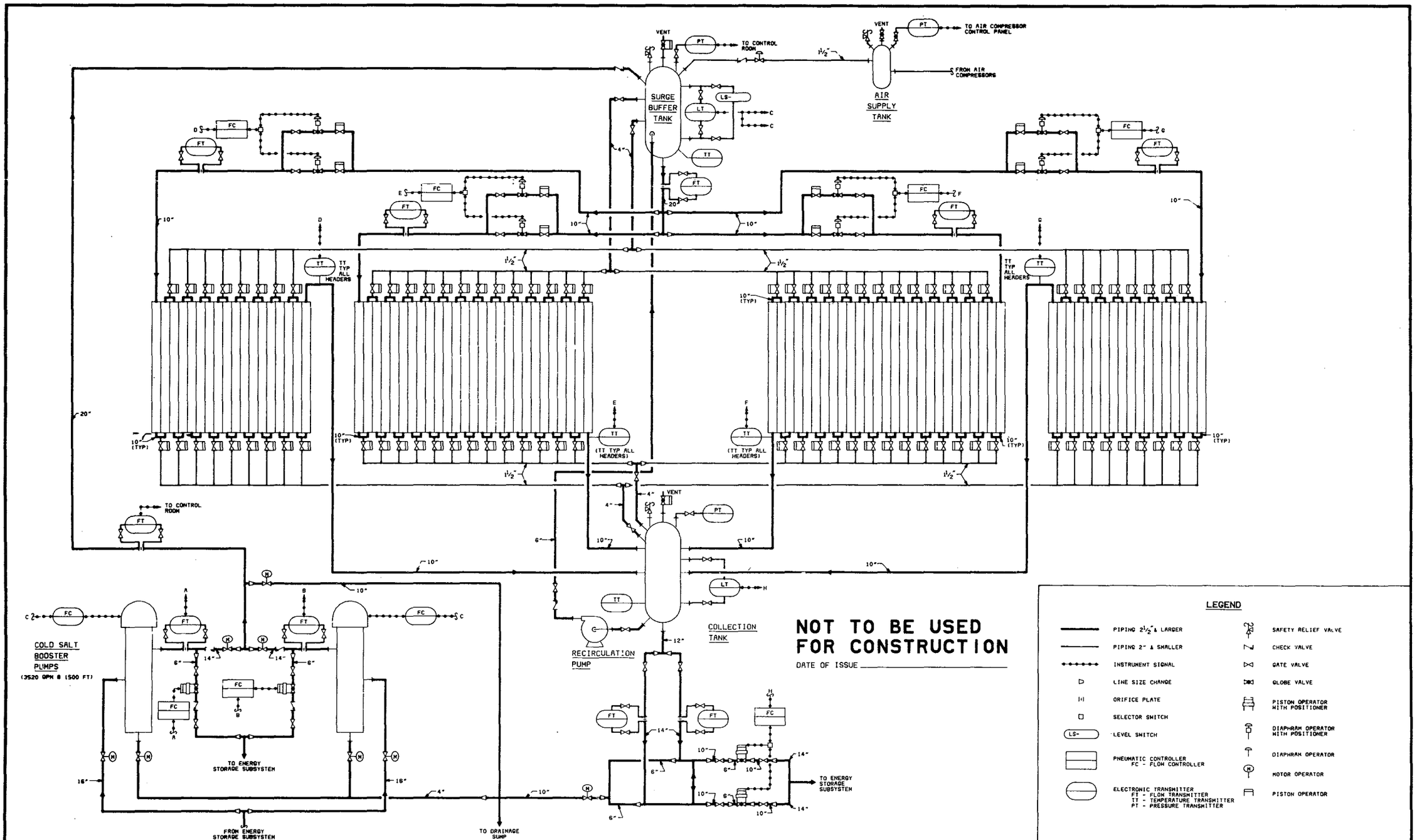

NOT TO BE USED FOR CONSTRUCTION

DATE OF ISSUE _____

FIGURE 3.1

NO.	DATE	REVISIONS AND RECORD OF ISSUE	BY	CHK	APP	ELM
2	12-01-82	GENERAL REVISIONS	ELD		JEH	
1	10-29-82	GENERAL REVISIONS	ELD		JEH	
0	09-28-82	PRELIMINARY ISSUE	ELD		JEH	

I HEREBY CERTIFY THAT THIS DOCUMENT WAS PREPARED BY ME OR UNDER MY DIRECT SUPERVISION AND THAT I AM A DULY REGISTERED PROFESSIONAL ENGINEER UNDER THE LAWS OF THE STATE OF
SIGNED _____
DATE _____ REG NO. _____

BLACK & VEATCH CONSULTING ENGINEERS

ENGINEER | DRAWN | CHECKED | DATE

SANDIA LABORATORIES/BABCOCK & WILCOX
MOLTEN SALT RECEIVER SUBSYSTEM
PIPING AND INSTRUMENT DIAGRAM
RECEIVER PIPING

PROJECT 9982 - | DRAWING NUMBER M1001 | REV 2
CODE | AREA

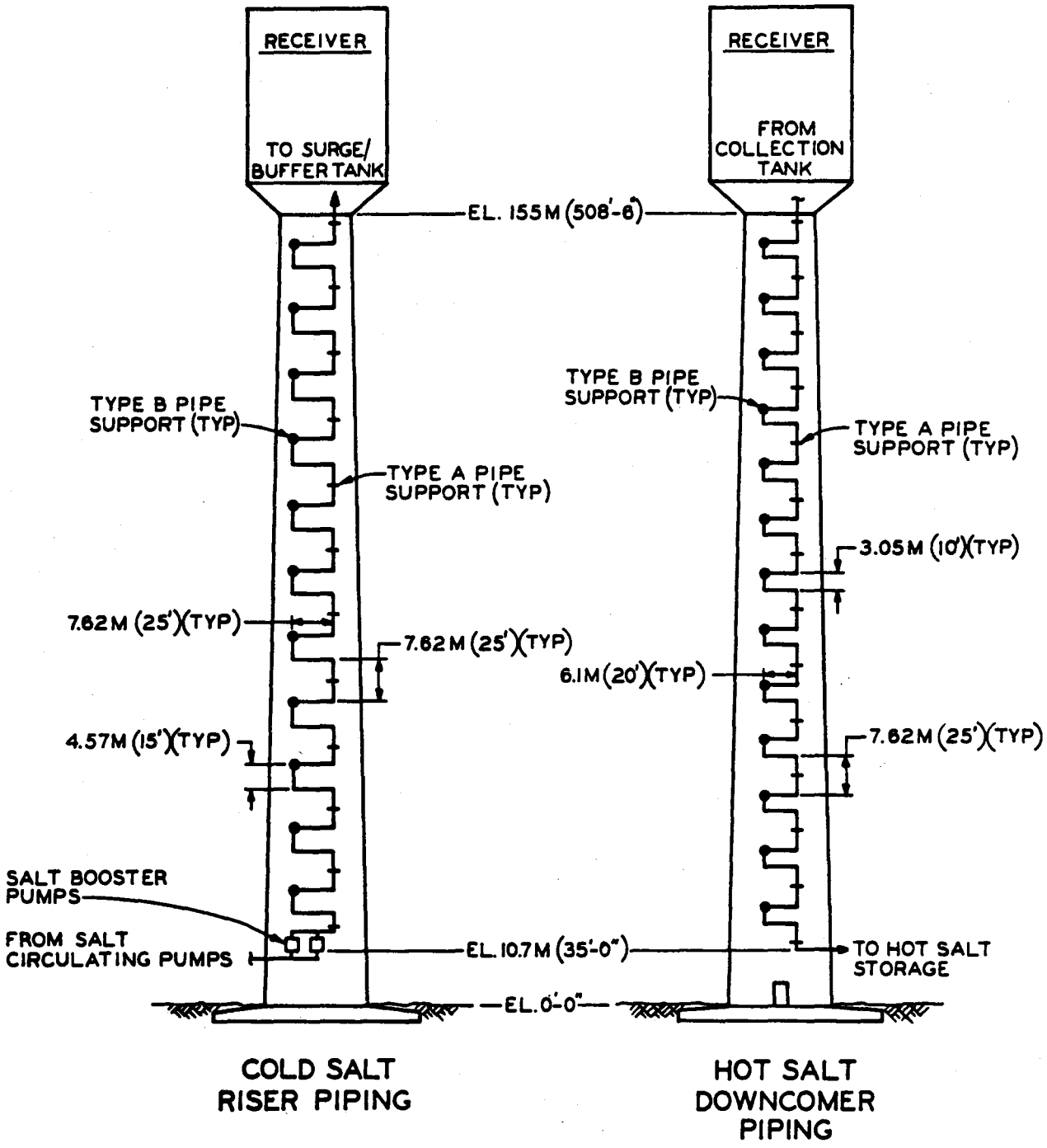

BLACK & VEATCH CONSULTING ENGINEERS PROJECT 9982	SANDIA LABORATORIES/BABCOCK & WILCOX MOLTEN SALT RECEIVER SUBSYSTEM	M1002
	RECEIVER TOWER PIPING ELEVATION VIEW	FIGURE 3.2

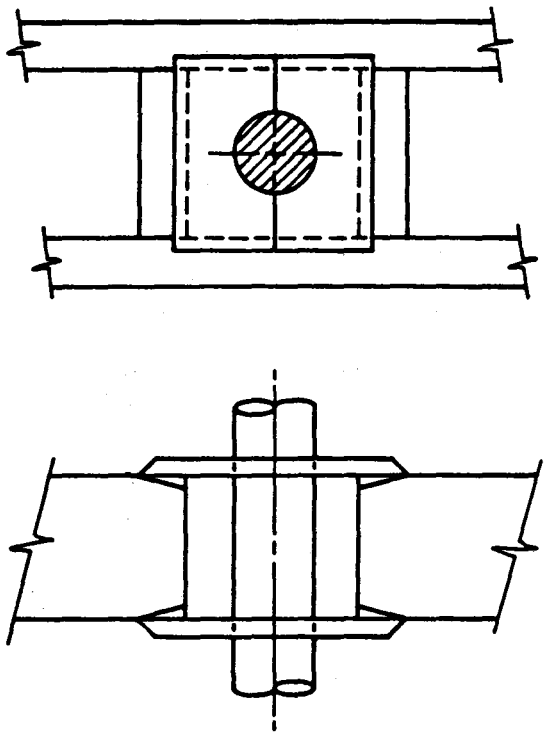

TYPE A PIPE SUPPORT
(ANCHOR)

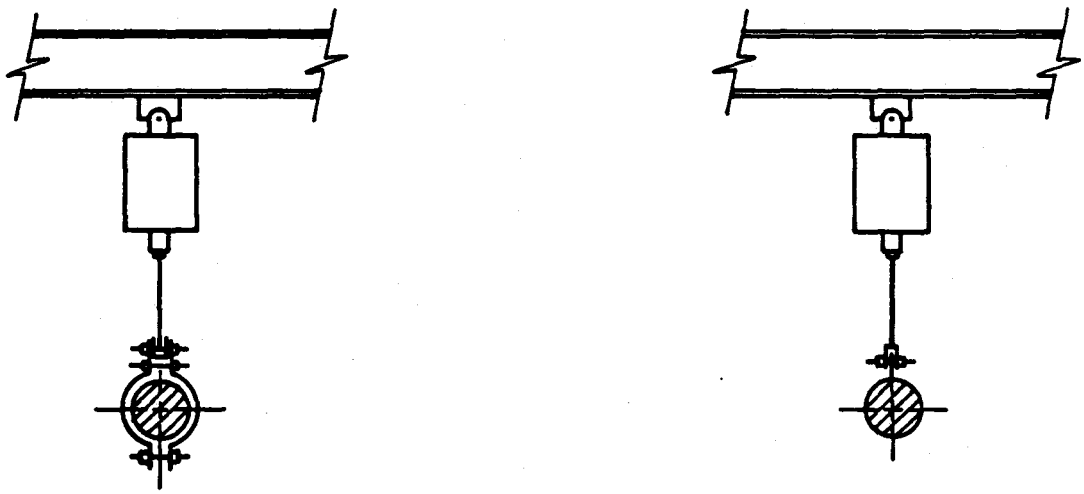

TYPE B PIPE SUPPORT
(SPRING HANGER)

BLACK & VEATCH CONSULTING ENGINEERS PROJECT 9982	SANDIA LABORATORIES/BABCOCK & WILCOX MOLTEN SALT RECEIVER SUBSYSTEM	M1004
	RECEIVER TOWER PIPING PIPE SUPPORTS	FIGURE 3.4

The recirculation line, which connects the collection tank to the surge/buffer tank, is used during the hot standby mode. This line pumps hot salt from the collection tank to the surge/buffer tank where it mixes with the cold salt to produce an intermediate temperature salt which is then distributed to the panels. The operation of the recirculation line maintains salt temperature above freezing rendering it unnecessary to drain the panels at night. When draining is required, a system of vent and drain lines, which are connected to the panels, facilitate the draining and filling of the panels.

The air supply line connects the air tank to the surge/buffer tank and is used to maintain pressure levels in the surge/buffer tank.

Figure 3.5 shows functional plan views of the absorption panels and crossover lines, both top and bottom. The salt flows from the surge/buffer tank to the first panels, center of the north and south walls, along the center walls and then out along the wing walls crossing back and forth. From the end of the wing walls the hot salt is then brought to the collection tank through the return lines. This arrangement of the crossover lines was chosen so that the salt flows from the panels with the highest heat flux to those with the lowest heat flux and also to give the crossover lines the best flexibility to allow for the thermal expansions.

Figure 3.6 is a sketch of the physical arrangement of the piping of the top of the wing wall in Zone 1. It shows how the headers, crossover lines and the vent lines are all interconnected. A similar arrangement is used for the bottom headers, crossover lines and drain lines with the exception that the bottom headers are all at the same elevation.

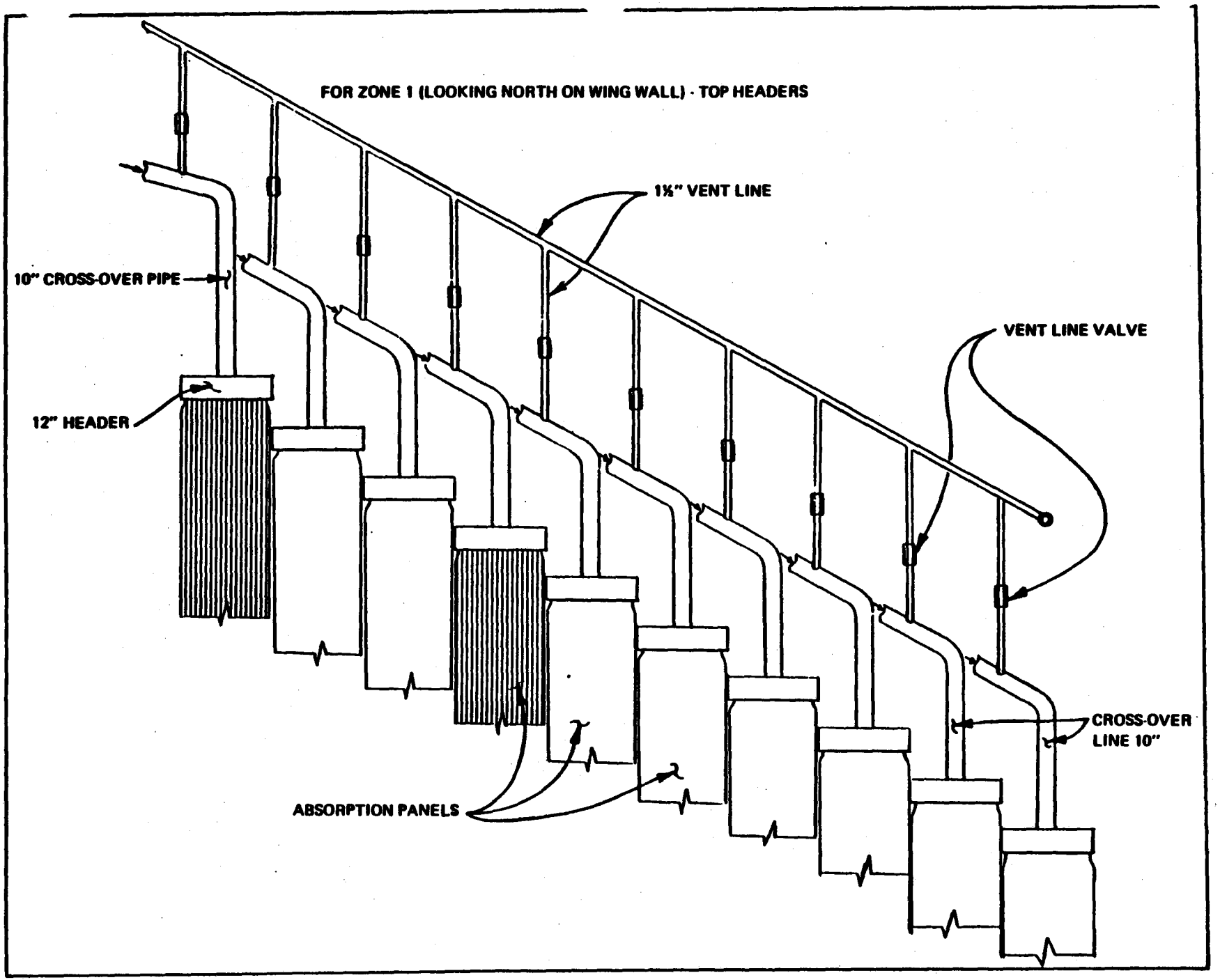

FIGURE 3.6 - VIEW OF HEADERS AND PIPING

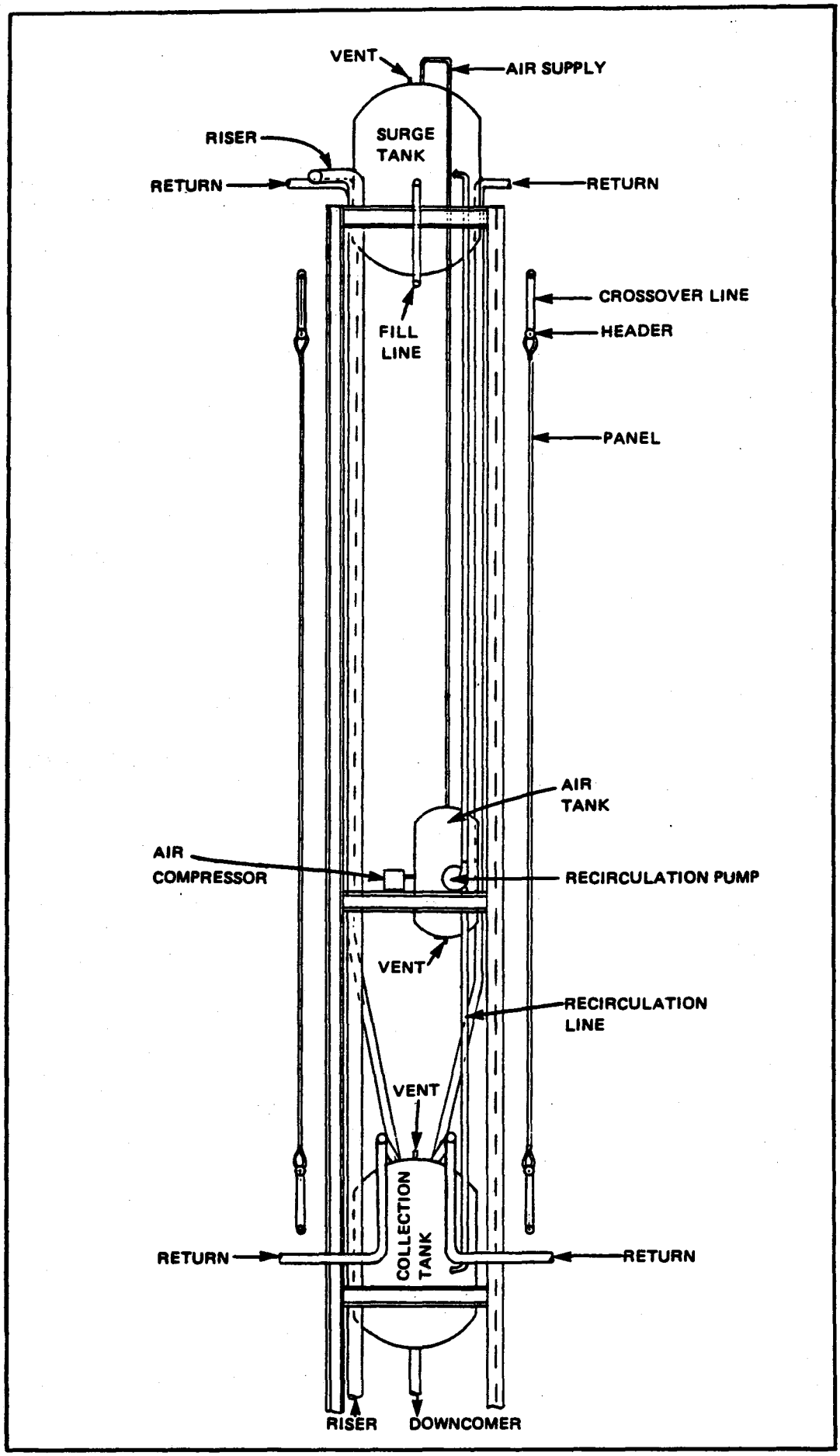

FIGURE 3.7 - ARRANGEMENT OF TANKS AND PIPING

TABLE 3-1. PIPE LISTING FOR RISER AND DOWNCOMER

Piping System	Pressure and Temperature		Pipe Size	Pipe Material
	Operating	Design		
Cold salt piping from energy storage interface to booster pump suction	288 C (550 F) 0.34 MP_a (50 psia)	316 C (600 F) 0.60 MP_a (100 psia)	450 mm (18") Std Wt	Carbon Steel ASTM A106 Gr B
Cold salt piping from booster pump discharge pump suction	288 C (550 F) 8.96 MP_a (1300 psia)	316 C (600 F) 11.7 MP_a (1700 psia)	500 mm (20") Sch 100	Carbon Steel ASTM A106 Gr C
Hot salt piping from receiver to energy storage interface	566 C (1050 F) 2.85 MP_a (414 psia)	593 C (1100 F) 3.1 MP_a (450 psia)	350 mm (14") XS	Stainless Steel ASTM A312 TP 304

3.1.3 Valves

The valve materials and pressure classes for the major valves are listed in Table 3-3. Valve materials were selected for compatibility with pipe material and design pressures and temperatures of the various piping systems. Valve pressure classes were selected in accordance with the American National Standards Institute Code for Steel Butt-Welding end Valves B16.34.

Isolation valves are gate type shutoff valves furnished with either a manual handwheel operator or an electric motor operator. Check valves are nonslam, tilting disc type nonreturn valves. Both types of valves utilize packing for shaft sealing; and will be heat traced to prevent solidification of salt in the packing.

Control valves are piston operated, self-draining, single piece body, cast steel valves. They are furnished with stainless steel bellow seals and equal percentage trim. Redundant control valve stations are provided in critical service applications. This arrangement allows maintenance to be performed on one station without shutting down the receiver or draining the lines.

3.1.4 Recirculation Pump

The salt recirculation pump is a vertical cantilever pump. The pump is cantilevered into a 1219mm (4 ft.) diameter by 2133 mm (7 ft.) long suction vessel and circulates salt from the collection tank to the surge/buffer tank during diurnal shutdown. The recirculation pump has a total developed head of 72 KPa (10.5 psi) sized to overcome piping losses plus a suitable design margin. The pump has a capacity of 147 m^3/hr (650 gpm) and an operating temperature range of 260°C (500°F) to 427°C (800°F).

3.1.5 Heat Tracing

Heat tracing of the receiver subsystem will use electric power from the grid and is designed to prevent salt solidifcation in the receiver headers, valves, pumps, tanks, and piping. Trace heaters are flexible type cabling with a two conductor element and covered with an Inconel sheath. Two completely redundant sets of electrical trace heaters are provided to insure integrity.

Provisions are made to monitor the temperatures adjacent to the trace heating elements and to disconnect power to the elements when 1) heating is no longer required or 2) temperatures would exceed maximum operating limits. The trace heaters are designed to preheat each component to a minimum temperature of 277°C (530°F). The heat-up time from ambient temperature 21°C (70°F) to design temperature is a minimum of 12 hours.

TABLE 3.5 INSULATION LISTING

ITEM	THICKNESS	INSULATION MATERIAL	LAGGING
Panels	2"	Med. Temp. Block (ASTM C-612 CL. 3)	Aluminum
	4"	Intermed. Temp. Block (ASTM C-612 CL. 5)	
Panel Seals	2"	Kaowool K3000	Aluminum
	2"	Med. Temp. Block (ASTM C-612 CL. 3)	
	2"	Med. Temp. Blanket (ASTM C-592 CL. 2)	
Roof & Enclosure 1/2	2"	Med. Temp. Block (ASTM C-612 CL. 3)	12 GA. CROLOY
Panels	4"	Intermed. Temp. Block (ASTM C-612 CL. 5)	3/16" A36
Roof & Enclosure 1/2 Seals		Med. Temp. Blanket (ASTM C-592 CL. 2)	12 GA. CROLOY
Headers	7 1/2"	Med. Temp. Blanket (ASTM C-592 CL. 2)	Aluminum
Floor Panels 1/2	2"	Calcium Silicate (ASTM C-533)	12 GA. CROLOY
	4"	Calcium Silicate (ASTM C-533)	3/16" A36
Floor Seals	2"	Mineral Fiber Blanket (ASTM C-612-70 CL.3)	Aluminum
Doors 1/2	2"	Med. Temp. Block (ASTM C-612 CL. 3)	12 GA. CROLOY
Panels	4"	Intermed. Temp. Block (ASTM C-612 CL. 5)	3/16" A36
Surge Tank	8"	Calcium Silicate Block	Aluminum
Collection Tank	8"	Calcium Silicate Block	Aluminum

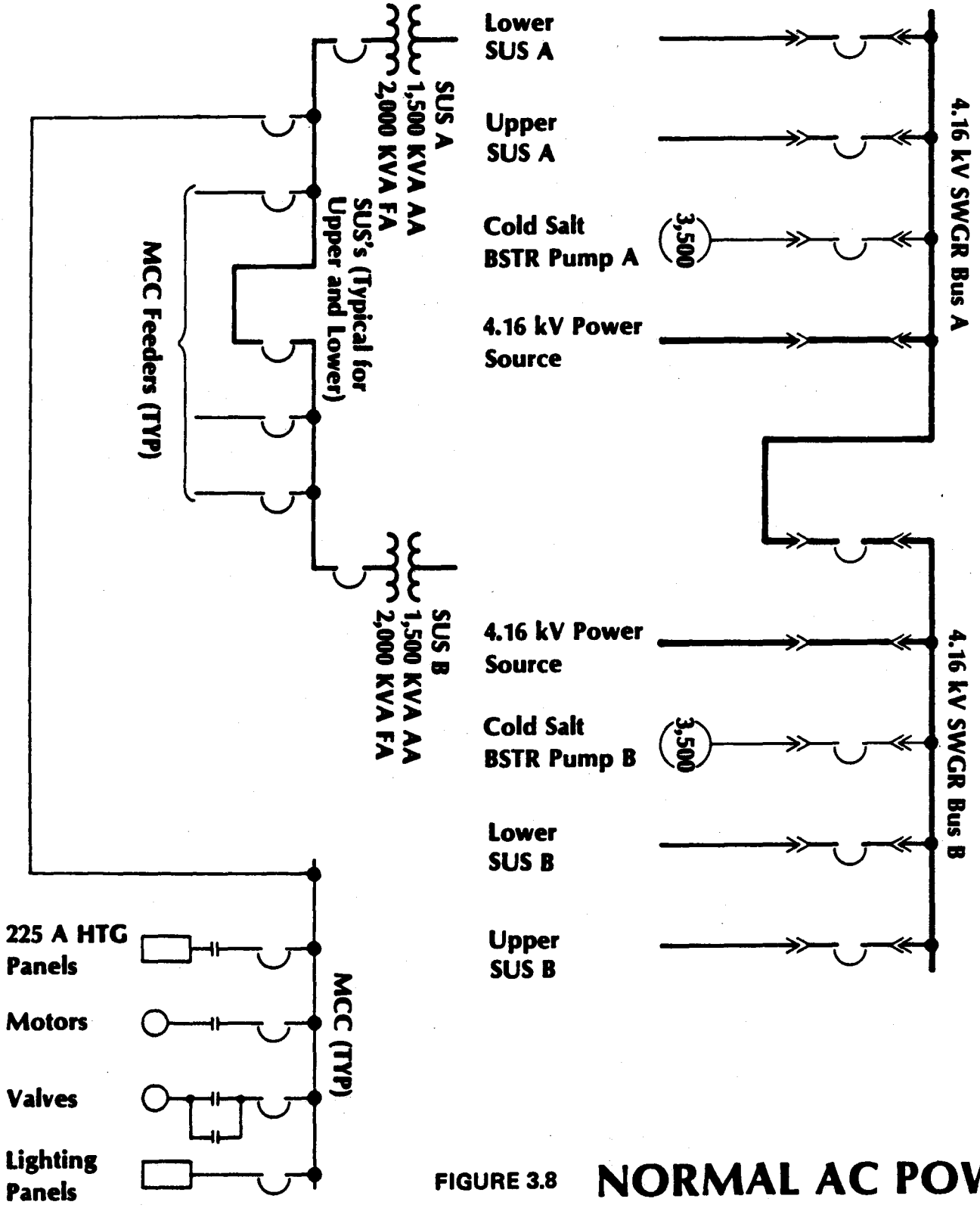

FIGURE 3.8 **NORMAL AC POWER SUPPLY ONE-LINE DIAGRAM**

Tower Electrical System Requirements

- The two Cold Salt Booster Pumps utilize two 2610 kW (3500 hp), 4000 volt motors to drive the pumps. The motors are located at elevation 10.7 m (35 ft.).
- The Trace Heating System requires 400 VAC and 277 VAC circuits having power requirements of approximately 295 kW operating and 1024 kW startup. The locations of these circuits are throughout the tower.

The vertical, turbine, multistage pump was selected because of its ability to deliver high flow rates at high pressures. An alternative vertical, cantilever pump was considered but rejected because of the necessity to place three or four of these pumps in a series pumping arrangement to achieve the required head. While the cantilever pump would not have bearings operating in the salt, the inability of this pump type to produce high pressures makes it an impractical pump for this service. Vertical turbine pumps are used in similar molten salt services by the petroleum industry with excellent results.

The pumps are each furnished with a 2610 kW (3500 hp) motor. The motors are variable speed units utilizing a changing input frequency to produce a wide range of operating speeds. With this arrangement, the pumps will always operate at their maximum efficiency for any given speed. Control valves are not required to throttle the discharge flow, and operating costs are minimized.

4.0 OPERATION AND CONTROL

The operating procedures for the receiver subsystem are designed to provide for safe, efficient plant operation, and maximum use of daylight hours for collection of thermal energy. The control system is designed to support these goals by maintaining close automatic control over system operating parameters, providing automatic protection of the absorption panels from transient effects, and providing the operator with system monitoring, warnings, and alarms.

4.1 Operational Modes

The operation of the receiver subsystem may be divided into two major categories; normal operation, and abnormal operation. Normal operation centers around the diurnal cycle and natural transients resulting from cloud cover. Abnormal operation is the response of the subsystem to upsets generally resulting from some failure within the plant system.

4.1.1 Normal Operation

The following discussion documents the proposed normal operating procedures for the receiver subsystem. Included in the discussion of each condition is a statement of the operating philosophy, and for transient conditions, a description of the sequence of events. The operating conditions that will be presented are:

- Steady-State
- Cloud Transients
- Hot Standby
- Startup from Hot Standby
- Shutdown to Hot Standby
- Cold Startup
- Prolonged Shutdown

Steady-State

Steady-state operation is defined as any operation during which only very slow changes in power occur, such as the changes caused by the tracking of the sun. The operating philosophy for steady state operation is to control the flow to maintain 565C (1050F)outlet salt temperature. This is a relatively easy control function and is accomplished by monitoring salt temperature and adjusting the panel flow control valves to match flow to the energy input in each circuit. This is performed under automatic control, without operator action. Steady operation is projected to encompass 73 percent of the available daylight hours at Barstow.

Operating Cloud Transient

An operating cloud transient is defined as any operation where significant portions of the collector field are shaded by clouds, but sufficient energy is available to justify operation. The philosophy for operating cloud transients is to keep the heliostats focused on the receiver to maximize the energy absorption of the system, and when necessary to sacrifice the salt outlet temperature by maintaining increased flow in the system to prevent high metal temperatures in any of the receiver panels. The principal difficulty of a cloud transient is that certain regions of the heat absorption panels may become shaded while other parts continue to be subjected to full flux. As a result, a high flow rate is needed to maintain the cooling of the heated regions, but since the total energy input to the circuit is down, the salt outlet temperature must drop. This results in the penalty of sending the low temperature salt down the downcomer to the thermal storage sub-system.

The thermal storage subsystem must, therefore, be prepared to handle low temperature salt. Operating cloud transients are the most complex conditions for which the control system must be designed. As a result of the rapid changes in heat flux at the absorption panels resulting from cloud passage, the control system must anticipate the salt outlet temperature resulting from transient heating patterns and adjust flow to protect the panels from overheating.

Hot Standby

Hot standby condition occurs during two modes of operation. First, during daylight hours when weather conditions prevent operation, and second, during diurnal shutdown. The operating philosophy during hot standby is to maintain forced recirculation in the absorption panels, to prevent freezing. The quad cavity receiver incorporates doors and insulation so that the individual cavities can be insulated to minimize heat loss. However, a great deal of heat will still be lost because of the large amount of external surface area of the enclosure. This heat is transported from the absorption panels themselves by convection and radiation within the cavities. The surge/buffer tank and collection tank have been sized to provide sufficient warm salt storage to allow hot standby operation overnight without recharging the system with hot salt from the ground.

Startup from Hot Standby

The sequence of events that occur to bring the system from hot standby to a steady state operating condition are first to bring all of the heliostats to a standby point in the vicinity of the receiver apertures. After that, in quick succession, the cavity doors must be

opened, the booster pump started, the subsystem isolation valves opened, recirculation shut off, and flow established from the booster pump up through the riser, the panels, and back down through the downcomer. Once flow has been established, a relatively high flow rate must be obtained in anticipation of power ramp up. This flow rate must be set higher than that required for the anticipated power from heliostat field to protect the absorption panels from high local heat fluxes that may occur during the power ramp up. Next, the heliostats are brought on to the target and power ramped up to the full operating level available for the current insolation conditions. Once all of the heliostats are on target, the system is turned over to the automatic control system and design temperatures in the system are established. During the power ramp up, however, low temperature salt must be sent down the downcomer to the thermal storage subsystem.

Shutdown to Hot Standby

Shutdown to hot standby from some steady state operating condition would normally be undertaken when overcast conditions occur or in preparation for overnight shutdown. The first step in this sequence is to remove the heliostats from the receiver and take them to their standby point. Once this is accomplished, the recirculation pump is started, the system is isolated at the riser and the downcomer, and the booster pump is shut down. At this point, if the shutdown is due to cloudy conditions, the operator must decide whether to leave the doors open and maintain salt temperature in the system with a few heliostats between cloud passages, or to close the cavity doors and set up for prolonged

shutdown and wait for the cloudy conditions to end. If the shutdown is in preparation to overnight standby, a set of warm up heliostats may be brought on target while the system is recirculating to bring the system to a higher temperature. This will allow initiation of the diurnal shutdown with enough storage to keep the receiver hot for a period of 12 to 16 hours.

Cold Startup

The first event in the cold startup sequence is trace heating of all the piping and tanks to a temperature above the salt freezing point so that salt may be introduced to those components without danger of freezing. Once the system is heated up, the heliostats are brought to the standby point and the cavity doors opened. Once the doors are open, a set of warmup heliostats are brought onto the panels in order to heat them up, in the dry condition, to a temperature that will allow introduction of salt without danger of salt freezing. Because of the large distances from the receiver to the outer heliostats, there is no problem bringing a small number of heliostats onto the panels to heat them to a temperature above the salt freezing temperature but below a temperature that would be dangerous to the panels. Once the panels are heated using these warmup heliostats, the booster pump can be started and the system may be filled with salt. While filling the system with salt, the fill/drain and vent lines are open in order to vent all of the gas out of the system. Next, a relatively high flow rate is established and then the heliostats are brought onto the target. Once all the heliostats are on target, the system is turned over to the automatic control system which will cut back the flow and establish design temperatures.

Prolonged Shutdown

The sequence of events for prolonged shutdown is fairly simple. First, the system must be brought to hot standby conditions. Then, starting at hot standby, the downcomer, riser, fill/drain and vent valves are opened allowing the molten salt to drain by gravity out of the system. Most of the salt will exit via the downcomer. Some of it will come down the riser. A bypass line around the riser check valve and the booster pumps is incorporated in the system to allow the riser to drain. The salt will be drained into the thermal storage system. Venting of the system is done with atmospheric air.

4.1.2 Abnormal Operation

The molten salt solar receiver subsystem has been designed for safe, economical operation, and will withstand common upsets without damage, and will withstand improbable upsets safely but with some potential for damage. The design of the receiver subsystem includes the following abnormal conditions:

- Loss of site power
- Loss of power to the heliostat field
- Molten salt pump trip
- Failure of a molten salt pipe
- Failure of panel tube
- Failure or improper operation of isolation, relief, or control valves
- Loss of salt flow control
- Heliostat field trip (inadvertent)
- Loss of surge tank pressurization

Definition of System

In designing for abnormal conditions, the subsystem incorporates a combination of features, controls, and instrumentation to ensure safe plant operation. Some of these items are:

- A large volume Surge/Buffer tank along with a high pressure air blowdown system is located at the panel inlet to maintain flow in the panels in the event that normal upward flow in the riser is interrupted.
- Check Valves are located in the riser to prevent loss of flow in the panels due to riser backflow.
- Control valves are designed to fail in a safe (full open) position.
- Sacrificial Shielding is incorporated on non-absorbing surfaces which may experience high solar fluxes if collector field control is lost.
- Flow Sensing is incorporated in the riser, the individual control zones, and in the downcomer such that large salt leaks may be detected.
- Temperature Measurements are made throughout the loop to allow normal control as well as sense temperature upsets.
- Pressure Measurements are made in the Surge/Buffer tank and Collection tank to allow monitoring of flow conditions
- Level Sensing is incorporated in the Surge/Buffer tank to monitor salt supply to the panels.
- Control valve positions are sensed by transducers to allow monitoring of control authority in all circuits.

- Redundant instrumentation and voting circuits are used to assure reliable shutdown of the equipment during emergency events.

Response to Abnormal Conditions

In response to each of the abnormal conditions, the system will detect the problem, alert the operator, and react in a manner to allow safe operation or shutdown of the plant. The response of the subsystem to each condition is discussed below. The sequence of presentation of the conditions is from the most critical to the least critical.

Loss of All On-Site Power

The loss of all on site power implies the combination of several upsets including the loss of power to the collector field and to the molten salt pumps and a loss of salt flow control. The subsystem response to this condition is simply the sum of the responses to each of these upsets.

Upon loss of power, the pumps rapidly stop. Check valves in the riser will close, preventing backflow through the pumps, control valves in each flow circuit and at the base of the downcomer will fail open, and the high pressure air blowdown system will vent high pressure air to the surge/buffer tank to maintain pressurization. In this condition, flow will be maintained for approximately two minutes.

For worst case, loss-of-power also assumes a loss of power to the heliostat field. Thus, the heliostat sun tracking motion stops and the result on the receiver is a gradual defocus of solar power at the aperture and a tracing of the solar image away from the aperture and onto the non-absorbing surfaces. The heat flux distribution on the heat

absorption panels will shift and gradually decrease. Since there is a loss of power to the flow control valves, these will fail open, and full flow from the surge tank is maintained by the high pressure air blowdown system. The exterior non-absorbing surfaces around the apertures are protected by sacrificial shielding which will protect the structural steel behind it if repowering by an emergency power supply and defocus of the heliostat field occurs within two minutes. Substantial damage to the heat absorption surface and receiver structural members will occur if defocus is not accomplished with emergency power within two minutes.

Loss of Power to the Heliostat Field

In the event of loss of power to the heliostat field, heliostat sun-tracking motion stops and an alarm is given by the collector control system. The result on the receiver is a gradual defocus of solar power at the apertures and a tracing of the solar image away from the aperture and onto non-absorbing surfaces. Within the receiver, the reduction of power is detected and flow will ramp-down under normal control. The exterior non-absorbing surfaces surrounding the apertures, protected by sacrificial shielding, will heat-up, possibly to the point of some damage. The design of the receiver subsystem assumes that this shielding can absorb the energy without damage to the structural steel behind it. Repowering and defocus (or refocus) of the heliostat field must however occur within two minutes to prevent damage to structural components.

Molten Salt Pump Trip

Two half capacity molten salt booster pumps supply salt to the riser inlet. A "pump trip" is defined as a rapid loss of pumping. The same sequence of events applies whether a single pump or both pumps fail

but events happen more rapidly with the failure of both pumps. Upon tripping or failure of a pump, the pump outlet check valve will close preventing the loss of flow from the receiver due to backflow through the pump(s). This condition is sensed electrically by the control system (opening of breakers, loss of current) and an alarm is issued to the operator.

The failure mode to be prevented is overheating of the heat absorption panels. If both pumps trip, the controls will automatically trip* the heliostats; thus removing the heat input to the absorption panels. As a result of a single pump trip, salt flow to the surge/buffer tank is reduced and the level in the tank will begin to drop. At a preset level, an alarm is issued, and at a second (lower) level, a signal is sent to the master control system to trip* the collector field (approximately 1 minute). As level drops in the surge/buffer tank, the pressure will tend to drop as well but the high pressure blowdown system will activate to support flow. The circuit control valves will remain open under normal control 565C (1050F) outlet salt temperature so flow in the panels is maintained until the heliostat trip is complete. During pressurization by the air blowdown system, the surge/buffer tank is protected from overpressurization by its own relief system.

Failure of a Molten Salt Pipe

The response of the receiver subsystem to the failure of a molten salt pipe will depend on the size of the resulting salt leak and the

---

*Heliostat trip is defined as rapid removal of the heliostats to the standby aim point.

location of the leak in the subsystem. The subsystem may be considered in three sections:

1) Piping between the cold storage tank and the surge/buffer tank (upstream of the riser check valve).

2) Piping between the surge/buffer tank and the collection tank.

3) Piping downstream of the collection tank (isolation valve).

A small leak in any of these regions will, in general, not be detectable by plant instrumentation nor will it affect the operation of the plant. Visual inspection on a regular basis is required for detection of such leaks to prevent their propagation or an accumulation of salt.

A leak of a moderate size in any of the three sections will be detectable by plant instrumentation as a flow mismatch based on sensing flow to the riser, the absorption panels, and the downcomer and sensing of the surge/buffer tank level. Detection of such a leak will result in an alarm being issued to the operator. A leak of this magnitude may affect the operation of the subsystem, but not to the point where the panel temperatures cannot be controlled.

A large leak (25% or more of the flow lost) will cause different consequences depending on where it occurs. If upstream of the surge tank, it will cause the system to react as a pump trip with a reduction of level in the surge/buffer tank. The high pressure blowdown system will allow the inventory in the surge/buffer tank to sustain flow while the field defocuses.

If such a leak were to occur in the downcomer, detection would be by comparison of flow and the operator would be alerted to trip the plant. In this case, the heat absorption panels are unaffected.

If a large leak occurs in piping between the surge and the collection tank, the flow loss will be detected by flow instrumentation signaling the operator to trip the plant. The panel control valve will go full open, but damage may occur in panels downstream of the break and possibly in parallel circuits due to overheating. The likelihood of such damage depends on whether the accident occurs when the plant is at or near full power.

Failure of a Panel Tube

The failure of a panel tube is a special case of piping failure between the surge/buffer tank and the collection tank. Small leaks will not affect operation but should be detected by scheduled (suggest nightly) inspection. Moderate leaks will be detected as a flow mismatch and the operator signaled. Large leaks will be detected and the operator alerted, but damage due to overheating may occur in downstream panels, parallel tubes in the leaking panel, and in panels in the parallel zones.

Failure or Improper Operation of Isolation, Relief, or Control Valves

Improper operation of a valve during normal plant operation, whatever the cause, may impact plant operation in many ways depending on the location of the valve in the system. For consideration of the impact of improper valve operation, the valves will be considered in the following groups:

1) Isolation and control valves upstream of the Surge/Buffer Tank.
2) The flow circuit control valves.
3) The downcomer isolation valve.
4) Isolation and control valves downstream of the downcomer.
5) The Surge/Buffer tank safety relief valve.

6) The Collection tank safety relief valve.

7) The Collection tank (Downcomer) power relief valve.

The subsystem response to each of these is described below.

1) Isolation and Control Valves Upstream of the Surge/Buffer Tank

Several valves exist in the receiver subsystem, or more generally in the plant system, which can restrict flow to the surge/buffer tank if improperly operated. The surge/buffer tank will detect the loss of flow as a level drop. The operator is notified by an alarm of the condition. A heliostat field trip will occur if the drop continues past a preset lower limit. While the heliostats are being defocused, flow will be supplied by the surge/buffer tank inventory supported by the high pressure blowdown system if necessary.

2) The Flow Circuit Control Valves

The flow in each of the four zones of the receiver is controlled by a control valve arrangement at its inlet. This control valve arrangement consists of two valves mounted in parallel, one of which is blocked open to permit 25% flow at full surge/buffer tank pressure with the other valve normally controlled to provide the required flow. In the event that the valve used for normal control should shut for any reason, the other valve could open under automatic control to provide flow for cooling of the panels. In no event, however, could the valves close further than the 25% flow position. Since the surge/buffer tank pressure will vary according to load, inadvertent closure of both valves will result in approximately

25% of the required flow. This could result in a rapid rise in the salt temperature within the system. At a preset temperature, an alarm is issued, and at a marginally higher limit, the subsystem controls will cause a heliostat field to trip. The high pressure blowdown system will also activate. Under full (or near full) power conditions, closure of these valves and restriction of the flow to 25% (loss of 75% flow) could result in damage to the panels resulting from overheating.

3) The Downcomer Isolation Valve

During any operation of the plant, the downcomer isolation valve is normally open. Inadvertent closure of this valve would result in overpressurization of the collection tank and a back-pressure on the system. The resultant decrease in flow will open the flow circuit control valves attempting to increase the flow to maintain the outlet temperature. Eventually the increase in panel salt temperatures will become uncontrollable as flow is choked off. To prevent overheating of the absorption panels, the controls will call for a heliostat field trip when over-pressurization of the collection tank is indicated. As further protection, the downcomer isolation valve is set up to operate slowly (approximately 30 seconds close fully) to allow time for the collector field to defocus.

4) Isolation and Control Valves Downstream of the Downcomer

Closure of any of the several valves downstream of the collection tank isolation valve in the receiver subsystem or

downstream further in the thermal storage subsystem would choke off flow in the absorption panels and overpressurize the Collection tank. The response is the same as when the downcomer isolation valve inadvertently closes, but some of the valves may be quick acting. Therefore, some provision must be made to relieve pressure in the Collection tank. Since venting salt in the tower should be avoided, a power operated relief valve is incorporated in the downcomer at ground level, upstream of the energy dissipation control valve, to allow venting of the Collection tank through the downcomer. This valve vents to an appropriate location in the storage subsystem and issues a signal to trip the heliostat field if the downcomer flow is blocked by a downstream valve. The collection tank is thus protected and flow in the panels maintained.

5) The Surge/Buffer Tank Safety Relief Valve

Inadvertent opening of the surge/buffer tank safety relief valve will result in loss of pressurization of the surge tank. Responding to this, the flow control valves will open in an attempt to maintain flow. When the position of the valves is nearly open, the high pressure blowdown system will be activated and a signal will be sent to trip the heliostat field. The surge/buffer tank is designed to be capable of venting the incoming air flow from the high pressure blowdown system, and the blowdown system itself has a relief valve to prevent overpressurization of the surge/buffer tank. However,

the relief system is matched to the capability of the blowdown system such that tank pressure will be maintained long enough to defocus the collector field.

6) The Collection Tank Safety Relief Valve

Inadvertent opening of the collection tank safety relief valve in the tower will result in hot salt being vented from the system and directed to a nearby sump. Venting of this valve must issue an alarm to the operator and trip the heliostat field. Venting of this valve will not interrupt cooling of the panels so no damage should occur.

7) The Collection Tank (Downcomer) Relief Valve

Inadvertent operation of this valve will vent salt to a sump on the ground. This should not affect plant operation, but instrumentation will be present to alert the operator so that appropriate measures can be taken to stop the loss of salt.

Loss of Salt Flow Control

Loss of flow control, resulting from failure of the control system or failure of pneumatic control power to the valves, will cause the flow control valves in each zone and the downcomer energy dissipation control valve to fail open. This causes maximum flow in the system. If unpowered, the high pressure blowdown system will be activated to support pressurization of the surge/buffer tank and support flow long enough to trip the collector field.

Heliostat Field Trip

The response of the receiver to a trip of the total or partial heliostat field is a normal operating control condition because it is similar to the response to a cloud transient. As the energy input to the apertures decreases due to the removal of heliostats, salt flow ramps down to a 25% minimum value and the operator is alerted. The operator may then elect to bring the plant back to full power by refocusing the heliostats or go to a hot standby condition in the receiver.

Loss of Surge/Buffer Tank Pressurization

Loss of surge/buffer tank pressurization will result in a decrease in flow in the heat absorption panels. This is countered by the flow control valves opening as the controls try to maintain flow. Eventually the pressure drops to the point where the high pressure blowdown system activates in an attempt to maintain surge/buffer tank pressure. Associated with the opening of the high pressure blowdown system, a signal is sent to trip the heliostat field. For most cases, the high pressure blowdown system will support surge/buffer tank pressure long enough to trip the collector field. For large failures, however, the system may not be able to support surge/buffer tank pressure and damage to the absorption panels due to overheating may result. The high pressure blowdown system will be tested periodically to ensure its integrity.

4.2 Control System Design

A complete report on the control system design analysis performed during this study is presented in Appendix C. A summary of the approach and of the principal results are given below.

4.2.1 Characterization of Transients

From a standpoint of receiver response, two classes of transients have been identified: "self similar" and "dissimilar", respectively. A self similar transient is associated with variable flux intensities at constant spacial distributions, whereas during a dissimilar transient both intensity and distribution of the incident fluxes vary with time. Previous studies, as well as initial results from this work have demonstrated the feasibility and practicality of salt outlet temperature control during steady state and self similar transient operation. The central problem to be resolved by the present study was to develop viable control schemes for dissimilar transients, with consideration to the possibility of transition from two-sided to one-sided heating of the wing walls.

4.2.2 Cloud Models

Available data on insolation variations due to cloud transients at the reference site have been reviewed and have been incorporated into two "worst case" cloud transient models: (1) the east-to-west sharp-edged cloud model; and (2) the group cloud model. The east-to-west model represents worst-case transients with regard to flux gradients and distributions along a control zone; a step-wise representation of the flux distributions for control zone No. 1 is shown in Figures 4.1, 4.2, and 4.3. The group cloud transient simulates the more frequent

occurrences of the passage of groups of smaller clouds (up to several hundred meters in diameter) over the heliostat field; the step-wise representation of the resulting flux distributions is shown for this transient in Figures 4.4 through 4.9.

4.2.3 Control Simulation Models

The MITAS computer code was used for the simulation of the control system. There have been two principal control schemes investigated: two-point temperature feedback; and quasi-feedforward control (QFFC). The former uses measurements of salt temperatures at two locations (e.g. midpoint and receiver outlet), and calculates the necessary adjustments in flow rate to minimize the deviation of outlet temperature from its setpoint. Only limited success has been achieved with this algorithm, and, consequently, it was dropped from further consideration. The quasi-feedforward algorithm calculates the heat absorbed by each pass from the temperature rise and flow rate through that pass, and determines the required flow rate to maintain the outlet temperature at the set point from heat balance considerations. As work progressed, several refinements have been incorporated into the basic quasi-feedforward algorithm, including salt temperature limit control, salt and wall temperature limit control, the use of optimal filters, and development of an optimal control scheme to minimize salt temperature fluctuations during dissimilar transients.

Simulation runs were performed with both "worst-case" transient models, at the design point, and under maximum thermal load conditions.

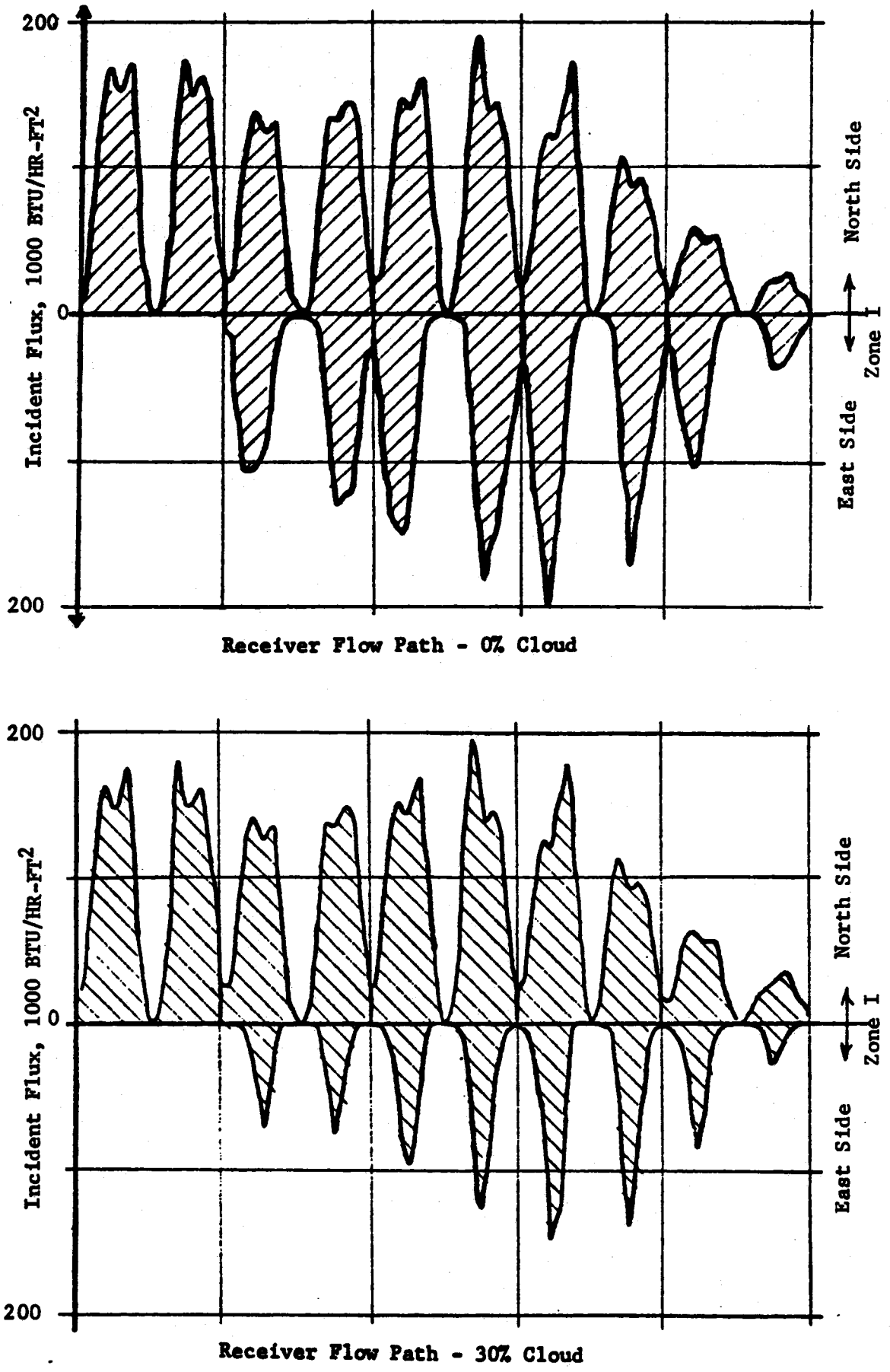

FIGURE 4.1 - OPERATIONAL CLOUD COVER TRANSIENTS 0% AND 30% EAST TO WEST CLOUD COVER

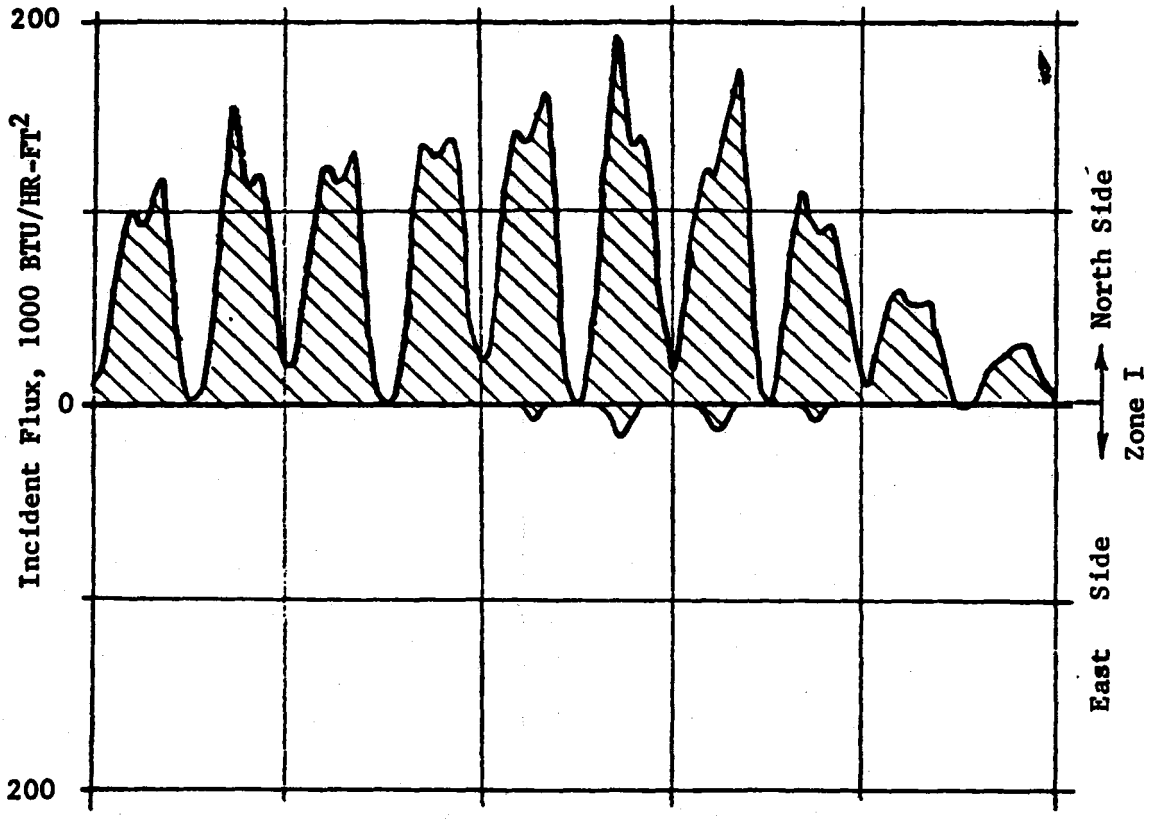

Receiver Flow Path - 50% Cloud

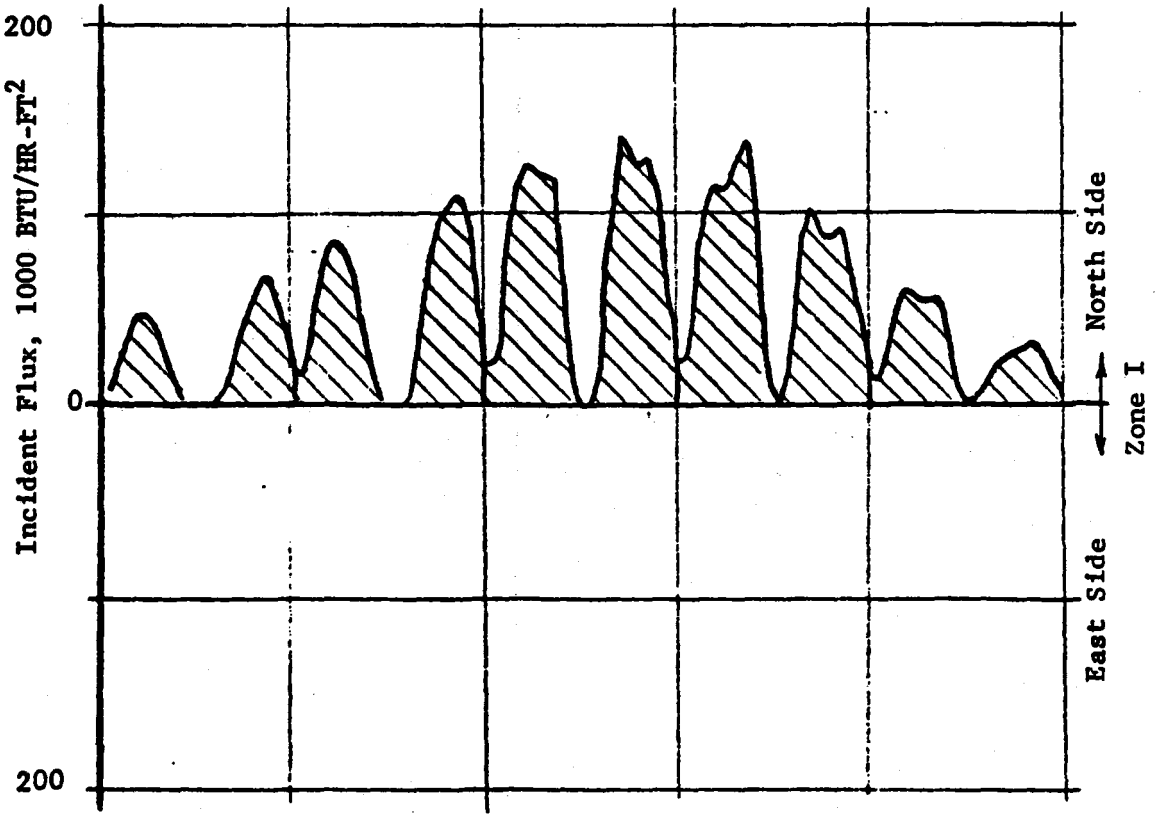

Receiver Flow Path - 60% Cloud

FIGURE 4.2 - OPERATIONAL CLOUD COVER TRANSIENTS 50% AND 60% EAST TO WEST CLOUD COVER

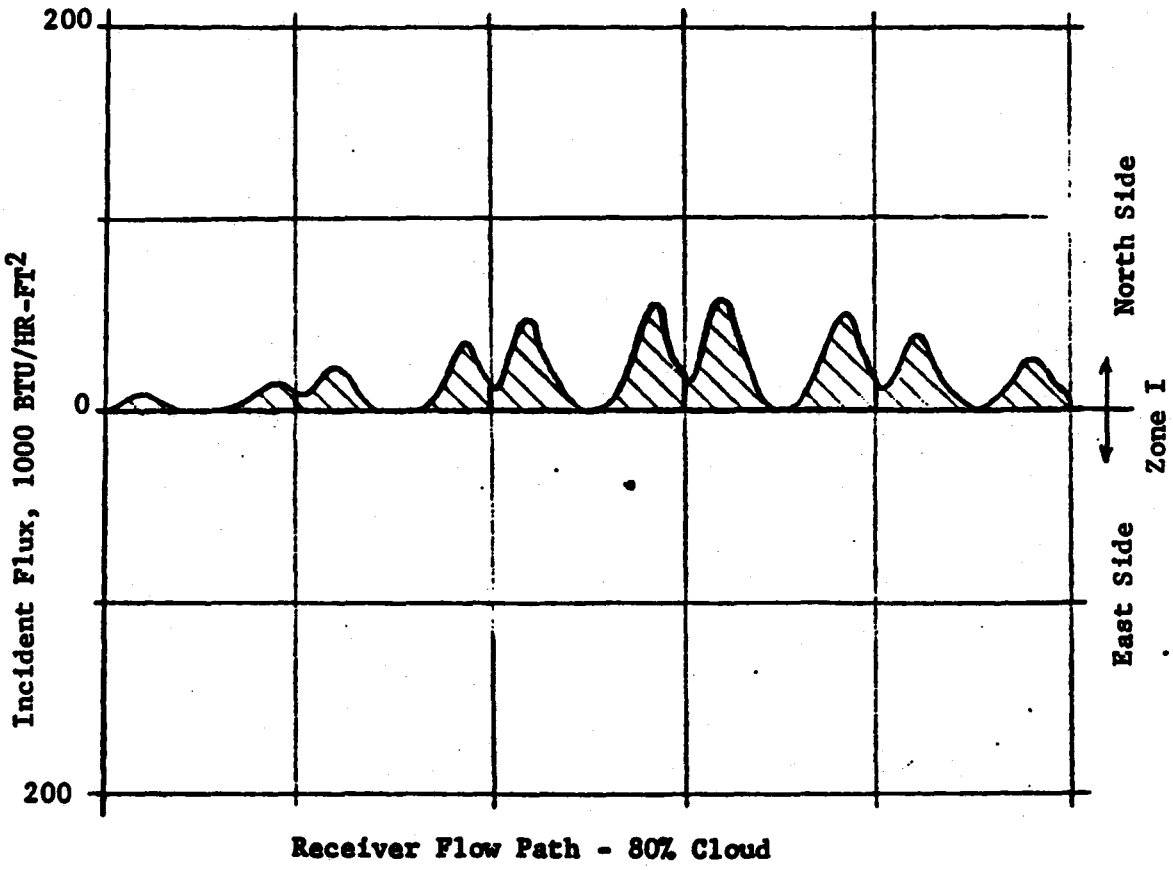

FIGURE 4.3 - OPERATIONAL CLOUD COVER TRANSIENT
80% EAST TO WEST CLOUD COVER

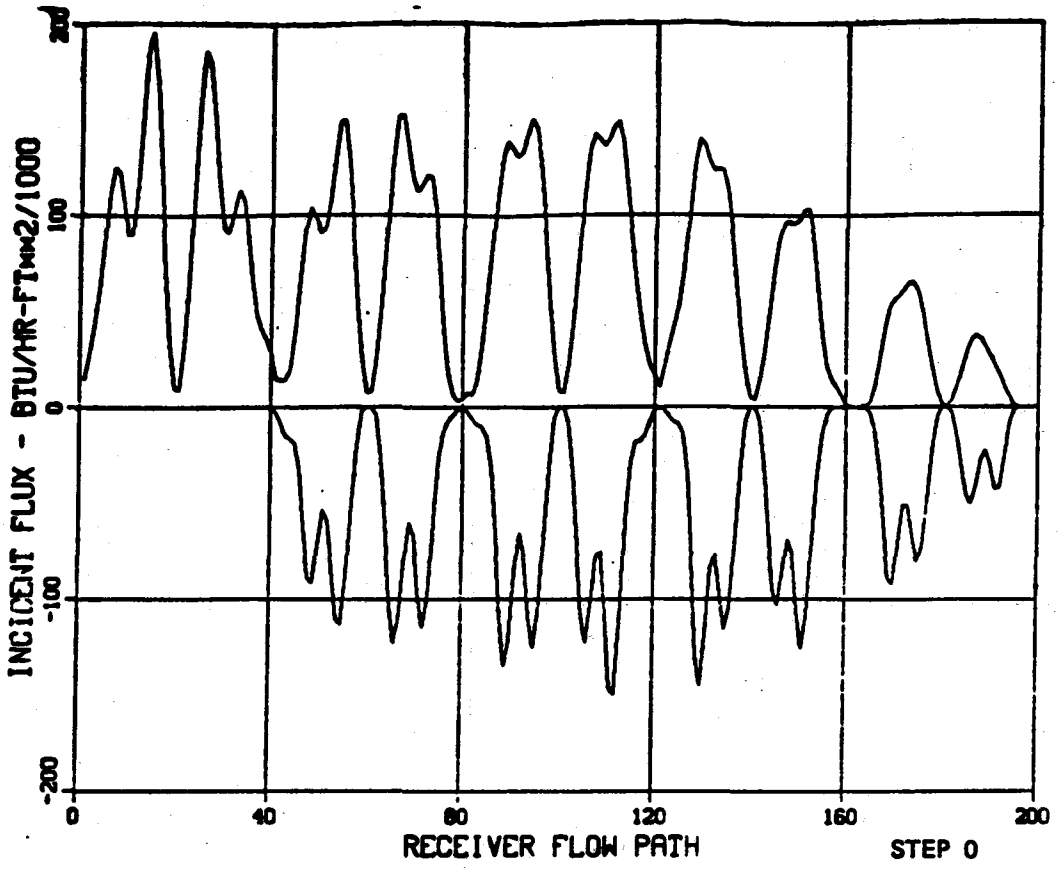

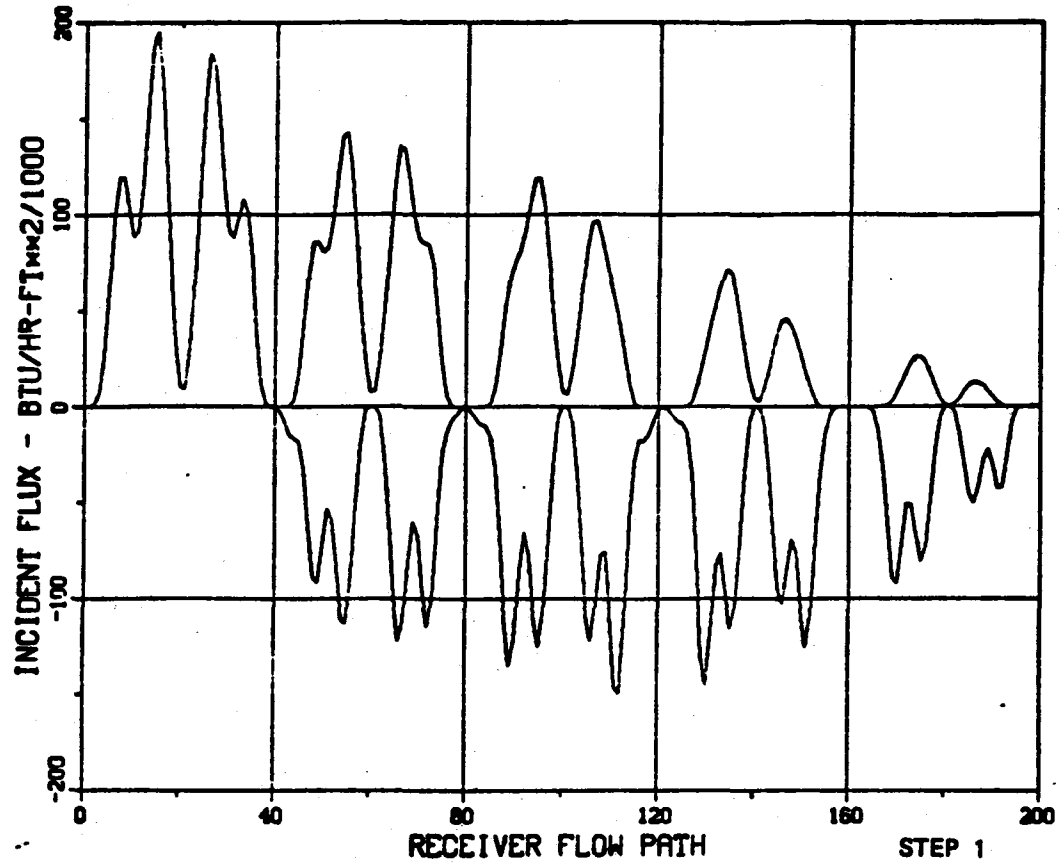

FIGURE 4.4 - GROUP CLOUD TRANSIENT

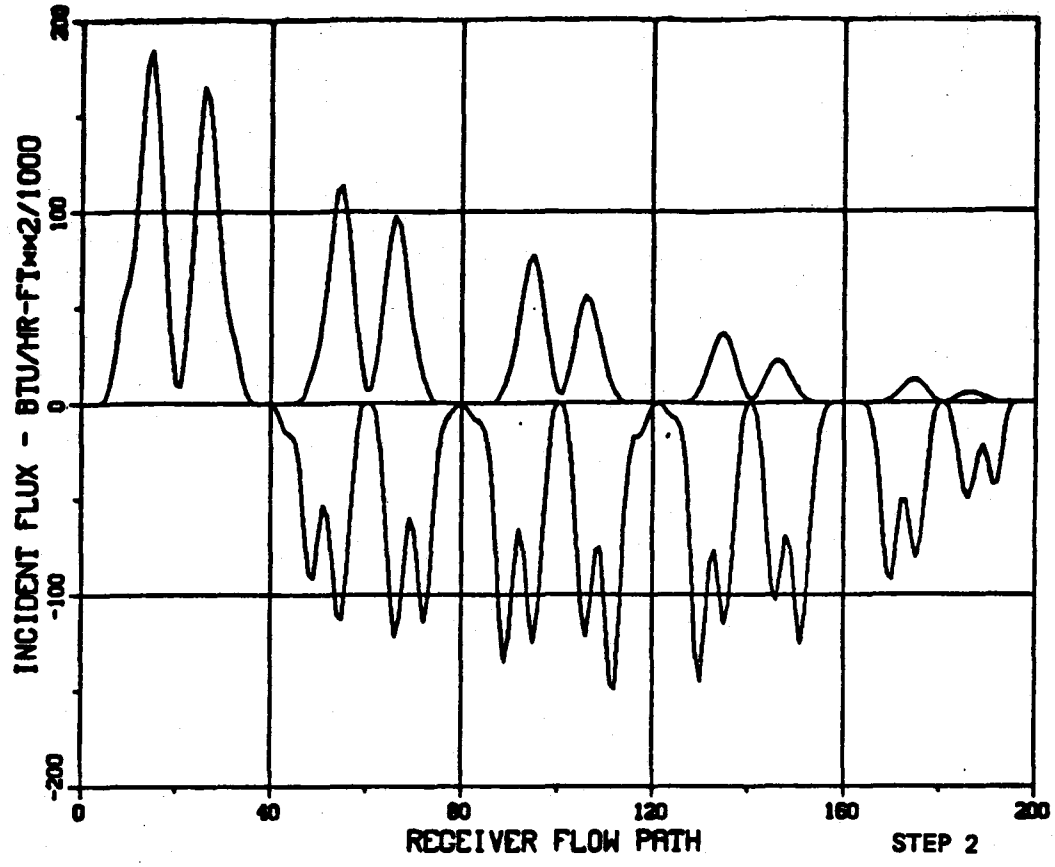

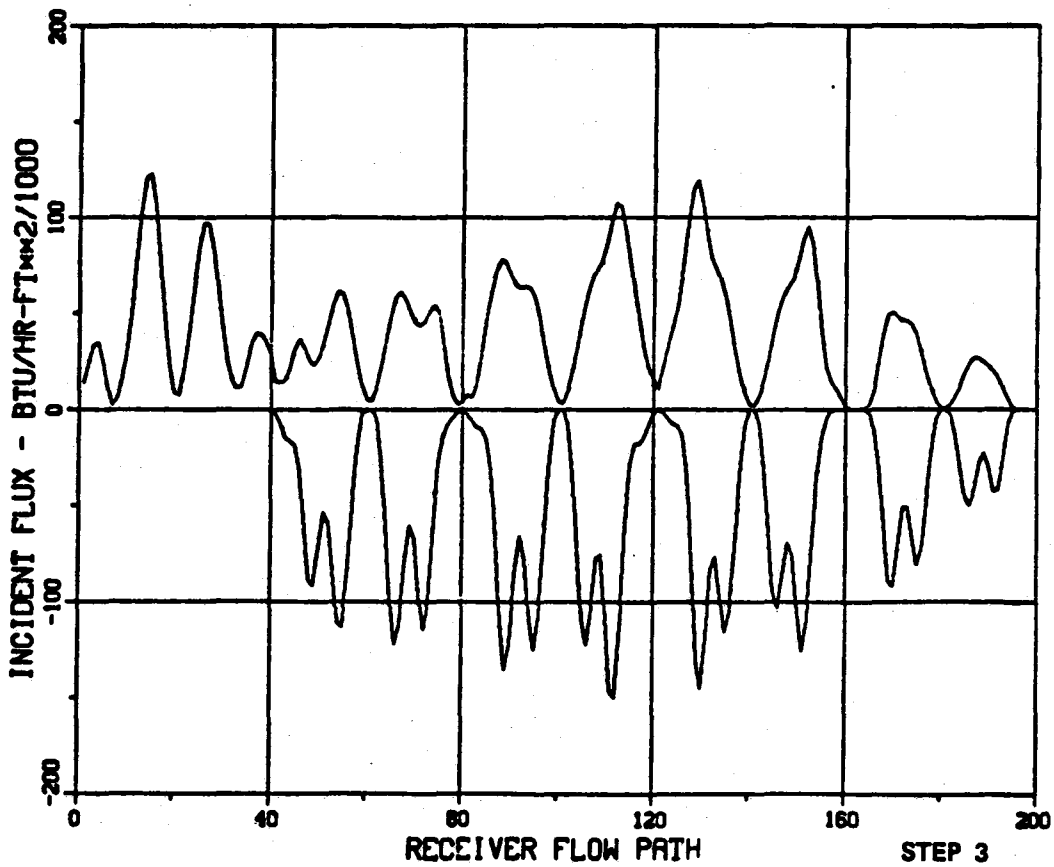

FIGURE 4.5 - GROUP CLOUD TRANSIENT

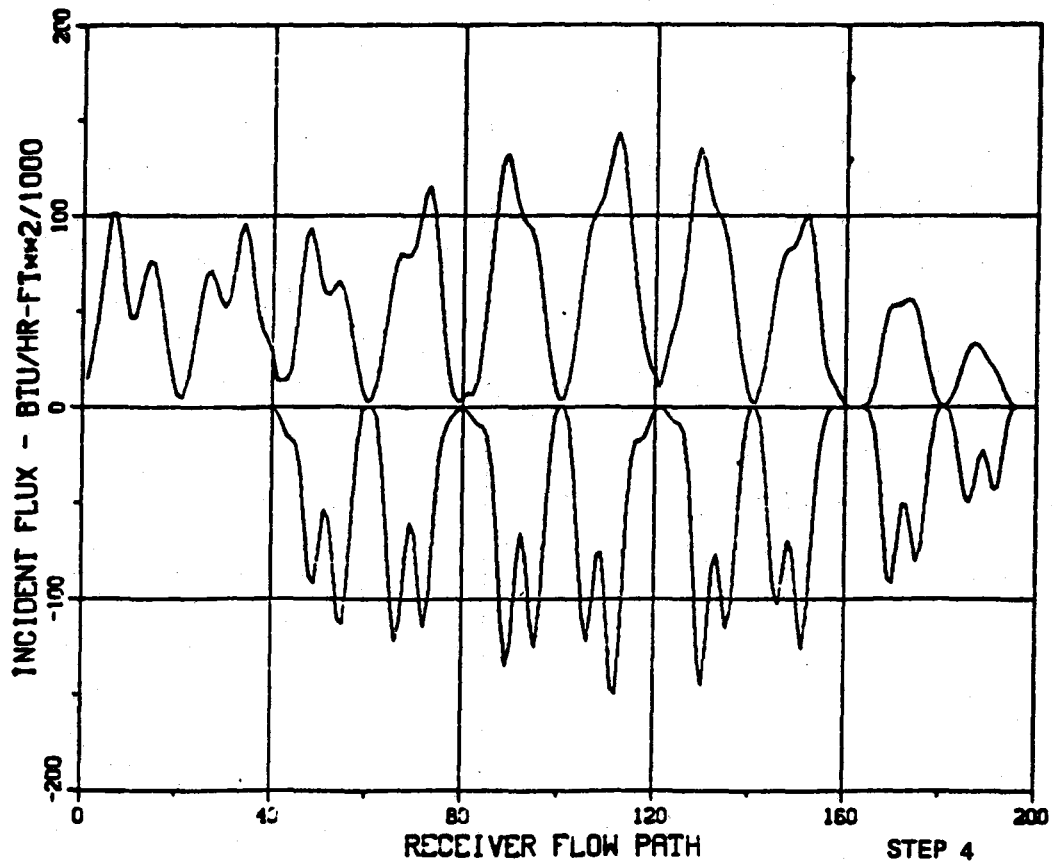

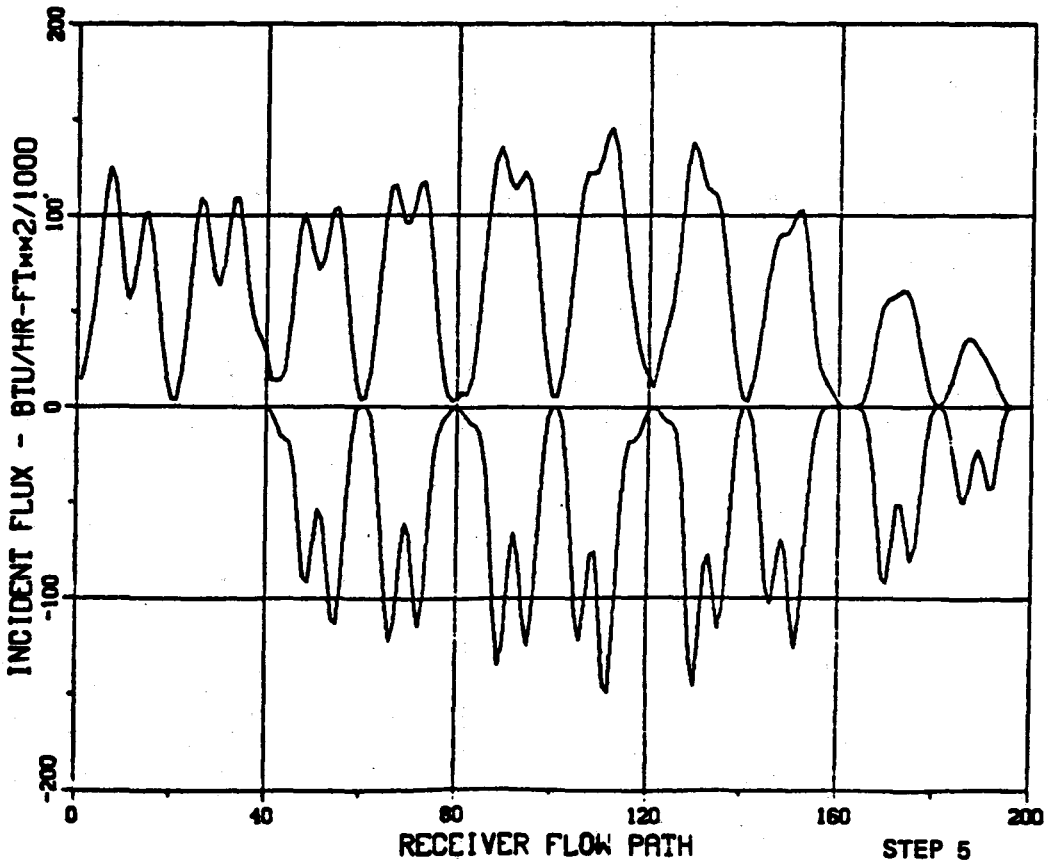

FIGURE 4.6 - GROUP CLOUD TRANSIENT

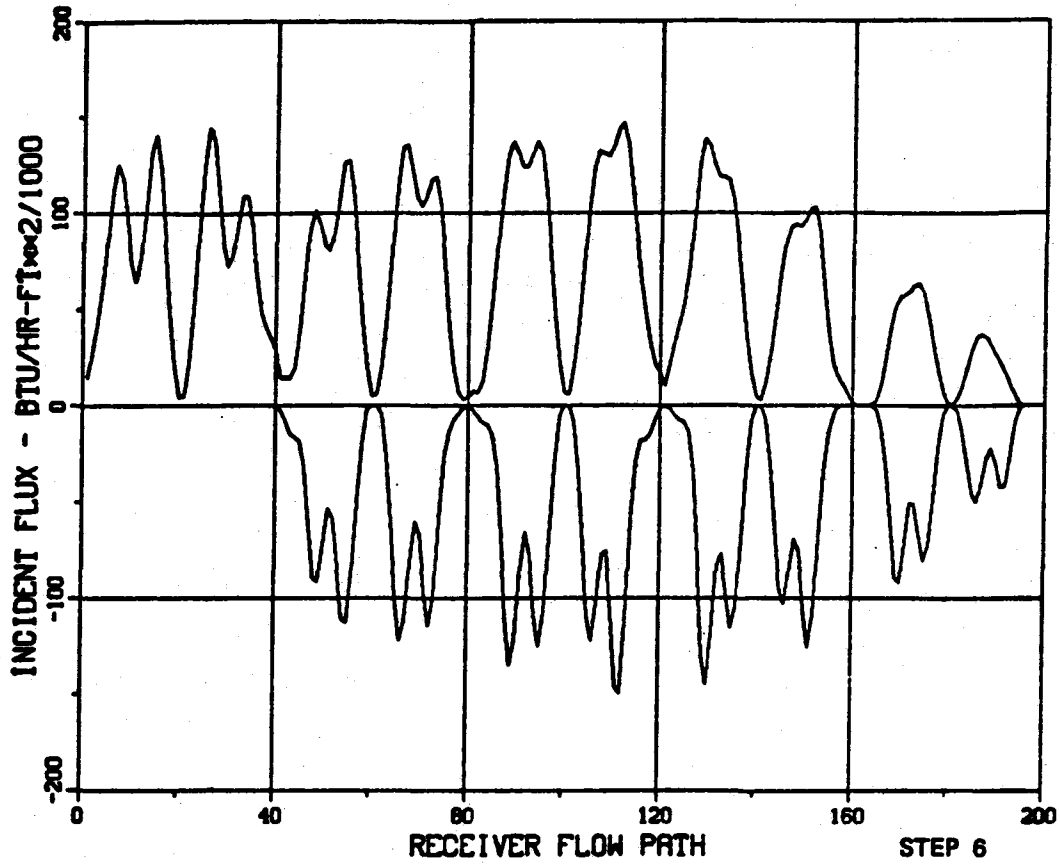

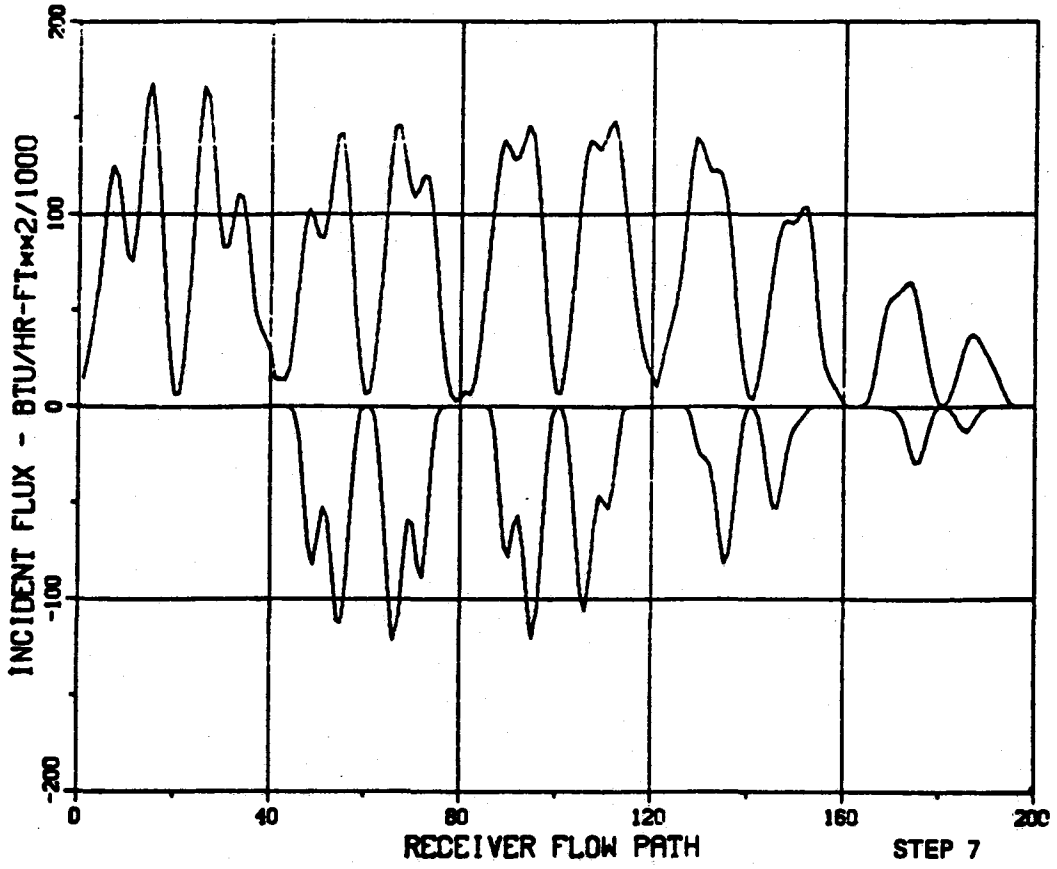

FIGURE 4.7 - GROUP CLOUD TRANSIENT

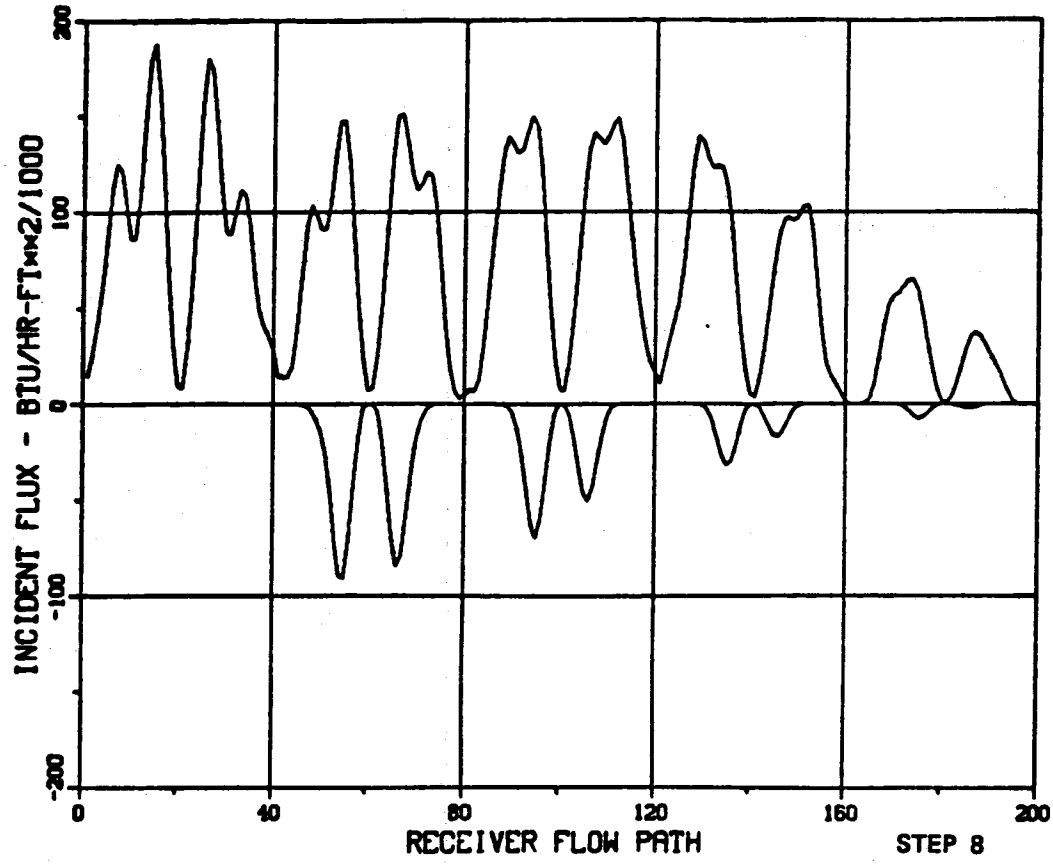

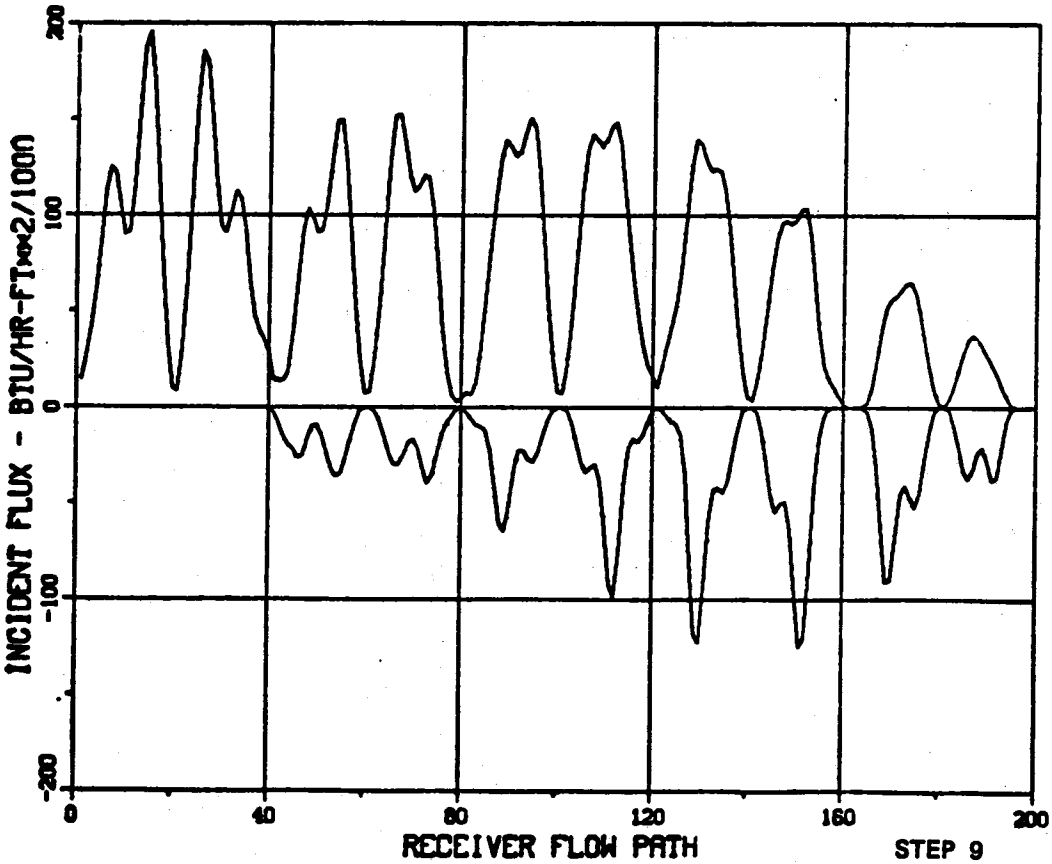

FIGURE 4.8 - GROUP CLOUD TRANSIENT

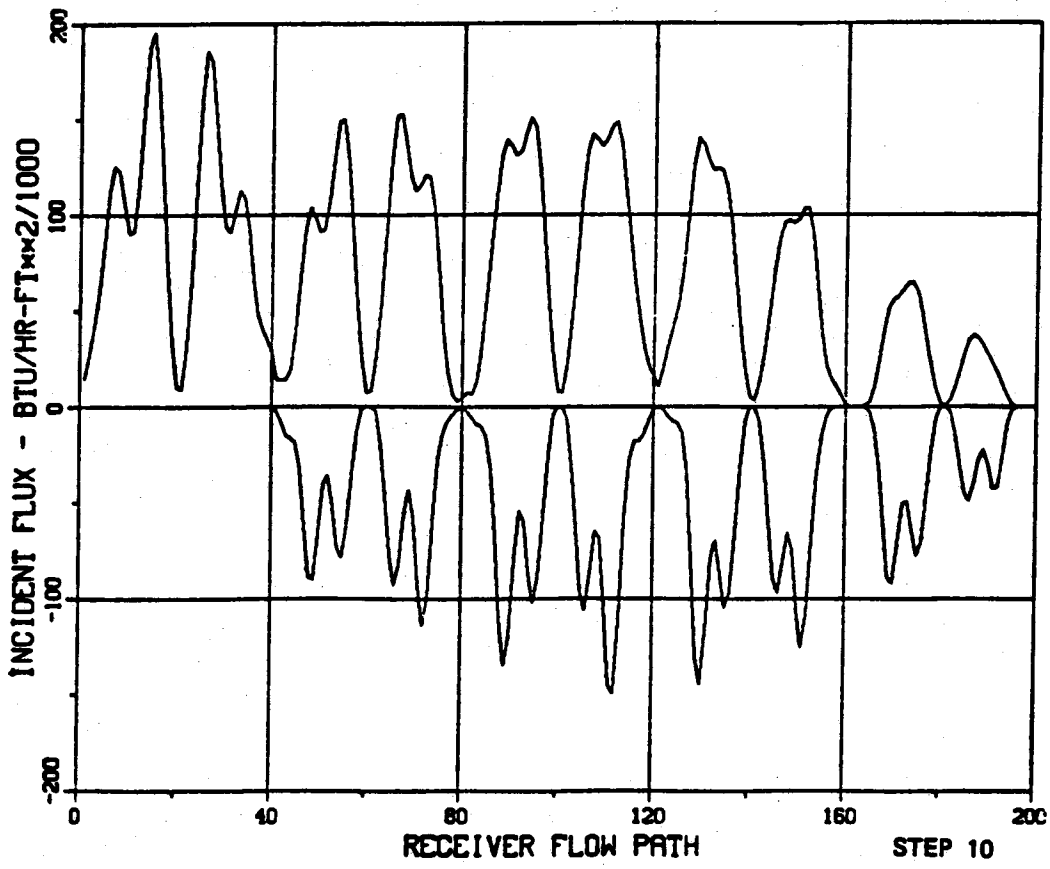

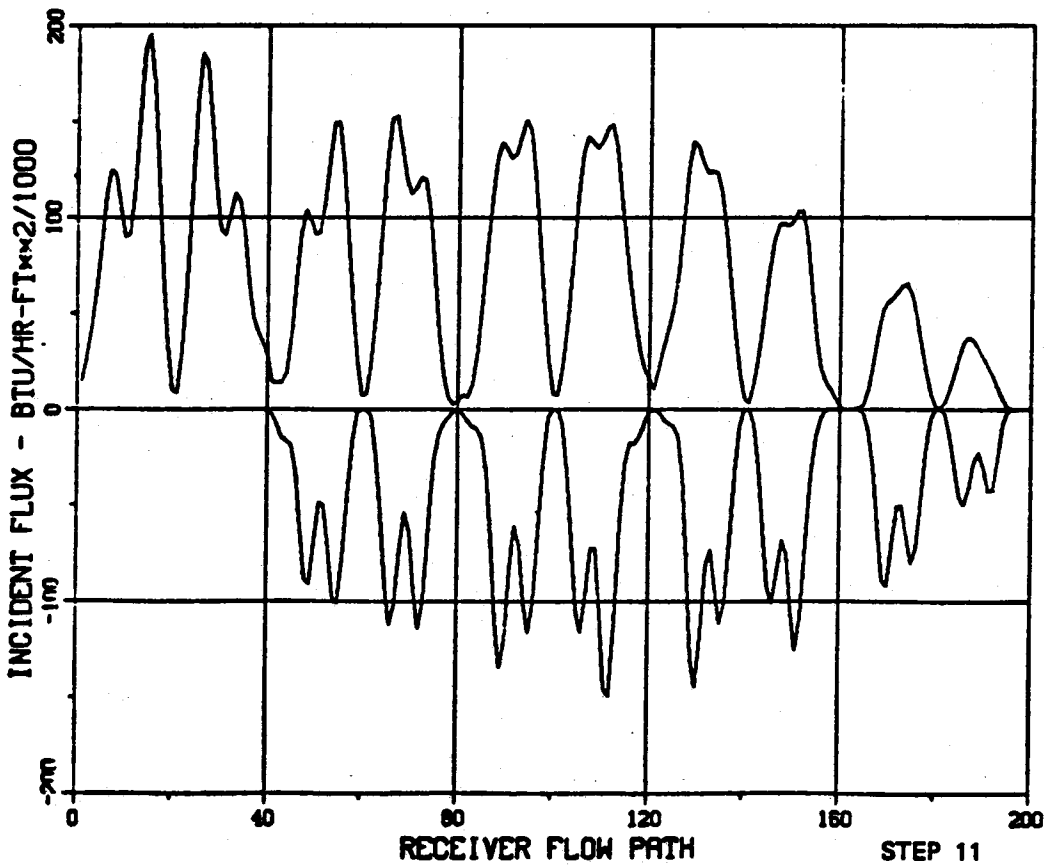

FIGURE 4.9 - GROUP CLOUD TRANSIENT

4.2.4 Simulation Results

Representative performance with the use of the quasi-feedforward control is shown for the east-west sharp-edged model, and the group cloud model, in Figures 4.10 through 4.13, respectively. The clouds were assumed to pass over the collector field at the maximum specified velocity of 13 meters/sec. Further discussion of these simulations may be found in Appendix C. It is readily apparent from these figures that the control system is capable of maintaining salt and metal temperatures within specified limits under worst-case transient conditions.

4.2.5 Control System Schematic

A control system functional diagram is shown on Figure 4.14. The instrumentation and control hardware requirements are discussed in Appendix C.

4.2.6 Conclusions

a. The analysis has shown that a quad-cavity receiver can be tightly controlled, comfortably within the requirements. Further analysis in the area of optimal control would be beneficial. Such study would be aimed at further reducing deviation in salt outlet temperature by modifying the cost function used for optimal control. Further attention to the control of parallel valves would also affect better control.

b. Peak metal temperatures on the panel surface can be limit controlled using a radiometer for temperature measurement. The control uses the temperature measurement of the point to be controlled to continuously update an adaptive model. The model is then used to predict the panel temperature in order

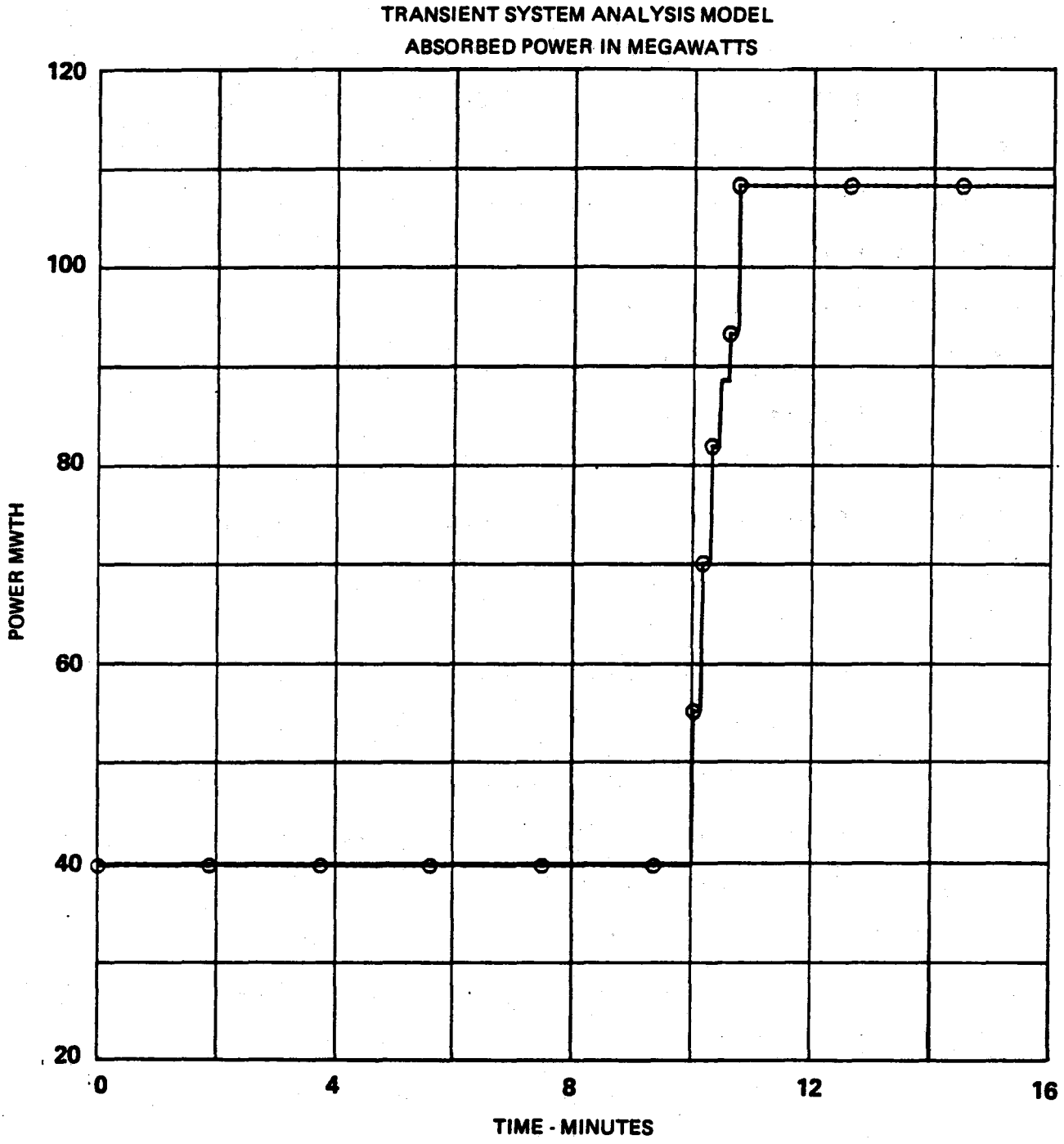

FIGURE 4.10 - E-W CLOUD SIMULATION - ABOSRBED POWER

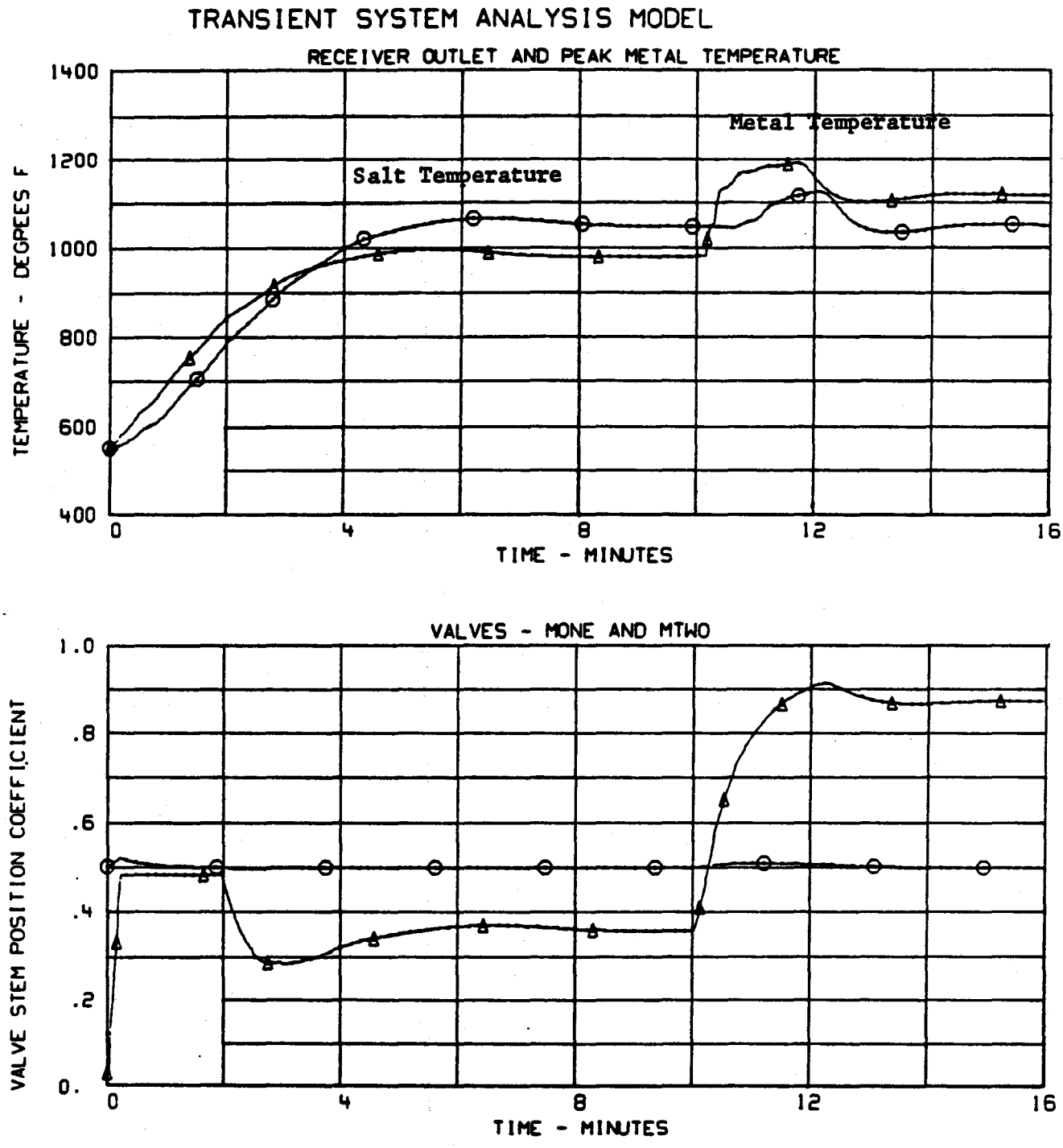

FIGURE 4.11 - E-W CLOUD SIMULATION - TEMPERATURE AND VALVE POSITIONS

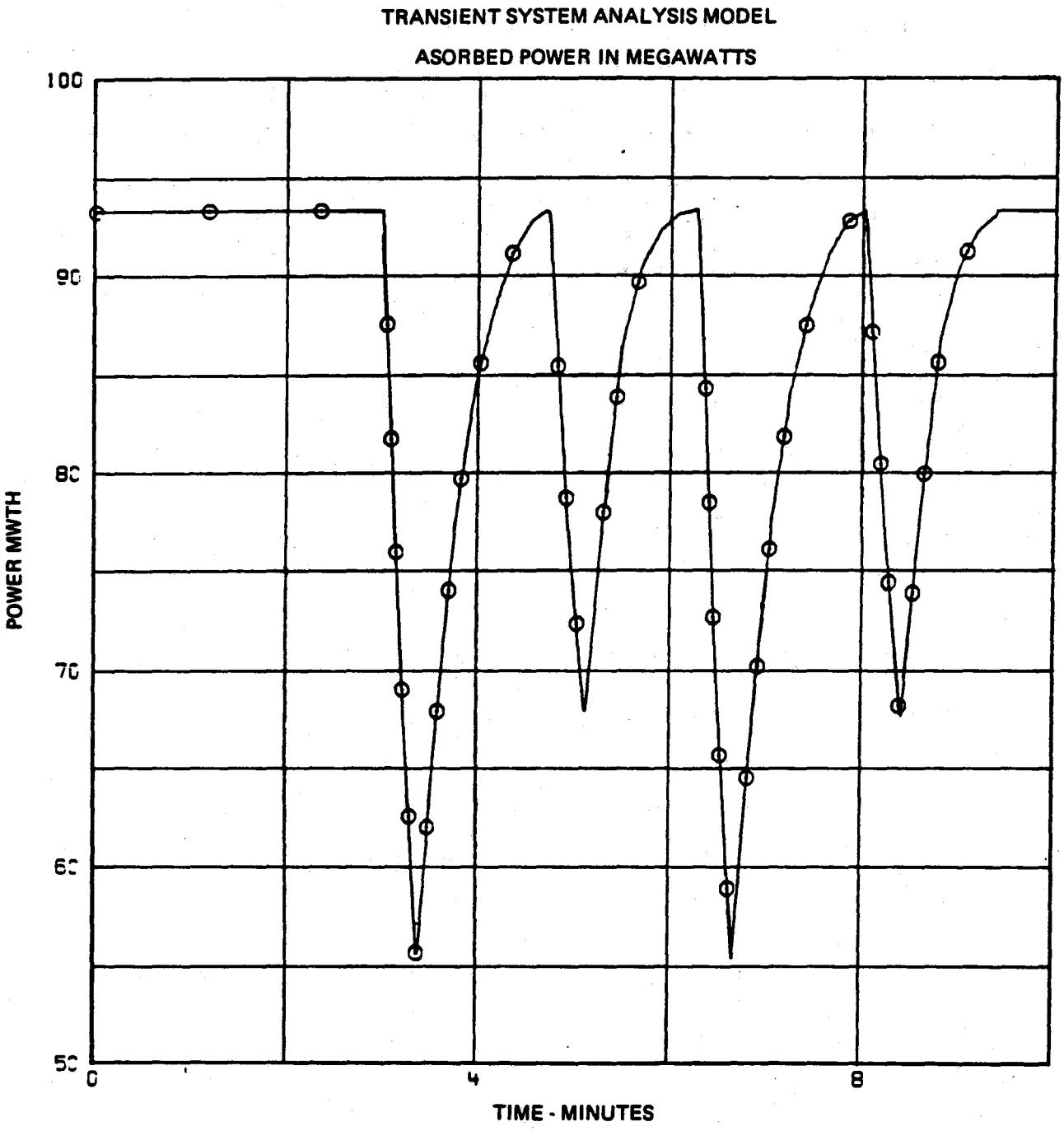

FIGURE 4.12 - GROUP CLOUD SIMULATION - ABSORBED POWER

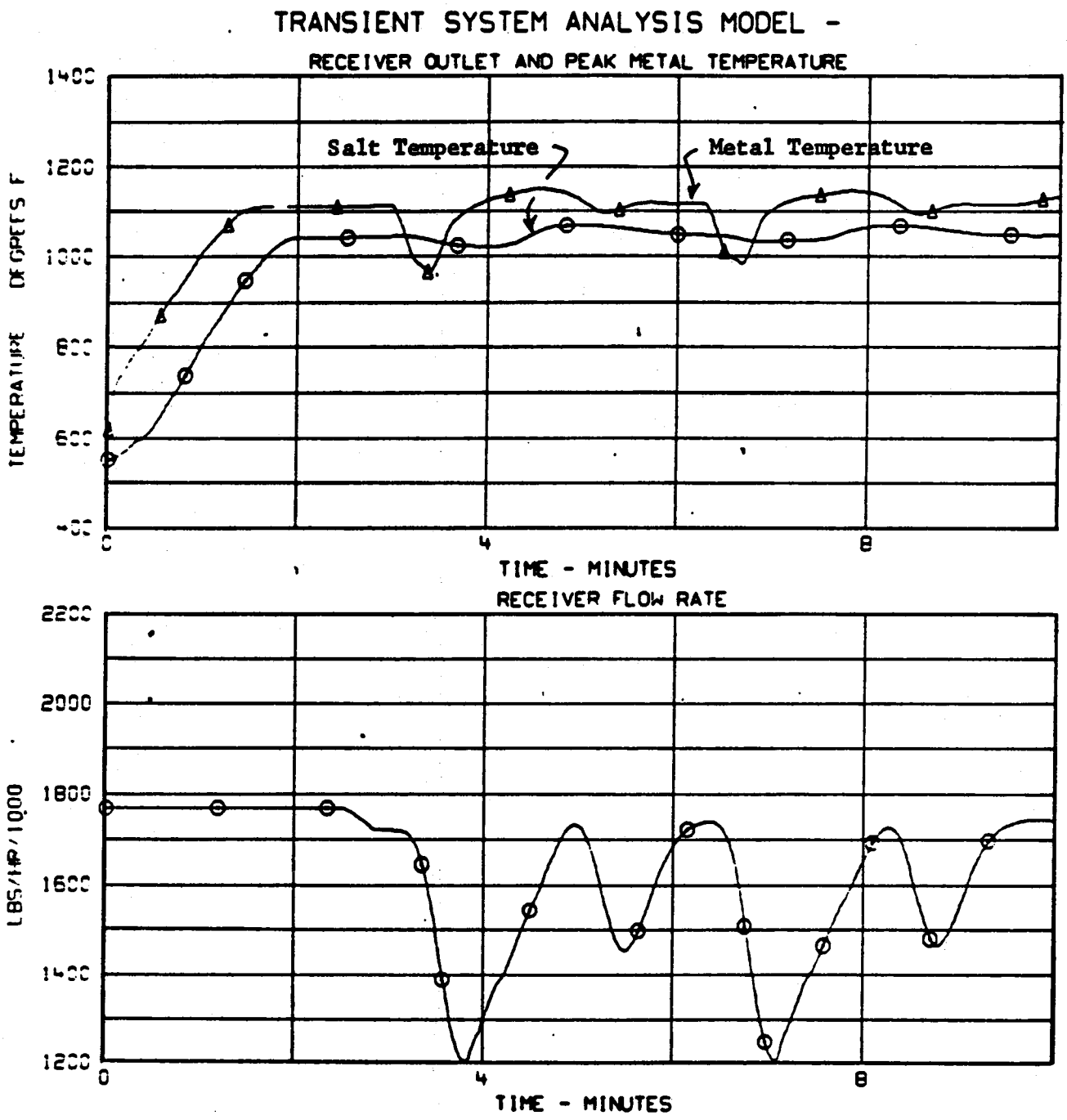

FIGURE 4.13 - GROUP CLOUD SIMULATION - TEMPERATURES AND FLOW

to control it by over-riding the salt flow rate control. As in the case of salt temperature limiting, this control is an extension of QFFC.

c. The control hardware required to implement QFFC is readily available. The PID controller can be adapted for QFFC to implement both QFFC and Optimal Quasi-Feedforward Control (OQFFC) with salt-temperature limiting. However, the availability of a high-level language programmable controller would improve the efficiency and reliability of control as fewer hardware components would be required. Furthermore, this type of controller is required to implement the optimal filtering used for metal-temperature control. The requirement for high-level language for control limits the scope of hardware available if fully distributed control is a further requirement. However, there is no such limitation with Distributed Digital Control and the high-level language type controllers are becoming more available with distributed control hardware as time proceeds. Consequently, implementing the more advanced control algorithms is not considered to be problematic.

d. Quasi-Feedforward control should be used in preference to two-point temperature feedback control. Two-point temperature feedback control is very sensitive to disparity between temperature set-points and flux distribution as well as being prone to instability. In comparison, QFFC uses the one set-point and is thus insensitive to the distortions in

flux distribution caused by cloud coverage. In addition to this advantage, QFFC is easily adapted and can be used to limit the peak salt temperatures by over-riding the main control.

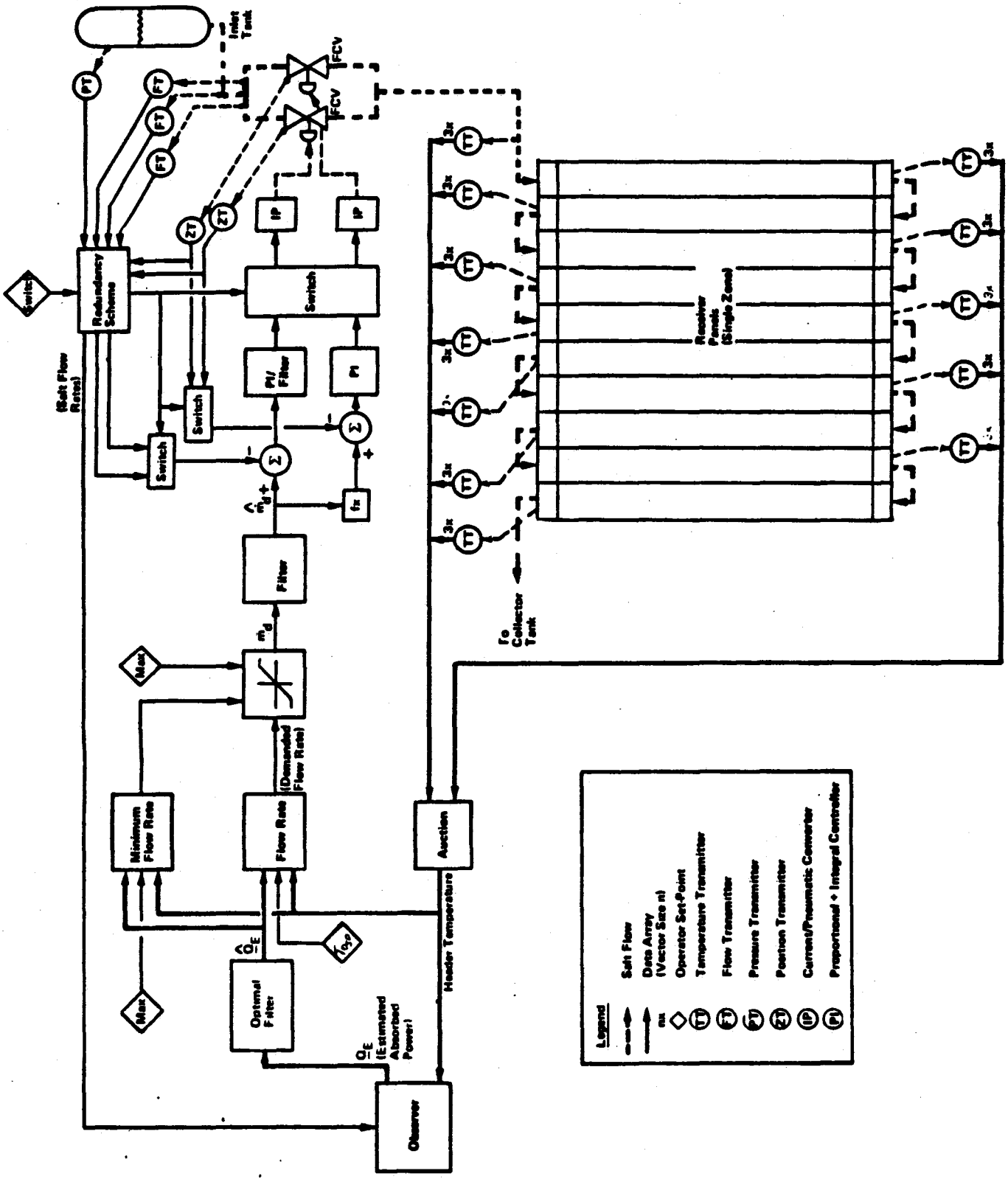

FIGURE 4.14 - CONTROL SYSTEM SCHEMATIC

5.0 FABRICATION AND FIELD ERECTION PLAN

Fabrication outlines were developed for shop fabricated components to identify significant operations in the fabrication sequence. The fabrication outlines were used to prepare detailed cost estimates and material ordering and fabrication spans. Erection steps for the receiver subsystem were developed to prepare erection cost estimates and spans.

An integrated shop fabrication and field erection schedule, as well as individual fabrication schedules for the major receiver subsystem components, are provided. Cost estimates were obtained using standards data, actual cost data from previous contracts, material vendor quotations and catalog prices.

5.1 Shop Fabrication

Fabrication outlines for shop fabricated components were developed. The heat absorption panels are completely shop fabricated as are the major pressure boundary components. Structural members of the receiver, including the roofs, walls, floors, center section, radiation shields and doors, are also shop fabricated. However, their sizes dictate that subassemblies be shop fabricated and shipped to the field for final assembly and erection.

The manufacturing activities required to complete fabrication of the heat absorption panels are briefly described below.

1. Detailed fabrication drawings will be prepared and reviewed to assure that design requirements are satisfied and that the components can be fabricated in a cost-effective manner.
2. Material ordering information will be prepared and reviewed.
3. Detailed fabrication processes will be prepared to provide manufacturing with instructions for fabrication, inspection, and testing. A brief narrative of the panel processing is herewith provided:

   Panel wall fabrication will begin with receipt of tubing in 50-70 foot lengths. Depending on comparative cost, the tubing may have integral fins, or may require that the fins be weld deposited. Since the material cost for a large production run of finned tubing is not available, it is assumed here that the fins will be weld deposited. The 50-70 foot tube lengths will be weld preped and butt welded using the automatic tungsten inert gas process as the full length tube is rotated. Required equipment will include rack type supports, and positioning and handling tooling. All butt welds will be liquid penetrant inspected.

   The full length tubes will then be moved to an automatic metal inert gas welding station for weld deposit of the fins. This station requires rigid full length support of the tubing and a tract to carry the welding head. Two weld passes are required for each fin, using tightly controlled parameters to assure proper dimensions of the finished build-up. After the first fin is deposited, the tube is

rotated exactly 180°, using fixturing to prevent twist, and the second fin is deposited. Grinding of the build-up after weld deposit is not required.

If tubing is purchased with integral fins, a short longitudinal manual build-up will be made to connect the fins that will have been machined back at the butt weld locations.

Prebent stainless steel safe ends will be fit to each end of the tube using fixturing to assure proper location. The safe-end to tube weld will be made by the automatic tungsten inert gas process as the tube is rotated. An alternative approach here is use of orbital welding equipment. The safe-end to tube welds will be liquid penetrant inspected.

The tubes will next be fit together to form the full width panel and tack welded for deposit of the membrane welds. The equipment would include a full length support fixture and gantry type welding equipment. The safe-ends are also fixtured to assure proper alignment. The membrane welds will be made by the automatic tungsten inert gas process. An initial weld pass will be made at each membrane location, joining groups of two tubes, then four, then eight, etc. to minimize the affect of weld shrinkage. The panel will then be turned over on its fixture, aligned, and a weld pass made on the opposite side of each membrane to provide full penetration. It is anticipated that multiple welding heads will be used on this station.

Panel mounting attachment clips will then be fit and welded to the panel tubing using the manual tungsten inert gas process. Headers will be fit to the safe-ends at each end of the panel and welded by the manual tungsten inert gas process. The safe end to header welds will receive liquid penetrant inspection. End caps will then be fit and welded to the header.

The completed panel will next be hydrostatic tested, followed by painting and baking to cure the paint. Insulation will be installed and the panel will be mounted to buckstays, loaded on a railcar and shipped.

4. The detailed processing will be reviewed, and the manufacturing operations will be spanned and scheduled for completion. Fabrication activities will be monitored and expedited as necessary throughout the project.

5. Fabrication, inspection, and testing will be completed in accordance with the detailed processing instructions, design drawings, and approved procedures. All operations will be documented as they are completed.

6. The detailed processing will be reviewed to assure proper completion and documentation of all operations before the components are code stamped and shipped.

Where appropriate, all shop fabricated components will be painted before shipment to the site.

Fabrication outlines for the major pressure boundary components are provided in an accompanying document. Fabrication schedules for the major pressure boundary components and the receiver structure are shown in Figures 5.1 through 5.3.

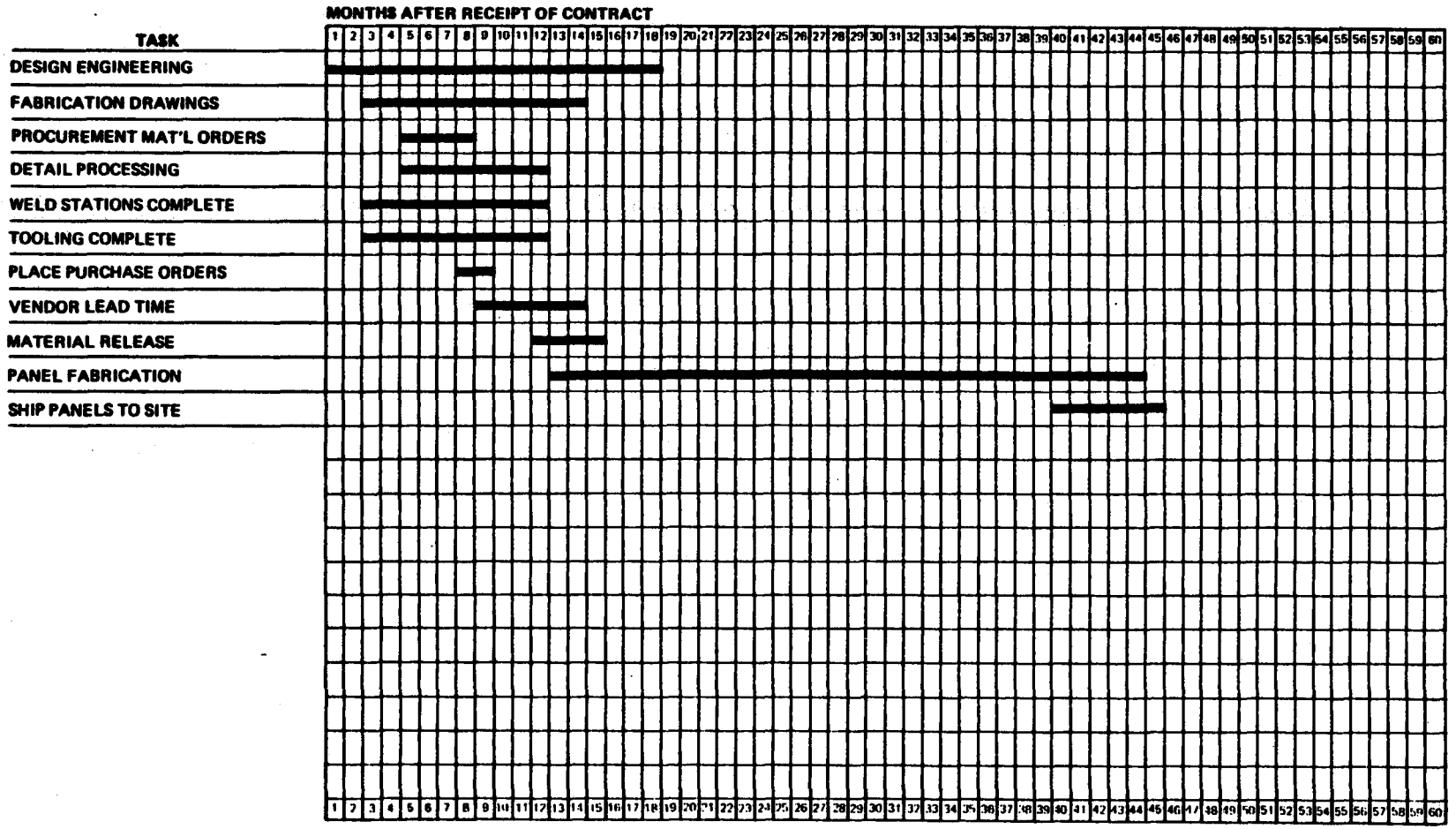

FIGURE 5.1 - FABRICATION SCHEDULE FOR RECEIVER PANELS

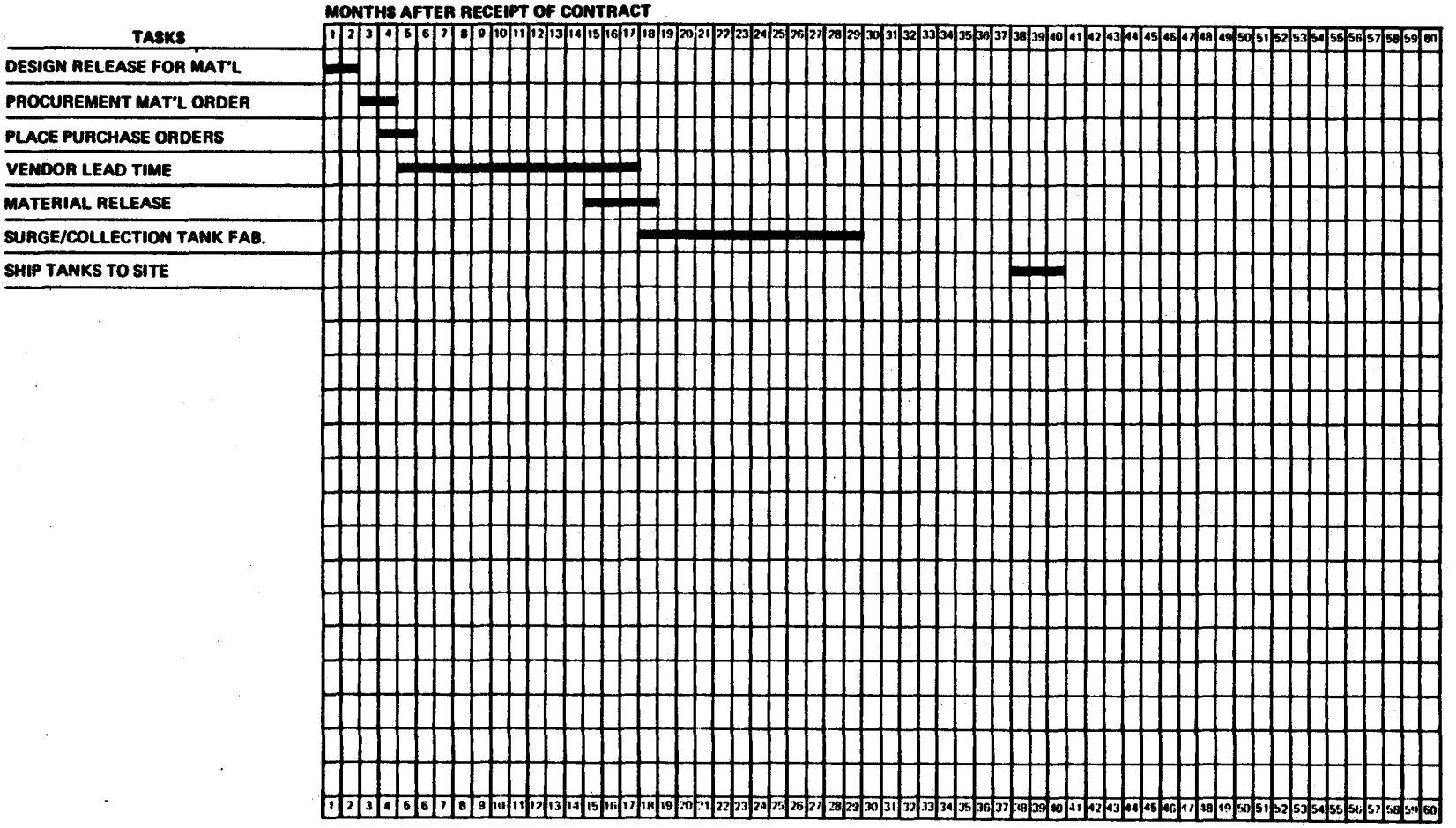

FIGURE 5.2 - FABRICATION SCHEDULE FOR SURGE/BUFFER AND COLLECTION TANKS

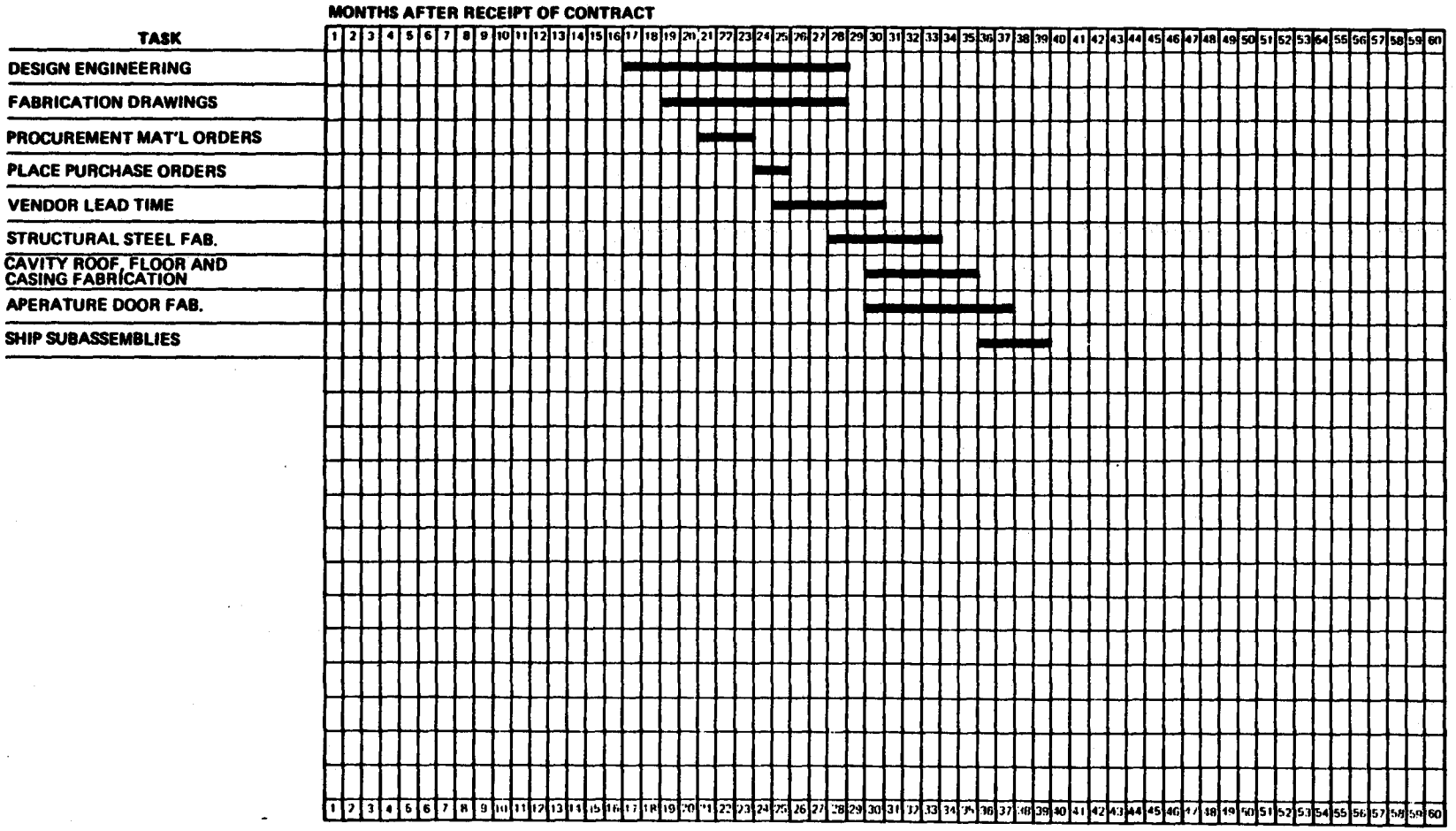

FIGURE 5.3 - FABRICATION SCHEDULE FOR RECEIVER

5.2 Field Erection

Erection details were developed for the receiver subsystem including tower and foundation, supports, piping, pumps, valves, panels, tanks, trace heating, and insulation. The receiver subsystem is erected in two phases. In the first phase, the tower foundation and the concrete tower are constructed. In the second phase, the receiver is erected to the top of the tower and the electrical distribution system is installed and interface connections made.

During the first month of the receiver erection phase, components, subassemblies, and procured materials are received and unloaded. Erection of the receiver support structure and structural frame will begin in the second month and continue for five (5) months. The tanks will be erected into the central box of the receiver, followed by the erection of the heat absorption panels, which will require approximately seven (7) months to complete. The timely delivery of heat absorption panels to the site is critical to the erection schedule since the span for panel erection is long and continued erection is dependent upon the panels being in place. Interconnecting piping, recirculation pump, valve, instrumentation, heat tracing and insulation erection will be in parallel with heat absorption panel erection, however, will lag panel erection by approximately one (1) month. Erection of the receiver cavity casings, roof, floors, walls, and doors, requires a five (5) month span. The last two (2) months of the receiver erection are primarily devoted to installing the electrical distribution system and making interface connections with the tower. From receipt of material through receiver hydrotest, the total receiver erection span is fifteen (15) months. Receiver erection will be followed by six months of field testing. The detailed receiver field erection plan is shown in Figure 5.4.

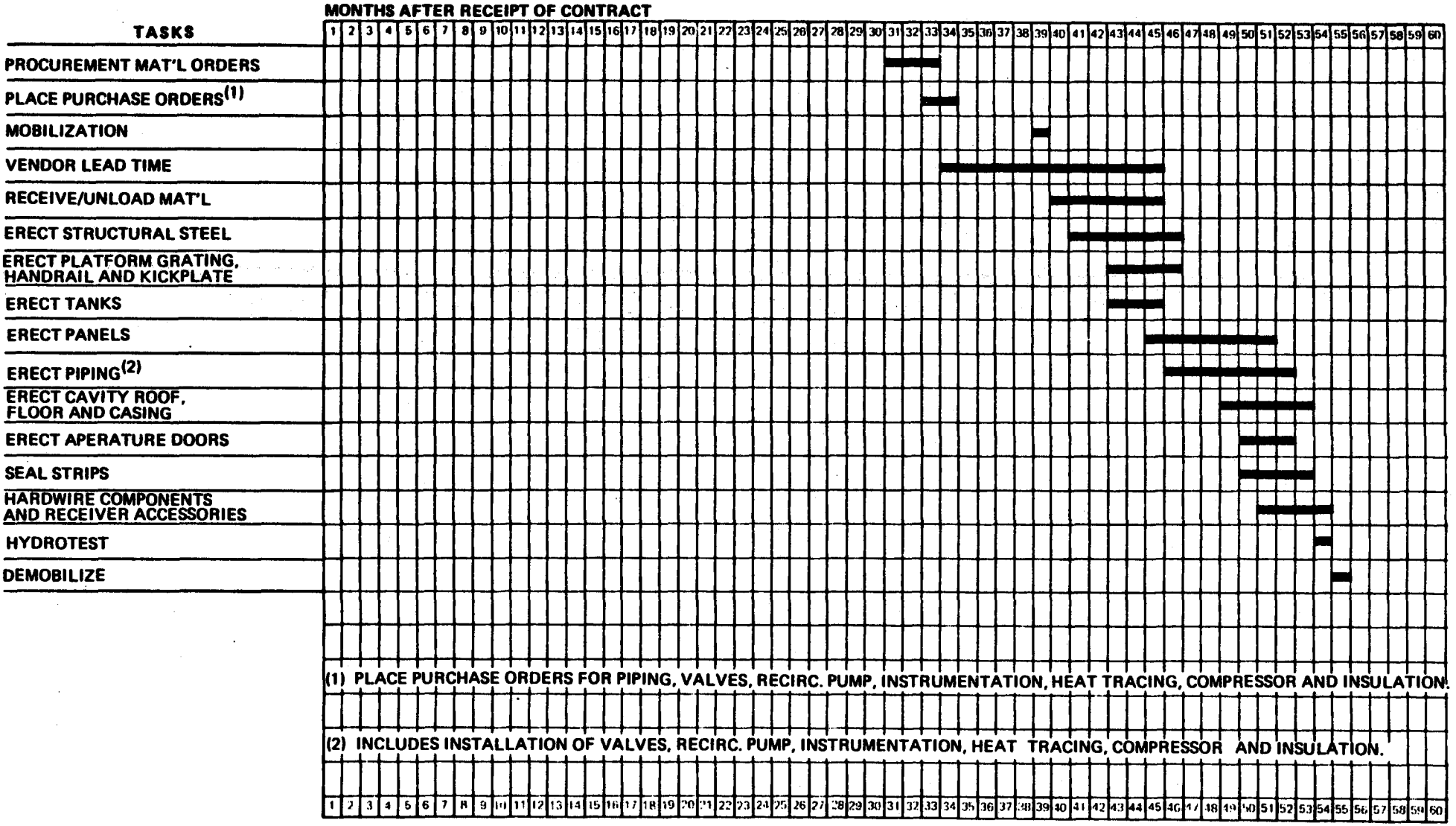

FIGURE 5.4 ERECTION SCHEDULE FOR RECEIVER

5.3 Integrated Schedule

The integrated design, fabrication, and field erection schedule is presented in Figure 5.5. The total span is five (5) years, from receipt of contract through subsystem testing. The critical path is identified and important events are identified by milestones.

5.4 Cost Estimates

Cost estimates for design, fabrication, and erection of the receiver subsystem are presented in Table 5.1. The assumptions used to develop the cost estimates are as follows:

- Costs are expressed in current (November 1982) dollars.
- The molten salt receiver subsystem is located near Barstow, California.
- The cost estimates exclude owner's cost such as land, licenses and permits, taxes, and the cost of capital.
- Riser and downcomer piping, and electrical cable are costed to one foot outside the tower wall.
- Interconnecting piping, vents, and drains are costed to connections on panel headers, surge tank and collection tank.

Cost estimates for shop fabricated components are based on standards data, actual cost data from previous contracts, vendor quotations, and catalog prices.

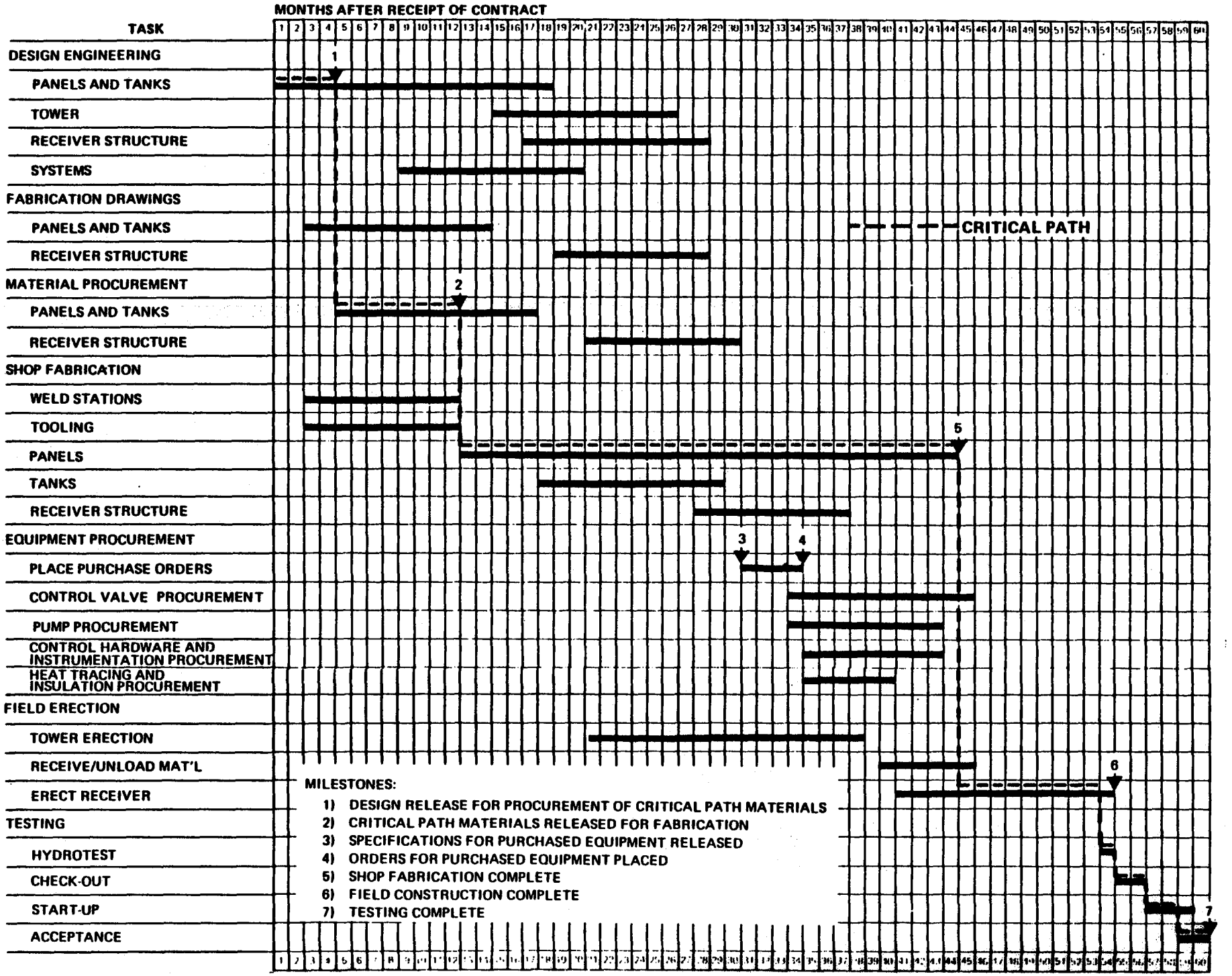
MONTHS AFTER RECEIPT OF CONTRACT
TASK
DESIGN ENGINEERING
PANELS AND TANKS
TOWER
RECEIVER STRUCTURE
SYSTEMS
FABRICATION DRAWINGS
PANELS AND TANKS
RECEIVER STRUCTURE
MATERIAL PROCUREMENT
PANELS AND TANKS
RECEIVER STRUCTURE
SHOP FABRICATION
WELD STATIONS
TOOLING
PANELS
TANKS
RECEIVER STRUCTURE
EQUIPMENT PROCUREMENT
PLACE PURCHASE ORDERS
CONTROL VALVE PROCUREMENT
PUMP PROCUREMENT
CONTROL HARDWARE AND INSTRUMENTATION PROCUREMENT
HEAT TRACING AND INSULATION PROCUREMENT
FIELD ERECTION
TOWER ERECTION
RECEIVE/UNLOAD MAT'L
ERECT RECEIVER
TESTING
HYDROTEST
CHECK-OUT
START-UP
ACCEPTANCE
CRITICAL PATH
1
2
3
4
5
6
7
MILESTONES:
1) DESIGN RELEASE FOR PROCUREMENT OF CRITICAL PATH MATERIALS
2) CRITICAL PATH MATERIALS RELEASED FOR FABRICATION
3) SPECIFICATIONS FOR PURCHASED EQUIPMENT RELEASED
4) ORDERS FOR PURCHASED EQUIPMENT PLACED
5) SHOP FABRICATION COMPLETE
6) FIELD CONSTRUCTION COMPLETE
7) TESTING COMPLETE

TABLE 5.1

COST ESTIMATE FOR 100 MWe RECEIVER SUBSYSTEM
(In Thousands of Dollars)

1.	Receiver		
	a) Engineering	1,943	
	b) Fabrication		
	Panels and Insulation	17,054	
	Surge/Buffer Tank	455	
	Collection Tank	578	
	Structural	5,415	
	c) Procured Equipment[1]	4,824	
	d) Erection	23,752	
	Subtotal		54,021
2.	Tower		
	a) Foundation and Erection	3,932	
	b) Electrical Equipment[2]	2,247	
	c) Accessories[3]	985	
	d) Procured Equipment[4]	3,898	
	Subtotal		11,062
3.	Systems		
	a) Engineering	625	
	b) Testing	709	
	Subtotal		1,334
4.	Indirect Costs[5] (15% on all Items Except Receiver and Systems Engineering)		9,577
	TOTAL		75,994

NOTES:
1. Includes pumps, valves, piping, compressor, air tank, trace heating, door motor and mechanism, instrumentation, and controls.
2. Includes all electrical equipment except lighting, communications, and lighting protection.
3. Includes stairs, elevator, lighting, communications, lighting protection, ventilation equipment, and painting.
4. Includes booster pumps, riser/downcomer piping, tower valves, and insulation.
5. Indirect costs cover field costs, field engineering, procurement, and construction management.

6.0 MANUFACTURING DEVELOPMENT PLAN

A detailed "Fabrication Process Development Plan" was prepared to address the critical fabrication issues relating to the receiver heat absorption panel design. The plan was to develop weld parameters, procedures, and fabrication techniques to fabricate a membrane wall heat absorption panel, using thin wall tubes, for solar thermal central receiver applications. The development work concluded with the fabrication of a 10 ft. x 8 tube mock-up panel to demonstrate the fabrication techniques that are applicable to the commercial fabrication of membrane wall solar receiver heat absorption panels.

Conventional fabrication techniques were used whenever possible. However, B&W's experience with membrane wall welding has been with thick wall tubing for fossil fired steam generation systems; thus, the techniques were not directly transferable.

The weld connections that required development and formed the basis of the fabrication process development plan were:

- Incoloy 800H tube-to-tube membrane wall (including single tube replacement).
- Incoloy 800H tube-to-304 Stainless Steel safe end butt weld.
- 304 stainless steel safe end to header.

The development work for each weld connection is briefly described in the following sections.

6.1 Incoloy 800H Tube-to-Tube Membrane Wall

Three approaches were taken to fabricate the membrane wall:

1) membrane bar concept
2) weld deposit concept
3) finned tube concept

Preliminary evaluations of the three concepts resulted in dropping the membrane bar concept. From the two remaining approaches, final selection of the fabrication method will be based on the thermal/hydraulic and mechanical design features, fabricability, and cost effectiveness.

6.1.1 Membrane Bar Concept

The membrane bar concept requires a bar placed between tubes and attached to the tubes by four fillet welds. The membrane bar welding was attempted using MIG and automatic cold wire TIG. Test results indicated that there was potential for a discontinuity, or stress riser, at the root of the weld due to incomplete penetration of the fillet weld. The stress riser reduces the integrity of the panel design and is unacceptable under the rigorous demands of the solar receiver absorption panel application. Figure 6.1 illustrates the case in point.

The narrow width and depth of the membrane bar, required for solar receiver applications, results in an extremely flexible bar which would be difficult to handle and set-up. Thus handling costs would be excessive and a potential for unforeseen problems would exist.

6.1.2 Weld Deposit Concept

The weld deposit concept employs weld deposits on opposite sides of each tube to form the membrane. Weld parameters and procedures were developed using the pulsed MIG welding process to deposit weld metal 180° apart on each side of the I800H tubing. Parameters and procedures were then developed using the TIG process to fuse the weld deposits between tubes to join the membrane. The TIG membrane weld passes were made from both sides of the membrane to ensure full penetration.

The key issues applying to the weld deposit approach were:

- bead size and shape
- tube wall penetration depth of weld bead
- weld parameters
- surface conditioning

Bead size and shape was important for build-up and membrane welds. A trial and error method was established to determine the number and size of weld deposits required to obtain the desired ligament dimensions (See Figure 6.2). Development work performed on membrane welds between tubes indicated that it was unnecessary to use filler metal to make the membrane weld.

Tube wall penetration depth of the weld bead was correlated with weld parameters and procedures (amps, volts, wire feed speed, travel speed). The tubes were water cooled to decrease weld bead penetration due to base metal temperature effect on weld puddle cooling, and to assure that burn through does not occur (See Figure 6.3 and 6.4). Water cooling was required for the weld buildup but was not required for the membrane weld.

Weld parameters were evaluated to obtain the desired weld configuration and quality with the goal of zero rework. The welding time was not considered to be very important since it is minimal compared to handling, set-up, cleaning, fitting, bending, etc.

Parameters were established that eliminated the need to machine weld preps on the weld buildup prior to making membrane welds. Hence, the only surface conditioning required is to smooth the high spots on the weld deposits (See Figure 6.5).

6.1.3 Finned Tube Concept

Weld buildups are expensive relative to base metal, so the third approach was to eliminate the weld buildup by obtaining tubes with extruded fins. This approach depends on what can be obtained from the tube mill and its cost. It is anticipated that some minor surface conditioning will be required to weld prep the fins before constructing the membrane weld. The specified tube diameter and rib dimensions are illustrated in Figure 6.6. The extruded finned tube has been successfully milled and meets the tube specifications.

6.1.4 Panel Tube Replacement

The development effort included replacing a single tube in a membrane panel. If a tube were damaged, it was determined to be more practical to replace the entire tube, rather than risk welding in a dutchman, since accessibility to make two butt welds is poor.

The procedure calls for cutting the membrane on both sides of the defective tube with a thin abrasive wheel. A weld prep is prepared on the adjacent panel tubes, and a new tube with weld deposited fins is tack welded into position. The membrane is welded on the front side of the panel by the manual TIG process with the addition of filler metal. It was assumed that the back side of the panel is inaccessible (without removal of insulation) to back weld the membrane. Figure 6.7 illustrates the panel tube replacement mock-up apparatus.

6.2 Incoloy 800H Tube-to-304 Stainless Steel Safe End Butt Weld

Parameters and procedures were developed for the thin wall Incology 800H tube-to-thick wall 304 stainless steel safe end butt weld. Prebent 304 stainless steel safe ends were fit to the end of the Incoloy 800H tubing and

fixtured to assure proper alignment. The butt weld was made by the automatic TIG process as the tube was rotated. The butt welds were then non-destructively examined by liquid penetrant inspection. Figure 6.8 illustrates the tube-to-safe end butt weld.

6.3 304 Stainless Steel Safe End-to-Header

Parameters and procedures were developed for socket welding the safe ends to the headers. The safe ends were fit into the headers and the weld was made by the manual TIG process with backing strip in place. The safe end to header welds were non-destructively examined by liquid penetrant inspection. Figure 6.9 illustrates the safe end to header socket weld.

6.4 Demonstration Panel

A 10 ft. long, 8 tube demonstration panel was fabricated using the weld buildup membrane wall concept and the parameters, procedures, and fabrication techniques developed during the fabrication process development plan.

The following narrative briefly describes the sequence to fabricate the demonstration panel:

Weld buildup of the membrane fins was deposited on the Incoloy 800H tubing by an automatic MIG process. The MIG station requires rigid full length support of the tubing and a track to carry the welding head. Two (2) weld passes were required for each fin. After the first fin was deposited, the tube was rotated 180°, using fixturing to prevent twist, and the second fin was deposited. Surface conditioning of the weld deposits was required only to smooth high spots in the weld buildup.

Prebent 304 stainless steel safe ends were fit to each of the Incoloy 800H panel tubes using fixturing to assure proper alignment. The safe end to tube weld was made by the automatic TIG process as the tube was rotated. The safe end to tube welds were then liquid penetrant inspected for surface discontinuities.

The tubes were fit together to form the full width panel and tack welded to position the tubes to make the membrane welds. The equipment included a full length support fixture and gantry type welding

equipment. The membrane welds were made by the automatic TIG process. The panel was then turned over, aligned, and a weld pass was made on the opposite side of each membrane to provide full penetration.

Panel attachment lugs for lateral support tees and insulation support pins were fit and welded to the back of the panel tubing by the manual TIG process.

The header was fit to the safe ends and socket welded by the manual TIG process with backing strip in place. The safe end to header welds were liquid penetrant inspected for surface discontinuities.

Header and caps were fit and welded to the header, hydrostatic plugs were welded into the panel tubing, and the panel was hydrotested.

Figures 6.10 through 6.17 illustrate the demonstration panel fabrication sequence. It is anticipated that the commercial fabrication of these membrane wall heat absorption panels will be similar to the demonstration panel fabrication, with the addition of multihead welding stations.

6.5 Metallurgical Examination

A metallographic evaluation was performed on Alloy 800H weld build-up membrane welds. Several samples of each weld type were sectioned at various areas (some corresponding to suspected weld defects), mounted, polished and etched for microstructure evaluation. Two samples were chosen from the membrane weld and two samples from the build-ups for microhardness evaluation. The samples were lightly etched to locate the fusion line. From the microhardness measurements, two traverses were made. One traverse was a radial progression from the ID of a tube to the weld. The other traverse was run tangential to the toe of the weld, approximately 45^{o} to the center of the weld bead. Hardness versus distance from the ID of the tube were plotted. All samples were then evaluated for microstructure. Photomicrographs were taken in representative areas of both types of welds.

Microhardness measurements indicated no unusual change in hardness through the tube and weld heat affected zone. A sharp increase occurred as readings progressed into the weld metal. In the membrane welds, three regions of higher hardness were detected: at the two fusion lines of the weld beads and in the weld center corresponding to the joining of the two weld beads. Residual stresses due to the welding process of joining the tubes were correlated with the variable hardness. Base metal hardness was fairly uniform in both weld build-ups and membrane welds. Typical scatter existed in the weld metal values in both types of welds.

Weld metal microstructure was composed of fine dendrites with some fissuring in a few of the samples. The base metal microstructure was composed of grains with grain boundaries delineated with carbides. The grain size up to the fusion line was essentially the same through the tube. No substantial microstructural difference existed between the heat affected zone and non-heat affected zones.

It was apparent that the tube cooling techniques used during welding the bead on the tube was sufficient to suppress significant grain growth in the weld heat affected zone. The cooling did not initiate any base metal defects. Minor fissuring was detected in the weld build-ups, but not any worse than is typically seen in this type of weld metal.

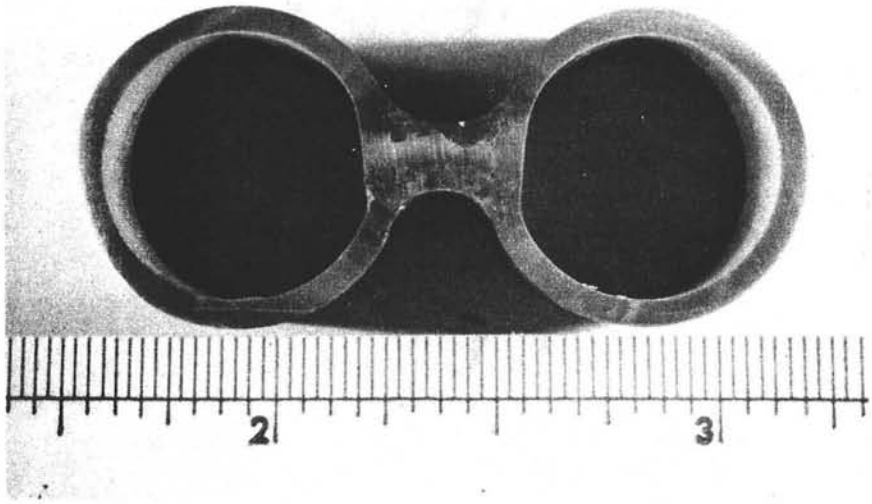

FIGURE 6.1 - MEMBRANE BAR CONCEPT

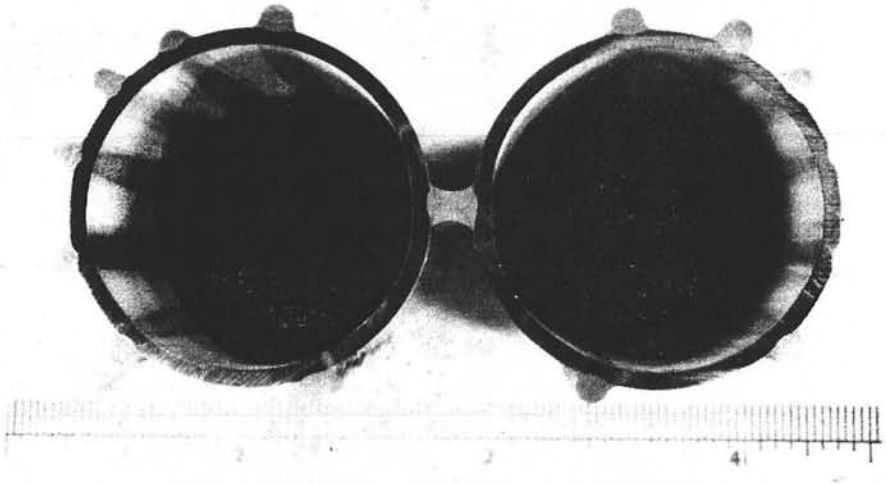

FIGURE 6.2 - WELD DEPOSIT BEAD SIZE

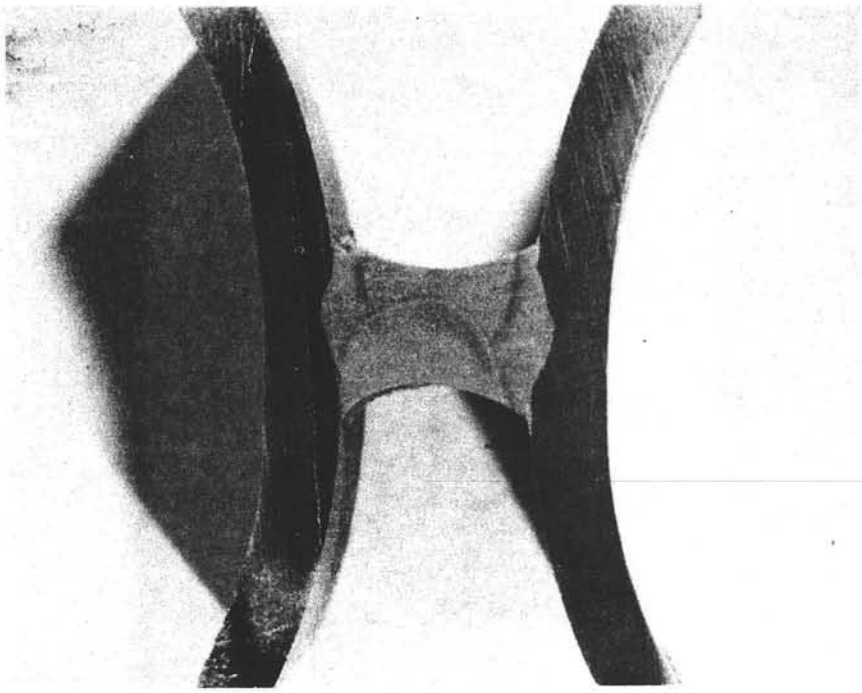

FIGURE 6.3 - WELD DEPOSIT MEMBRANE WELD CONCEPT

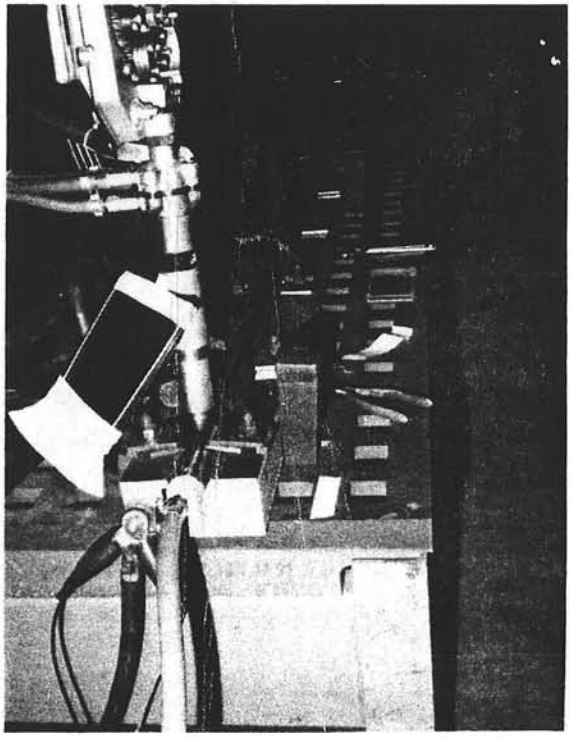

FIGURE 6.4 - WELD DEPOSIT–WATER COOLING

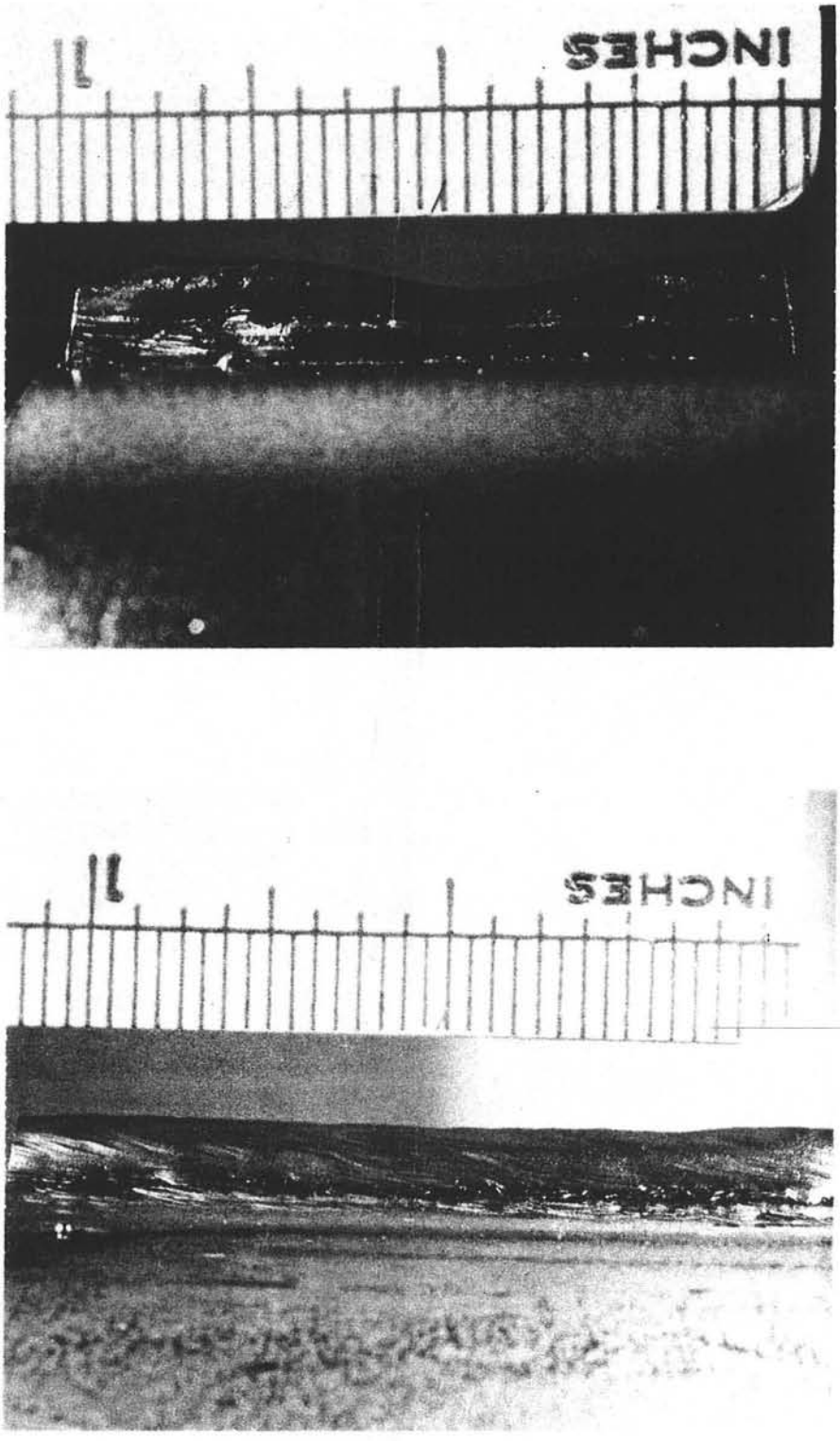

FIGURE 6.5 - WELD DEPOSIT SURFACE CONDITION

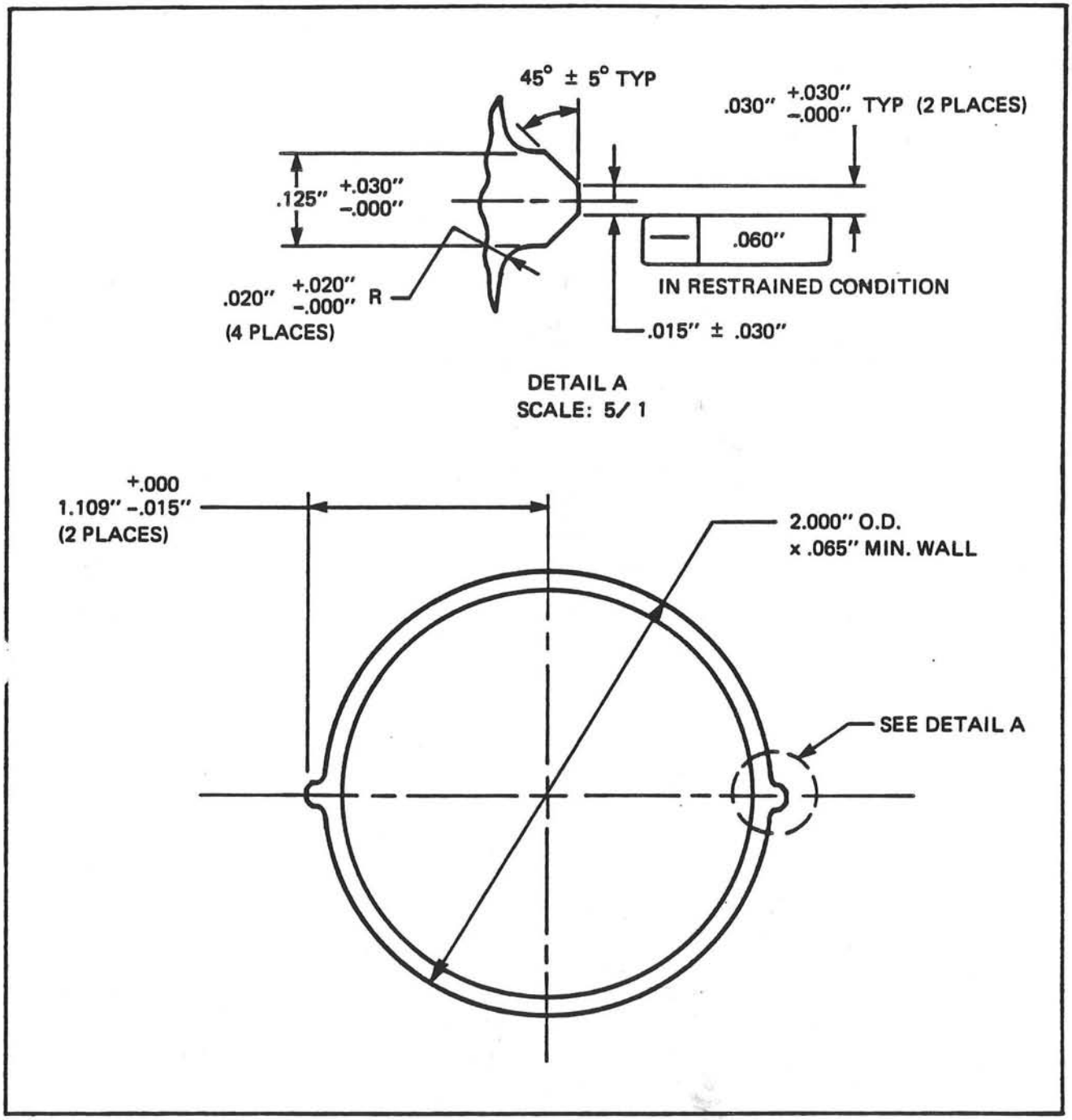

FIGURE 6.6 - FINNED TUBE CONCEPT

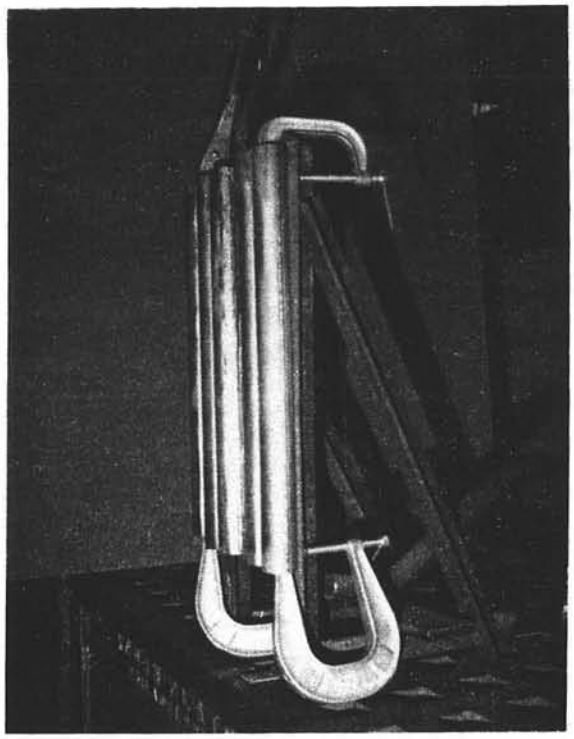

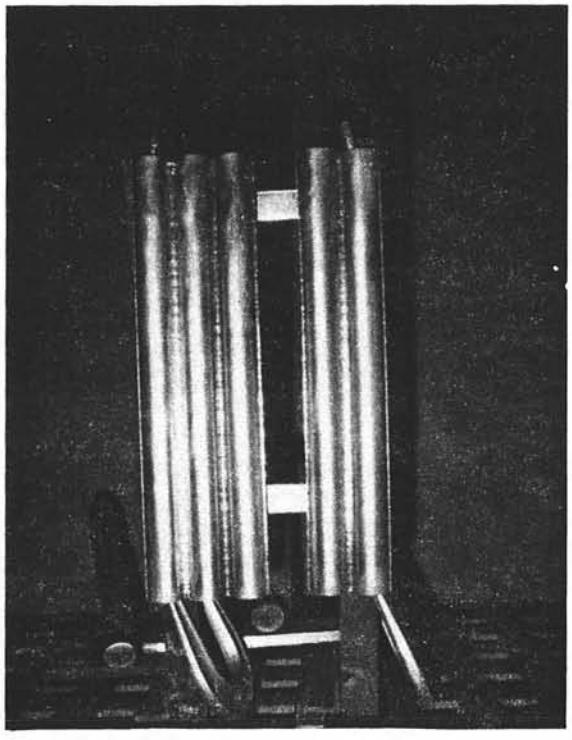

FIGURE 6.7 - PANEL TUBE REPLACEMENT

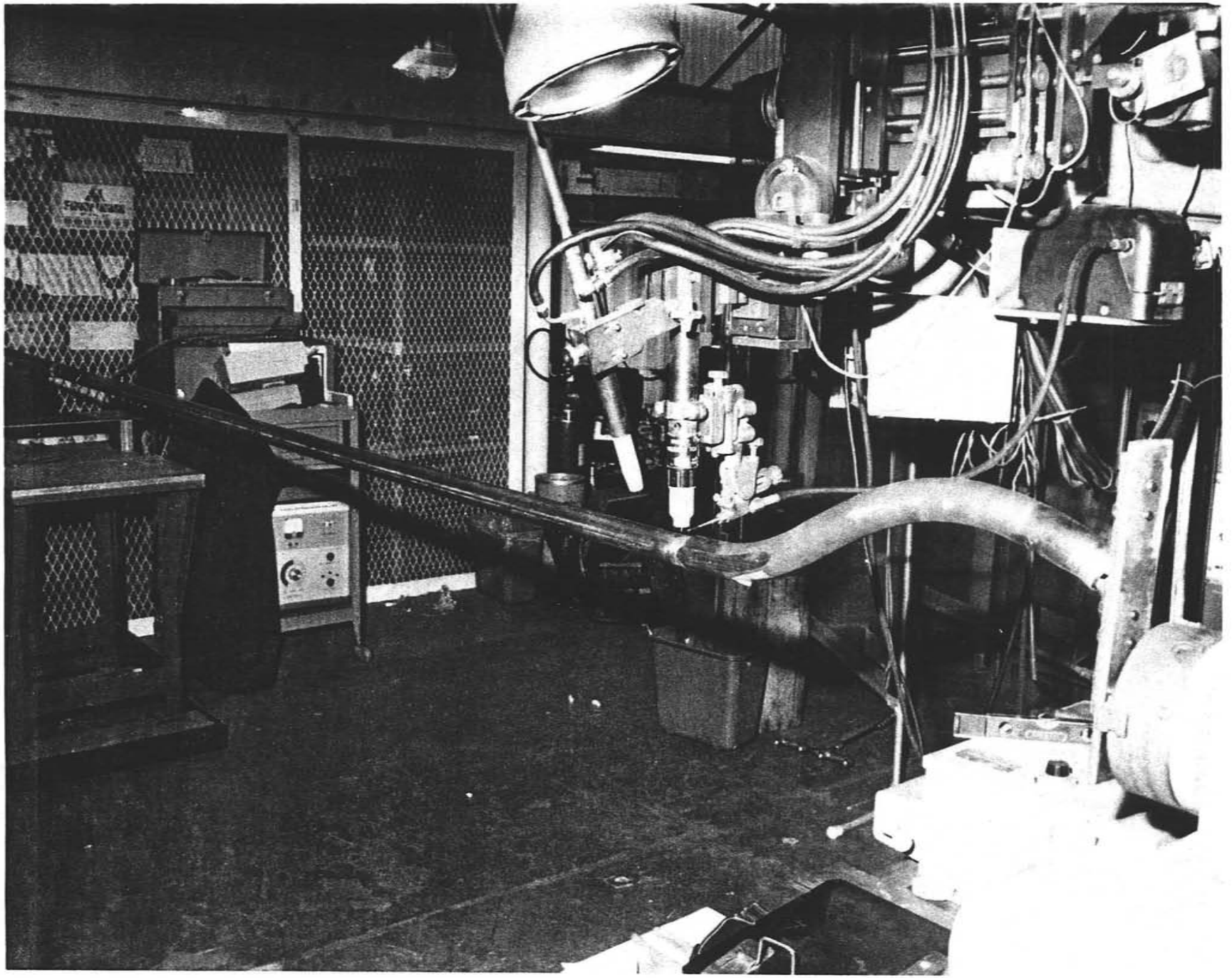

FIGURE 6.8 - TUBE-TO-SAFE END BUTT WELD SET-UP

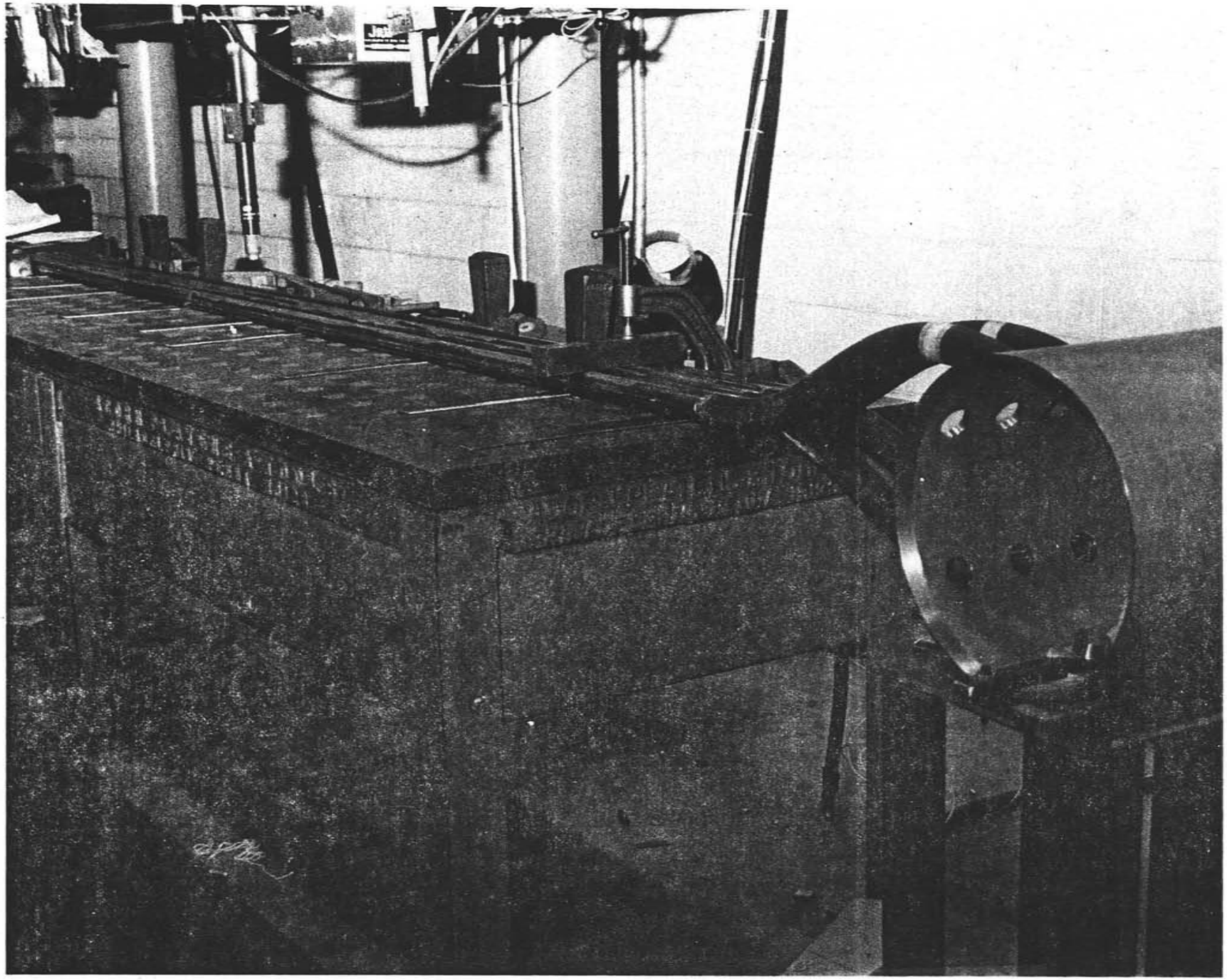

FIGURE 6.9 - SAFE END-TO-HEADER SOCKET WELD

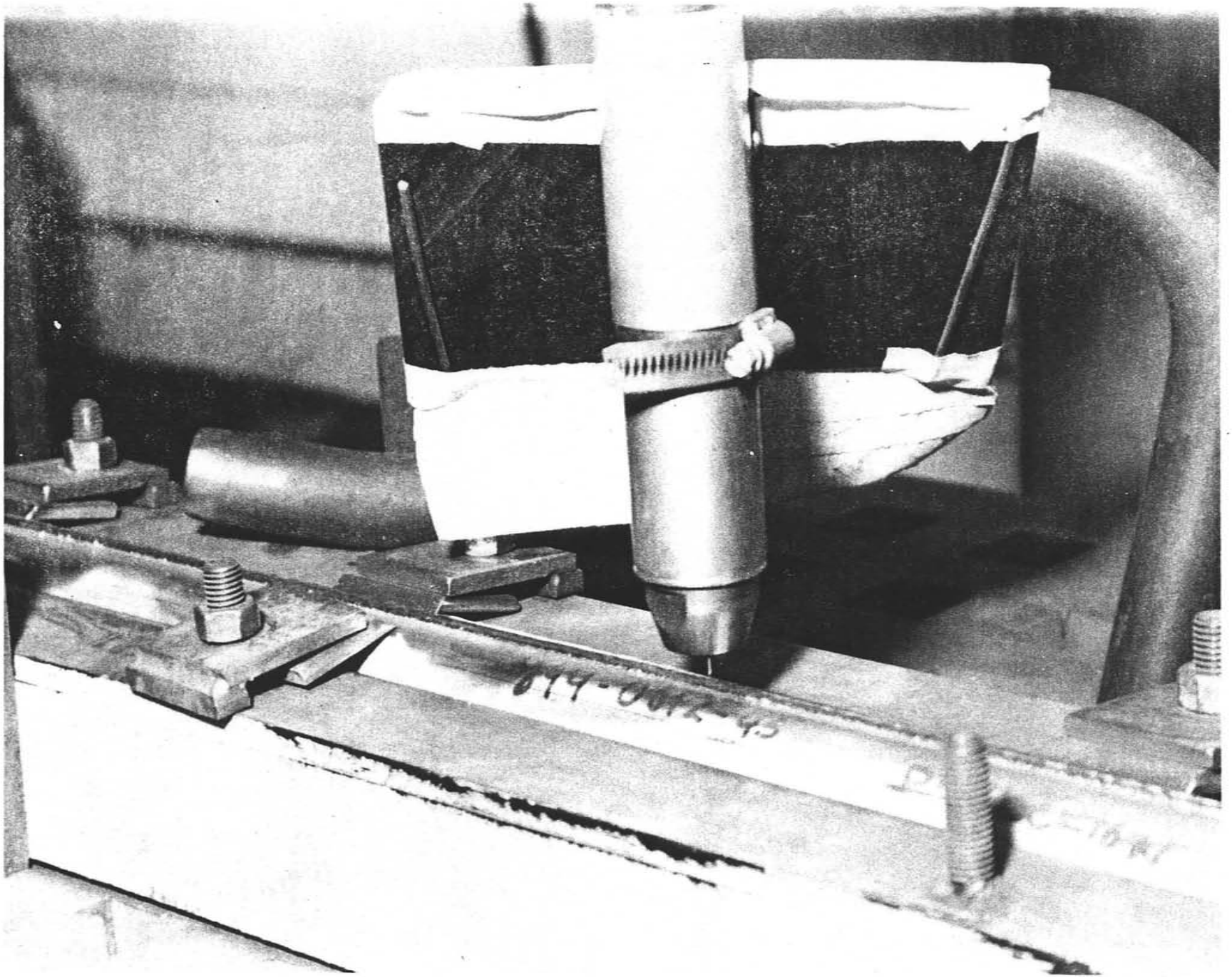

FIGURE 6.10 - MIG WELD BUILDUP OF MEMBRANE FINS

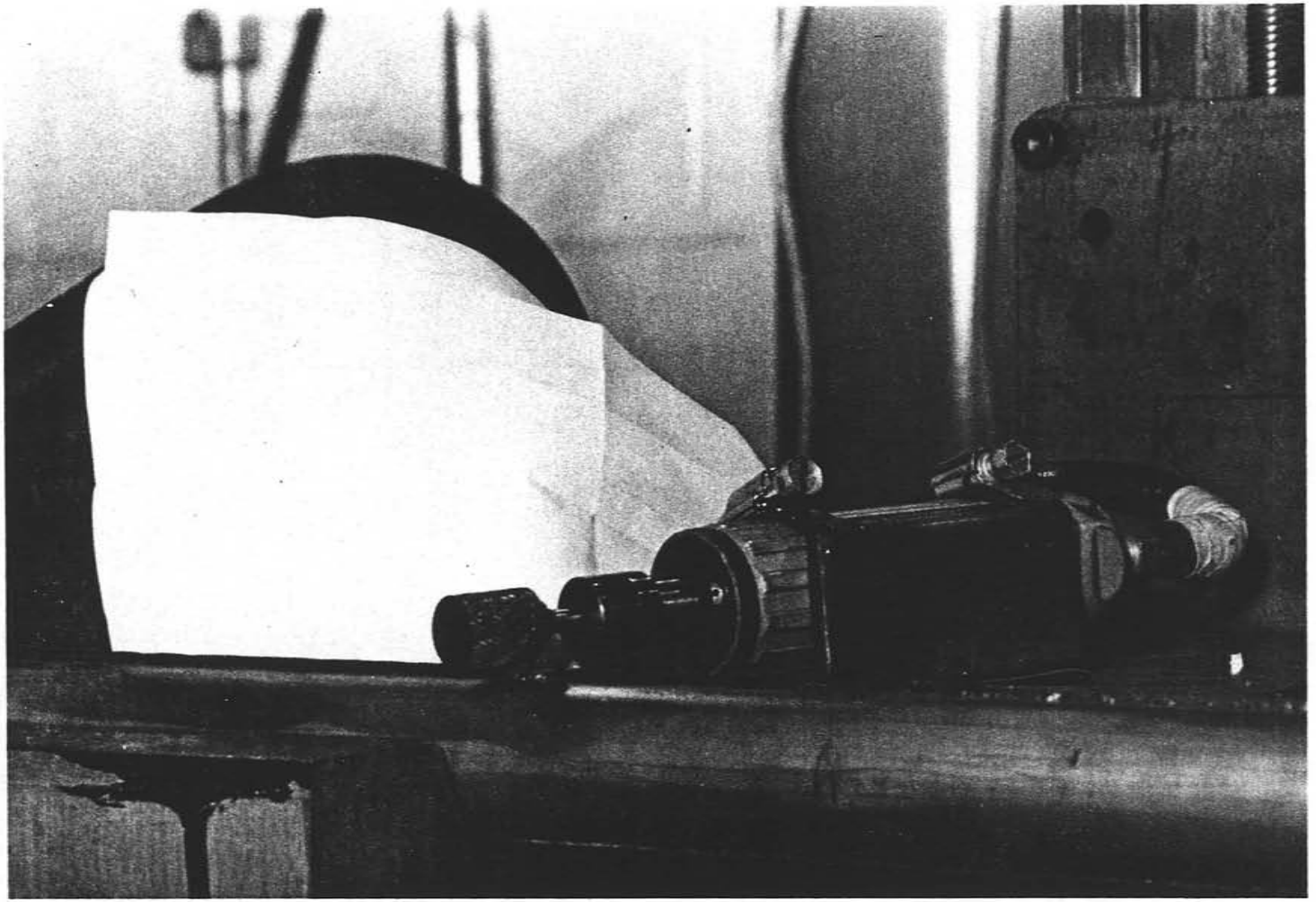

FIGURE 6.11 - WELD DEPOSIT SURFACE CONDITIONING

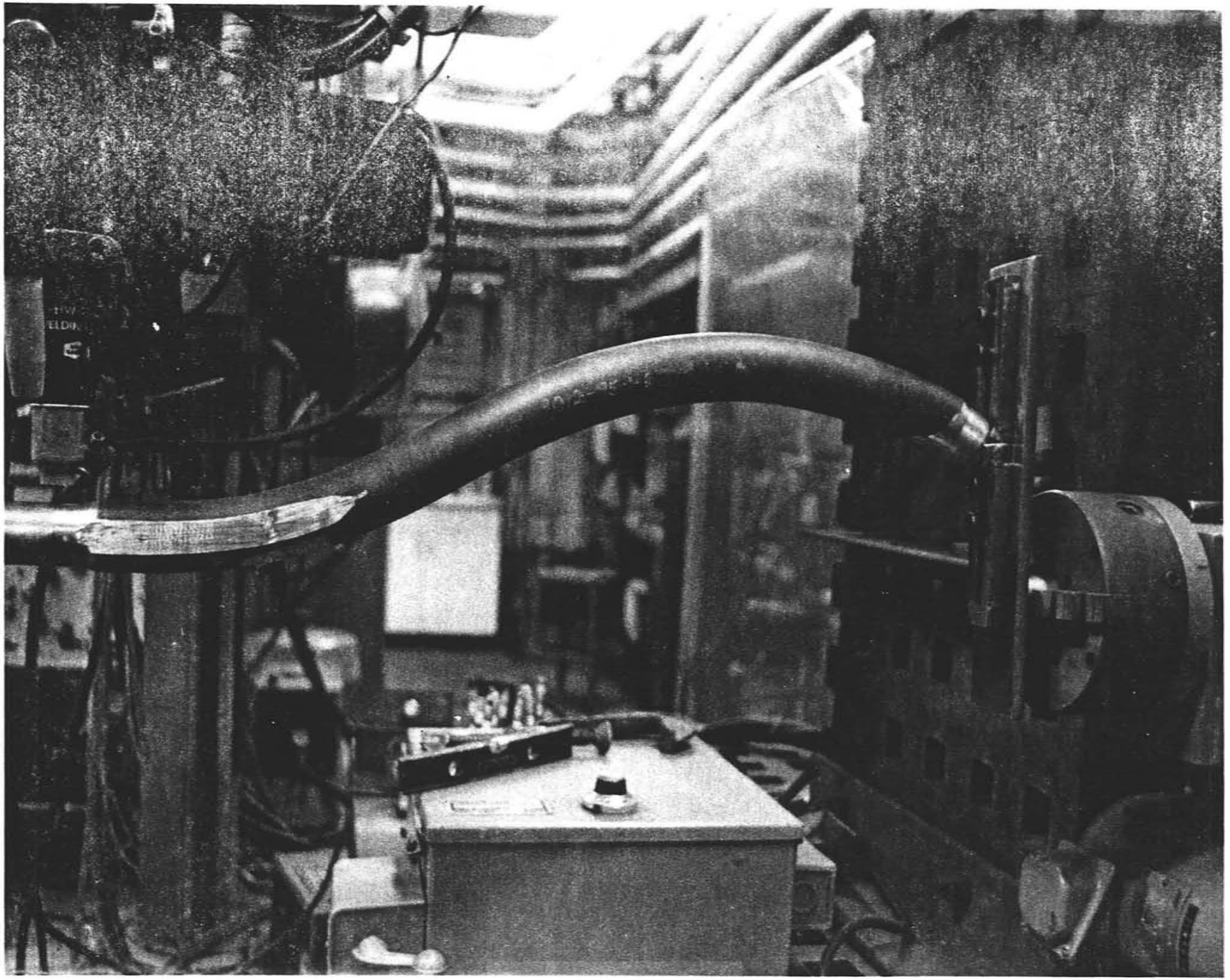

FIGURE 6.12 - SAFE END-TO-TUBE WELD BY TIG PROCESS

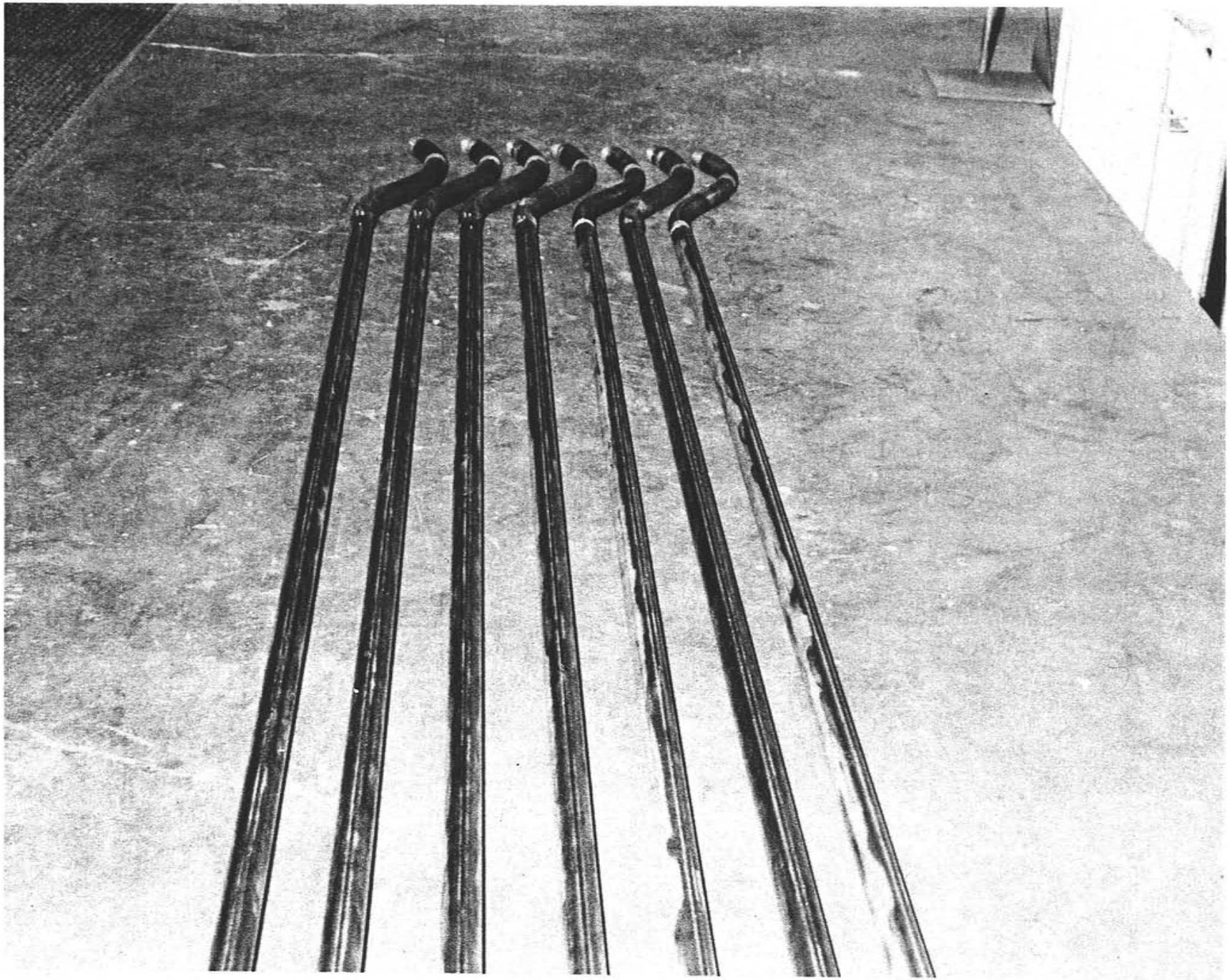

FIGURE 6.13 - COMPLETED SAFE END ATTACHMENT

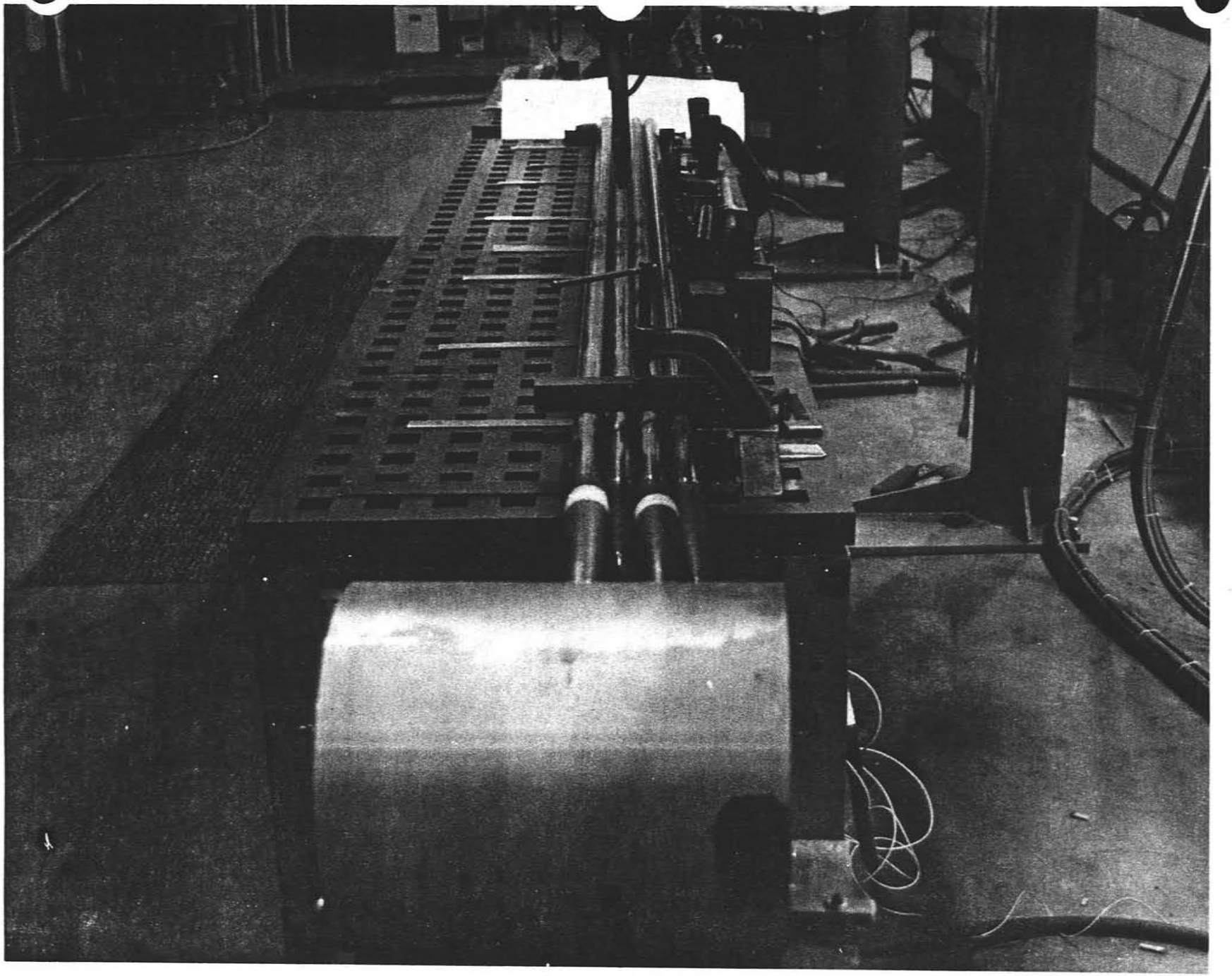

FIGURE 6.14 - MEMBRANE WALL CONSTRUCTION

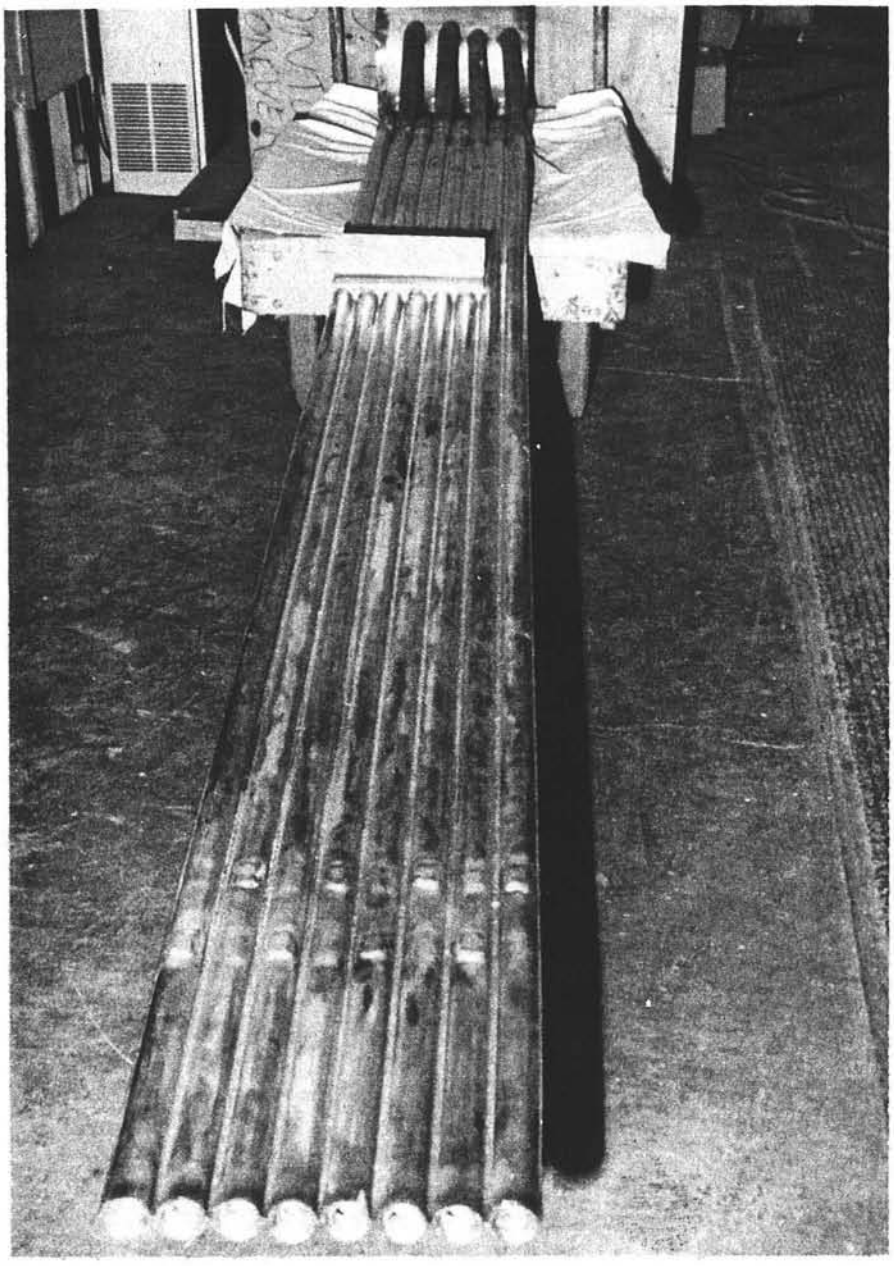

FIGURE 6.15 - PANEL ATTACHMENT LUGS

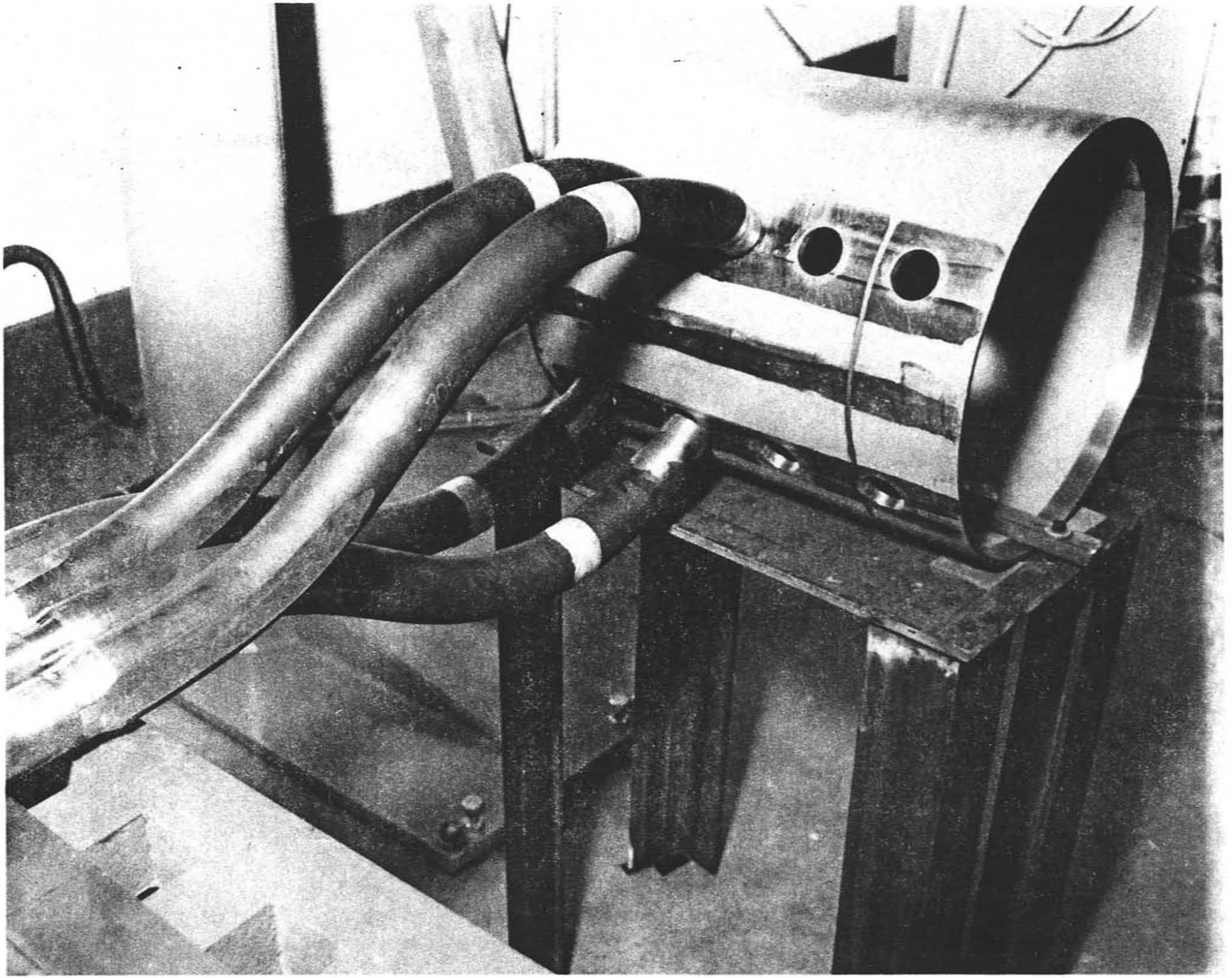

FIGURE 6.16 - SAFE END-TO-HEADER SOCKET WELD

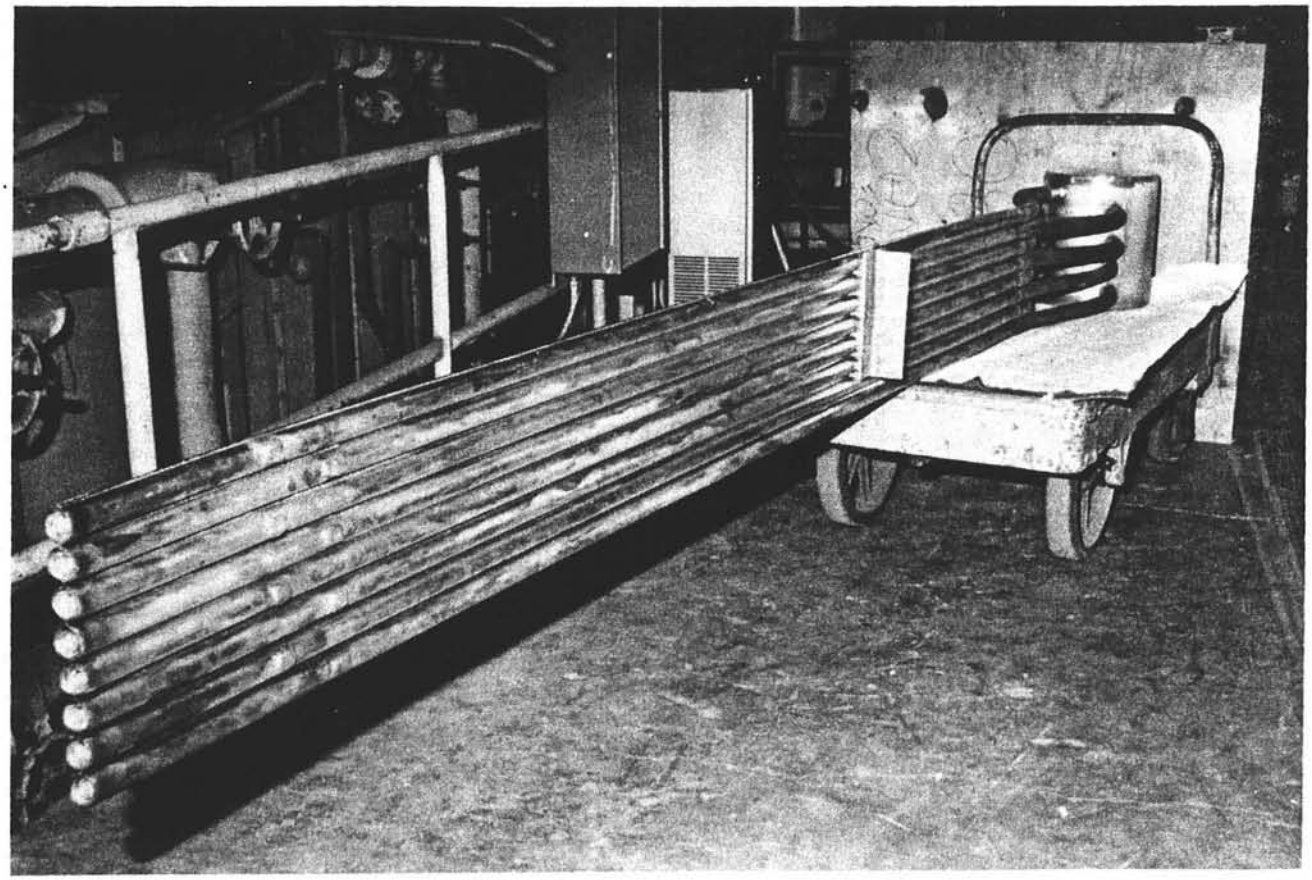

FIGURE 6.17 - COMPLETED DEMONSTRATION PANEL

7.0 SRE AND DEVELOPMENT PLAN

The objectives of Task 7 were to identify problem areas and uncertainties associated with the full sized commercial receiver and to develop a program through which these problem areas and uncertainties could be resolved. To meet these objectives, the program was divided into two parts.

Part 1 - designated the SRE Design, is the design of a subscale receiver subsystem that will demonstrate the design adequacy and operational capability of the commercial receiver subsystem.

Part 2 - designated the Development Plan, is a program of analytical studies, field testing, and laboratory testing to resolve specific areas of uncertainty.

The purpose of the SRE and Development Plan is to resolve any uncertainties with the design, fabrication, or operation of the full scale commercial receiver subsystem. Resolving the uncertainties is a critical step in the process of developing the technology necessary to provide cost competitive solar power. Descriptions of both parts of the program are presented in Sections 7.1 and 7.2.

7.1 Solar Research Experiment (SRE) Design

It seems likely that the commercialization of the solar industry will progress in relatively small steps, that is, large extrapolations in size will not take place. At present the industry knowledge of the molten salt system is based on the equipment built for the CRTF. To reach large commercial plant sizes, it may be prudent to establish some test experience on unit sizes somewhere in between these two extremes.

It is proposed that the industry examine the design, fabrication, and test of receivers in two size ranges. First, it is recommended that a 5 MW_t unit be tested at CRTF with the major objective of proving out some features of the units proposed for large plants. Second, a receiver of approximate size 30-50 MW_t should be tested to demonstrate the hardware viability with panel and tube sizes that are close to those needed for large plants. Testing of the larger unit may be possible at the Barstow site or at some repowered facility.

For the purposes of documenting a plan outline, the following sections are written around two receiver sizes - 5 MW_t and 30 MW_t. An outline of the potential benefits of designing, fabricating, and testing these two units is described in Section 7.1.1.

7.1.1 Subscale Modeling

The specific objectives of the subscale modeling are:

1) Demonstrate panel fabrication.
2) Demonstrate cavity enclosure fabrication.
3) Measure thermal performance.
4) Demonstrate control system operation.
5) Demonstrate operation of high pressure blowdown system.
6) Demonstrate ability of the panel supports to accommodate thermal expansion.
7) Provide data for verification of structural design calculations and methods.
8) Evaluate effects of solar flux on insulating materials.

This broad range of objectives has led to a two phase plan for carrying out the receiver subscale modeling. The first phase is a 5 MWt receiver to be tested at CRTF. This receiver would duplicate the commercial receiver with respect to

--salt inlet temperature

--salt outlet temperature

--salt velocity

--overall heat transfer coefficient

--peak heat flux

--average heat flux

--tube to tube attachment

--panel supports

The duplication of these thermal/hydraulic parameters permits a thorough checkout of the receiver control system and a verification of the thermal performance predictions. Due to the scaling factor, the degree of similarity for some of the geometric parameters is not as high as for those listed above. These parameters include tube diameter, tube length, number of tubes per pass, and number of passes. Although valuable data, such as deflections, temperatures, and stresses can be obtained from the 5 MWt SRE, the extrapolation to a 300 or 400 MWt commercial receiver would be enhanced if a larger subscale receiver was tested.

The second phase of the subscale modeling is the testing of a 30-50 MWt receiver which will be referred to as the Large Receiver Test Program (LRTP).

The large receiver test program would be geared towards providing more quantitative data on the thermal/mechanical behavior of the commercial receiver than was obtainable from the 5 MWt tests. A 30 MWt receiver would employ full sized tubes, 2.000" O.D. x .065 wall, and the panel lengths would be in the range of 60 to 80 feet. The number of tubes per pass would closely approximate the commercial receiver. Besides providing a high degree of geometric similarity there are also some thermal/hydraulic parameters that would be better simulated with the LRTP receiver than with the 5 MWt test. In particular are the salt temperature increase per pass, the axial flux gradient, and the lateral flux gradient. The overall heat transfer coefficient would be the same as in the commercial receiver.

When combined with the CRTF program, the data from the LRTP would greatly reduce the uncertainty in extrapolating from a 5 MWt receiver to a 300 MWt or 400 MWt commercial receiver. Table 7.1 illustrates how the combination of tests will encompass the whole spectrum of receiver features/parameters.

In an effort to keep costs at a minimum, it may be possible to test a 30 to 40 MWt receiver at the Barstow site by erecting another tower adjacent to the existing collector field. If this plan is not viable due to scheduling and/or technical limitations, another option may be to approach a potential repowering customer with a proposal to construct a large test facility with the intent to expand into a repowering installation at the completion of the test program.

TABLE 7.1

FEATURES AND PARAMETERS OF THE FULL SCALE RECEIVER

THAT ARE SIMULATED IN THE TEST PROGRAMS

Feature/Parameter	CRTF	LRTP
Cavity w/aperture	X	
Exposed		X
Salt inlet and outlet temperature	X	
Maximum salt temperature per pass		X
Tube size		X
Tube length		X
Multi-tube pass	X	X
Membrane wall	X	X
Tangent Tube	X	X
Panel Support	X	X
Salt Velocity and U	X	X
Aperture Flux Measurement	X	
Axial Flux Gradient		X
Lateral Flux Gradient		X

7.1.2 Description of 5 MWt SRE Receiver

The 5 MWt receiver has been designed to simulate the commercial receiver with respect to salt velocity, overall heat transfer coefficient, peak and average heat flux, and inlet and outlet salt temperatures. In conjunction with these thermal/hydraulic parameters, the receiver incorporates as many of the structural and mechanical characteristics of the commercial receiver as possible.

The receiver would be a cavity type with an aperture door (or doors) that could be tightly closed during non-flux periods. The door seals would be the same type as those proposed for the commercial receiver.

The heat absorption surface consists of 36 vertical panels with 6 tubes per panel. The tubes are 1.000" O.D. x .065" wall with a heated length of approximately 15 feet. The overall dimensions of the receiver surface is roughly 15 feet high by 20 feet wide. The length was governed by the horizontal buckstay spacing which, for the 1.000" tubes, is 11 feet. The buckstay spacing was based on the same criterion used for the commercial receiver which was tube stresses due to wind and seismic loading. Two other criteria were tube vibration and tube deflection, and these are also satisfied by the 11 foot spacing. The upper buckstay is approximately 4 feet below the upper headers and 2 feet below the top of the active length as shown in Figure 7-1.

With the receiver height known, the width was selected to provide a total surface area of approximately 300 square feet. This absorption area gives the same average heat flux as in Zone 1 of the commercial quad-cavity receiver.

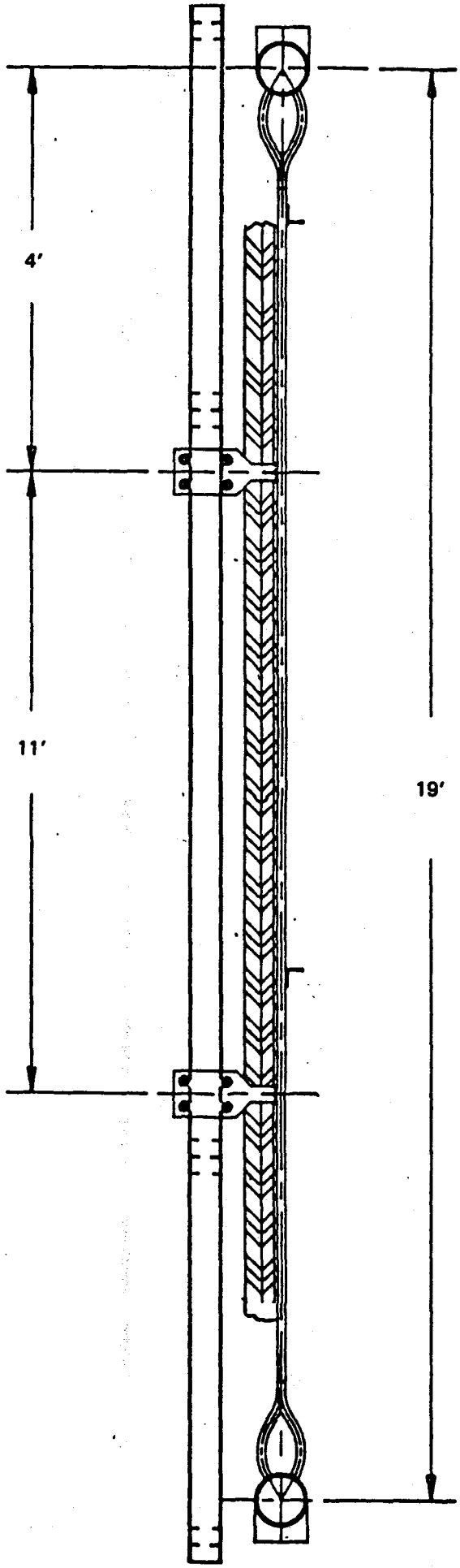

FIGURE 7.1 - SIDE ELEVATION 5 MWt PANEL

There are two types of tube-to-tube attachments that are under consideration for a commercial receiver - a continuous welded web or membrane and a tangent tube construction in which the tubes are attached to the lateral buckstay but not to each other. To provide data for a more in depth trade study, the SRE receiver will have both types of panels. Two passes of membrane panels would be alternated with two passes of tangent tube panels. Alternating every two panels was chosen over every other panel so that there would be both up-flow and down-flow passes of each type of construction. A flow schematic of the receiver subsystem is shown in Figure 7-2.

7.1.3 Description of 30 MWt Receiver

The 30 MW_t receiver would employ a single control zone with 8 vertical passes. Each pass consists of 16, 2.000" O.D. x .065" wall tubing. The tube length would be the same as for a commercial sized receiver - 60 to 80 ft. Assuming an average flux of approximately 60000 Btu/hr-ft^2 results in an absorption area of 1700 ft^2 and a receiver width of 21-28 ft.; a summary of the design characteristics are presented in Table 7-2. The panel construction type would probably be either membrane wall or tangent tube but not both as in the 5 MWt receiver. It is anticipated that the 5 MWt testing and the receiver development work would result in a conclusion as to the optimum receiver construction.

The receiver configuration for this size model would be an exposed design. The reason for this is that the geometry of the test receiver, relatively tall and narrow, does not correspond to an aperture and cavity design that is prototypical of the commercial receiver. It was felt that simulating full length passes was of higher priority than duplicating the cavity configuration in this phase of the subscale modeling program.

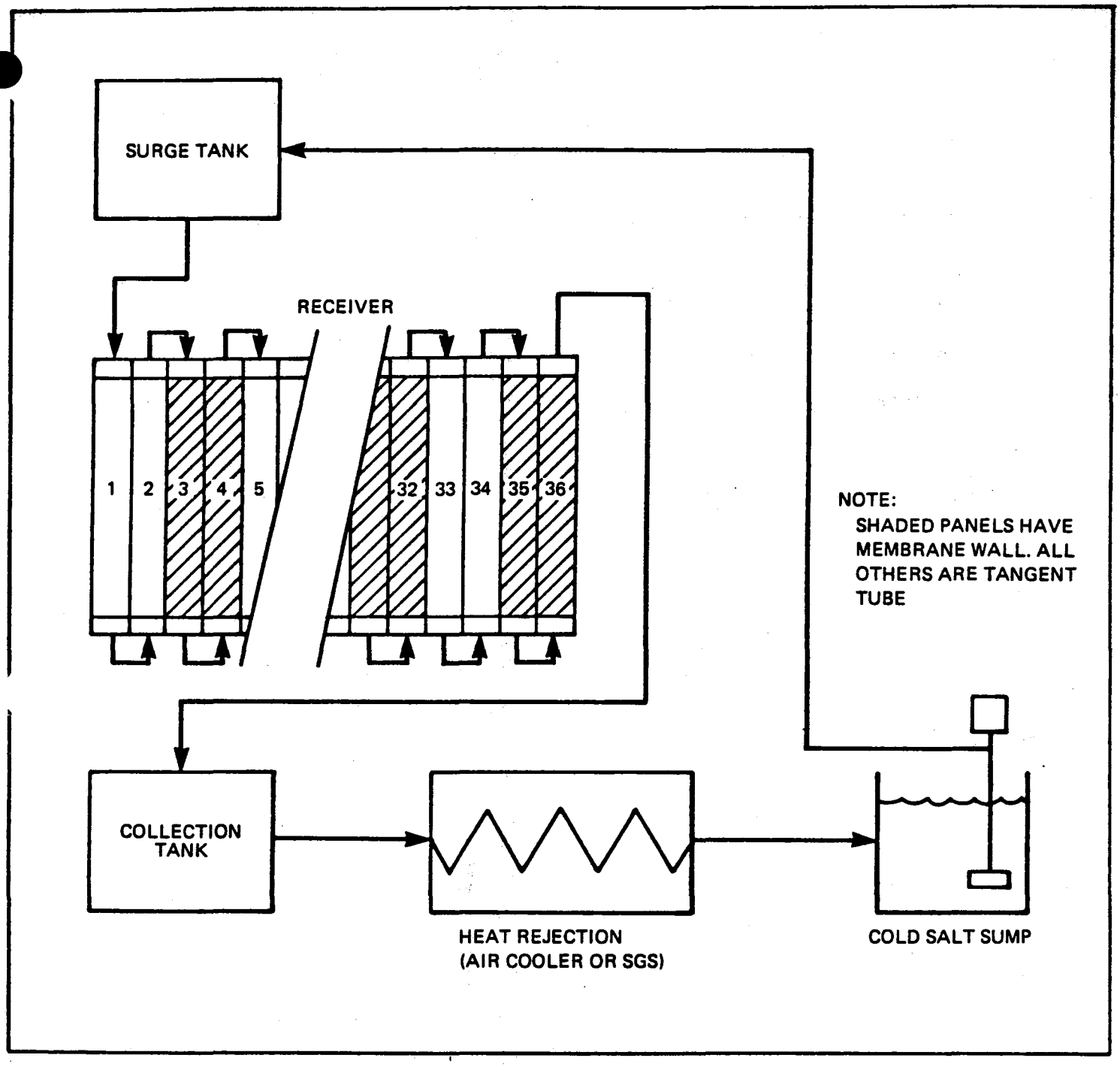

FIGURE 7.2 - FLOW SCHEMATIC FOR 5 MWt SRE

TABLE 7.2

DESIGN CHARACTERISTICS

	CRTF	LRTP
Thermal Rating	5 MWt	30 MWt
Receiver Configuration	cavity	exposed
Salt Inlet Temperature	550	T_{in}
Salt Outlet Temperature	1050	T_{in} + 200F
Salt Flow Rate	93250 lb/hr	1.4 x 10^6 lbm/hr
Average Heat Flux	60000 Btu/hr-ft^2	60000 Btu/hr-ft^2
Peak Heat Flux*	160000 Btu/hr-ft^2	160000 Btu/hr-ft^2
Absorption Surface Area	300 ft^2	1700 ft^2
Tube O.D. x Wall Thickness	1.000" x .065"	2.000" x .065"
Tube Length	15 ft.	70 ft.
No. of tubes per pass	4	16
No. of passes	36	8
Receiver Width	20 ft.	25 ft.

* The receivers are designed for this flux but will be subjected to higher flux levels.

7.1.4 Means of Meeting Specific Objectives

The two phase plan for carrying out receiver subscale modeling allows a broad range of objectives to be satisfied. The means of meeting these objectives are described below.

1) Demonstrate Panel Fabrication

The methods proposed to fabricate both the 5 MWt and 30 MWt receiver panels will, as much as possible, be the same as those used to fabricate the commercial receiver. Particular emphasis will be placed on simulating the techniques used for tube-to-tube and tube to buckstay attachments. Building the subscale models is expected to provide invaluable information regarding fabrication techniques and costs which will permit a higher degree of accuracy in the fabrication cost estimates for the commercial receiver.

2) Demonstrate Cavity Enclosure Fabrication

One of the unknowns in predicting performance of a cavity receiver during both normal operation and hot standby is the infiltration of cold air into the cavity enclosure. During normal operation, portions of the ceiling and walls are expected to be in excess of 1000F. Maximizing receiver efficiency and minimizing heat loss during hot standby requires that the junctures between the ceiling, walls, floor, and aperture be designed and constructed such that gaps do not develop due to thermal expansion as these components heat up. Most of the large junctures in the commercial design are sealed with a "plug" of insulation as discussed in Section 2.4.1. These will be duplicated in the 5 MWt SRE receiver.

The effectiveness of these seals will be difficult to measure although thermocouples and anemometers could possibly be used to measure air temperature and velocity in the vicinity of the junctures. These measurements would be used to estimate the convection heat losses through the seals.

The aperature door seals are also important with respect to hot standby. The door seals are described in Section 2.5.2 and are subject to the same problems of quantifying their effectiveness. The same measurements for air temperature and velocity could be made around the edges of the aperture door.

3) Measure Thermal Performance

The thermal output of both the 5 MWt and 30 MWt receivers can be determined by measuring the salt mass flow rate and the receiver inlet and outlet temperature. Thermocouples will also be placed at each pass outlet so that the temperature increase in each pass can be determined. These thermocouples would also provide input to the receiver control system. Receiver efficiency will be calculated using analytical procedures and compared to test results for both heated and unheated (no flux) tests. With both the 5 MWt and 30 MWt receivers, these tests will allow refinement of the analytical techniques for more accurate forecasting of the performance of a commercial scale unit.

4) Demonstrate Control System Operation

Demonstrating the operation of the Optimal Quasi Feedforward Control System is one of the primary objectives of the 5 MWt test program at CRTF. The control system is

designed to maintain salt outlet and tube metal temperatures within acceptable limits during steady state, startup, shutdown, and during cloud transients by matching the salt flow rate to the heat flux. Operation of the control system will be checked by measuring salt and tube metal temperatures and comparing them to the set points.

5) Demonstrate Operation of High Pressure Blowdown System

To prevent the receiver tubes from overheating due to a loss of flow caused by a pump, valve, or pipe failure upstream of the surge tank, a passive high pressure blowdown system has been designed. This system consists of a high pressure air storage tank and a remotely set regulator that maintains the surge tank pressure and salt driving force.

Operation of this system is critical to protection of the receiver during a loss of flow. Testing of the system can be performed with minimal solar flux on the receiver and would be carried out under a variety of operating conditions simulating startup, shutdown, steady state, and cloud transients. Salt flow rates and durations would be monitored and compared to the time required to scram the heliostat field.

6) Demonstrate the Ability of the Panel Supports to Accommodate Thermal Expansion

The horizontal buckstay-to-vertical buckstay connection is made via a set of steel rollers as shown in Figure 2.4.1. It is felt that this is the optimum arrangement for both lateral support and vertical motion under all operating conditions. The displacement of the horizontal buckstay will

be measured and compared to the predicted displacement for the given tube temperatures. The temperatures of the buckstay members will be measured so that the ability of the roller assembly to operate at various, and potentially uneven, temperatures can be evaluated, first for a small panel in the 5 MWt design and later for a long panel in the 30 MWt test.

7) Provide Structural Data for the Verification of Design Calculations and Methods

In order to verify the methods and analytical tools used to design the receiver, instrumentation will be installed on the absorption panels and supports that will give the following information:

1. Strain Level - back side of tube (O.D.)
   - web between tubes (membrane wall)
   - horizontal buckstay T-beam
2. Temperature - back side of tube (O.D.)
   - front side of tube (I.D.)
   - back side of insulation lagging
   - horizontal buckstay members
   - vertical buckstay members
3. Lateral Displacement - absorption tubes
   - headers
4. Vertical Displacement - horizontal buckstays
5. Flux Measurement - web between tubes
   - aperture plane using Real Time Aperture Flux System (5 MWt only)

8) Evaluate Effects of Solar Flux on Insulating Materials

To accommodate lateral thermal expansion and manufacturing tolerances, a small gap is left between adjacent absorption panels. This gap is filled with B&W 3000 Board to protect structural members behind the panels. A sketch of a typical panel-to-panel joint is shown in Section 2.4.1.

Close observation of the insulation in these gaps over the duration of the testing would provide data on the long term performance of this material. Specifically, the insulation would be examined for cracking, flaking, and melting.

Summary of SRE Program

The two-part subscale modeling program is intended to demonstrate to potential users the design adequacy and operational capability of the commercial receiver subsystem. Information obtained from the modeling will be used to update the design of the receiver subsystem. Performance estimates, structural design, fabrication and erection techniques, operational procedures, control system design, and maintenance requirements will all be upgraded based on the results of the 5 MWt and 30 MWt test programs.

7.2 Development Plan

The purpose of this development plan is to identify and briefly discuss proposed work activities associated with the design and fabrication of commercial receiver subsystems. These work activities consist of analytical studies, laboratory testing, and field testing. The work would be directed towards resolving uncertainties, broadening the technical and economic data bases, and reducing design margins.

The development plan has been broken down into the following items:

1) Receiver thermal and mechanical design
2) Corrosion testing
3) Insulating materials testing
4) Salt properties verification
5) High head salt pump
6) Tower design

The following paragraphs contain brief work statements and recommendations for each task.

1) Receiver Thermal and Mechanical Design

Design studies should be performed to determine the feasibility of reducing receiver size and weight, and associated material and fabrication cost, without performance penalty. This work would include:

a) Re-assessment of thermal design criteria to determine if peak heat flux limitations can be increased, thus reducing total heat absorption surface requirements.

b) Examination of innovative approaches to design of panel restraints to permit greater flexibility and relieve thermal stresses.

The thermal design criteria are linked to the creep/fatigue properties of the tube material. The limited amount of creep/fatigue data available for candidate materials indicates that additional testing would reduce the uncertainties associated with receiver tube stress analysis.

2) Corrosion Tests

The general corrosion characteristics of candidate receiver materials in molten nitrate salt should be investigated. The work would consist of short-term electro-chemical tests performed in the laboratory. It is intended for critical comparison with currently available data which exhibit wide scatter, and to supplement longer-term data to be derived from the Olin loop at the CRTF site.

The test matrix is shown in Table 7-3. Both isothermal and cyclic thermal corrosion rates will be measured.

TABLE 7.3 CORROSION TEST MATRIX

	Isothermal				
Temperature (^{o}F)	1050	1075	1100	1125	1150
Type 410 SS	X	X	X	X	X
Incoloy 800H	X	X	X	X	X
Alternate					

	Cyclic Thermal		
		$Temp_1$ (^{o}F)	$Temp_2$ (^{o}F)
Type 410 SS		550	1050
I 800 H		550	1050

The limiting use temperature and design corrosion allowance for the candidate materials will be determined. Available data indicates that Incoloy 800H undergoes a rapid increase in corrosion rate in the range of current design temperatures (approximately 1100^{o}F). Since remedies which involve reducing the receiver outlet temperature could introduce significant penalties associated with loss of cycle efficiency and in thermal storage inventory, it is desirable to verify or refine the existing data and to take a closer look at other materials.

3) Insulating Material Testing

Both laboratory and field testing of insulating materials is required to determine the long term performance of commercially available products. Previous work has identified the failure threshold for various materials and now there is the need to complement this information with long term data that includes the effects of weathering and thermal cycling.

There are three basic applications which expose the insulation to solar flux.

1) spillage protection
2) cavity lining
3) panel shine-through protection

The geometry and flux level is different for each application and each may require a different material. In the first two applications, the flux levels would likely be low (less than 80,000 Btu/hr-ft^{2}) although large areas would be illuminated. For use as shine-through protection the insulation would be exposed to the

maximum flux levels but only in very narrow (approximately .50 inch) strips. The flux distribution on the test specimens should duplicate the distribution expected on the actual receiver.

4) Salt Properties Verification

Variations in the transport properties of molten nitrate salt exist in the literature. In particular, there is wide scatter in the reported values of specific heat. The salt mass flow rate and heat transfer coefficient are sensitive to the specific heat and the salt side coefficient is generally the dominant resistance to heat transfer. Therefore, accurate knowledge of this property is imperative to minimizing heat transfer surface in both the receiver and steam generator subsystems. Additionally, the salt flow rate affects the size of thermal energy storage tanks.

Because of the importance of specific heat, a literature study should be made to evaluate the existing data. Following this, a laboratory testing program should be enacted to (1) establish the specific heat of molten nitrate salt over the operating range of 500F to 1100F and (2) assess the chemical stability of the composition when cycled between these temperatures.

5) High Head Salt Pump

There is a need to develop and demonstrate a high head molten salt pump that is compatible with the requirements of the full scale receiver subsystem. The major issues to be resolved are:

1) whether or not the pump shaft bearings can operate in a salt environment, and
2) what design and materials should be used in the pump seals.

Three pump configurations are under consideration:

--vertical turbine

--vertical cantilever

--horizontal split case

The vertical turbine pump has the potential disadvantage of having a set of pump shaft bearings in contact with the molten salt. Pump manufacturers are making conflicting claims for bearing life in this environment. The vertical cantilever pump is not capable of high head so a series of pumps would be required to develop the required head. Horizontal split case pumps offer simple mounting and reliable bearings but the pump seals are in contact with the molten salt which raises reliability questions.

Based on the lack of supporting data for the various configurations, it would be prudent to conduct lifetime testing on pump seals and bearings in a molten salt environment.

6) Tower Design

There are two aspects of tower design which warrant additional analytical studies. These are:

--reduction in seismic amplification factors

--integration of tower top and receiver support structure

The realization of these improvements could substantially reduce the amount of structural steel in the receiver with a corresponding reduction in the costs of material, fabrication, and erection.

Successful completion of the work proposed in these six areas will reduce the risk and uncertainty in predicting receiver subsystem performance and make solar thermal systems more economically competitive with other forms of energy.

8.0 CONCEPTUAL STUDIES

At the start of the contract, the receiver design was essentially that reported in conceptual design studies of solar repowering for the Saguaro Plant (Ref. 8). As reported, the receiver base design was the four cavity arrangement with single wing walls heated from two sides.

The major argument for adoption of the single wing walls was the advantages of two sided heating which offers minimum receiver cost and weight. In comparison with panels which are heated on one side only, two sided heating results in greatly reduced heat transfer surface area requirements. With smaller surface area, the single wing wall arrangement offers great potential for reduced weight and cost over other arrangements.

To support the single wing wall arrangements against wind and seismic loads, a series of horizontal buckstay supports were designed to provide support at several elevations. The buckstays were arranged on both sides of the wing wall and supported at the ends by structural steel. Due to the intensity of the incoming heat flux, the exposed surfaces of the buckstays were protected by tubes attached to the surfaces and carrying cold salt to maintain the buckstays at the required temperature. Details of the layout of the cavity, the panel arrangement, and the panel supports, as proposed prior to the contract are shown in Figures 8.1 and 8.2.

During the initial phase of the contract work, it was recognized that the implementation of exposed buckstays introduced complexities into the design arrangement with corresponding potential design weaknesses. Two approaches were tried. The first was to design an adequate buckstay arrangement and the second was to attempt to eliminate all exposed, integral-cooled supports.

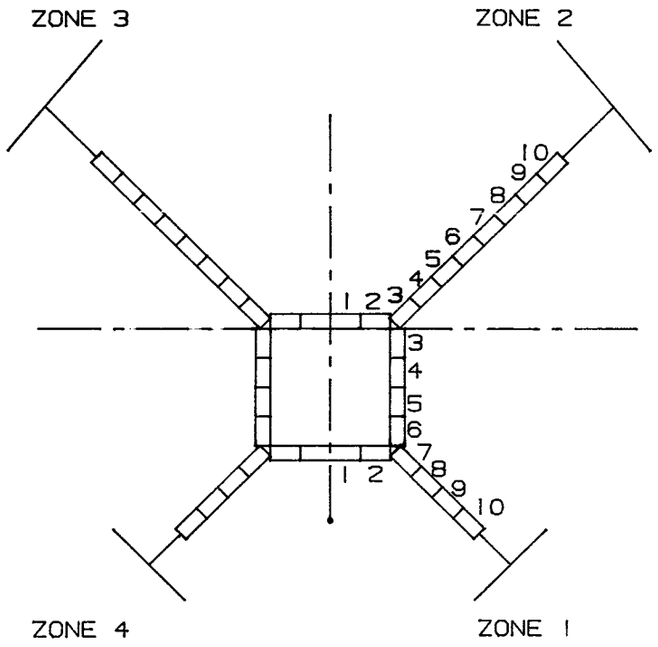

PANEL LAYOUT

PANEL SUPPORT BEAM

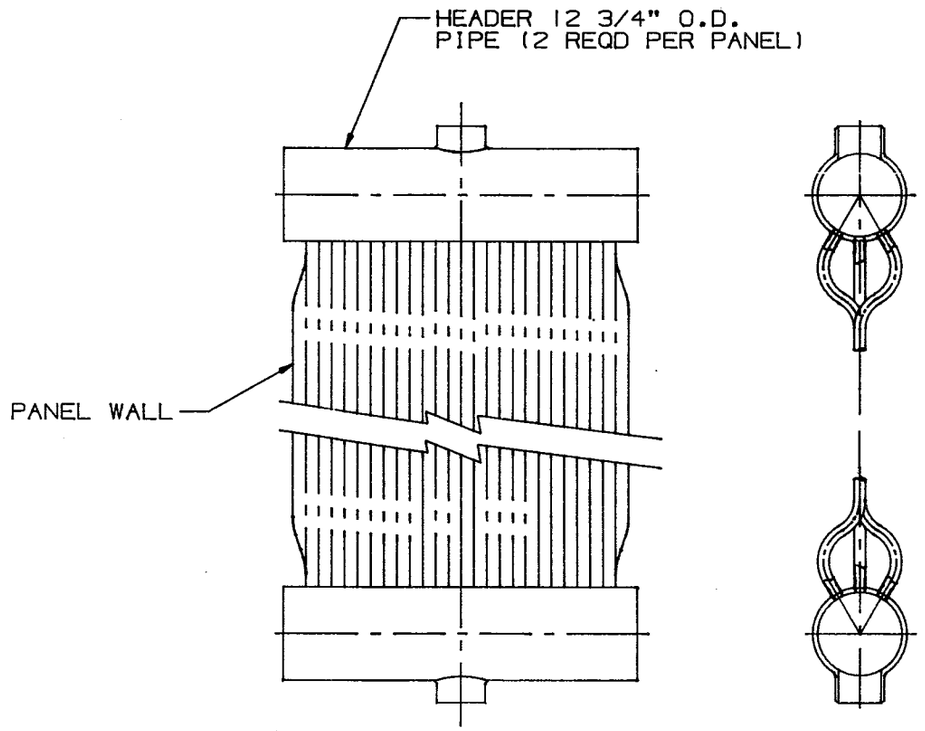

HEAT ABSORPTION PANEL

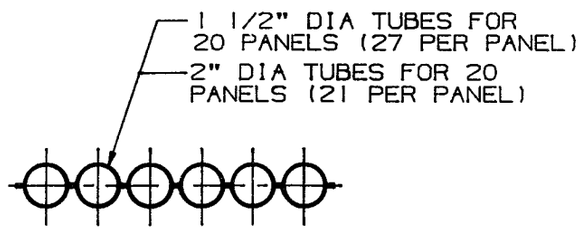

MEMBRANE WALL

Figure 8.1 Panel Wall and Cavity Arrangement

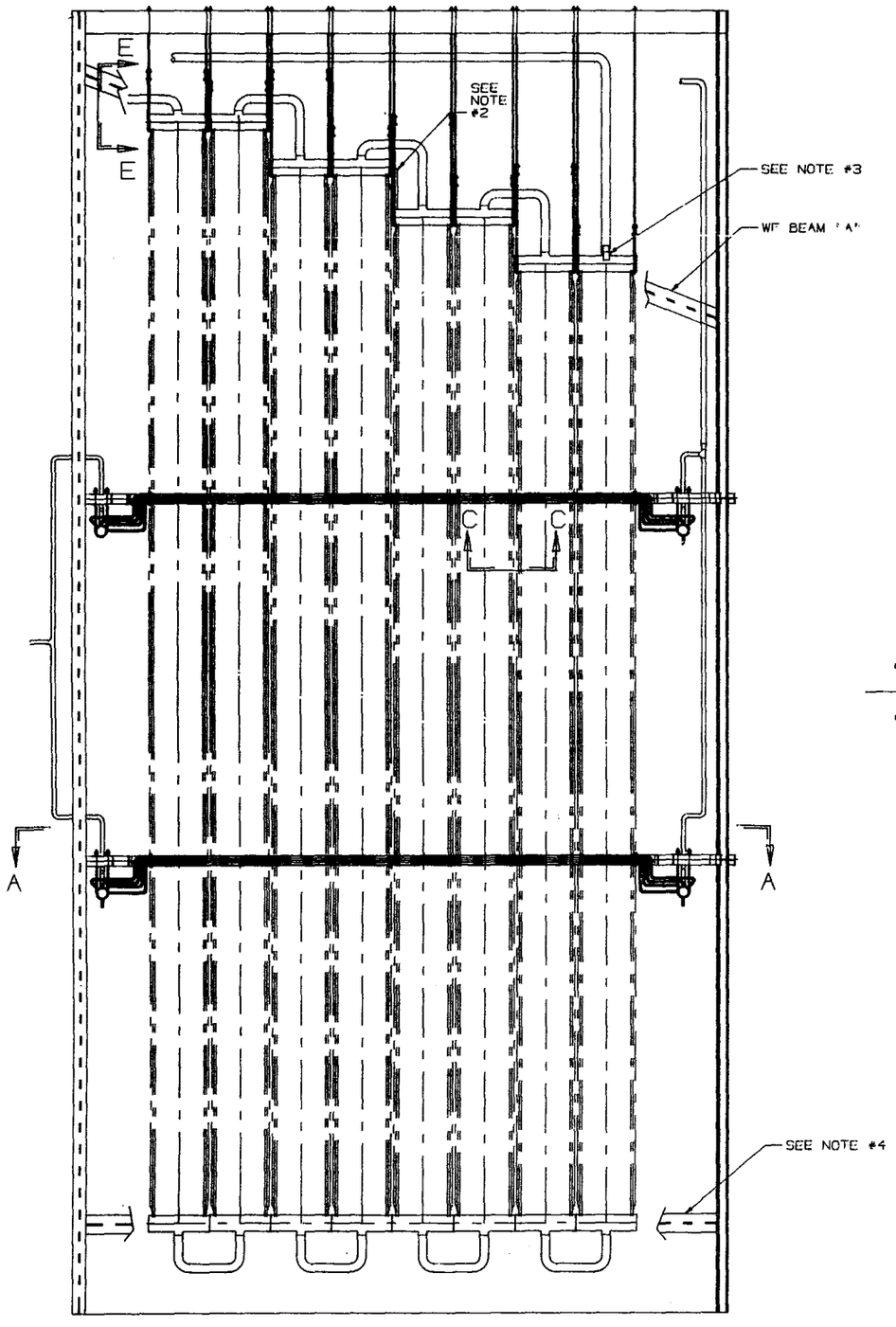

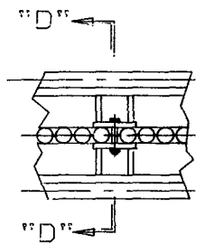

SECTION C-C

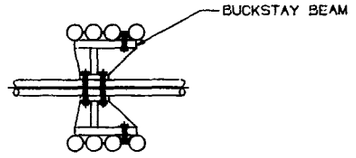

VIEW "D"

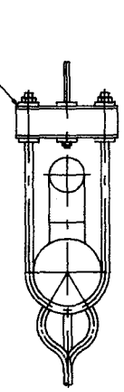

VIEW E-E

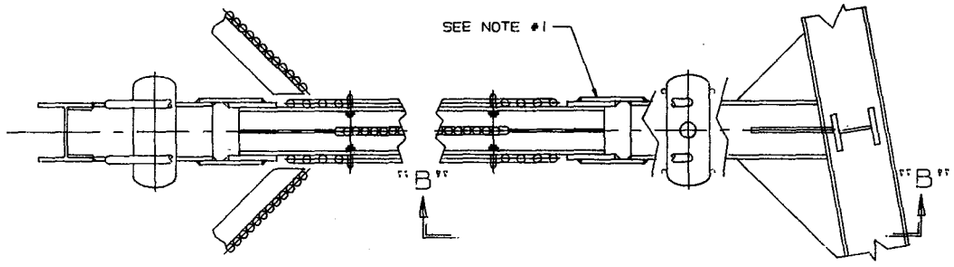

SECTION A-A

NOTES

1. ALTERNATIVE END TIE WOULD BE USING A PAIR OF VERTICAL ROLLERS WITH EXTERNAL TRACKS.
2. LOCATION OF IN-PLANE SEISMIC TIE TO STRUCTURAL BEAMS 'A' AT CENTER HEADERS ONLY.
3. LOCATION OF OUT-OF PLANE SEISMIC AND WIND TIES FROM EACH HEADER NOZZLE TO BEAMS 'A'.
4. LOWER HEADERS ARE BETWEEN A PAIR OF BRACED BEAMS TO TAKE OUT-OF PLANE SEISMIC AND WIND LOADS FROM ABSORPTION PANELS.

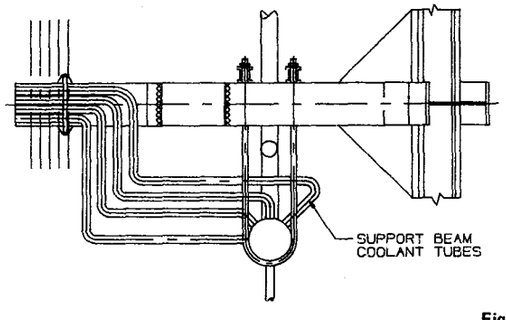

VIEW "B"

THE BABCOCK & WILCOX COMPANY		
DWN BY P HUBER	SOLAR RECEIVER	
CHKD BY	TYPICAL HEAT ABSORPTION PANEL ARRANGEMENT AND SUPPORTS	
PASSED BY		
APPVD BY		
EC7-7013		DWG NO 203290 E REV
	SCALE	

Figure 8.2 Typical Heat Absorption Panel Arrangement and Supports

During detailed evaluation of the first approach, i.e., the buckstay arrangement, it became apparent that the complex supports introduced design problems that were not readily amenable to analysis. Because the buckstays spanned the entire wing wall, crossing many panels, the determination of the variations in metal temperature along the length of the buckstay was extremely difficult. Also, an examination of wind and seismic loadings showed the need for additional support for the horizontal buckstay and was accommodated by re-designing with vertically oriented buckstays. The addition of the vertical buckstays then added to the complexities of the original design. After evaluation of several variations of the buckstay support arrangement the concept of supported wing walls was dropped from further consideration. The major reasons were:

1) Indeterminate nature of the temperature variations along the length of the buckstays leading to design uncertainties.
2) The interaction between the panel and the buckstay to provide restraint yet allow differential expansion of the parts gave rise to complex designs with many small parts.
3) The complex buckstay arrangement required extensive extra cooling circuits which incurred extra capital costs and would also make panel replacement extremely difficult.

Efforts were then concentrated on the second approach, i.e., to try to remove all exposed supports from the panels. Analysis showed that with supports at the top and bottom headers only, the panels could withstand reasonable levels of wind and seismic loadings, the major problem with the unsupported panel arrangement was the excessive bowing of the panels due to temperature differentials from one face of the panel to the other and due to wind loads. During operation, the large deformation of the panels would incur

thermal losses due to "blow through" and "shine through" at the gaps between the panels. In addition, the unsupported panels had a very low natural frequency, and it was believed they would be unacceptable to flow induced vibration problems under the action of winds. The unsupported panel arrangement was then dropped from further consideration.

Following the evaluation of the single wing wall designs, it was concluded that while the single wall offered large potential cost and weight reductions, the design problems were such as to incur a high risk in the design. All design efforts on the single wing wall were then discontinued and all further efforts were then concentrated on the double wing wall approach.

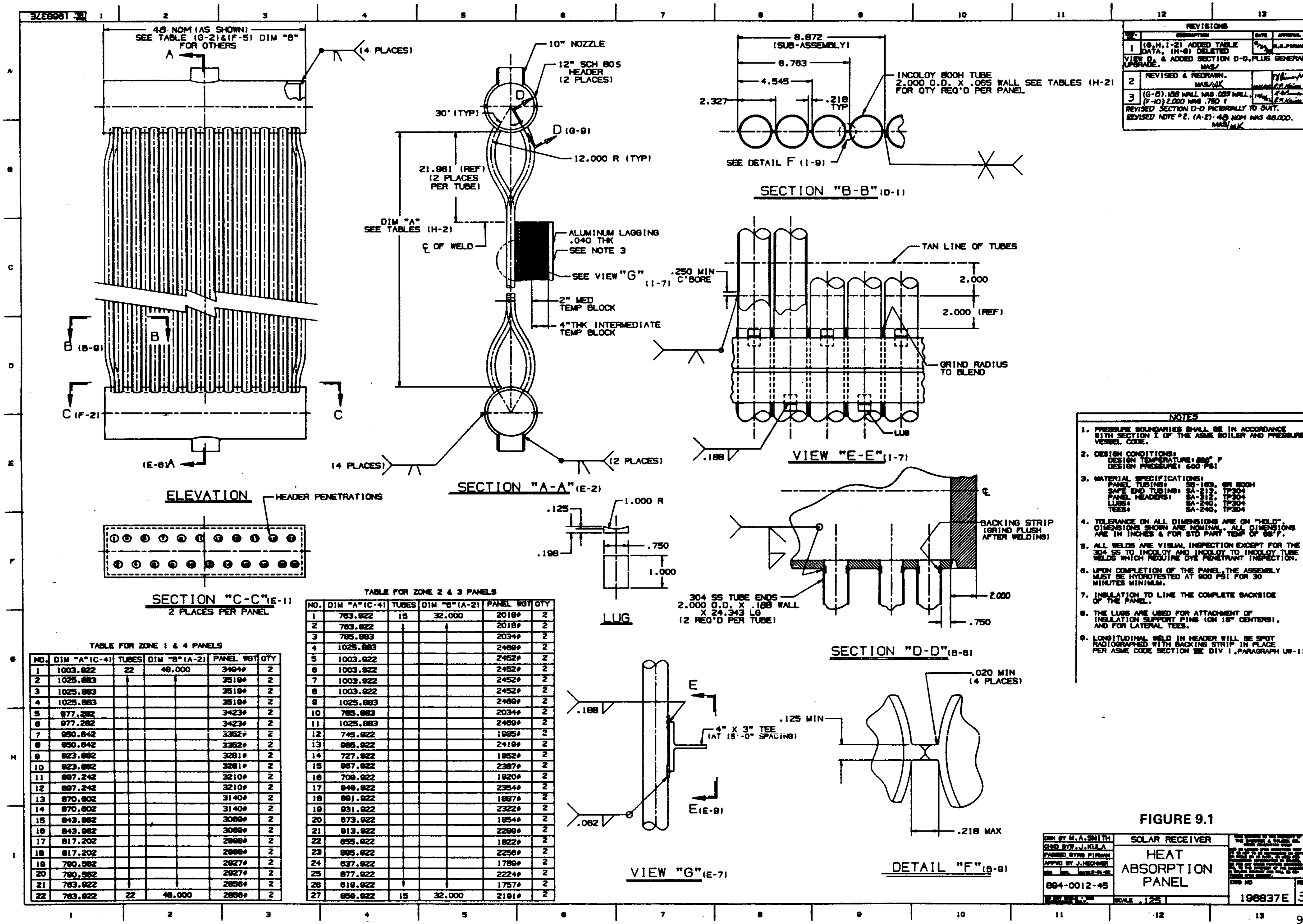

TABLE FOR ZONE 1 & 4 PANELS

NO.	DIM "A" (C-4)	TUBES	DIM "B" (A-2)	PANEL WGT	QTY
1	1003.922	22	48.000	3404#	2
2	1025.883			3519#	2
3	1025.883			3519#	2
4	1025.883			3519#	2
5	977.282			3423#	2
6	977.282			3423#	2
7	950.642			3352#	2
8	950.642			3352#	2
9	923.882			3281#	2
10	923.882			3281#	2
11	897.242			3210#	2
12	897.242			3210#	2
13	870.602			3140#	2
14	870.602			3140#	2
15	843.962			3069#	2
16	843.962			3069#	2
17	817.202			2998#	2
18	817.202			2998#	2
19	790.562			2927#	2
20	790.562			2927#	2
21	763.922			2856#	2
22	763.922	22	48.000	2856#	2

TABLE FOR ZONE 2 & 3 PANELS

NO.	DIM "A" (C-4)	TUBES	DIM "B" (A-2)	PANEL WGT	QTY
1	763.922	15	32.000	2018#	2
2	763.922			2018#	2
3	785.883			2034#	2
4	1025.883			2469#	2
5	1003.922			2452#	2
6	1003.922			2452#	2
7	1003.922			2452#	2
8	1003.922			2452#	2
9	1025.883			2469#	2
10	785.883			2034#	2
11	1025.883			2469#	2
12	745.922			1985#	2
13	985.922			2419#	2
14	727.922			1952#	2
15	967.922			2387#	2
16	709.922			1920#	2
17	949.922			2354#	2
18	691.922			1887#	2
19	931.922			2322#	2
20	673.922			1854#	2
21	913.922			2289#	2
22	655.922			1822#	2
23	895.922			2256#	2
24	637.922			1789#	2
25	877.922			2224#	2
26	619.922			1757#	2
27	859.922	15	32.000	2191#	2

NOTES

1. PRESSURE BOUNDARIES SHALL BE IN ACCORDANCE WITH SECTION I OF THE ASME BOILER AND PRESSURE VESSEL CODE.
2. DESIGN CONDITIONS:
   DESIGN TEMPERATURE: 880° F
   DESIGN PRESSURE: 600 PSI
3. MATERIAL SPECIFICATIONS:
   PANEL TUBING: SB-163, GR 800H
   SAFE END TUBING: SA-213, TP304
   PANEL HEADERS: SA-312, TP304
   LUGS: SA-240, TP304
   TEES: SA-240, TP304
4. TOLERANCE ON ALL DIMENSIONS ARE ON "HOLD". DIMENSIONS SHOWN ARE NOMINAL. ALL DIMENSIONS ARE IN INCHES & FOR STD PART TEMP OF 68°F.
5. ALL WELDS ARE VISUAL INSPECTION EXCEPT FOR THE 304 SS TO INCOLOY AND INCOLOY TO INCOLOY TUBE WELDS WHICH REQUIRE DYE PENETRANT INSPECTION.
6. UPON COMPLETION OF THE PANEL, THE ASSEMBLY MUST BE HYDROTESTED AT 900 PSI FOR 30 MINUTES MINIMUM.
7. INSULATION TO LINE THE COMPLETE BACKSIDE OF THE PANEL.
8. THE LUGS ARE USED FOR ATTACHMENT OF INSULATION SUPPORT PINS (ON 18" CENTERS), AND FOR LATERAL TEES.
9. LONGITUDINAL WELD IN HEADER WILL BE SPOT RADIOGRAPHED WITH BACKING STRIP IN PLACE PER ASME CODE SECTION VIII DIV I, PARAGRAPH UW-11.

FIGURE 9.1

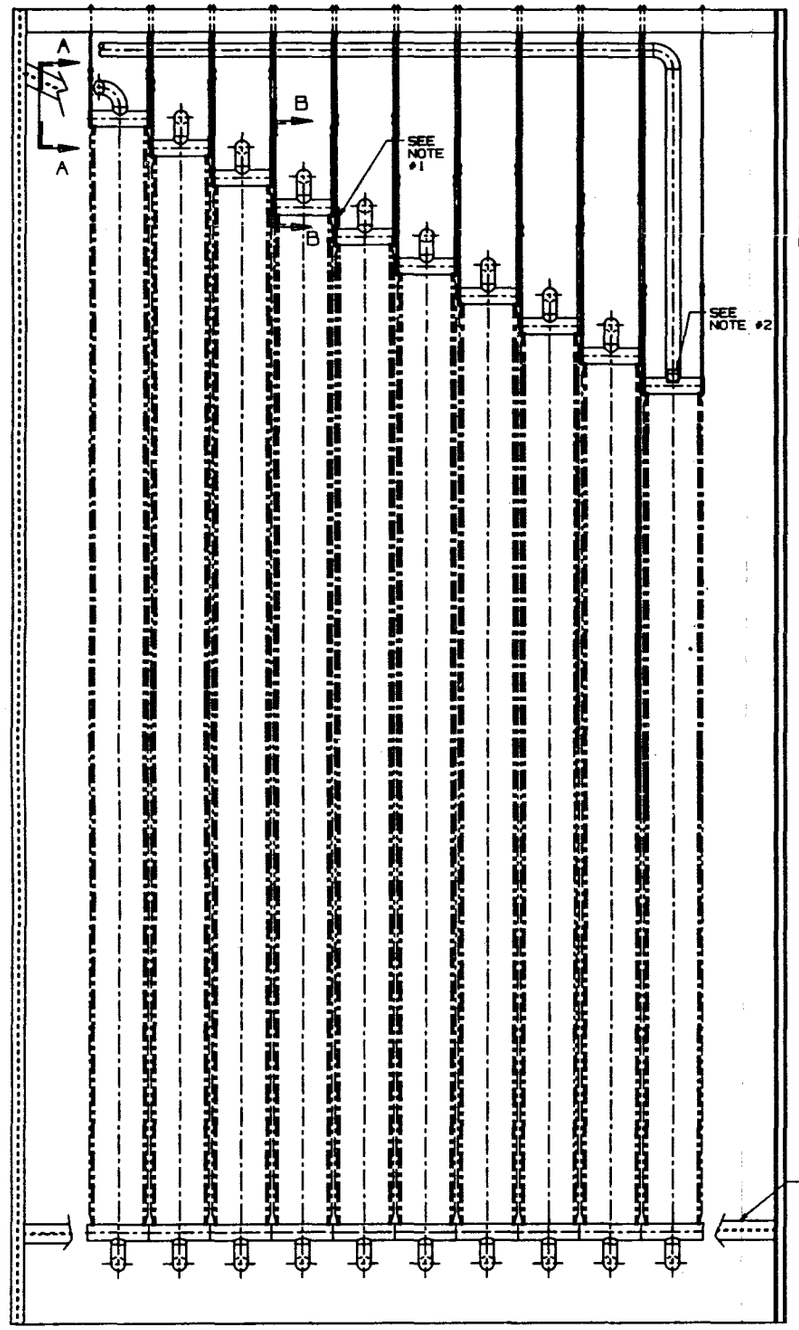

TYPICAL WING WALL
(ONE SIDE)

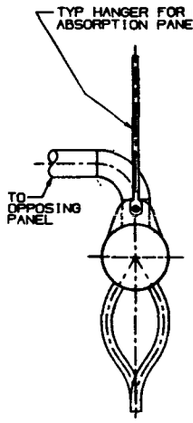

SECTION "B-B"

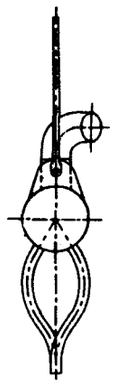

SECTION "A-A"

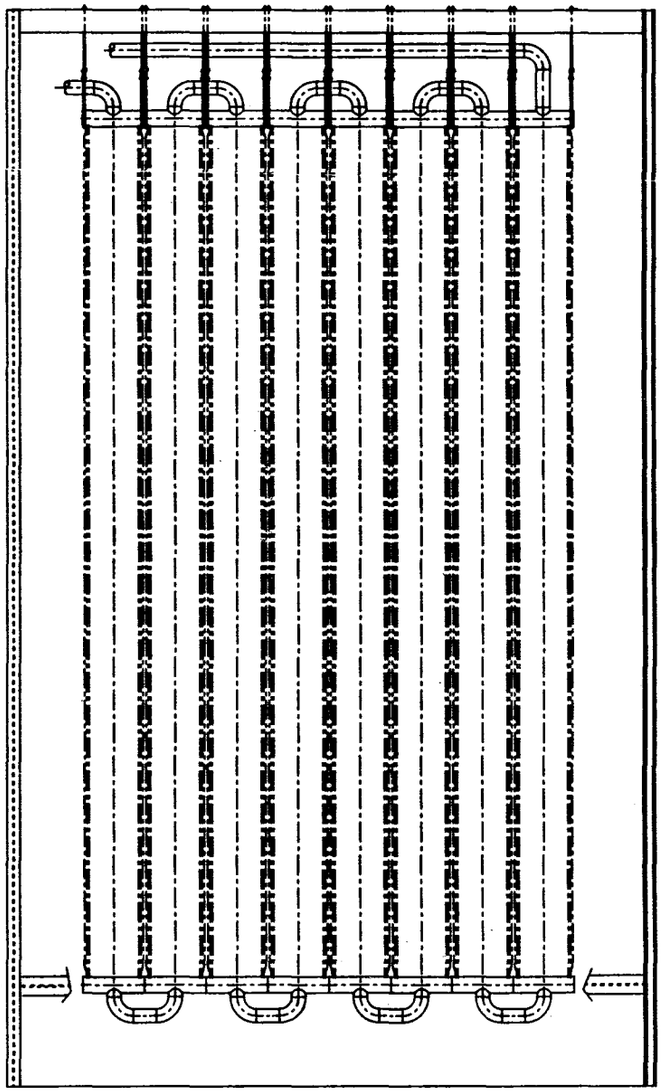

TYPICAL BACK WALL

REVISIONS			
NO.	DESCRIPTION	DATE	APPROVAL
1	REVISED & REDRAWN. MAS/MK	7/6/81	
2	PICTORIALLY REVISED SECTION A-A & SECTION B-B. MAS/MK		

NOTES

1. LOCATION OF IN-PLANE SEISMIC TIE TO STRUCTURAL BEAMS "A" AT CENTER HEADERS ONLY.
2. LOCATION OF OUT-OF-PLANE SEISMIC AND WIND TIES FROM EACH HEADER NOZZLE TO BEAMS "A".
3. LOWER HEADERS ARE BETWEEN A PAIR OF BRACED BEAMS TO TAKE OUT-OF-PLANE SEISMIC AND WIND LOADS FROM ABSORPTION PANELS.

FIGURE 9.2

THE BABCOCK & WILCOX COMPANY

DRN BY M.A. REBISH	SOLAR RECEIVER	
CHKD BY R.J. KULA	TYPICAL HEAT ABSORPTION PANEL ARRANGEMENT AND SUPPORTS	
APPVD BY J. MECHLER 3-6-82		
894-0012-45	SCALE 1/42	238877 E 2

REVISIONS			
REV. NO.	DESCRIPTION	DATE	APPROVAL
1	REVISED & REDRAWN. MAS/MK		
2	REVISED SIZE & ARRANGEMENT OF RISER & DOWNCOMER PIPING. (8-8) ADDED CHECK VALVE. (8-9) ADDED "REDUNDANT". ADDED (8) FLOW CONTROL ISOLATION VALVES TO CIRCULATION LINES. (8-7) DELETED CHECK VALVE. (8-11) ADDED COMPRESSOR. RW/MK		

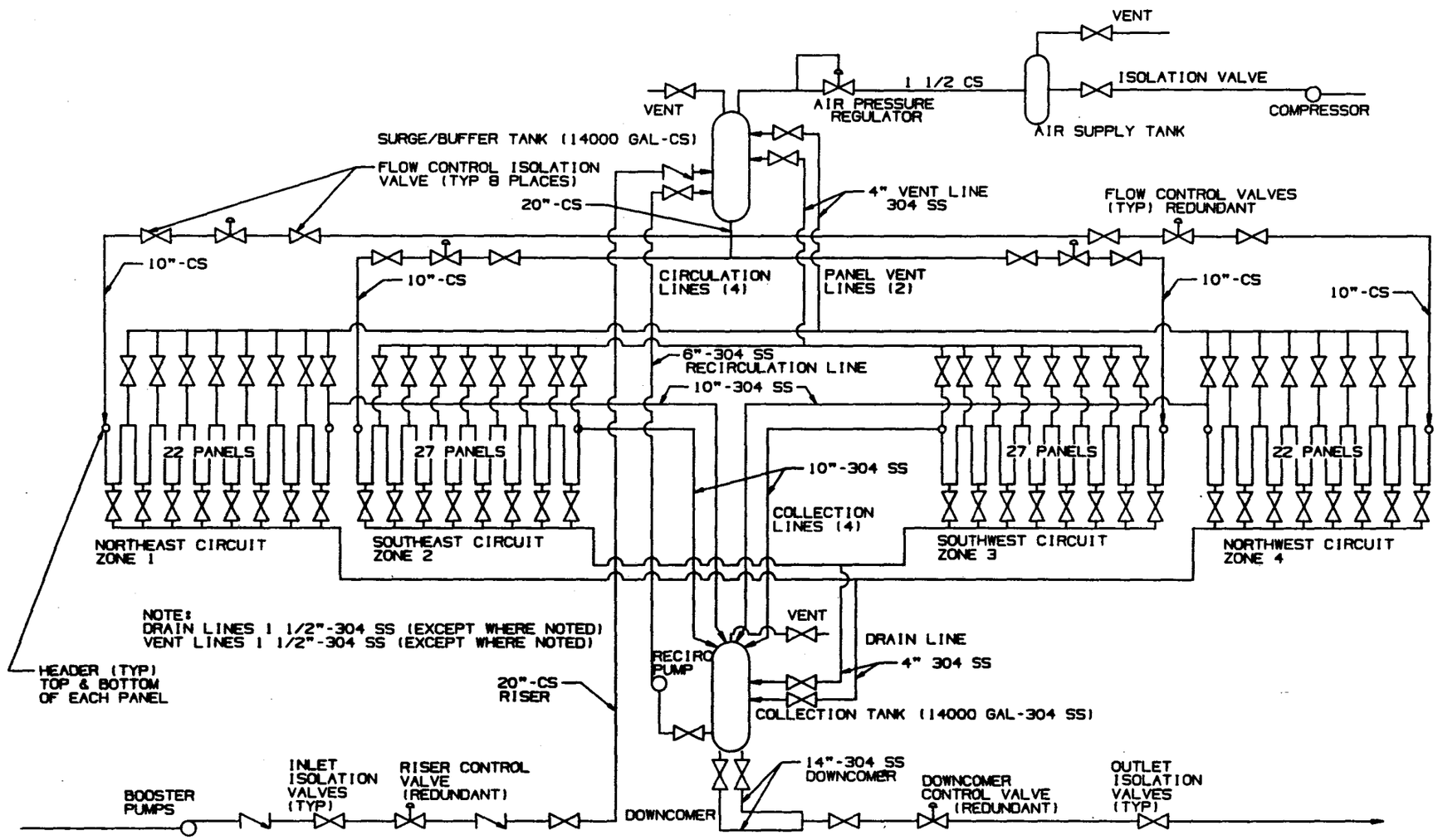

FIGURE 9.3

THE BABCOCK & WILCOX COMPANY

SOLAR RECEIVER

PIPING SCHEMATIC

894-0012-45

SCALE 1/8

238878E REV 2

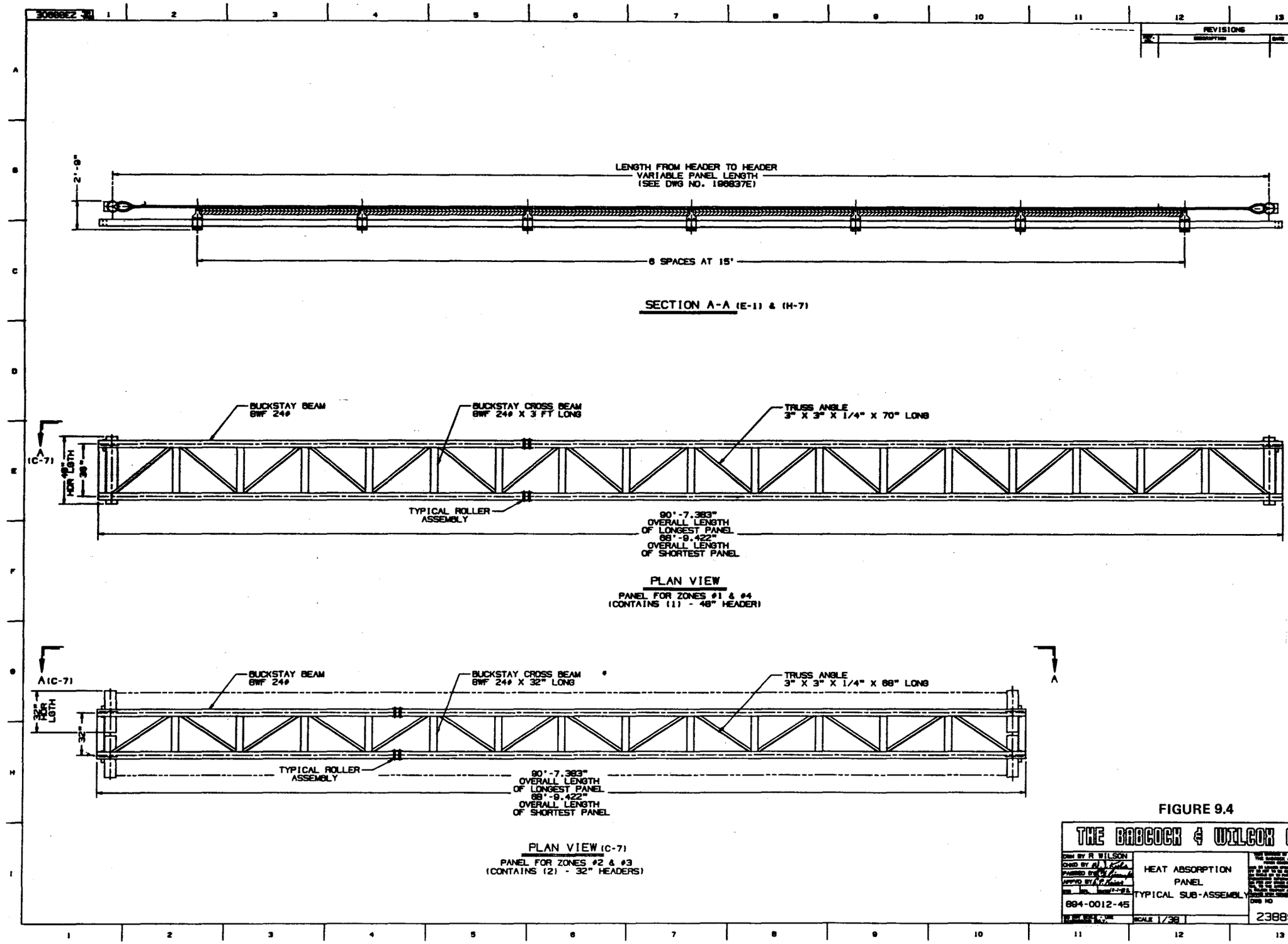
REVISIONS
LENGTH FROM HEADER TO HEADER
VARIABLE PANEL LENGTH
(SEE DWG NO. 198837E)
2'-6"
6 SPACES AT 15°
SECTION A-A (E-1) & (H-7)
BUCKSTAY BEAM
8WF 24#
BUCKSTAY CROSS BEAM
8WF 24# X 3 FT LONG
TRUSS ANGLE
3" X 3" X 1/4" X 70" LONG
A
(C-7)
HDR LGTH
36"
TYPICAL ROLLER
ASSEMBLY
90'-7.383"
OVERALL LENGTH
OF LONGEST PANEL
88'-9.422"
OVERALL LENGTH
OF SHORTEST PANEL
PLAN VIEW
PANEL FOR ZONES #1 & #4
(CONTAINS (1) - 48" HEADER)
A(C-7)
BUCKSTAY BEAM
8WF 24#
BUCKSTAY CROSS BEAM
8WF 24# X 32" LONG
TRUSS ANGLE
3" X 3" X 1/4" X 68" LONG
HDR LGTH
32"
TYPICAL ROLLER
ASSEMBLY
90'-7.383"
OVERALL LENGTH
OF LONGEST PANEL
88'-9.422"
OVERALL LENGTH
OF SHORTEST PANEL
PLAN VIEW (C-7)
PANEL FOR ZONES #2 & #3
(CONTAINS (2) - 32" HEADERS)
THE BABCOCK & WILCOX CO.
DRN BY R WILSON
CHKD BY
APPRD BY
884-0012-45
HEAT ABSORPTION
PANEL
TYPICAL SUB-ASSEMBLY
SCALE 1/38
DRG NO
238890E
REV
0

FIGURE 9.4

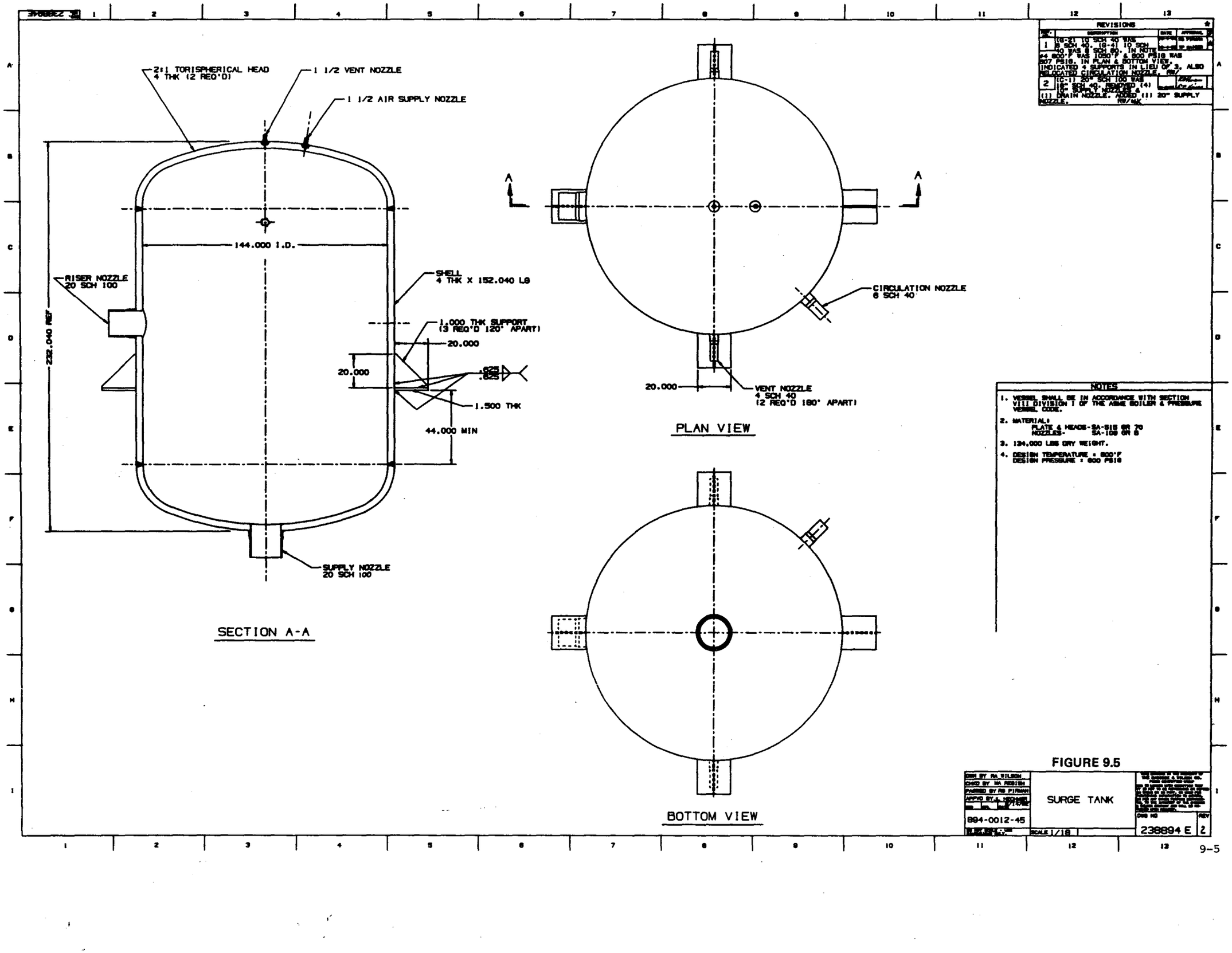
2:1 TORISPHERICAL HEAD
4 THK (2 REQ'D)
1 1/2 VENT NOZZLE
1 1/2 AIR SUPPLY NOZZLE
144.000 I.D.
232.040 REF
RISER NOZZLE
20 SCH 100
SHELL
4 THK X 152.040 LG
1.000 THK SUPPORT
(3 REQ'D 120° APART)
20.000
20.000
.625
.625
1.500 THK
44.000 MIN
SUPPLY NOZZLE
20 SCH 100
SECTION A-A
A
A
CIRCULATION NOZZLE
6 SCH 40
20.000
VENT NOZZLE
4 SCH 40
(2 REQ'D 180° APART)
PLAN VIEW
BOTTOM VIEW
REVISIONS
NOTES
1. VESSEL SHALL BE IN ACCORDANCE WITH SECTION VIII DIVISION 1 OF THE ASME BOILER & PRESSURE VESSEL CODE.
2. MATERIAL:
PLATE & HEADS- SA-515 GR 70
NOZZLES- SA-106 GR B
3. 134,000 LBS DRY WEIGHT.
4. DESIGN TEMPERATURE = 600°F
DESIGN PRESSURE = 600 PSIG
SURGE TANK
894-0012-45
238894 E
2
SCALE 1/18

FIGURE 9.5

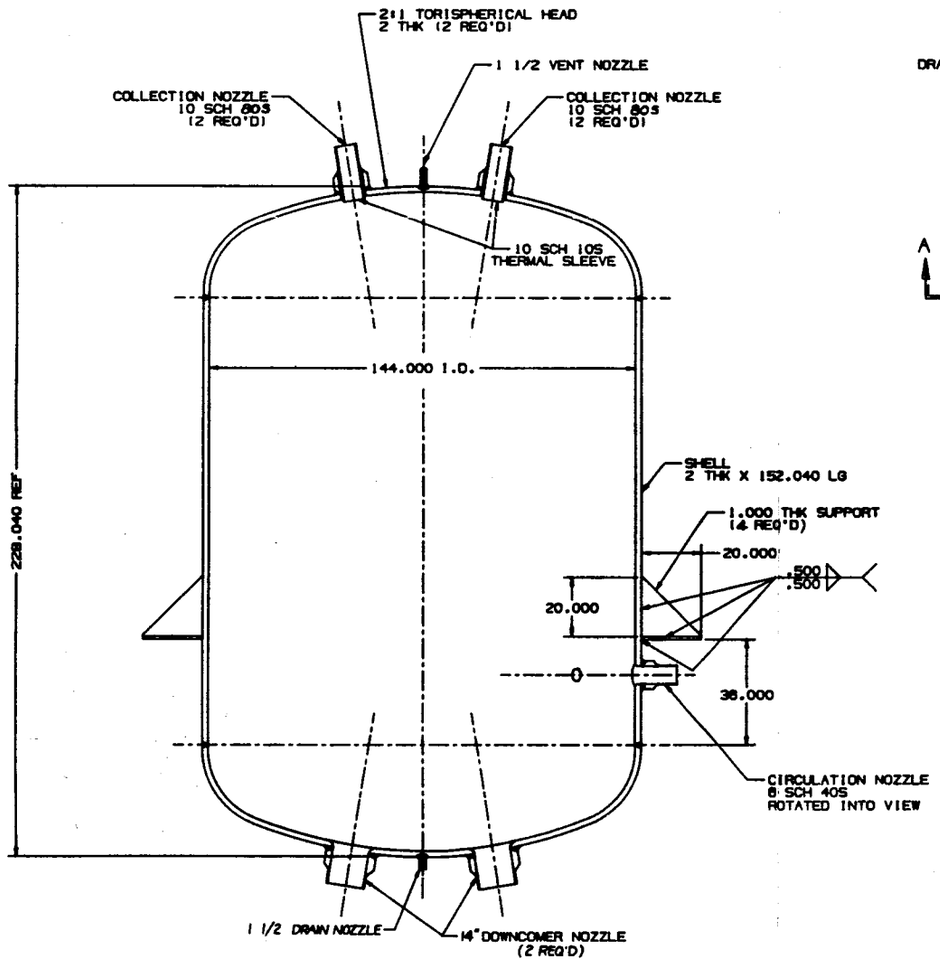

SECTION A-A

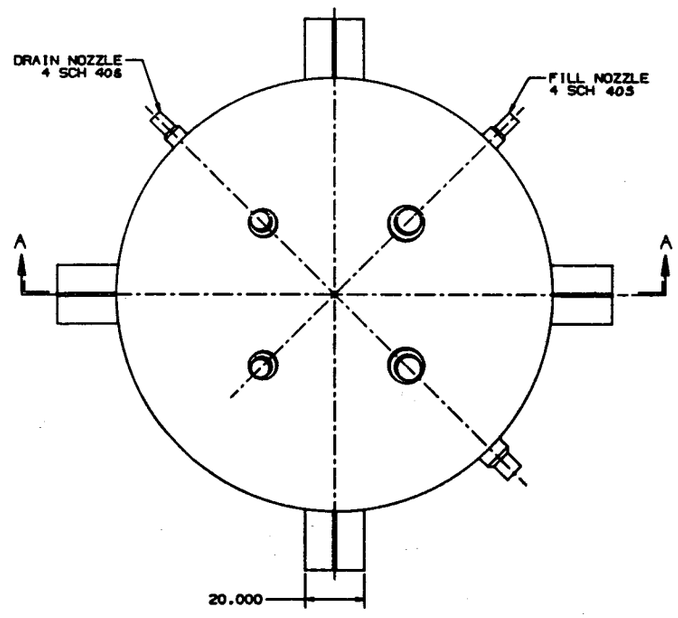

PLAN VIEW

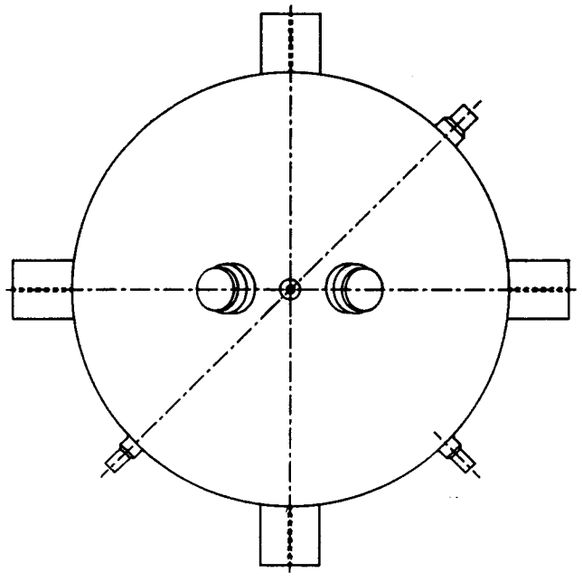

BOTTOM VIEW

REVISIONS			
REV. NO.	DESCRIPTION	DATE	APPROVAL
1	(A-2) 10 SCH 80S WAS 8 SCH 10S. (A-3) 10 SCH 80S WAS 8 SCH 10S. (B-3 & 4) ADDED THERMAL SLEEVES. IN NOTE #4 1050°F WAS 900°F. IN PLAN & BOTTOM VIEW, INDICATED 4 SUPPORTS IN LIEU OF 3, ALSO RELOCATED NOZZLES. RW/MK	7/9/91	
2	(G-3\4) 14" DOWNCOMER NOZZLE (2 REQ'D) WAS DOWNCOMER NOZZLE 12 SCH 10S, ADDED 1 1/2 DRAIN NOZZLE, REVISED SECTION A-A & BOTTOM VIEW PICTORIALLY TO SUIT. MAS/MK	7/10/92	

NOTES

1. VESSEL SHALL BE IN ACCORDANCE WITH SECTION VIII DIVISION 1 OF THE ASME BOILER & PRESSURE VESSEL CODE.
2. MATERIAL:
   PLATE & HEADS - SA-240 TP 304
   NOZZLES - SA-312 TUBE
3. 67,000 LBS DRY WEIGHT.
4. DESIGN TEMPERATURE = 1050°F
   DESIGN PRESSURE = 90 PSIG

DRN BY RA WILSON
CHKD BY MA REDISH
PWRKD BY RB FITMAN
APPVD BY LJ HECHNER 7/10/92

894-0012-45

COLLECTION TANK

SCALE 1/18

DWG NO 238895E REV 2

FIGURE 9.6

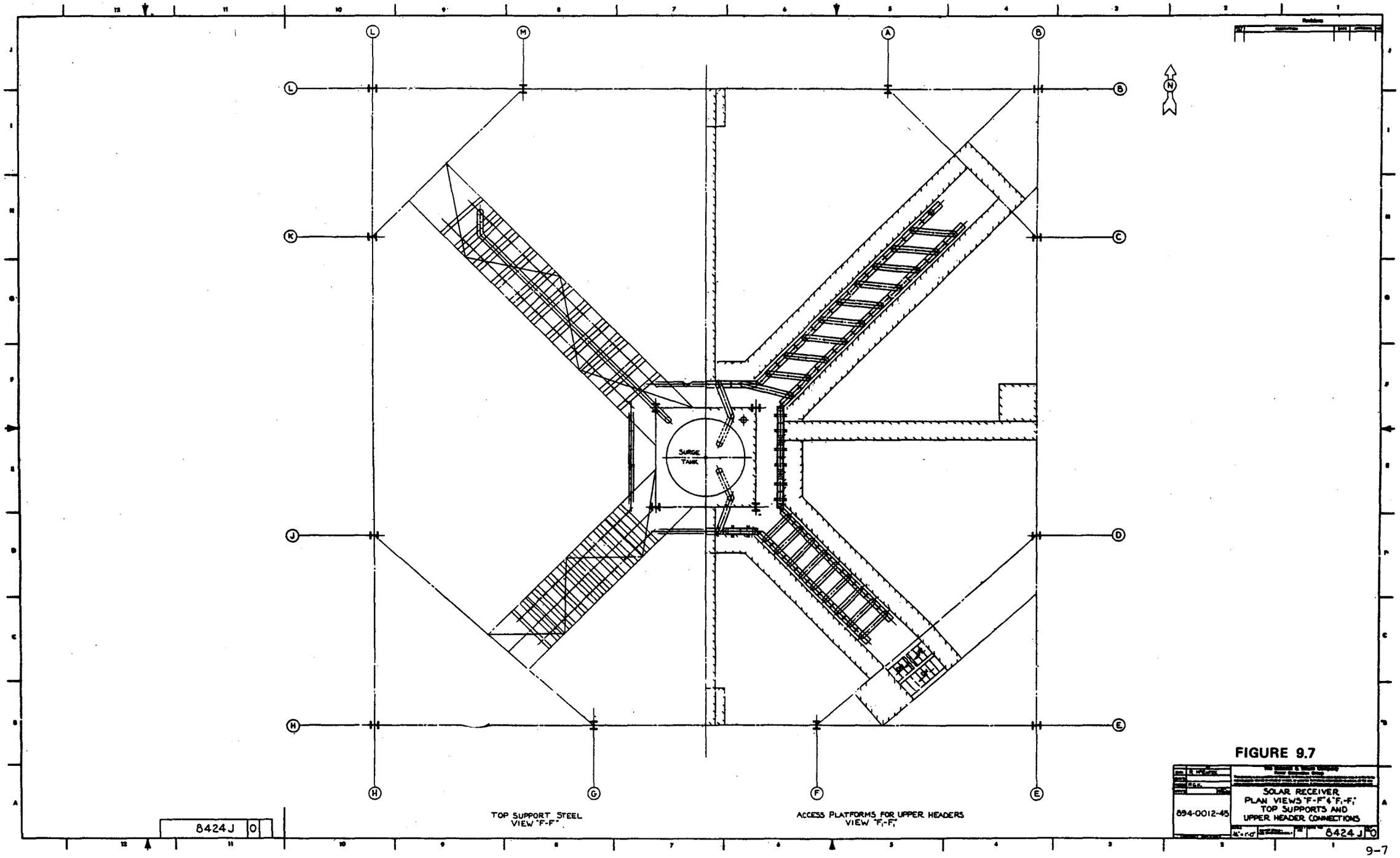
L
M
A
B
K
C
J
D
H
G
F
E
N
SURGE TANK
TOP SUPPORT STEEL
VIEW "F-F"
ACCESS PLATFORMS FOR UPPER HEADERS
VIEW "F1-F1"
8424J 0
SOLAR RECEIVER
PLAN VIEWS "F-F" & "F1-F1"
TOP SUPPORTS AND
UPPER HEADER CONNECTIONS
894-0012-45
8424J 0

FIGURE 9.7

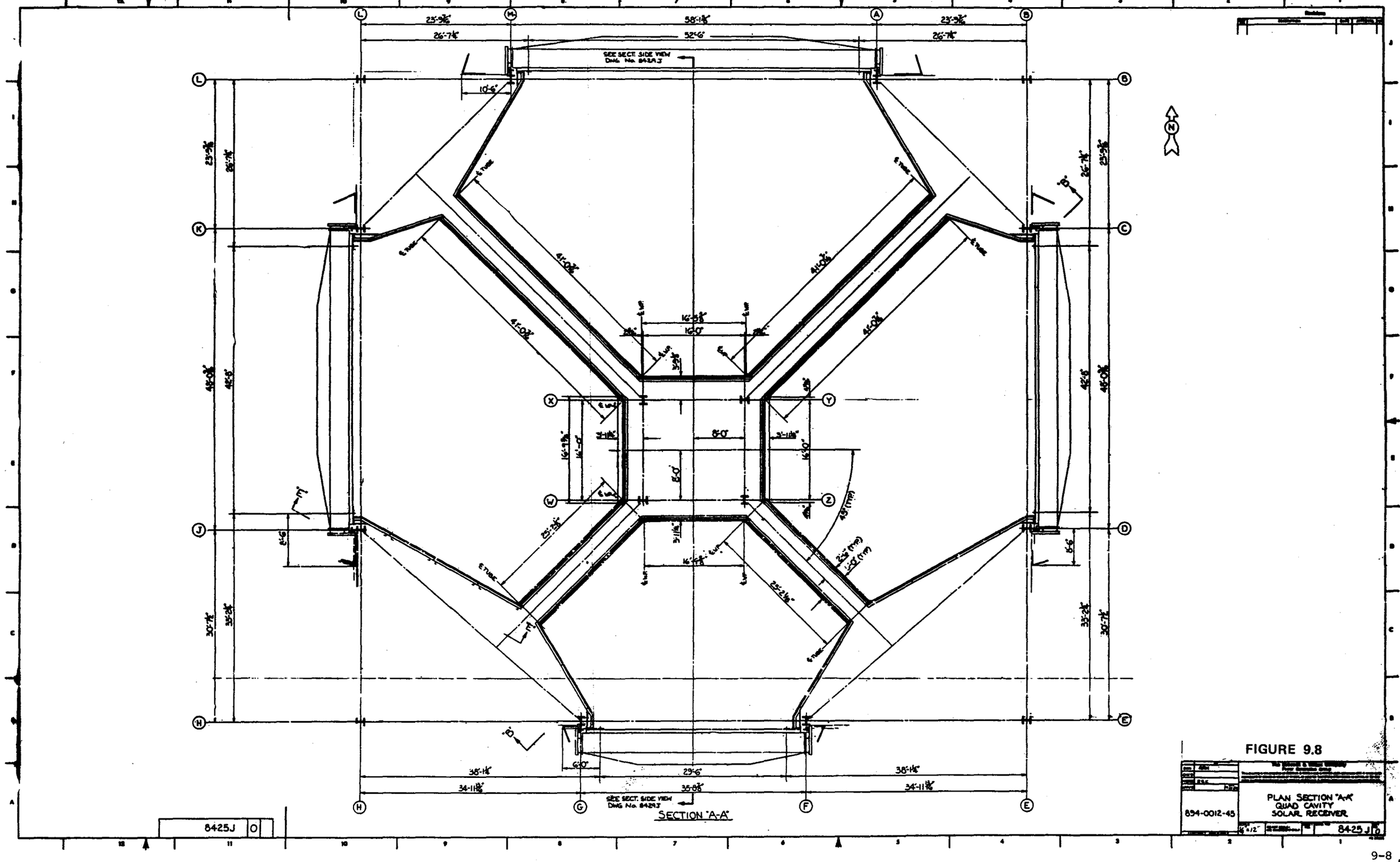

FIGURE 9.8

894-0012-45

PLAN SECTION "A-A"
QUAD CAVITY
SOLAR RECEIVER

8425 J

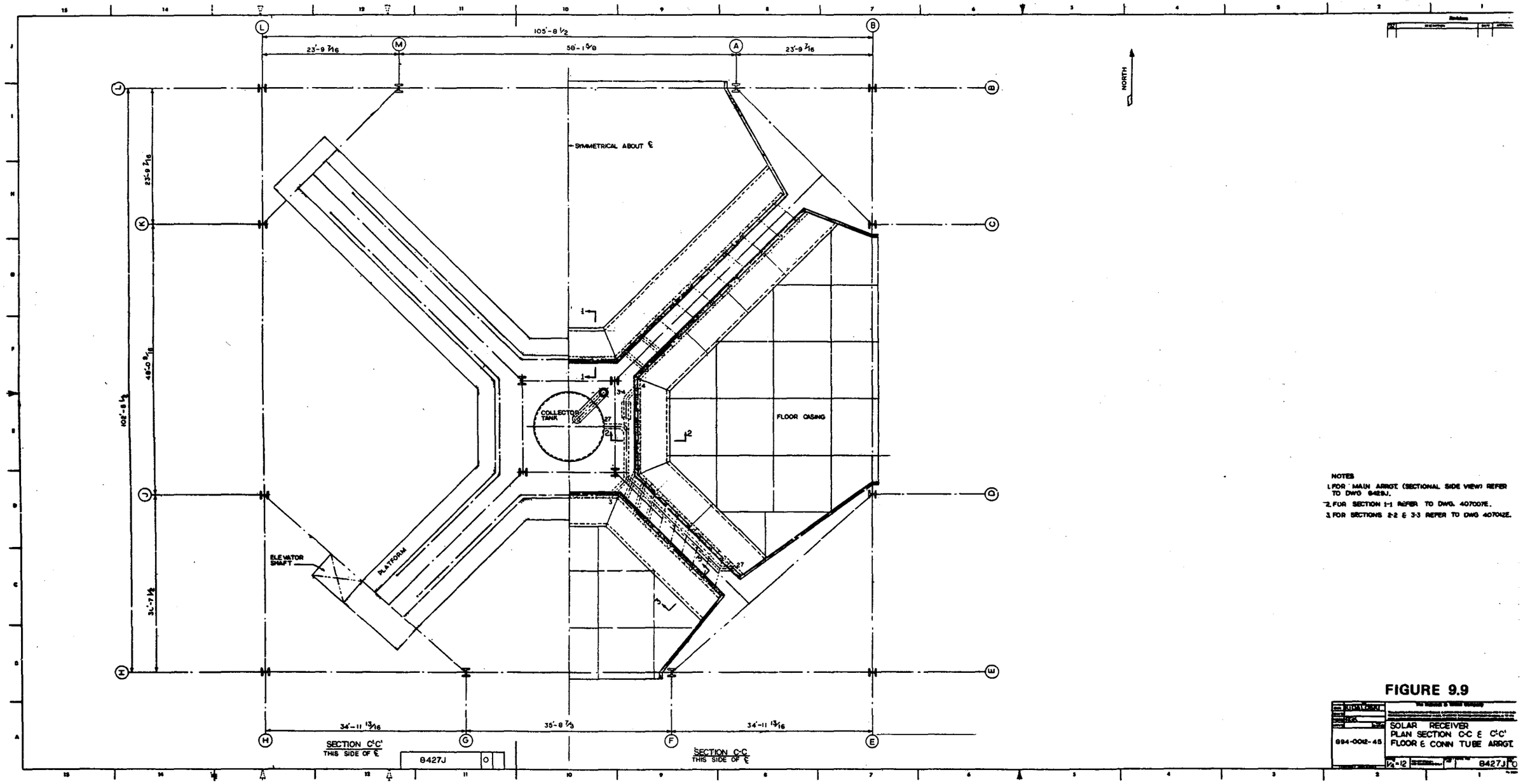

NOTES

1. FOR MAIN ARRGT. (SECTIONAL SIDE VIEW) REFER TO DWG 8429J.
2. FOR SECTION 1-1 REFER TO DWG. 407007E.
3. FOR SECTIONS 2-2 & 3-3 REFER TO DWG 407042E.

FIGURE 9.9

	SOLAR RECEIVER
	PLAN SECTION C-C & C'C'
884-0012-45	FLOOR & CONN TUBE ARRGT.
1/4-12	8427J

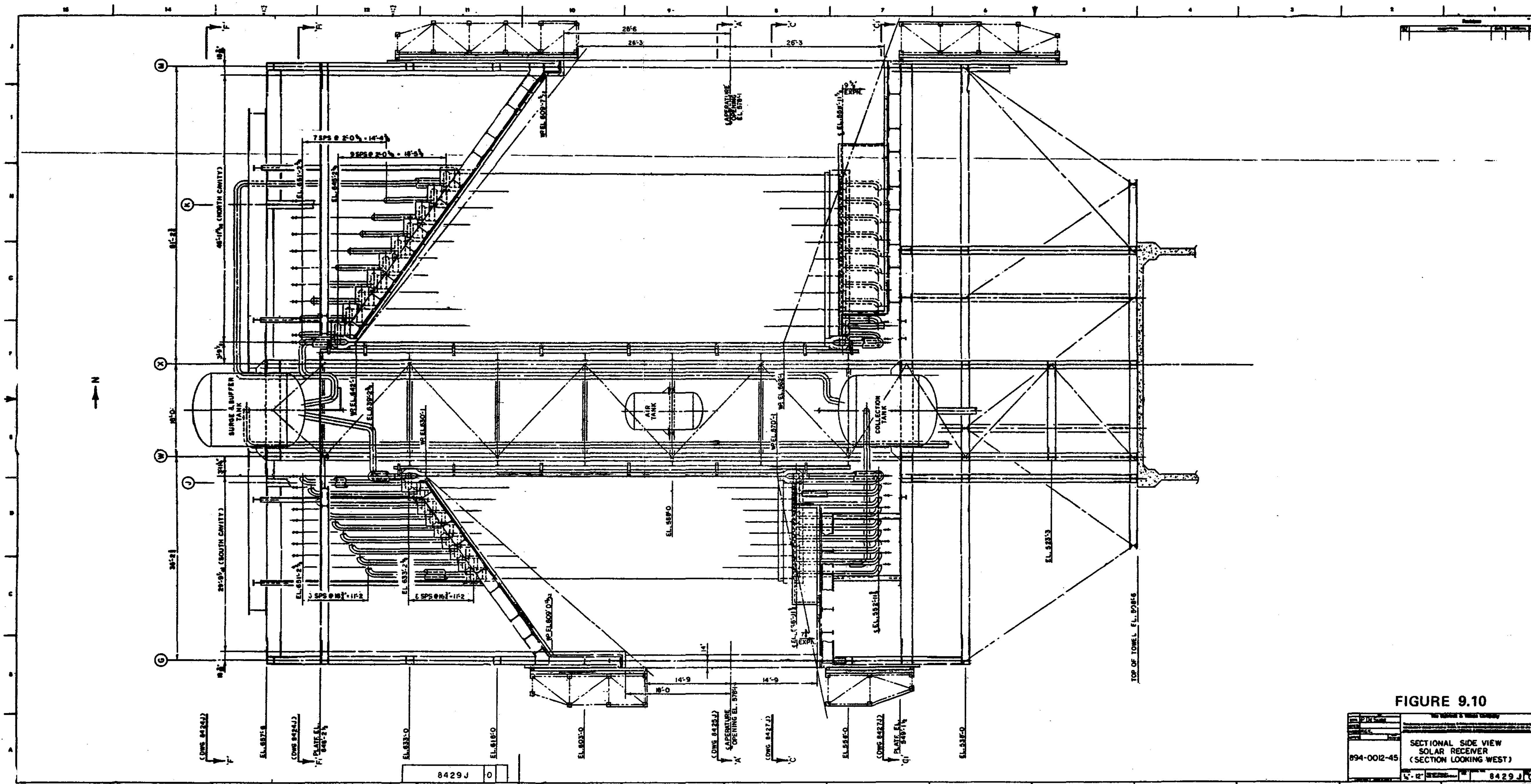

28'-6
26'-3
26'-3
(NORTH CAVITY)
(SOUTH CAVITY)
N
SURGE & BUFFER TANK
AIR TANK
COLLECTION TANK
EXPN.
14'-9
14'-9
18'-0
(DWG 8424J)
EL. 657'-6
(DWG 8424J)
EL. 633'-0
EL. 618'-0
EL. 603'-0
(DWG 8425J)
(DWG 8427J)
EL. 588'-0
EL. 558'-0
(DWG 8427J)
EL. 538'-0
8429J
SECTIONAL SIDE VIEW
SOLAR RECEIVER
(SECTION LOOKING WEST)
894-0012-45
8429 J

FIGURE 9.10

REVISIONS

SYMBOL	DESCRIPTION	DATE	APPROVAL

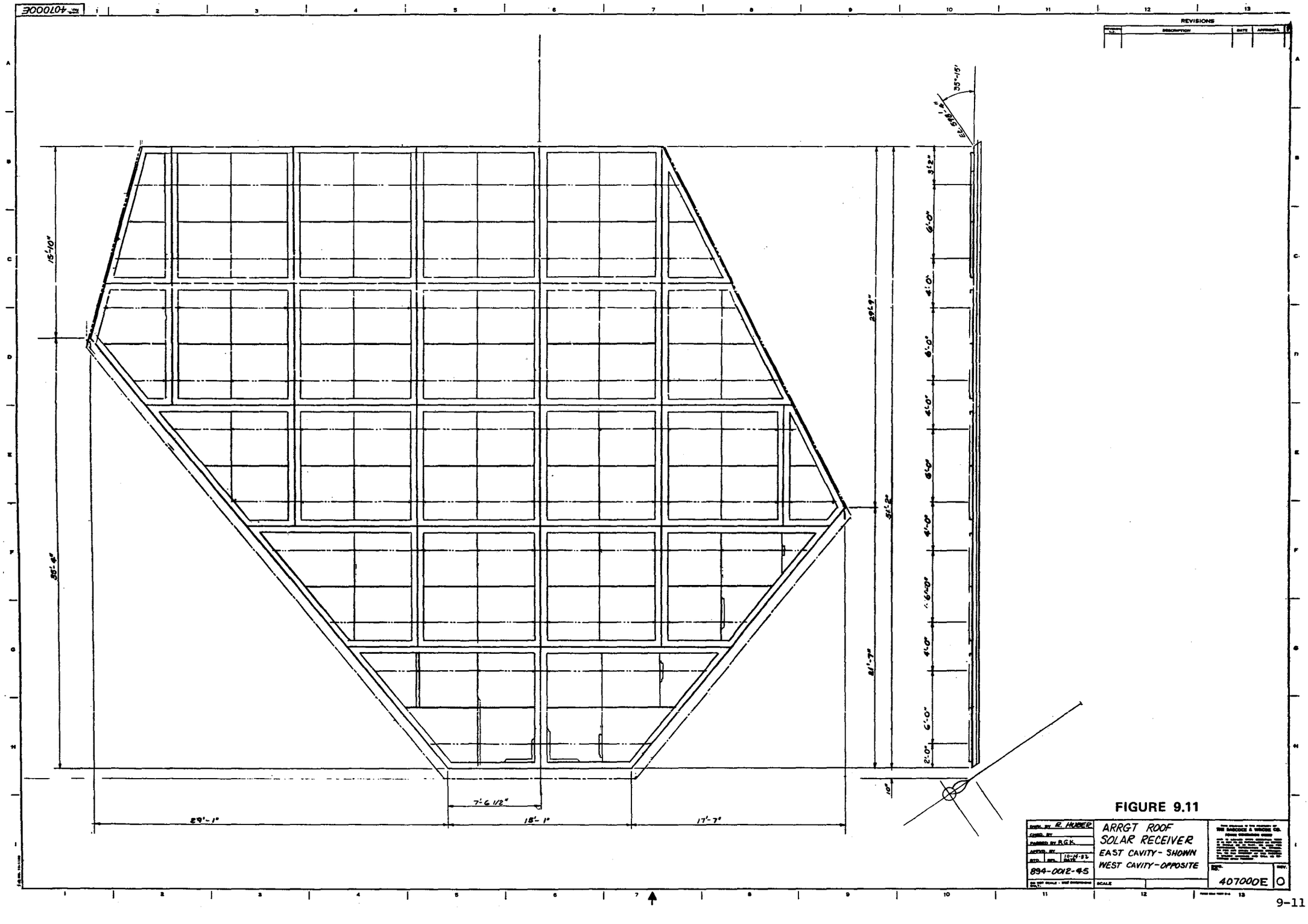

FIGURE 9.11

DRAWN BY R. HUBER	ARRGT ROOF SOLAR RECEIVER	
CHKD. BY	EAST CAVITY - SHOWN	
PASSED BY R.G.K.	WEST CAVITY - OPPOSITE	
APPVD. BY		
STD. DEV. DATE 10-14-93		
894-0012-45	SCALE	407000E O

REVISIONS

WEST APERTURE

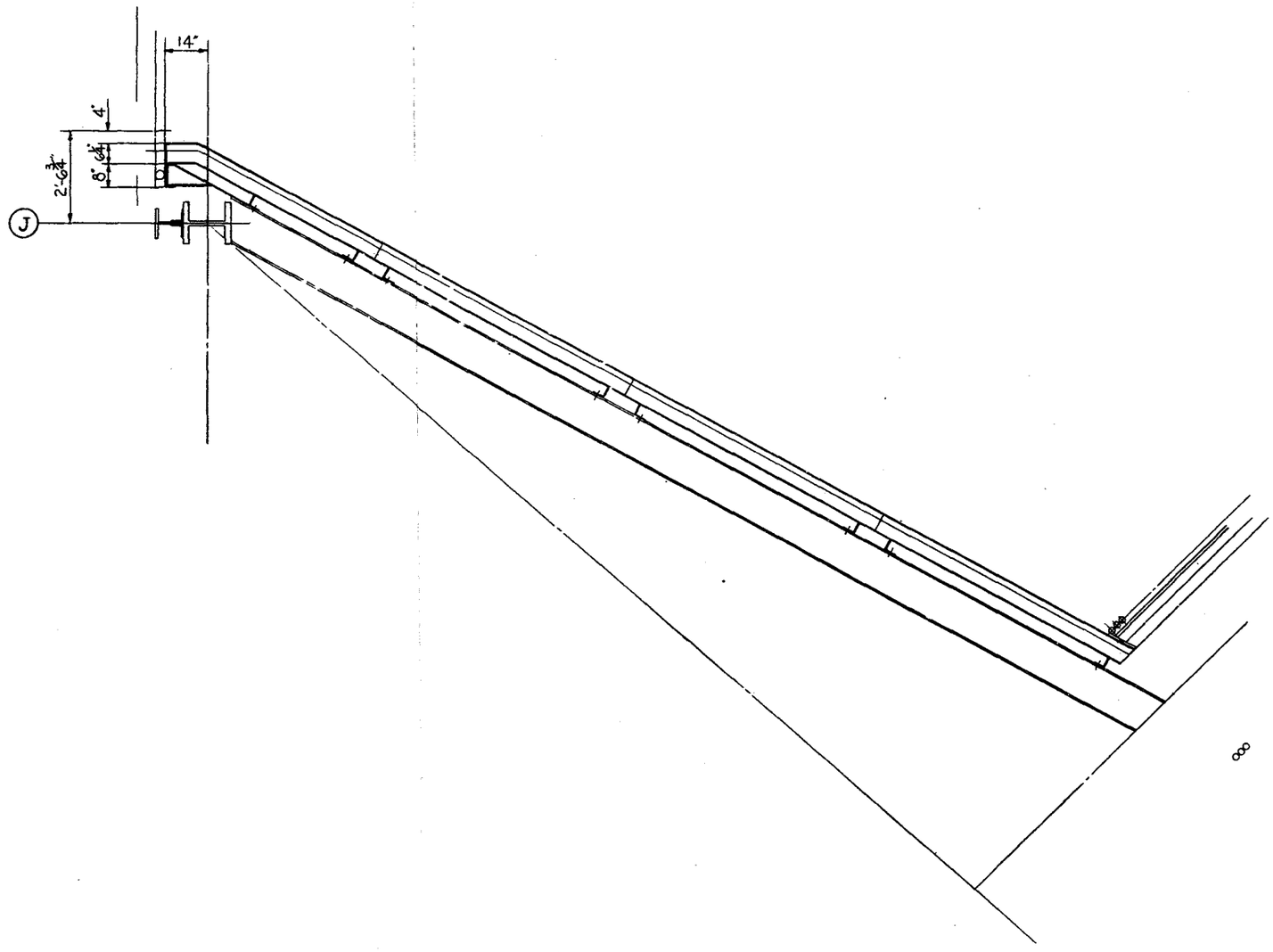

FIGURE 9.12

DWN. BY RRM	SECTION "D-D" ENLARGED PLAN VIEW CASING WALL SOUTH WEST	THE BABCOCK & WILCOX CO.
CHKD. BY		
PLANNED BY RG P.		
APPVD. BY		
SYS. APPL. DATE 10-16-92		
894-0012-45	SCALE	407003E REV. 0

REVISIONS

NO.	DESCRIPTION	DATE	APPROVAL

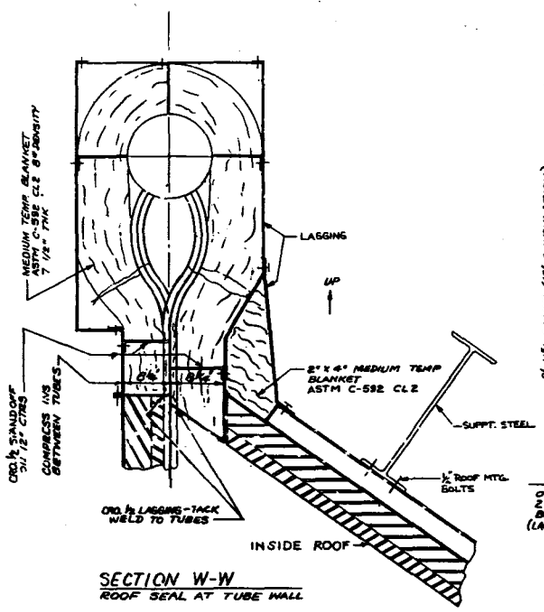

SECTION W-W
ROOF SEAL AT TUBE WALL

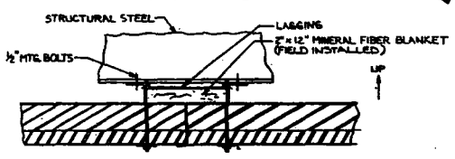

SECTION X-X
ROOF SEAL BETWEEN PANELS
1½" = 1'-0"

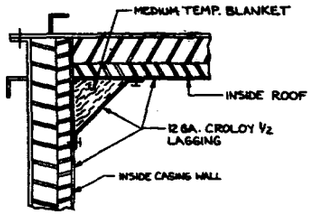

SECTION Y-Y
ROOF SEAL AT CASING WALL
1½" = 1'-0"

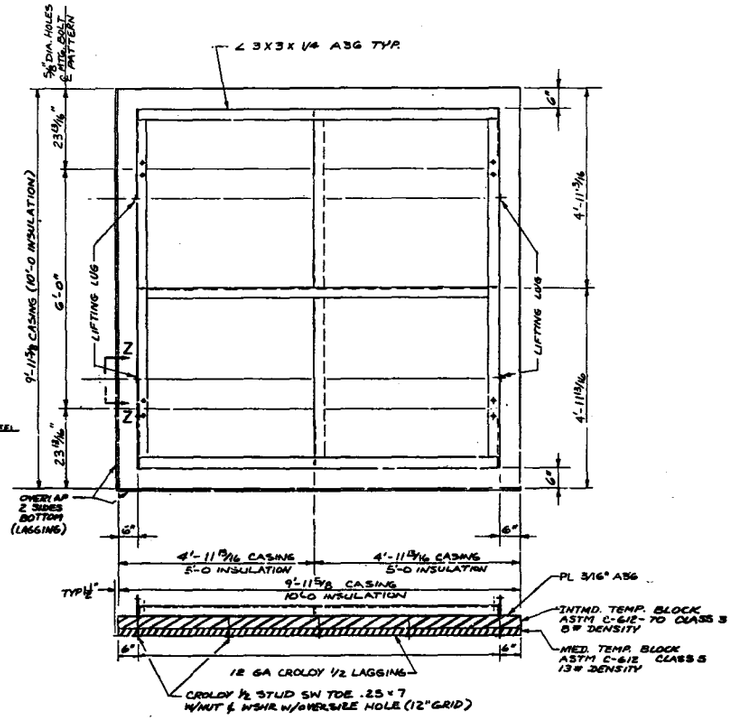

TYPICAL ROOF & CASING PANEL
3/8" = 1'-0"

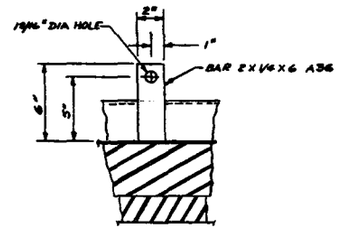

SECTION Z-Z
LIFTING LUG
1 1/2" = 1'-0"

NOTES
1. FOR MAIN ARRGT SEE DWG. 8425 J & 8426 J.

FIGURE 9.13

DWN. BY HUBER/LAMB	SECTIONS & VIEWS SOLAR RECEIVER	THE BABCOCK & WILCOX CO.
CHKD. BY		
PROJECT ENGR. K		
APPVD. BY		
STD. MFR. 10-8-82 DATE		
894-0012-45	SCALE AS	407005E REV. 0

REVISIONS

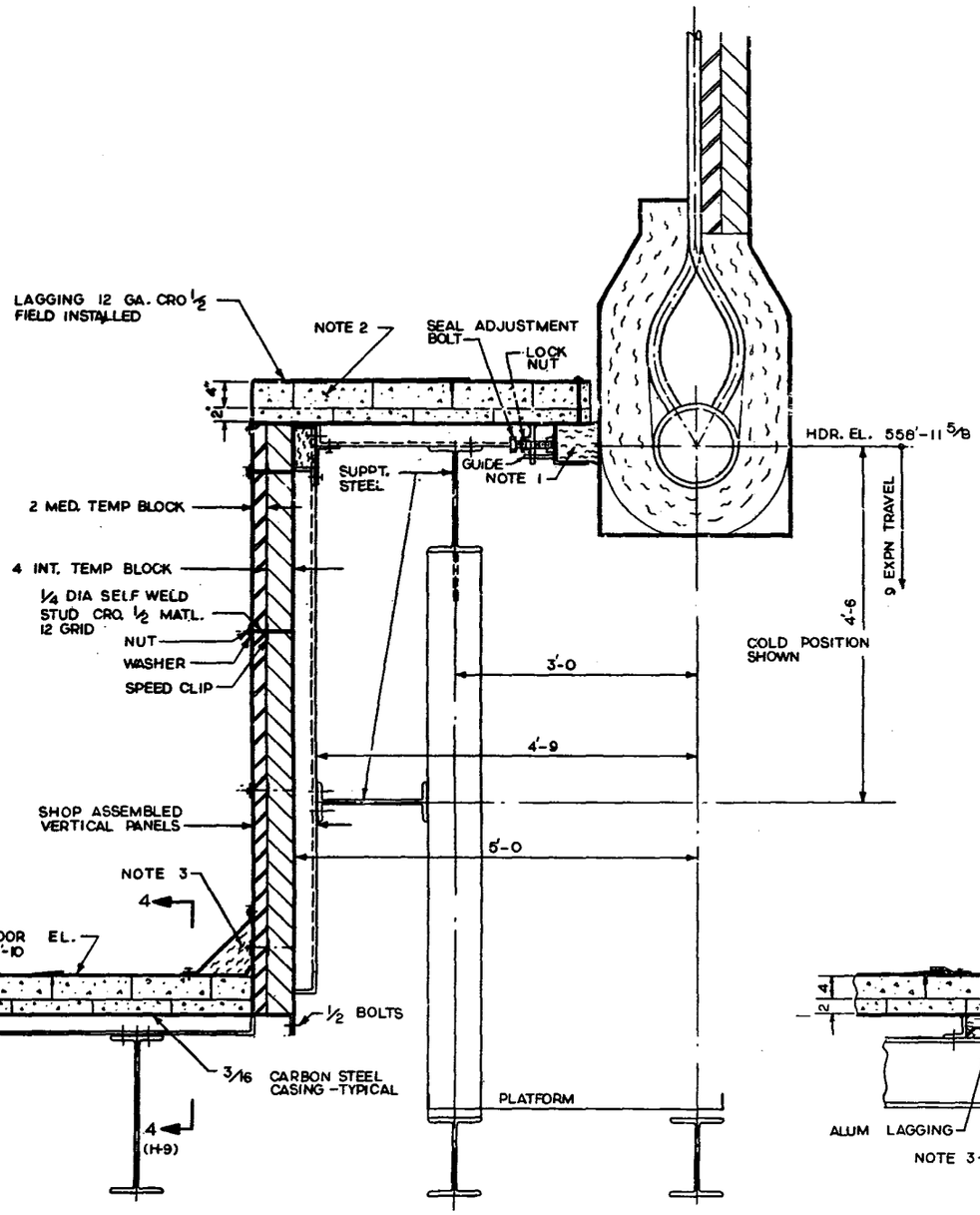

SECTION 1-1
NORTH CAVITY

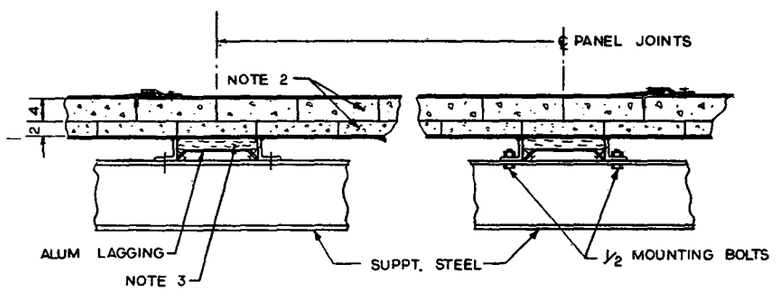

SECTION 4-4
(G-2)

NOTES:

1 MED TEMP BLANKET ASTM - C-592 - CL 2 6" THK. (MINERAL FIBER BLANKET 8# DENSITY).

2 MED TEMP BLOCK ASTM C 533 (CALCIUM SILICATE BLOCK) 12" x 36" BLOCKS THK. AS SHOWN. FIELD INSTALLED.

3 MINERAL FIBER BLANKET ASTM C 612-70 - CL 3.

4 FOR MAIN ARRGT SEE DWG 8427J

FIGURE 9.14

DRWG. BY KIDALOSKI	ENLGD VIEWS & SECTIONS FLOOR JUNCTIONS	THE BABCOCK & WILCOX CO.
CHKD. BY		
PLANNED BY RGK		
APPVD. BY		
STD. NO.	DATE 10-14-81	
894-0012-45	SCALE 1/2"=1'-0"	DWG. NO. 407007E REV. 0

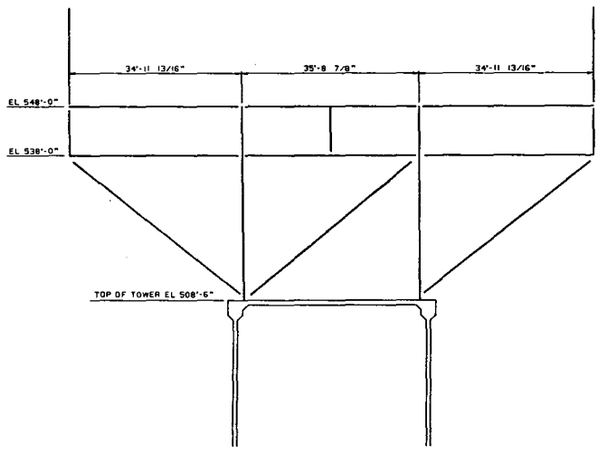

SECTION A-A

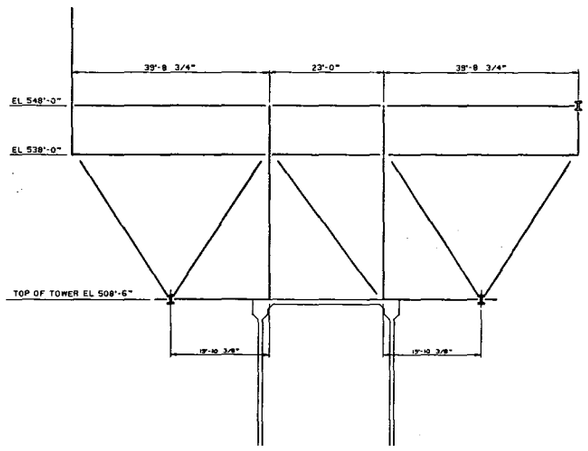

SECTION C-C

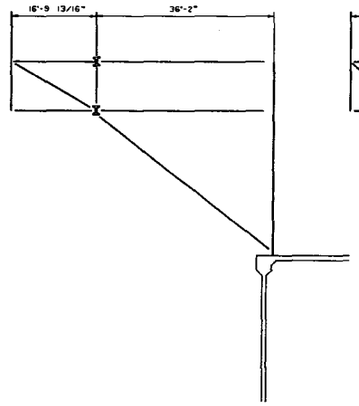

SECTION B-B

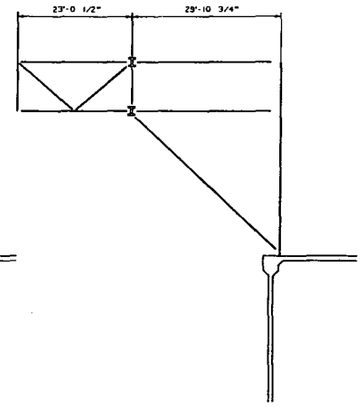

SECTION D-D

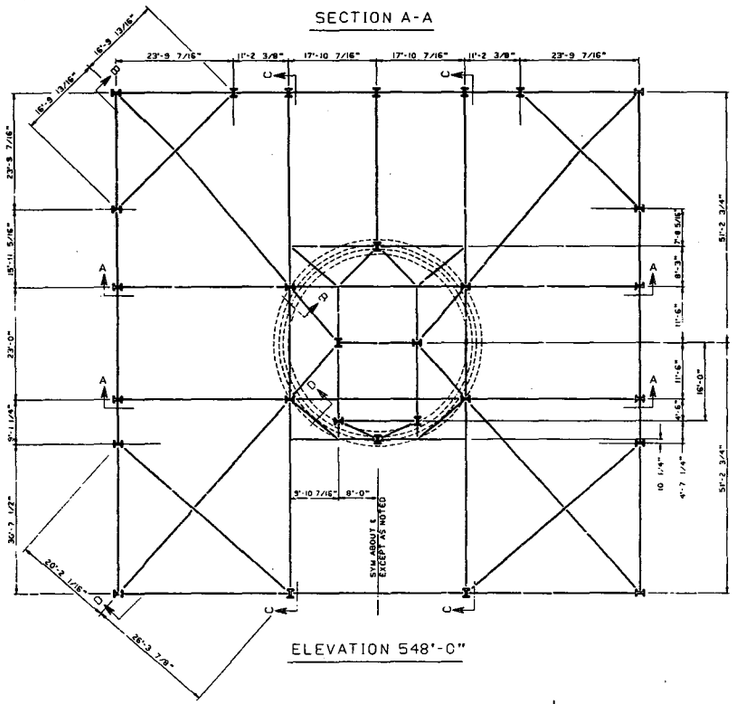

ELEVATION 548'-0"

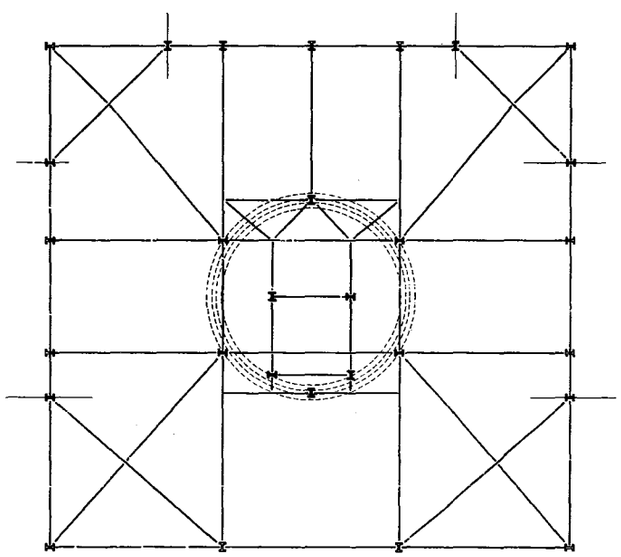

ELEVATION 538'-0"

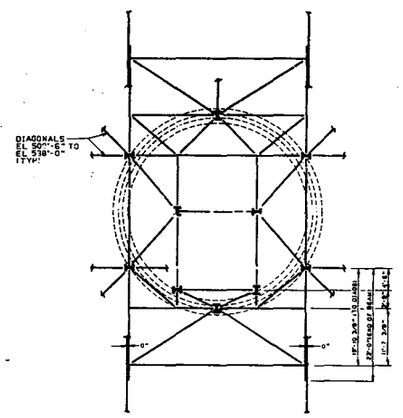

ELEVATION 508'-0"
TOP OF TOWER

NOTES

ALL ELEVATIONS ARE FROM GROUND

- COLUMN FRAMING INTO TOWER
- COLUMN IN CAVITY TOWER
- COLUMN IN OUTER WALLS
- TRUSS POSTS

FIGURE 9.15

DO NOT REVISE MANUALLY

DRN	R.A.HOPSON
CHK	R.S.D.
APPD	R.B.DAVENPORT
DSGN	R.D.FREEMAN

BABCOCK & WILCOX
A McDERMOTT COMPANY

RECEIVER
SUPPORT STRUCTURE

894-0012-45

SCALE: 1/8"=1'-0" | DWG. NO. 6542J | REV. 0

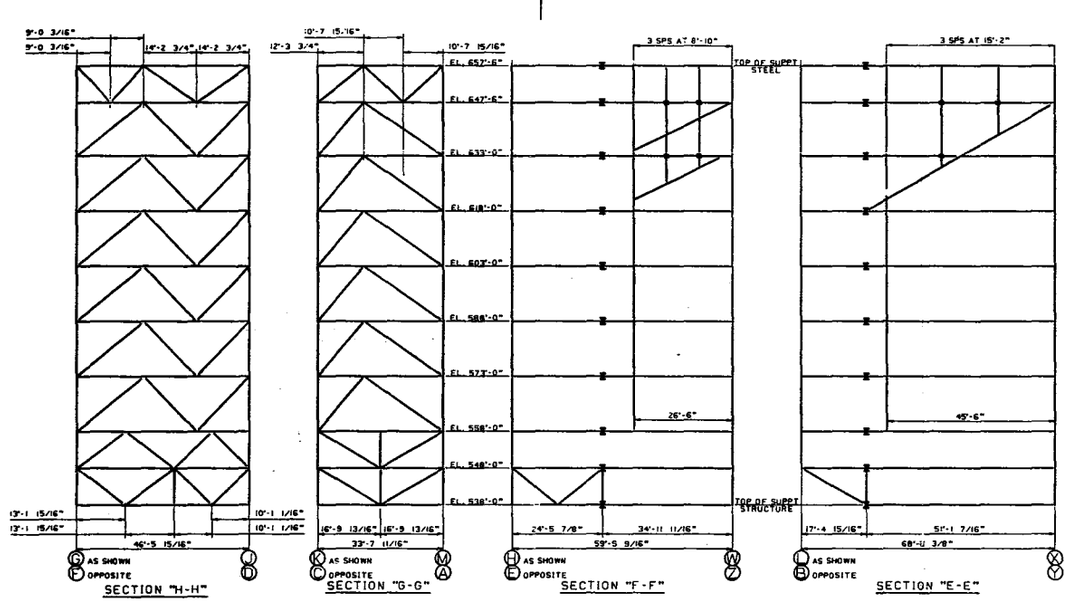

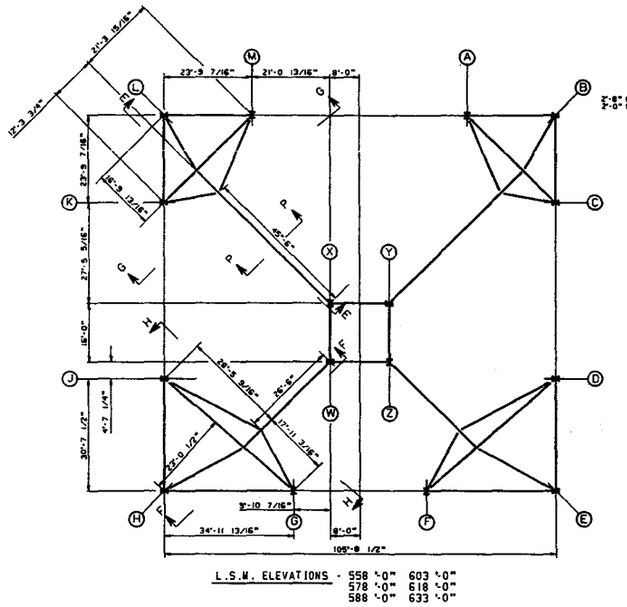

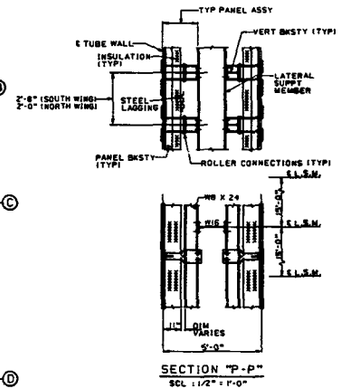

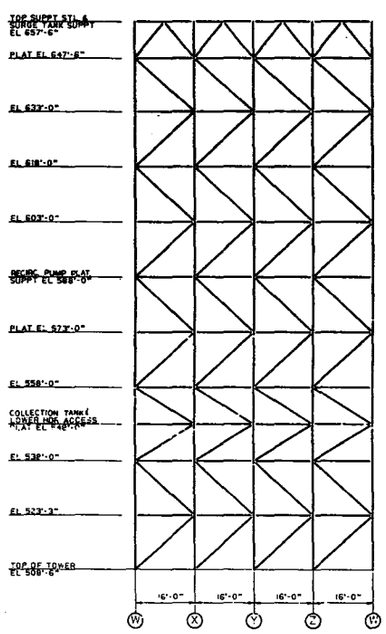

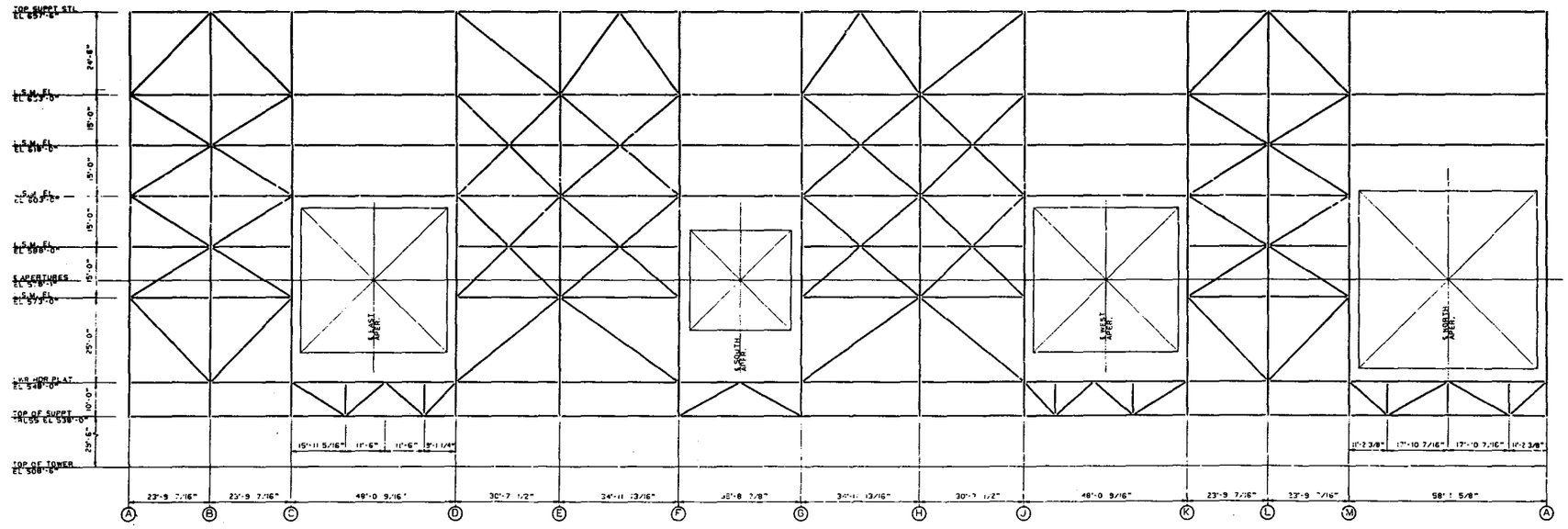

FIGURE 9.16

	A.PREVERSLIK	BABCOCK & WILCOX, A McDERMOTT COMPANY
	R.D.S.	
	R.B.DAVENPORT	
	R.J.GREEN	ELEVATION VIEW, CENTRAL TOWER, L.S.W. PLAN & SECTIONS
	894-0012-45	6543J 0

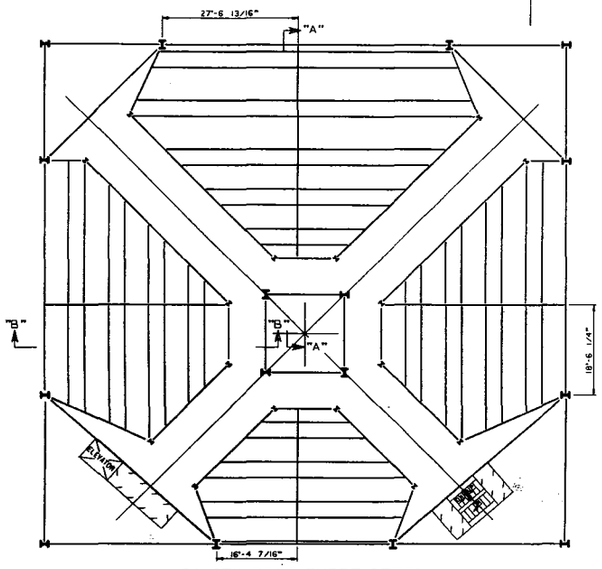

CAVITY ROOF SUPPT STEEL

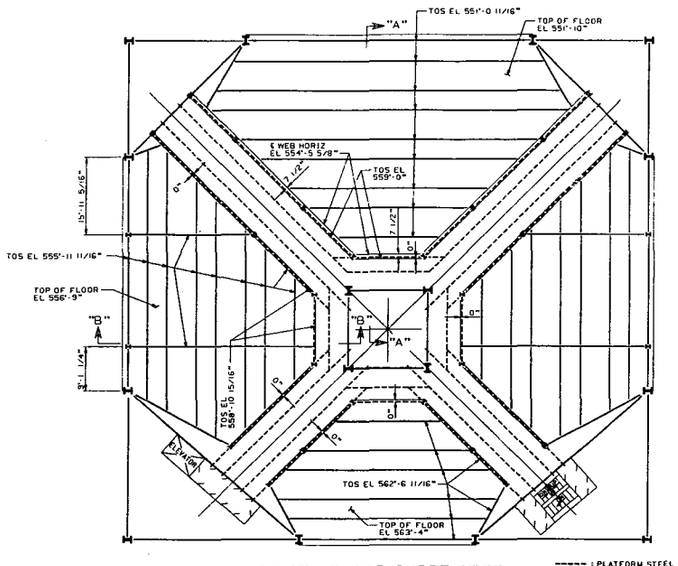

CAVITY FLOOR SUPPT STEEL

------ : PLATFORM STEEL

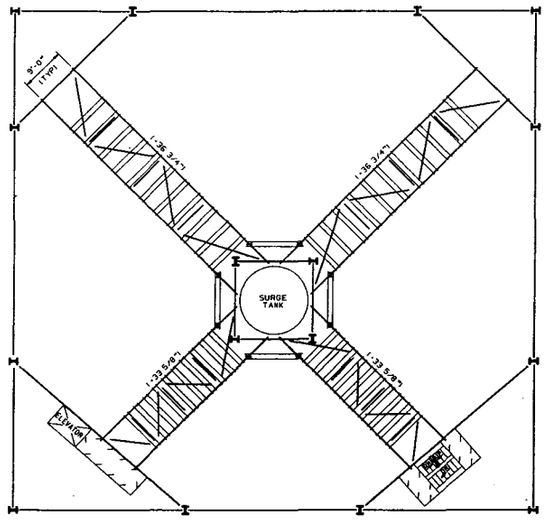

TOP SUPPORT STEEL EL 657'-6"

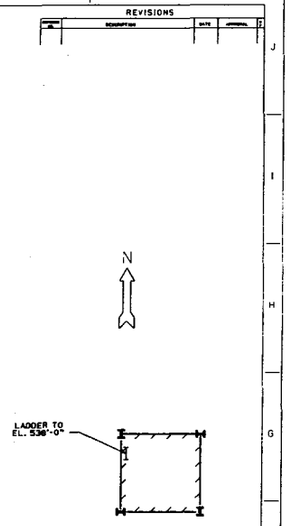

RECIRC. PUMP PLAT.

EL. 588'-0"

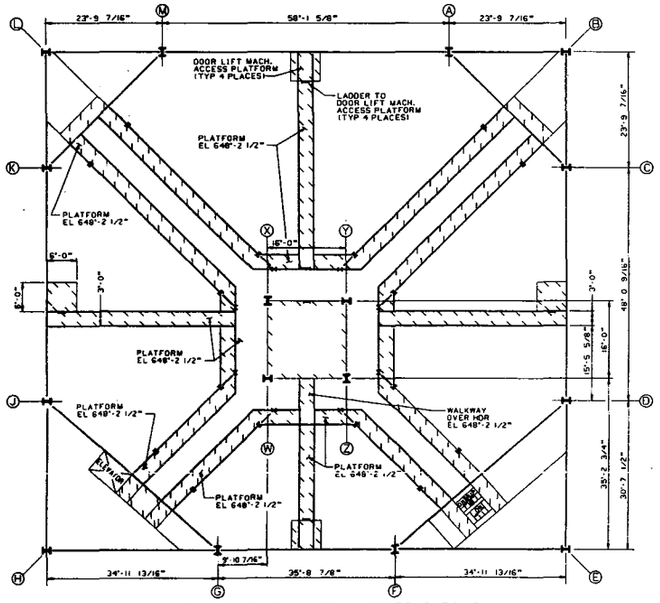

ACCESS PLATFORMS FOR UPPER PIPING

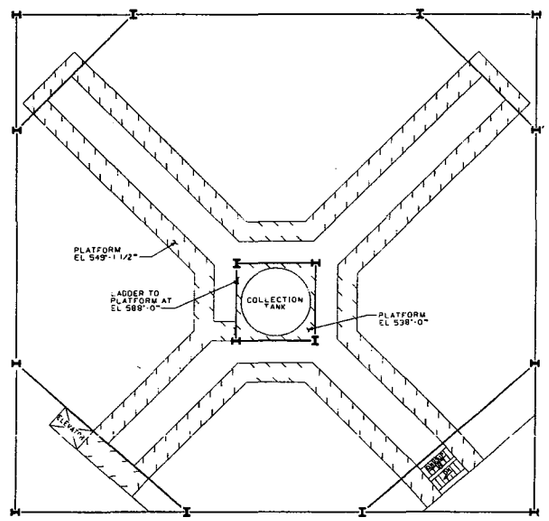

ACCESS PLATFORMS FOR LOWER PIPING

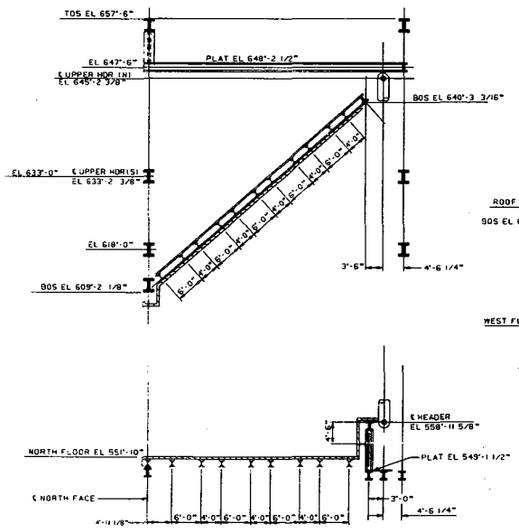

SECTION A-A

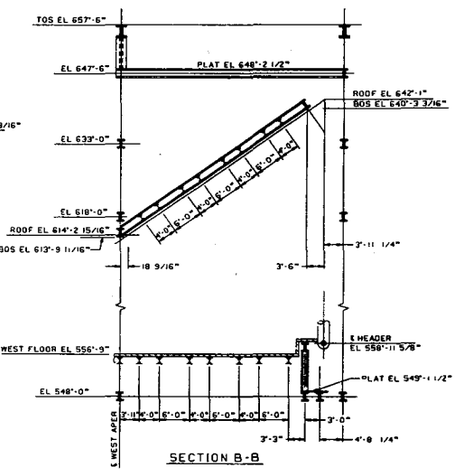

SECTION B-B

FIGURE 9.17

DRAWN	D.GALLINA	BABCOCK & WILCOX A MCDERMOTT COMPANY
		RECEIVER PLAN VIEWS
	894-0012	

DWG NO 6544J REV

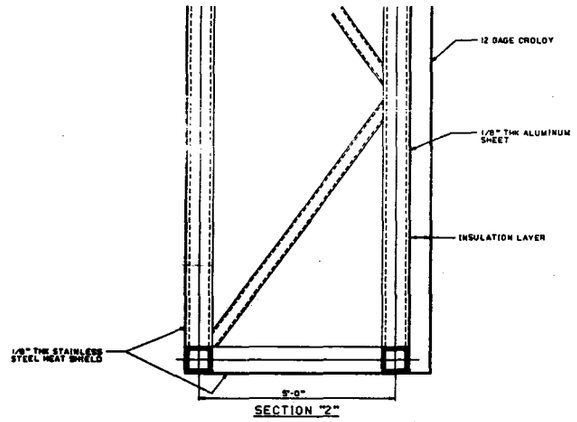

SECTION "2"
SCL : 1" = 1'-0"

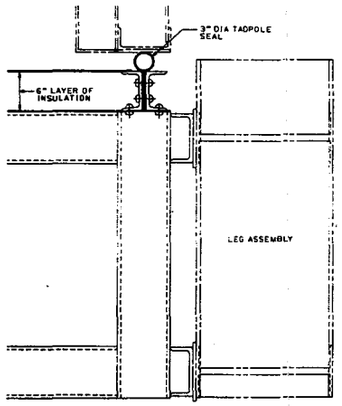

SECTION "1"
SCL : 2" = 1'-0"

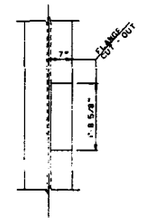

SECTION "Z-Z"
SCL : 1" = 1'-0"

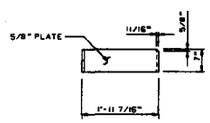

SECTION "X-X"
SCL : 1" = 1'-0"

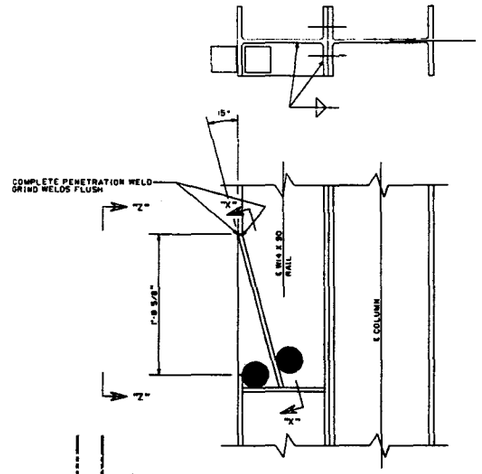

DETAIL "C"
SCL : 2" = 1'-0"

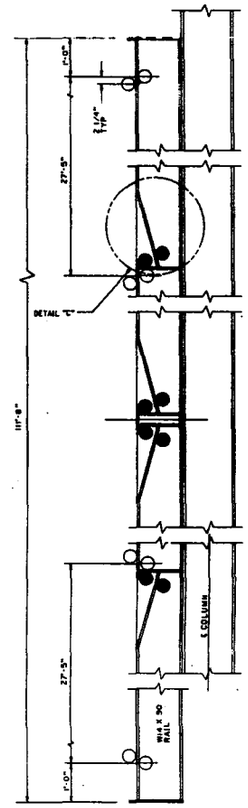

RAIL ASSEMBLY (NORTH DOOR)
SCL : 1" = 1'-0"
NOTE : OTHER DOORS SIMILAR DIMENSIONS SHOWN ARE FOR NORTH DOOR ONLY

● WHEEL OF DOOR IN CLOSED POSITION
○ WHEEL OF DOOR IN OPEN POSITION

SECTION "C-C"

SECTION "B-B"

SECTION "A-A"

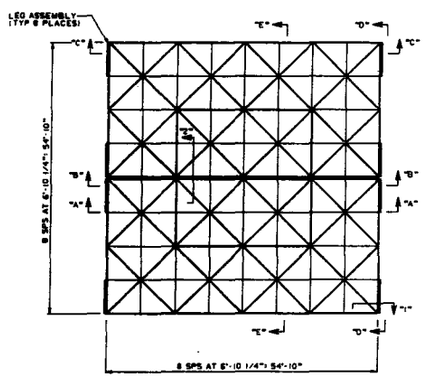

DOOR PLAN VIEW

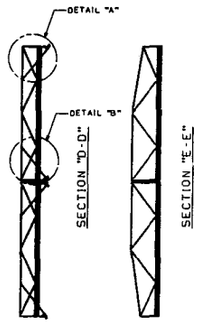

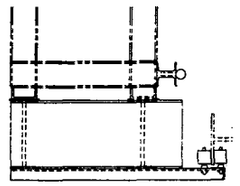

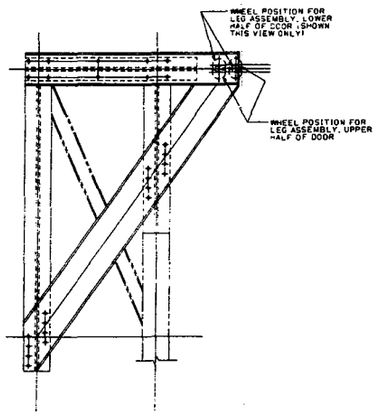

DETAIL "A"
SCL : 1" = 1'-0"
RIGHT SIDE (SHOWN)
LEFT SIDE (OPPOSITE)

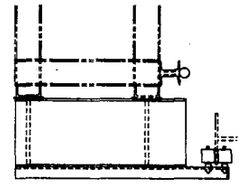

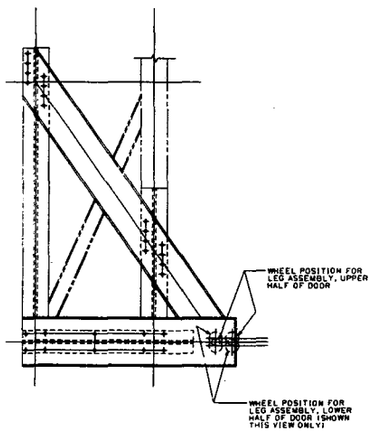

DETAIL "B"
SCL : 1" = 1'-0"
RIGHT SIDE (SHOWN)
LEFT SIDE (OPPOSITE)

REVISIONS

FIGURE 9.18

DRAWN	T. MACCOLL '81
CHKD	R.B.D.
APPROVED	R.B. DAVENPORT
ISSUED	R.D. GILLESPIE '82
894-0012-45	

BABCOCK & WILCOX
A McDERMOTT COMPANY

L/O DOOR AND TRACK ARRANGEMENT, SECTIONS AND DETAILS

SCALE: AS NOTED
DWG NO. 6545J-10
REV

DWG NO 6545J SH REV

10.0 REFERENCES

1. MCR 81-1707, "Alternate Central Receiver Power System Phase II, Volume III, Molten Salt Materials Tests," May 1981, Martin Marietta Aerospace Corporation.
2. SAND80-8052, "Molten Nitrate Salt Technology Development Status Report," C. M. Kramer (March 1981).
3. SAND81-8210, "Thermal Convection Loop Corrosion Test of 316SS and I800 in Molten Nitrate Salt," R. W. Bradshaw, (February 1982).
4. Howell, John R., "A Catalog of Radiation Configuration Factors," McGraw-Hill, 1982.
5. Clausing, A. M., "An Analysis of Convective Losses from Cavity Solar Central Receivers, Solar Energy, Vol. 27, No. 4, 1981.
6. Clausing, A. M., "Convective Losses from Cavity Solar Receivers - Comparison between Analytical Predictions and Experimental Results," Solar Engineering - 1982, Proceedings of 4th Annual ASME Solar Energy Conference, Albuquerque, NM, April, 1982, pp. 388-394.
7. Clausing, A. M., "Natural Convection Correlations for Vertical Surfaces Including Influences of Variable Properties." Preliminary Release.
8. "Saguaro Power Plant Solar Repowering Project," Final Report, Executive Summary and Vols. I, II, & III, DOE/SF 10739-1, 2, 3, & 4, Arizona Public Service Company, Phoenix, AX, July 1980.

INITIAL DISTRIBUTION
UNLIMITED RELEASE

Department 8450 Files (2)
Publications Division 8265, for TIC (27)
Publications Division 8265/Technical Library Processes Division, 3141
Technical Library Processes Division, 3141 (3)
M. A. Pound, 8024, for Central Technical Files (3)